PHYSICAL REVIEW

A JOURNAL OF EXPERIMENTAL AND THEORETICAL PHYSICS

PUBLISHED BY THE

AMERICAN PHYSICAL SOCIETY

Second Series *May, 1928* *Vol. 31, No. 5*

THE

PHYSICAL REVIEW

THE INTENSITY OF REFLECTED X-RAYS AND THE DISTRIBUTION OF ELECTRONS IN CRYSTALS

By G. E. M. Jauncey and W. D. Claus

Abstract

From the intensities of x-rays reflected in different orders, atomic structure-factor (or F) curves may be obtained from Darwin's formula. Duane and Compton, using different arguments, have shown that the method of Fourier analysis may be applied to a set of F values to obtain radial electron-distribution (or U) curves for the atoms of a crystal. However, Williams (Phil. Mag. **2,** 657) and Jauncey (Phys. Rev. **29,** 757) have suggested that the intensity of reflected x-rays is less than that on the classical theory because of the modified scattering of the Compton effect occurring at the expense of regular reflection. According to Williams and Jauncey, the number of electrons scattering coherently in the reflection process is a function of the angle of scattering and hence the method of Fourier analysis is invalid because this method depends on the assumption that the number of diffracting centers per atom of the crystal is independent of the angle of reflection. Havighurst (Phys. Rev. **31,** 16) takes issue with Williams and Jauncey on the following grounds: (1) A Fourier analysis of an experimental F curve gives a U curve which is reasonable (2) A Fourier analysis of the unmodified F values calculated for a model atom gives a U curve which agrees with the model and which roughly agrees with the experimental U curve (3) A Fourier analysis of the modified F values (i.e. F values modified by the Compton effect) gives a U curve which is unreasonable and does not at all agree with the experimental U curve.

The present paper is a reply to the criticisms of Havighurst. By trial a reasonable Bohr model of the chlorine ion has been found which gives modified F values at all angles in good agreement with the experimental values. Furthermore, the theoretical modified F curve has a kink at the same angle as that at which a kink occurs in the experimental F curves. This kink occurs at $\sin\theta=0.45$ (for Mo $K\alpha$ x-rays) and is connected with the result on Jauncey's theory that at this angle the M electrons entirely cease to act as diffracting centers. Havighurst's F curves do not show this kink because he draws smooth curves. From the theoretical modified F values a U curve is plotted for a grating space of $D=3.06$A. This U curve is similar to Havighurst's experimental U curve for the chlorine ion and has an area of 16.64 electrons in good agreement with 16.74 electrons for the experimental curve. Yet the theoretical U curve carries no particular information concerning the model from which it is derived. This is because the method of Fourier analysis is invalid.

The accuracy of experimental F values and U curves is discussed. The experimental F values for chlorine seem to be subject to an absolute error of 0.3, while the area under a U curve is easily subject to an error of 0.5 electron. Objection is raised to the practice by some authors of obtaining U curves for fictitious grating spaces. It is shown that the area under a U curve is a function of D and has no precise meaning even if crystal reflection is unaffected by modified scattering.

1. Introduction

SEVERAL papers on the distribution of electrons in the atoms of crystals as revealed by the intensities of x-rays reflected in different orders by the crystals have recently been published by R. J. Havighurst. For brevity we shall in the present paper refer to these papers as Papers I[1], II[2], III[3], IV.[4] In papers I and II, Havighurst describes how atomic structure-factor curves, or F curves, are obtained from the experimental values of the intensities in the various orders of reflection from powdered crystals. In Paper III, Havighurst applies the Fourier analysis method, as developed by Duane[5] from his quantum theory of diffraction and also subsequently by A. H. Compton[6] from the classical theory, to his experimental F curves and so obtains the distribution of the electrons in the atoms of the crystals.

Various authors have tried to find a model atom which would give F values in agreement with the experimental values and an excellent account of these efforts appears in a paper by Bragg, Darwin and James.[7] The models used, however, have until recently been based on the Bohr orbit theory of the atom. None of these models has been successful. This fact led Williams[8] and Jauncey[9] to inquire whether there might not be some effect which had been omitted from consideration when F values were calculated for a given Bohr model. It seemed to both Williams and Jauncey that such an effect might be the Compton effect. On Jauncey's theory of the unmodified line in the Compton effect,[10] coherent or unmodified scattering takes place from one set of electrons in an atom, while modified scattering takes place from a second set of electrons. Jauncey refers to the electrons of the first set as u electrons, and those of the second set as s electrons. *The effect of the application of the ideas of Williams and Jauncey to crystal reflection of x-rays is that the Fourier analysis method of finding the electron disribution in an atom is rendered invalid. This is because one of the assumptions underlying the validity is that the number of diffracting centers per atom remains constant as the angle of reflection varies; whereas the ideas of Williams and Jauncey lead to the result that the numbers of diffracting centers or u electrons, is a function of the angle of reflection.*

In Paper IV, Havighurst criticises the ideas of Williams and Jauncey and brings forward arguments to show that there is no need to apply a Compton effect correction to the electron distribution as obtained by a Fourier analysis of the experimental F curves since the electron distribu-

[1] R. J. Havighurst, Phys. Rev. **28,** 869 (1926).
[2] R. J. Havighurst, Phys. Rev. **28,** 882 (1926).
[3] R. J. Havighurst, Phys. Rev. **29,** 1 (1927).
[4] R. J. Havighurst, Phys. Rev. **31,** 16 (1928).
[5] W. Duane, Proc. Nat. Acad. Sci., **11,** 489 (1925).
[6] A. H. Compton, X-Rays and Electrons, Chap. 5.
[7] Bragg, Darwin and James, Phil. Mag. **1,** 897 (1926).
[8] E. J. Williams, Phil. Mag. **2,** 657 (1926).
[9] G. E. M. Jauncey, Phys. Rev. **29,** 757 (1927).
[10] G. E. M. Jauncey, Phys. Rev., **25,** 314 (1925); **25,** 723 (1925); Jauncey and Compton, Nature, October 15, 1927.

tion so obtained is a reasonable one. The present paper is a reply to the criticisms of Havighurst.

Before considering Havighurst's paper in detail, the authors wish to remark that they are aware of the papers by Waller[11] and Wentzel[12] on the application of wave-mechanics to the scattering of x-rays by bound electrons. According to Waller and Wentzel coherent scattering takes place according to the classical theory and the number of diffracting centers in an atom of a crystal remains constant as the angle of reflection varies. Hence, the Fourier analysis is valid. In its present stage, however we are not prepared to accept fully Schroedinger's wave-mechanics. For the present the authors prefer to keep the Bohr model and to see how far one can go with this model. We now proceed to the detailed consideration of Havighurst's paper IV.

2. Summary of Havighurst's Criticism

On careful consideration of Havighurst's Paper IV, it seems to us that his most weighty objection to the ideas of Williams[8] and Jauncey[9] is that the experimental F values lead, on the application of a Fourier analysis, to electron distribution curves which are reasonable, whereas a model atom gives F values which when modified by the Compton effect in the way proposed by Williams and Jauncey lead to electron distribution curves which are not reasonable. For brevity, the radial distribution is represented by U and a radial distribution curve is called a U curve. The relation between U and the F values is given by Compton as

$$U=(8\pi r/D)\sum_{1}^{\infty}(nF_n/D)\sin(2\pi nr/D) \tag{1}$$

where r is the distance from the center of the atom. If U is plotted against r, the area under the U curve is equal to the effective number of diffracting electrons associated with an atom. For instance, in Fig. 2, Paper IV, the curve a represents the radial distribution of the electrons in a model argon atom. The area under this curve is 18 electrons for a grating space of $D=$ 2.814A. Further there are two humps in the curve corresponding to the ten (K+L) electrons at $r=0.22$A and eight M electrons at $r=1.0$A. The K and L electron orbits overlap each other because of the thermal vibrations of the atoms. These vibrations are estimated by James and Firth[14] to have an amplitude of about 0.2A. Havighurst then calculates F values, modified to take account of the Compton effect, for his model, and from these modified F values he obtains a U curve represented as c in Fig. 2, Paper IV, for $D=2.814$A. The area under curve c is 14.1 electrons. This means that the radius of the atom is greater than $D/2$ or 1.407A. On taking a grating space of $D=5.628$A, he obtains curve b of Fig. 2, Paper IV, which

[11] I. Waller, Nature **120,** 155 (1927); Phil. Mag. **4,** 1228 (1927).
[12] G. Wentzel, Zeits. f. Physik, **43,** 779 (1927).
[14] James and Firth, Proc. Roy. Soc. **117A,** 62, (1927).

has an area of 18.2 electrons. The area of the curve is correct (the true number of electrons being 18), but the grating space is such that an atom of radius about 2.814A is obtained. Furthermore, neither curve *b* nor curve *c* has a second hump at $r=1.0$A corresponding to the *M* electrons. Since his experimental *F* values for chlorine as obtained from a crystal of rocksalt lead to a *U* curve, Fig. 6, Paper III having an area of 17.85 electrons (nearly 18) for $D=3.25$A and humps at $r=0.26$, 0.75 and 1.23A corresponding to the $(K+L)$, M_{III} and M_I electrons and so corresponds fairly closely to the *U* curve obtained from the unmodified *F* values of his model argon (or Cl^-) atom, and since the *U* curve obtained from the experimental *F* values does not agree anywhere nearly so closely with the *U* curve obtained from the modified *F* values of the model, Havighurst then concludes that there is no room for the Compton effect correction to the *F* values.

3. Remarks in Rebuttal

A sufficient reply to Havighurst is to invent a model which gives modified *F* values which agree with the experimental *F* values and which contains a reasonable distribution of electrons and for which the *K*, *L* and *M* critical absorption wave-lengths used in calculating the modified F values according to Jauncey's formula are also reasonable.

Before proceeding to this model, we shall examine into what is meant by "experimental" *F* values for chlorine. These values are not calculated directly from Eq. (1), Paper I. The real experimental *F* values which are obtained for a crystal of rocksalt are for (Cl+Na) and (Cl−Na). However, as a (Cl+Na) reflection cannot occur at the same angle as a (Cl−Na) reflection and as an *F* value for chlorine at a given angle is determined by taking one half of the sum of the *F* values for (Cl+Na) and for (Cl−Na) at the same angle, it is impossible to obtain a real experimental *F* value for chlorine. On account of this, it is the practice of Havighurst and others to draw smooth curves through the real experimental *F* values for (Cl+Na) and (Cl−Na) respectively. Then from these two curves, the F curve for chlorine is calculated and so-called "experimental" values for chlorine are found from this curve. As a result these "experimental" *F* values for chlorine are obtained sometimes from two interpolated *F* values for (Cl+Na) and (Cl−Na), sometimes from one interpolated and one experimental value, sometimes from two extrapolated values. Havighurst on page 872 of Paper I states that in his experiments the relative intensities of the reflected beams from a crystal of rocksalt can be measured with an error of less than five percent except in the case of weak reflections. Now *F*-values as calculated from Eq. (1), Paper I vary as the square root of the ratio of the reflected to the primary intensity, so that the *F* values are subject to an error of 2.5 percent. At the first order reflection of Mo $K\alpha$ x-rays ($\lambda=0.71$A) from the (100) planes of rocksalt, when $\sin\theta=0.126$, the experimental *F* value for (Cl+Na) is 20.80 as shown in Table IIA, Paper I. Hence the *F* values for (Cl+Na) at $\sin\theta=0.126$ is subject to an absolute error of 0.5. For the first order reflection from the (111) planes when $\sin\theta=0.109$, the experimental *F*

value for (Cl−Na) is 4.55 and hence is subject to an absolute error of 0.1. Hence the so-called "experimental" F value for Cl at sin $\theta = 0.109$ is subject to an absolute error of $(0.5+0.1)/2 = 0.3$. We have verified this by drawing different smooth curves, through the experimental F values for (Cl+Na) and (Cl−Na) and we find we can obtain a variation of 0.2 to 0.3 from the mean value. The percentage error of the F values for chlorine increases as sin θ increases and we are of the opinion that the absolute error falls to about 0.2 as the large angle reflections are approached. Havighurst's statement that his "experimental" U curve for chlorine, obtained from his "experimental" F values for chlorine and shown in Fig. 6 Paper III, has an area of 17.85 (nearly 18) electrons depends amongst other things on his value of F for sin $\theta = 0.109$. In Table III, Paper III, the value of F is 13.60. This may easily be 13.40 in which case the area under the curve is not 17.85 but 17.45 electrons, since the area under a U curve from r = 0 to r = D/2 is obtained from Compton's formula[6]

$$A = -2\sum_{1}^{\infty}(-1)^{n}F_{n} \tag{2}$$

Accurate F values at all parts of the F curve are required in order to obtain the true value of A. Using the present experimental F values the writers do not believe that it is possible to obtain U curves the area under which is subject to an error of less than 0.5 electron. As a result the question as to whether the chlorine in crystal of rocksalt exists as a neutral atom or a negative ion cannot at present be decided by means of a Fourier analysis of "experimental" F values. The writers are supported in this belief by Bearden,[15] who states that absolute intensity measurements must be made precise to less than one percent in order to obtain reliable electron distribution curves for the atoms of a crystal. This means that the F values must be known to within 0.5 percent.

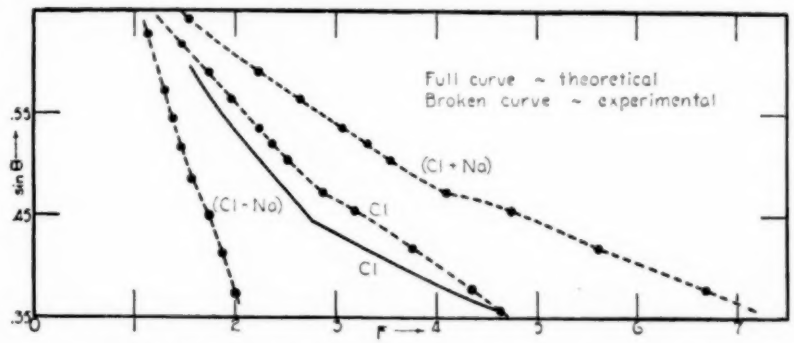

Fig. 1. Atomic Structure Factor for the Atoms in Rocksalt.

The drawing of a smooth "experimental" F curve for chlorine masks any real kinks in the curve which might occur if the true F curve could be found. This is a very important point for on Jauncey's theory small kinks

[15] J. A. Bearden, Phys. Rev. **29**, 20 (1927).

should occur in an F curve. In the experimental F curve for (Cl+Na) the experimental F values do not fall on a smooth curve. This is very evident in the F curve for (Cl+Na) at sin $\theta=0.47$ as shown in Fig. 1. Since the F values of (Cl−Na) apparently fall on a smooth curve, the writers have obtained a set of "experimental" F values for chlorine by adding the interpolated F values for (Cl−Na) to the experimental F values for (Cl+Na) and halving the result. The experimental F values of (Cl+Na) are taken from Table IIA, Paper I. This set of values is shown in the second column of Table I.

TABLE I. *F values for chlorine*

sin θ	"Experiment"	Theory	sin θ	"Experiment"	Theory
(.109)	(13.40)	13.22	.418	3.74	3.25
.126	12.32	12.37	.455	3.23	2.66
.178	9.22	9.82	.472	2.86	2.50
.218	7.84	8.16	.504	2.52	2.21
.252	6.94	7.10	.520	2.38	2.12
.309	5.58	5.65	.535	2.24	2.00
.357	4.63	4.61	.564	1.97	1.75
.378	4.35	4.10	.590	1.74	1.58
.399	3.98	3.66	.617	1.47	1.37

The F value for sin $\theta=0.109$ was obtained from the experimental F value for (Cl−Na) and a slightly extrapolated F value for (Cl+Na). This extrapolation is necessary since the smallest experimental value of sin θ for (Cl+Na) is 0.126. We have used a grating space of $D=3.06$A which is intermediate between $D=2.814$A for the (100) planes and 3.25A for the (111) planes of rocksalt. This was done in order to obtain an F value for the first order as near a real experimental value as possible. For $D=3.06$A, the first order reflection of Mo Kα x-rays occurs at sin $\theta=0.116$. A curve is drawn through the "experimental" F values of Table I so as to show any kinks which appear. F values are read off from this curve at multiple values of sin $\theta=0.116$ and a U curve obtained. The U curve so obtained is shown as the broken curve in Fig. 2, and is similar to Havighurst's curve in Fig. 6, Paper III. Like Havighurst's curve, it has three definite humps at $r=$ 0 27, 0.76, and 1.21A. However, our curve differs from Havighurst's curve in that while his has an area of 17.85 electrons, ours has an area of 16.74 electrons, the two values differing by 1.11 electrons. Some of this difference is due to the fact that Havighurst used a grating space of 3.25A while we have used a grating space of 3.06A. Using a grating space of 3.25A we have obtained an area of 17.2 electrons. The remainder of the difference is due to the different ways in which an F curve may be drawn through the experimental values, and to the different ways of extrapolating at small angles. We have used Havighurst's own extrapolated values at large angles to obtain our F values in this region, but we disagree with Havighurst that the particular kind of extrapolation of the F values to zero at large angles does not make an appreciable difference in the area under the U curve, although

the general shape of the U curve seems to be unaffected. We shall return to this point later. Obviously from Eq. (2) if the area is measured out to $D/2$ the area depends on the high order F values. We also disagree with Havighurst that his experimental U curve resembles so very closely the U curve for the model argon atom. The U curve for the model argon atom has only two humps while the experimental U curve for chlorine has three humps. We now proceed to our model.

In our model we suppose the chlorine to exist as an ion with the various electrons distributed as in Table II. The critical absorption wave-lengths for the various electrons are also shown.

TABLE II. *Model Cl^- ion*

Kind of electrons	Number	Radius of Orbit	Critical absorption Wave-length λ_s	$(2h/mc\lambda_s)^{1/2}=(2\alpha_s)^{1/2}$
K	2	0.033A	4.38A	0.106
L	8	0.29	69.0	0.0265
M	8	0.925	310.0	0.0125

For simplicity in calculation we have assumed circular orbits, and have omitted the fine structure of the L and M levels. On Jauncey's theory[9] the proportion of, say, the K electrons which are in the u state is

$$y_K=0.5-\frac{\alpha\sin\theta}{2(2\alpha_K)^{1/2}}+\frac{(2\alpha_K)^{1/2}}{8\alpha\sin\theta} \tag{3}$$

where $\alpha=h/mc\lambda$, $\alpha_K=h/mc\lambda_K$, λ is the wave-length of the primary x-rays and λ_K is the K critical absorption wave-length. The numerical values of y for the K, L and M electrons are obtained from the following equations:

$$\left.\begin{aligned} y_K&=0.5-0.160\sin\theta+0.390\ /\sin\theta\\ y_L&=0.5-0.635\sin\theta+0.0965/\sin\theta\\ y_M&=0.5-1.350\sin\theta+0.0454/\sin\theta \end{aligned}\right\} \tag{4}$$

We can now calculate what Havighurst calls the f values from Eq (10) of Jauncey's paper.[9] The F values (Havighurst's notation) are calculated from these by multiplying the f values by the Debye temperature factor $\exp.(-2.39\sin^2\theta)$ which is the factor used by Havighurst. The theoretical F values so found are shown in the third column of Table I. It will be noticed that the greatest differences between the experimental and theoretical F values are 0.57 at $\sin\theta=0.455$ and 0.60 at $\sin\theta=0.178$. We have put the error in the experimental F values at 0.3. With the exception of the two regions mentioned the differences are of the order of the experimental error. However, we have used a simple model in which there is no fine structure of the L and M levels and in which the orbits assumed are circular and we are confident that if we split up the L and M levels into sublevels and consider elliptical as well as circular orbits we can find a model

which will everywhere give theoretical F values differing from the experimental values by no more than the experimental error. The theoretical and experimental F curves for chlorine are shown as full and broken curves respectively in Fig. 1 for the range sin $\theta = 0.35$ to sin $\theta = 0.65$.

It will be noticed that both the experimental and theoretical curves show a kink at about sin $\theta = 0.45$. At present the writers do not believe that the experimental accuracy is such as to prove the existence of a kink in the experimental curve, yet it is interesting that a kink occurs in both curves at the same place. Havighurst's curves do not show the kink because he draws smooth curves. The kink in the theoretical curve comes at a value of sin θ which makes y_M of Eqs. (4) zero. This means that at this angle the M electrons entirely cease to act as diffracting centers, all of them being in the s state. This critical value of sin θ is determined by the value of λ_M assumed in our model which is 310A. From curves by Compton and Mohler[16] the critical absorption wave-length for the M_I level is 270A while that for the M_{III} level is 1000A. Our value of λ_M is therefore of the proper order of magnitude. It is very likely that the M levels of chlorine vary with the chemical compound. In Paper I, Havighurst has found that different experimental F curves are found for sodium according to whether NaF or or NaCl is used. According to Havighurst, this difference indicates a tightening of the electron atmosphere of sodium in NaF. On our ideas this tightening means amongst other things a decrease in the critical absorption wave-lengths. Hence some variation in the critical absorption wave-lengths in our model from those given by Compton and Mohler is to be permitted. We therefore feel that the values we have used in Table II are reasonable. Also, the radii of the circular orbits are reasonable. We therefore believe that by the method of trial we have found a model of the chlorine ion which is a reasonable one and which gives F values in reasonable agreement with the experimental F values.

TABLE III. *Experimental and theoretical F values used in Fourier analysis*

n	sin θ	F_n Experiment	F_n Theory	n	sin θ	F_n Experiment	F_n Theory
1	0.116	(13.00)	12.81	5	0.580	1.83	1.65
2	0.232	7.46	7.68	6	0.696	(.78)	.98
3	0.348	4.78	4.76	7	0.812	(.03)	.48
4	0.464	3.03	2.57	8	0.928	(.00)	(.15)

The theoretical and experimental F values for D = 3.06A (or first order reflection at sin $\theta = 0.116$) are shown in Table III, the extrapolated values being shown in parentheses.*

[16] Compton and Mohler, Nat. Res. Council Bull., **48**, 109 (1924).

* It will be seen that the theoretical F value for sin $\theta = 0.928$ is extrapolated. We have used this extrapolated value because the calculated F values do not approach zero quickly enough at large angles. Our extrapolation of the theoretical F values is of the same nature as the extrapolation used for the experimental F values at large angles.

Theoretical and experimental U curves plotted from these values are shown as the full curve and dotted curves respectively in Fig. 2. It is seen that our theoretical U curve corresponds very well with the experimental U curve. Our curve has three humps at $r=0.27$, 0.56 and 1.28A, agreeing roughly with the three humps on the experimental U curve obtained by us from Havighurst's experimental F values for (Cl+Na) and (Cl−Na), and also with Havighurst's own U curve of Fig. 6, Paper III. The area under our theoretical U curve in Fig. 2 out to $r=D/2=1.53$A is 16.64 electrons as found by Eq. (2). To show that the area under a U curve is susceptible to the F values at large angles, we have only to remember that in Table III the theoretical F values for n = 6, 7, and 8 correspond to what are the extrapolated values in the experimental set of F values. We could stop our calculated theoretical F values at F_5 and then extrapolate for the higher

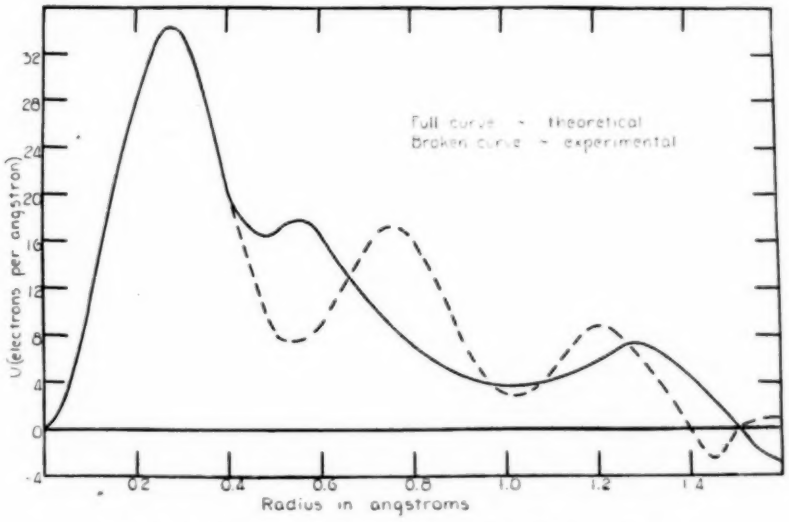

Fig. 2. Radial Distribution Curves or the Chlorine Ion.

F values. A reasonable set of such values would be $F_6=0.94$, $F_7=0.23$ and $F_8=0.00$, which would give a U curve area of 16.92 electrons.

The point to which we call attention is that we have devised a model chlorine ion which gives theoretical F values, these values being modified by the Compton effect according to Jauncey's theory,[9] in fair agreement with the experimental F values for chlorine. Also when a Fourier analysis is applied to our theoretical F values, a U curve is obtained which agrees in its general shape with the experimental U curve and gives the number of electrons within experimental error of the number given by the experimental U curve. Yet our U curve carries with it no particular information concerning the model from which we have derived the modified F values which have been used in obtaining our U curve. Had we used our model to calculate unmodified F values (that is, F values in which no account has been taken of the Compton effect) we would have obtained a U curve similar

to curve *a* for the argon model in Fig. 2, Paper IV, that is, a *U* curve with a hump due to the $(K+L)$ electrons at about 0.29A and a second hump due to the *M* electrons at about 1.0A. In this latter case the *U* curve does tell us something about the model.

The reason that our theoretical *U* curve tells us very little about the model from which it is calculated is that the Fourier analysis is not valid in this case since this validity is based on the assumption that the number of diffracting centers per atom remains constant as the angle of scattering varies. On Jauncey's theory, this number does depend on the scattering angle and hence the Fourier analysis is invalid and the *U* curve has no particular meaning.

It seems to us that the need for the Compton effect correction can neither be proved nor disproved from a consideration of the experimental *F* curves and the *U* curves resulting therefrom. On the other hand, a reasonable Bohr model of an atom cannot be found which will give unmodified *F* values in agreement with the experimental *F* values while it is possible to find a reasonable Bohr model which will give modified *F* values which differ from the experimental values by no more than the experimental error. We believe that the experimental *F* curves show that either the *F* values for a Bohr model atom must be modified to take account of the Compton effect or that the Bohr type of model must be abandoned. If we accept the idea of Schroedinger that the square of his function ψ is a measure of the electric density in the atom then the *U* curves which are obtained from the *F* values give us a measure of the continuous distribution of electric density in the atom, provided that the coherent scattering from this diffuse distribution of electricity is not affected by the Compton effect. Until it can be shown experimentally that the coherent scattering from an atom is not affected by the modified scattering, we believe that there is something to be said from the point of view of this paper.

4. Concluding Remarks

We regard it as extremely unfortunate that our views on the role of the Compton effect in crystal reflection require that the Fourier analysis method of unravelling atomic structure is invalid. There is no way as far as we can determine to make allowance for the Compton effect in a Fourier analysis. The only method is to assume a model and then to test it. This method of trial is extremely tedious. Nevertheless we feel that at present any electron distribution curve obtained by applying a Fourier analysis to a set of *F* values has very little basis of reality. We note in the literature on the subject that many writers in applying the Fourier analysis method use fictitious grating spaces. Usually these fictitious grating spaces are of the order of two or three times the real grating space between planes in the crystal. We object to this use of large fictitious grating spaces because they cause the first *F* value to come at an angle where there is no possibility of measuring the intensity of reflected x-rays. Such an *F* value for chlorine, for instance, is obtained from extrapolated *F* values for (Cl+Na) and (Cl−

Na). We feel that, even if the Compton effect does not enter into the reflection process in the way supposed by Jauncey, the U curves obtained by the use of fictitious F values are themselves largely fictitious. We have found the area under a U curve to be very susceptible to the particular grating space used. It is assumed by some writers that when a grating space of a certain size has been found to give, say, 18 electrons in the case of Cl^-, then all greater values of D give the same number of electrons for the area under the U curve out to $r = D/2$. This, however, is not necessarily the case. Using the experimental F values of Table I and adding an F value of 18 at zero value of $\sin\theta$, we have plotted an experimental F curve. From this curve we have read off various sets of F values for various values of D. From each of these sets of F values a U curve may be plotted and the area under the U curve from $r = 0$ to $r = D/2$ may be found from Eq. (2). In Table IV the values of the area for the several values of D are shown under "experiment." The values under $\sin\theta_1$ are for first order reflection of Mo $K\alpha$ x-rays by the corresponding grating spaces. Similarly, sets of theoretical F values have been found and the areas under the corresponding U curves obtained. The values of the area for the several values of D in this case are shown under "theory" in Table IV.

TABLE IV. *Area under U curves*

D	$\sin\theta_1$	Area (electrons) "Experiment"	"Theory"	D	$\sin\theta_1$	Area (electrons) "Experiment"	"Theory"
∞	.00	18.00	18.00	3.94A	.09	19.00	16.68
35.50A	.01	18.08	18.02	3.55	.10	18.34	17.16
7.10	.05	18.18	19.28	3.26	.109	17.28	17.18
5.92	.06	18.36	18.88	3.23	.11	17.20	17.14
5.07	.07	18.64	18.50	2.73	.13	16.04	15.74
4.44	.08	19.74	17.96	2.36	.15	13.90	14.10

In addition to the area at $D = \infty$, there is one other value of D for which the area is 18 electrons for both the "experimental" and the "theoretical" areas. It is interesting to note that the maximum area in either case is above 19 electrons. For the "experimental" areas the maximum occurs at D = 4.44A. If 19.74 electrons are included between $r = 0$ and $r = D/2 = 2.22$A, one would not expect that a less number of electrons would be included between $r = 0$ and $r > 2.22$A. This seems to us to prove that the Fourier analysis method of unravelling the structure of the atom is not suited to settling fine distinctions and differences, or, in other words, its resolving power is low.*

WASHINGTON UNIVERSITY,
ST. LOUIS, MO.,
January 24, 1928.

* The calculations in this paper were made by means of a Monroe calculating machine. Such a machine adds greatly to the facility with which a U curve may be plotted.

THE SPACE-DISTRIBUTION OF THE PHOTO-ELECTRONS EJECTED BY X-RAYS

By E. C. Watson

Abstract

None of the theories which have heretofore been proposed to account for the apparent emis ion of x-ray electrons from the atom over a wide range of angles instead of in one defin te direction is entirely satisfactory. Since the scattering of the electrons which takes place in neighboring atoms has not been completely eliminated in any of the experimental work, the Rutherford theory of nuclear scattering is applied to the problem. This theory together with the assumption that the electrons all start out from the parent-atom in the same direction can be made to explain in a satisfactory way all the details of the observed space-distribution. It gives the amount of the spread quantitatively; it gives the form of the distribution curves; it explains the difference between the lateral and longitudinal distributions; it explains the dependence of the amount of the spread upon the nature of the atoms from which the electrons are ejected and the frequency of the x-rays which do the ejecting; and it accounts for the disagreement among various observers regarding this dependence.

Incidentally it is pointed out that the scattering of 17 kv electrons by hydrogen nuclei is many times greater than can be accounted for on the classical theory.

THE problem of the nature of the force exerted upon an electron by a field of radiation is a fundamental one. Much light is thrown upon it by studies of the directions in which photo-electrons are ejected by x-rays. Experiments of this kind have recently been performed by C. T. R. Wilson[1] in England, Auger[2] in France, Bothe[3] and Kirchner[4] in Germany, and by Bubb[5], Loughridge[6], and the writer[7] in this country. These experiments show that while the most probable direction of ejection is exactly that of the electric vector of the incident radiation except for a forward component, there is apparently a very considerable spread in the directions of the individual electrons. Theories to account for this apparent emission from the atom over a wide range of angles instead of in one definite direction have been given by Bubb,[8] Bothe,[9] Auger and Perrin,[10] Wentzel,[11] Beck,[12] and Oppenheimer,[13] but none of them is entirely satisfactory in explaining all the

[1] C. T. R. Wilson, Proc. Roy. Soc. **A104,** 1 and 192 (1923).
[2] P. Auger, Comptes rendus **178**, 929, 1535 (1924); Jour. de Phys. et Rad. **8,** 85 (1927).
[3] W. Bothe, Zeits. f. Physik **26,** 59 (1924).
[4] F. W. Bubb, Phys. Rev. **23,** 137 (1924); Nature **112,** 363 (1923).
[5] D. H. Loughridge, Phys. Rev. **26**, 697 (1925) and **30**, 488 (1927)
[6] F. Kirchner, Phys. Zeits. **27,** 385 and 799 (1926); also Ann. d. Physik **83,** 521 (1927).
[7] E. C. Watson, Phys. Rev. **30,** 479 (1927).
[8] F. W. Bubb, Phil. Mag. **49,** 824 (1925).
[9] W. Bothe, Zeits. f. Physik **26,** 74 (1924).
[10] P. Auger and F. Perrin, Comptes rendus **180,** 1742 (1925), Jour. de Phys. et Rad. **8,** 93 (1927).
[11] G. Wentzel, Zeits. f. Physik **40,** 574 (1927).
[12] G. Beck, Zeits. f. Physik **41,** 443 (1927).
[13] J. R. Oppenheimer, Zeits. f. Physik **41,** 291 (1927).

now known experimental facts. The purpose of this paper is to point out that nuclear scattering of the sort postulated by Rutherford with such brilliant success in the case of α-particles has not been sufficiently considered in this connection and that it may account for the whole effect.[14]

I. The Experimental Situation

The experiments bearing upon this question have been of two general types: those which make use of unpolarized x-rays and study the distribution of electrons about the direction of the x-ray beam (this is usually called the *longitudinal distribution*) and those which use polarized x-rays and study the distribution about the direction of the electric vector in a plane perpendicular to the x-ray beam (this is called the *lateral distribution*).

The expansion-chamber technique of C. T. R. Wilson furnishes what is unquestionably the most powerful method which has been used in studies of this kind. It has been employed by Auger and Loughridge to study the longitudinal distribution and by Bubb and Kirchner to determine the lateral distribution.

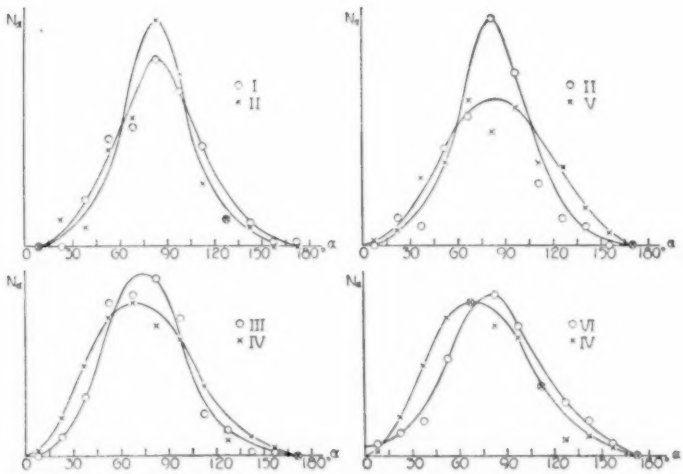

Fig. 1. Longitudinal distribution of photo-electrons ejected by x-rays as found by Auger.
I. *K* electrons of oxygen or nitrogen ejected by 15 kv primary x-rays.
II. *K* electrons of oxygen or nitrogen ejected by 20 kv primary x-rays
III. *K* electrons of argon ejected by 80 kv primary x-rays
IV. *L* electrons of xenon ejected by 80 kv primary x-rays
V. *K* electrons of krypton ejected by 22 kv primary x-rays
VI. *K* electrons of xenon ejected by 45 kv primary x-rays

Auger's results are shown in Fig. 1 in which the number of photo-electron tracks is plotted as a function of the angle of ejection measured from the forward direction of the x-ray beam for a number of experimental conditions. As heterogeneous x-radiation from a Coolidge tube was used the exact frequency of the rays which are most effective in each case is not known, but

[14] See also E. C. Watson, Phys. Rev. **29**, 752 (1927) and Proc. Nat. Acad. **13**, 584 (1927).

it is clear that the amount of the spread (i.e. the fraction of the whole number of tracks which start out at angles other than the most probable one) depends, to some extent at least, upon both the frequency of the incident x-rays and the nature of the gas in the expansion-chamber. This is in agreement with the results obtained by Bothe using a point-discharge ion-counter and those of Seitz[15] who studied the ionization on the two sides of very thin metallic films.

Loughridge, using zirconium-filtered radiation from a tube with molybdenum target driven at 40 kv, found that the amount of the spread was practically the same when argon or air was introduced into the expansion-chamber, but that it was less in hydrogen.

Kirchner, on the other hand, interprets his results on the lateral distribution as proving that the lateral spread is independent of both the frequency of the incident x-rays and the nature of the gas in the expansion-chamber. His results together with those previously obtained by Bubb are shown in Fig. 2 which is taken from Kirchner's paper. Here again the number of tracks is plotted against the direction of emission, the direction of the electric vector being at 90°. Heterogeneous radiation from an x-ray tube driven at approximately 50 kv was used in these experiments, but Kirchner finds nearly the same distribution for the tracks which are shorter than 15 mm that he does for those longer than 15 mm. This fact may not be significant, however, as the length of the track depends upon other factors than the energy of ejection and consequently the average energy of ejection of the longer tracks may not be much greater than that of the shorter tracks. Thus Nuttall and Williams[16] using strictly monochromatic x-rays found that the length of tracks varied as much as 30% each side of the mean. The results of Auger and Bothe which do show a variation with frequency are therefore the more convincing.

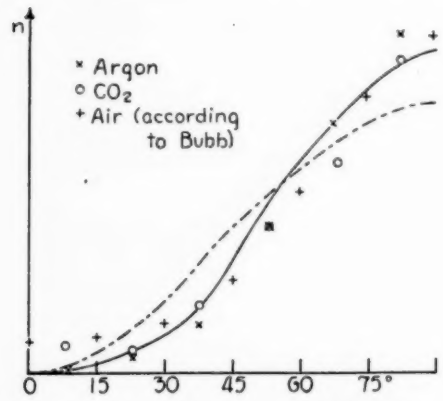

Fig. 2. Lateral distribution of photo-electrons ejected by x-rays as given by Kirchner.

Moreover as regards the dependence of the spread upon the nature of the gas in the expansion-chamber, Kirchner's results are not as convincing as are those of Auger, Bothe, and Loughridge, because the range of molecular weights used in his experiments was not so large. We conclude therefore that the evidence favors a variation in spread both with the nature of the gas and the frequency of the incident x-rays.

The results of Loughridge on air and hydrogen are of particular interest in this connection. They show that the spread is determined not so much by

[15] W. Seitz, Ann. d. Physik **73,** 183 (1924); Phys. Zeits. **25,** 546 (1924) and **26,** 610 (1925).
[16] J. M. Nuttall and E. J. Williams, Phil. Mag. **2,** 1109 (1926).

the nature of the atom from which ejection takes place as by the sort of molecules which surround it; for a simple calculation based upon the fact that the absorption of x-rays is proportional to the fourth-power of the atomic number shows that when hydrogen is the gas in the expansion-chamber practically all the electrons are ejected from the oxygen atoms of the water-vapor which must always be present. Consequently the difference between the spreads in air and hydrogen cannot be due to an appreciable difference in the atomic number of the atom from which the electron is ejected.

The dotted line in Fig. 2 is an attempt to fit the experimental points by a sine-square function, while the solid curve is a sine-cube function. No such functions can be made to fit the facts satisfactorily, however, because the experimental curves do not fall to zero at 0°. This is in marked contrast with the curves for the longitudinal distribution which do fall to zero at both 0° and 180° (as of course they must because the ordinate for any abscissa α is the number of tracks which start out through the solid angle between α and $\alpha+d\alpha$ to the direction of the x-ray beam and this solid angle becomes zero when α equals 0° and 180°). The failure of the curves for the lateral distribution to fall to zero may be due to lack of complete polarization of the incident x-rays, but this is unlikely as the non-polarized portion of the x-ray beam was carefully corrected for by both Bubb and Kirchner.

A comparison of the curves for the lateral distribution obtained by Bubb and Kirchner with those of the longitudinal distribution obtained by Auger and Loughridge shows that the amount of the spread is greater in the former than it is in any of the latter. Exact data upon this point are given in Tables II and III, below.

Finally it must be pointed out (and this is the consideration which makes the writing of this paper necessary) that the results of the expansion-chamber experiments are not as unambiguous as they are usually supposed to be. Thus it seems to have been universally assumed that these experiments give the actual directions of the electrons as they leave the individual atoms. This is not strictly true. The x-ray when it ejects an electron ionizes the atom and a water droplet condenses upon it. The diameter of this droplet was found by measurement upon the plates obtained by Loughridge to range from 0.5 to 0.9 mm.[17] Thus the space around the atom from which the electron is ejected is obscured and any change in the direction of motion of the electron which takes place in this distance cannot be detected. This fact has heretofore been thought to be of no significance because calculations of the amount of scattering to be expected in this distance were not made and simple scrutiny of the tracks themselves (which are often apparently quite straight for comparatively large distances) leads one to believe that no appreciable

[17] Mr. E. J. Williams has kindly written me that in his experiments the average diameter of the initial droplet is only about 0.1mm. In this case however the distance between droplets is probably larger. In any case it seems to the writer that it would be exceedingly difficult, if not impossible, to make exact measurements upon the direction of the tracks down to less than 0.5 mm from the atom from which the electron is ejected.

change in direction can take place in so small a distance. The calculations to be presented in this paper indicate, however, both that a considerable scattering will take place in a distance of the order of 0.5 mm and that the apparent straightness of the tracks is very deceptive.

II. Discussion of Previous Theories

Theories of the space-distribution have been of two kinds; those which account for the spread by compounding the momentum (assumed random in direction) of the electron in its atomic orbit just before ejection with the momentum imparted by the ejecting radiation (Bubb and Bothe), and those which deduce a probability function for the angle of ejection from general postulates, such as those of symmetry (Auger and Perrin) or those of the new quantum mechanics (Wentzel, Beck, and Oppenheimer).

Theories of the first kind seem to the writer to be definitely invalidated by the experimental results just given. Such theories demand that the spread be very great when the energy of the electron in its atomic orbit is only a little less than the energy of the incident quantum. The results of Auger show that this is not the case. Thus curve VI in Fig. 1 (for which the orbital energy $h\nu_0$ is 35 kv and the incident energy $h\nu$ is 45 kv) is practically no wider than curve IV (for which $h\nu_0 = 5$ kv and $h\nu = 80$ kv); nor is curve V (for which $h\nu_0 = 14$ kv and $h\nu = 22$ kv) any wider than is to be expected from considerations to be given later. The difficulty cannot be avoided by recourse to the new quantum mechanics which allows the moment of momentum of the K-electrons to be zero, as the writer[18] has recently shown that the spread is certainly not markedly greater for the L_{III} electrons of gold ejected by the $K\alpha$ rays of molybdenum ($h\nu_0 = 12$ kv and $h\nu = 17$ kv) than it is for the N and O electrons whose orbital energies are negligible.

All of the theories of the second kind so far proposed have led to a lateral distribution which is proportional to the cosine-square of the angle of ejection measured from the direction of the electric vector. There are four objections to such a distribution: (1) while Kirchner has succeeded in bringing his latest experimental results into fair agreement with this distribution, his earlier curves as well as those obtained previously by Bubb show a much sharper maximum than is given by the cosine-square law (this is shown in Fig. 2 where, as stated above, the dotted curve represents the cosine-square distribution); (2) the curves of the longitudinal distribution show a sharper maximum than is given by the corresponding cosine-cube law; (3) as has previously been pointed out the experimental curves do not fall to zero at 90° from the direction of the electric vector; and (4) such theories cannot without additional assumptions account for the variations in spread which Bothe, Auger, and Loughridge found when they changed the frequency of the incident x-rays and the nature of the gas in the chamber.

We conclude therefore that none of the theories so far proposed is entirely successful in accounting quantitatively for the observed space-distribution. Since the theoretical distributions are if anything already too broad, the

[18] E. C. Watson, Proc. Nat. Acad. **13**, 659 (1927).

agreement becomes still worse when allowance is made for the scattering in neighboring atoms. It therefore seemed worth while to calculate what the effect of scattering alone would be.[19]

III. Scattering in Neighboring Atoms

The Rutherford theory of nuclear scattering applied to β-rays leads to the equation[20]

$$\rho_\phi = \pi n t (Ze^2/2T)^2 \cot^2(\phi/2) \qquad (1)$$

where ρ_ϕ is the fraction of a beam of β-rays of charge e and kinetic energy T scattered through an angle equal to or greater than ϕ by a thickness t of scattering material containing n nuclei per cc of charge Ze.

This formula[21] (when modified by the inclusion of a relativity correction[22] worked out by C. G. Darwin for the change in mass of the electron with velocity in its orbit around the nucleus) has been completely verified in the case of the scattering of β-rays from radium E by Chadwick and Mercier[23] and for 30-77 kv cathode-rays by Schonland[24] provided thin enough foils are used so that Wentzel's criterion[25] for "single" scattering holds. It may therefore be used to calculate the fraction of the whole number of tracks which experience deflections greater than any given amount in going a distance of the order of 0.4 mm in the expansion-chamber experiments of Auger, Bubb, Kirchner, and Loughridge, on the assumption that all the electrons start out initially in the same direction. This fraction we shall call simply the "amount of the spread."

[19] That scattering in neighboring atoms might be made to account for the whole of the observed spread was suggested by the writer's results on the longitudinal distribution obtained with exceedingly thin metallic films. These showed that, in this case at least, nuclear scattering was the principal factor in bringing about the spread and that the ratio of the number of electrons leaving in a forward or backward direction to the number leaving at right angles to the x-ray beam became smaller as the thickness of the film decreased. This made plausible the assumption that for an infinitesimally thin film all the electrons would be ejected in a direction a little forward of normal to the x-ray beam.

[20] E. Rutherford, Phil. Mag. **21,** 669 (1911). See also J. A. Crowther and B. F. J. Schonland, Proc. Roy. Soc. **A100,** 526 (1922).

[21] For cathode-rays of small velocity Davisson [(Phys. Rev. **21,** 637 (1923) and **22,** 242 (1923)] has shown that equation (1) must be modified to take into account the screening effect of the outer electrons in the scattering atom. The velocities of the electrons in all the experiments on the space-distribution are, however, large enough so that corrections of this sort are negligible.

[22] For electrons ejected by the $K\alpha$ rays of molybdenum this correction is negligible except at large angles of scattering. For higher velocity electrons it may multiply ρ_ϕ by a factor of 2 or 3. Since, however, the exact frequencies of the ejecting x-rays are not known in the experiments of Auger, Bubb, and Kirchner, this correction cannot be made accurately and it is therefore omitted in the calculations which follow. In any case it always operates to increase the scattering.

[23] J. Chadwick and P. H. Mercier, Phil. Mag. **50,** 208 (1925).

[24] B. F. J. Schonland, Proc. Roy. Soc. **A113,** 87 (1926).

[25] G. Wentzel, Ann. d. Physik **69,** 335 (1922). See also Chadwick and Mercier, loc. cit. and Schonland, loc. cit.

Before applying equation (1) to this calculation, however, it is necessary to determine whether Wentzel's criterion for "single" scattering holds for distances of 0.4 mm in air, argon, hydrogen, etc.

a. *Wentzel's criterion for "single" scattering.* Wentzel's criterion for "single" scattering may be simply stated as follows: the scattering will be "single" provided the angle of scattering ϕ is at least some small multiple of ω, where ω is given by the equation

$$\cot(\omega/2) = 2TR/Ze^2 \tag{2}$$

where $R=(2/\pi nt)^{1/2}$ and T, Z, e, n, and t have the same meaning as above.

The smallest value of the ratio $\phi/4\omega$ for which the scattering will be certainly "single" has been made precise by experiments on the scattering of both α-and β-rays by thin foils. The smallest value of $\phi/4\omega$ in the α-ray experiments of Chadwick was 7, and the scattering was certainly "single." In the β-ray experiments of Crowther and Schonland for which $\phi/4\omega$ varied from 3.1 to 1.7, the value of ρ_ϕ was in general several times that given by equation (1) and the scattering has been shown to have been mainly "plural,"[26] while in the β-ray experiment of Chadwick and Mercier in which the scattering was certainly "single," $\phi/4\omega$ ranged from 4.5 to 7.5. The most precise evaluation of $\phi/4\omega$ for electrons has, however, been made by Schonland. With aluminum foil and both 59,900 and 77,300 volt electrons he obtained a linear relation between ρ_ϕ and t until, as the thickness increased, $\phi/4\omega$ became less than 3, when ρ_ϕ began to increase much more rapidly. This shows that the scattering will be "single" if $\phi/4\omega$ is greater than 3, but that it will be "plural" or "multiple" if $\phi/4\omega$ is less than 3.

For 15 and 24 kv electrons scattered in going a distance of 0.04 cm in argon, air, and hydrogen under standard conditions equation (2) gives the values of $\phi/4\omega$ in Table I.

TABLE I. *Values of* $\phi/4\omega$

Angle	$\phi/4\omega$ for 15 kv electrons			$\phi/4\omega$ for 24 kv electrons		
	argon	air (oxygen)	hydrogen	argon	air (oxygen)	hydrogen
90°	1.7	4	32	2.8	6.4	50
80°	1.5	3.6		2.5	5.6	
70°	1.3	3.1		2.2	5.0	
60°	1.1	2.7		1.8	4.2	
50°	1.0	2.2		1.5	3.5	
40°	0.8	1.8	14	1.2	2.8	22

This shows that the scattering in both air and argon is mainly "plural" even for distances of 0.04 cm. Such a result is very surprising in view of the apparent straightness of the tracks themselves, particularly as the number of right-angle bends in a distance of a whole cm has actually been counted by

[26] Plural scattering seems to be the preferred translation of the German "mehrfachstreuung." It is used to denote the intermediate case between single and multiple scattering in which the number of deflections experienced by a single particle is neither one nor large enough so that a Gaussian distribution may be assumed.

C. T. R. Wilson[27] and found to be in good agreement with equation (1). Since Wentzel's criterion for "single" scattering in thin metal foils should apply equally well to scattering in gases, this discrepancy must mean either that in the expansion-chamber experiments only the comparatively straight portions of the tracks are recognized as such, or that because of the appreciable size of the water droplets which make up the tracks many of the bends are obscured. Since the scattering is "plural" even for a distance which is less than the width of the tracks, it is not impossible that a series of droplets which seem to form a perfectly straight track may be due to an electron which actually followed a somewhat zigzag path.[28]

In view of this uncertainty in the interpretation of the experimental results, we shall assume, except where there is unambiguous evidence to the contrary, that the scattering takes place in accordance with equation (1). Furthermore, since in the cases which we shall consider the scattering is "plural" according to Wentzel's criterion, we shall multiply the value of ρ_ϕ obtained from equation (1) by a factor of 2 or 3. This is necessitated by the results of Crowther and Schonland which show that when $\phi/4\omega$ lies between 3 and 1.7 the scattering is between 2 and 3 times that given by equation (1).

b. *Lateral distribution.* Equation (1) was derived for the case of the scattering of a narrow beam of electrons traversing a thin lamina of the scattering material. If the photo-electrons are all ejected in the direction of the electric vector, this equation can be applied directly[29] to the calculation of the lateral distribution on the assumption that it is due entirely to nuclear scattering. The only modification necessary is caused by the fact that in this case electrons will be ejected in both the positive and negative directions of the electric vector and since the cot $\phi/2$ falls to zero at 180° from the direction of emission instead of at 90°, electrons ejected at angles between 90° and 180° will add themselves to those emitted between 90° and 0°

TABLE II. *Lateral spread*

	$\rho_{30°}$	$\rho_{50°}$	$\rho_{70°}$	$\rho_{90°}$	$\rho_{50°}$	$\rho_{40°}$
Observed	1.2%	1.9%	3.2%	5.1%	9.7%	19%
Calculated	1.1%	1.5%				
Calculated×2			4.4%	6.4%	10%	
Calculated×3						23%

[27] C. T. R. Wilson, Proc. Roy. Soc. **A104,** 205 (1923).

[28] Several discrepancies now outstanding between experiment and theory will be explained if the actual path of the electron is appreciably longer than the more or less straight track which envelopes it. Thus both C. T. R. Wilson (Proc. Roy. Soc. **A104,** 195 (1923) and Williams (Nature **119,** 489 (1927) in their expansion-chamber experiments found that the ionization per cm along the track was greater than that given by the theory of J. J. Thompson for the ionization per cm along the electron path. This difference disappears if the actual path length is greater than the distance measured along the track.

[29] There is some uncertainty as to whether the experiments of Bubb and Kirchner give as a function of ϕ the number of tracks which go out through solid angle $2\pi \sin\phi\, d\phi$ or their projection upon the plane normal to the x-ray beam. If the latter, the calculated values of ρ_ϕ will be smaller than those given in Table II.

respectively. If the composite curve of Bubb's and Kirchner's results (Fig. 2) is corrected for this effect and the fractions (ρ_ϕ) of the tracks which start out at angles greater than 90°, 80°, 70°, etc., are determined from the corrected curve the values given in the first row of Table II are obtained. The calculated values are for argon using equation (1) and putting $n=2.7\times10^{19}$, $t=0.04$ cm, $Z=18$, $T=23{,}000$ volts $=77\times4.774\times10^{-10}$ ergs.[30]

The close agreement between the calculated and experimental values shows that scattering in neighboring atoms is sufficient to account for the whole *magnitude* of the spread without unreasonable values of t and T being assumed, and the fair agreement for all values of the angle of scattering between 40° and 90° even when integral multipliers are used proves that the theory also gives the *shape* of the distribution very exactly.

To obtain the same agreement for the distribution in air and CO_2, either larger values of t or smaller values of T must be assumed. It is not necessary to modify either very largely, however, as the molecules of air being diatomic and those of CO_2 being triatomic are nearly as effective in scattering as are the monatomic molecules of argon. That this is the case is shown by some unpublished results of Mr. C. D. Anderson in this laboratory who counted roughly the number of right-angle bends in the first cm of path on the plates of Loughridge and found that 11% of the tracks in air showed such bends and 14% in argon. Moreover since heterogeneous x-rays were used in Bubb's and Kirchner's experiments, the frequencies of the x-rays which were most effective in ejecting electrons were probably different in the various gases. These considerations are sufficient to account for the fact that Kirchner found no difference in the spread for these gases.

c. *Longitudinal distribution.* In the case of the longitudinal distribution equation (1) must be further modified. If we assume that each electron leaves the atom exactly in the direction of the electric vector of the ejecting radiation, then electrons ejected by unpolarized x-rays will start out at random in a plane containing the electric vector and perpendicular to the direction of the x-ray beam. This means that in discussing the longitudinal distribution we must treat the scattering as from a plane instead of from a line. This may easily be done as follows:

Differentiating equation (1) we find that the number of electrons scattered through solid angle $2\pi \sin\phi d\phi$ is

$$\pi nNt(Ze^2/2T)^2 \cot(\phi/2)\,\mathrm{cosec}^2(\phi/2)d\phi \qquad (3)$$

where N is the total number of electrons and ϕ is the angle of scattering

[30] The exact value of T which should be used in this calculation is uncertain, since as has already been said the frequencies of the x-rays which are most effective in ejecting electrons in the experiments of Bubb and Kirchner are not known. The value used here is justified by Kirchner's observation that in his experiments the majority of the tracks were less than 12 mm long (corresponding to a value of T of about 23 kv), even though his x-ray tube was driven at 50–60 kv, and by Loughridge's observation that in argon the tracks were considerably shorter when heterogeneous radiation from a tungsten-target tube driven at 40 kv was used than they were for the zirconium-filtered radiation from a molybdenum-target tube driven at the same voltage (T for molybdenum $K\alpha$ rays $=15$ kv.)

measured from the direction of the electric vector. The number scattered through unit solid angle will therefore be

$$\frac{\pi nNt(Ze^2/2T)^2 \cot(\phi/2)\operatorname{cosec}^2(\phi/2)d\phi}{2\pi \sin\phi d\phi} = nNt\left(\frac{Ze^2}{2T}\right)^2 \frac{1}{(1-\cos\phi)^2}$$

But with unpolarized x-rays the direction of the electric vector will be at random in a plane perpendicular to the direction of the x-ray beam. If then θ represents the angle which any specified direction (in which we wish to calculate the scattering) makes with this plane and ω is the azimuth of that direction measured from the direction of the electric vector, we have

$$\cos\phi = \cos\theta\cos\omega$$

and therefore the number of electrons scattered through unit solid angle at an angle θ to the plane will be

$$\frac{nNt}{2\pi}\left(\frac{Ze^2}{2T}\right)^2 \int_0^{2\pi} \frac{d\omega}{(1-\cos\theta\cos\omega)^2} = nNt\left(\frac{Ze^2}{2T}\right)^2 \frac{1}{\sin^3\theta}$$

and the number scattered through solid angle $2\pi\cos\theta d\theta$ will be given by

$$dN = 2\pi nNt\left(\frac{Ze^2}{2T}\right)^2 \frac{\cos\theta}{\sin^3\theta}d\theta = 2\pi nNt\left(\frac{Ze^2}{2T}\right)^2 \cot\theta\operatorname{cosec}^2\theta d\theta. \tag{4}$$

Integrating we get the fraction scattered at angles equal to or greater than θ to be

$$\rho_\theta = \pi nt(Ze^2/2T)^2 \cot^2\theta \tag{5}$$

The distribution in this case is therefore a function of the whole-angle instead of the half-angle as in the case of the lateral distribution. The coefficient $\pi nt(Ze^2/2T)^2$ is moreover the same as that in equation (1) and therefore, since $\cot\theta$ is always less than $\cot(\theta/2)$, the spread of the longitudinal distribution will be less than that of the lateral under similar experimental conditions.[31]

It is possible also to choose reasonable values of t and T such that equation (5) will give quantitatively both the magnitude and shape of the longitudinal

[31] Since the most probable direction of ejection of the electrons is not exactly in the plane of the electric vector, but instead is a little forward of it, we should have treated instead of scattering from a plane, scattering from the surface of a cone whose axis is the direction of the x-ray beam and whose semi-angle is a little less than 90°, the exact angle depending upon the frequency of the incident x-rays. A treatment of this case, similar to that given above for the case of scattering from a plane, leads to the equation

$$dN = \frac{\pi}{2} nNt\left(\frac{Ze^2}{2T}\right)^2\left[\frac{1}{\sin^2(\alpha+\beta)/2} + \frac{1}{\sin^2(\alpha-\beta)/2}\right]\frac{\sin\alpha\, d\alpha}{\cos\beta - \cos\alpha}$$

where α is the angle of scattering measured now from the forward direction of the x-ray beam and β is the semi-angle of the cone. This equation reduces to equation (3) when $\beta=0$ and to equation (4) when $\beta=90°$ as it should. In the experimental work to be discussed, however, β is in all cases close to 90° and consequently equation (5) gives the spread with sufficient accuracy.

spread. Thus in Table IIIA the experimental values of ρ_θ obtained by Loughridge for electrons ejected in argon by the $K\alpha$ rays of molybdenum are compared with corresponding values calculated from equation (5) putting $n=2.7\times10^{19}$, $t=0.04$ cm, $Z=18$, and $T=14.1$ kv. Similarly, in Table IIIB the spreads obtained from curve I of Fig. 1 are compared with values obtained from equation (5) when $n=2.7\times10^{19}$, $t=0.08$ cm, $Z=8$, and $T=12$ kv; and Table IIIC compares values obtained from cuve II of Fig. 1 with those calculated for 15 kv electrons in oxygen.[32]

TABLE III. *Longitudinal spread.*

	$\rho_{90°}$	$\rho_{80°}$	$\rho_{70°}$	$\rho_{30°}$	$\rho_{50°}$	$\rho_{10°}$
	A. 14 kv electrons in argon (Loughridge)					
Observed	0%	0.15%	0.8%	2.2%	5.6%	12%
Calculated×2	0%	0.18%	0.75%	1.9%		
Calculated×3					6.0%	12%
	B. 12 kv electrons in oxygen (Auger I.)					
Observed	0%	0.08%	0.65%	2.3%	6.3%	13.5%
Calculated	0%	0.09%				
Calculated×2			0.8%	2.0%		
Calculated×3					6.6%	13.2%
	C. 15 kv electrons in oxygen (Auger II.)					
Observed	0%	0%	0.1%	1.0%	3.8%	9.4%
Calculated	0%	0.06%	0.26%			
Calculated×2				1.3%		
Calculated×3					4.2%	8.4%

The factors 2 and 3 are introduced only where Wentzel's criterion and the experimental results of Crowther and Schonland indicate that they should be. The improvement in the agreement between theory and experiment which is brought about by their use is a further argument that the scattering is "plural." If however the introduction of these factors is objected to on the ground that Wentzel's criterion cannot be applied in gases and that C. T. R. Wilson's count of the number of right-angle bends along the tracks was sufficiently accurate to show that the scattering is "single," the theory of nuclear scattering can still be made to fit fairly well (quite well in the case of argon) by choosing larger values of t and smaller values of T which are still consistent with the experimental facts.

Finally the variations in the amount of the spread with the frequency of the incident x-rays and the nature of the gas, which Bothe[33] and Auger found, take place in the way demanded by the coefficient $\pi nt(Ze^2/2T)^2$. Thus curves I and II of Fig. 1 show that when the voltage on the x-ray tube is raised from 15 to 20 kv, other conditions remaining the same, the spread decreases in the way required by the theory. Again if curves III and IV are compared it is seen that when argon is replaced by xenon, the voltage being kept constant, the curve broadens as it should. That the effect is not larger is probably due

[32] The exact values of T to be used in these last two cases are again uncertain. The values used (12 kv and 15 kv) are for reasons already given (see footnote 30) less than the voltages actually applied to the x-ray tube.

[33] According to Wentzel's criterion the scattering was also "plural" in the experiments of Bothe except at large angles.

to the fact that only small quantities of argon and xenon were introduced, the gas in the expansion-chamber being principally hydrogen. The same effect is shown by a comparison of curves II and V. The fact that Loughridge found no difference between the spread in air and in argon has already been explained in the discussion of the lateral distribution. That the variations with voltage are not larger may be due to the effect of the relativity correction to which reference has already been made. It is more probable, however, that even when the voltage on the x-ray tube is high the majority of the electrons are ejected by x-rays of low energy because their absorbability is so much greater. Experiments of the sort made by Nuttall and Williams with strictly monochromatic x-rays will be necessary to settle this point.

One apparently serious difficulty for the theory still remains, however. Loughridge found the spread in hydrogen only a little less than in argon and the theory of nuclear scattering here given demands that it be several hundred times less. This is too great a discrepancy to be accounted for by simple inadequacy in the number of tracks counted. It can only mean that either the theory is wrong or the scattering in hydrogen is actually much greater than that predicted by the classical theory. Fortunately the order of magnitude of the scattering in hydrogen can be ascertained independently of the space-distribution by studying the sharp bends in the tracks themselves and Dr. Loughridge very kindly allowed Mr. Anderson to count the number of tracks on his plates which showed sharp bends of 90° or more within the first cm of their range. In hydrogen 18 out of 190 tracks (9.5%) showed such bends, while in argon only 12 out of 85 (14%) did so. This means that the nuclear scattering in hydrogen is actually only a little less than it is in argon, and consequently it is quite sufficient to account for the observed space-distribution. The difficulty thus turns out to be an argument for, rather than against, the theory here presented.

The fact that the nuclear scattering in hydrogen is actually many times greater than was predicted by the theory probably means that the inverse-square law of force between the nucleus and the electron breaks down when the distance of approach becomes sufficiently small. A similar effect was found by Rutherford[34] and Chadwick and Bieler[35] in the case of close collisions between α-particles and hydrogen nuclei. This is, however, so far as the writer knows, the first time such an effect has been observed for collision between electrons and nuclei and a further study of it would seem to offer further possibilities for determining the exact limits of the inverse-square law and perhaps also of studying the structure of the electron and proton, or of determining their magnetic moments.[36]

IV. Scattering in Getting Out of the Parent-Atom

An elementary calculation of the probability of an electron having its direction changed in getting out of the parent-atom, based upon the assump-

[34] E. Rutherford, Phil. Mag. **37**, 537 (1919).
[35] J. Chadwick and E. S. Bieler, Phil. Mag. **42**, 923 (1921).
[36] See in this connection E. Rutherford and J. Chadwick, Phil. Mag. **4**, 605 (1927).

tions (1) that the impulse received by the electron is sensibly instantaneous, (2) that the field of the nucleus of the parent-atom acts upon the electron in exactly the same way as do the fields of the nuclei of neighboring atoms through which it passes, (3) that the electron originates in a circular Bohr orbit whose radius is given by the simple Bohr theory, and (4) that the orientation of the electron with respect to the nucleus at the moment of ejection is a random one, leads to the following approximate formula, when the absorption frequency ν_0 of the electron in the atom is small compared with the frequency ν of the ejecting x-ray, namely

$$\rho_\phi = (\nu_0/4\nu) \cot^2 (\phi/2) \tag{6}$$

where ρ_ϕ is as before the fraction of a large number of electrons which will have their direction changed by an amount equal to or greater than ϕ. This equation is of the same form as that for the scattering in neighboring atoms, but the amount of the spread given by it is, in the case of the lighter atoms, much smaller than that already considered. In the case of argon and the $K\alpha$ rays of molybdenum, however, ρ_{40° comes out about 6%, which would have to be taken into account if the effect were a real one. However, in the neighborhood of an absorption edge, i.e. when ν_0 is only a little less than ν, this scattering in getting out of the atom should be large. The results of Auger show that such is not the case. This may mean that a particular orientation of the atom with respect to the direction of the ejecting x-ray is necessary for photo-electric ejection, or that the ejection is always radial, but the theoretical considerations involved are too uncertain to warrant any definite interpretations.

V. Summary and Conclusion

The results of this investigation may be summarized as follows: The Rutherford theory of nuclear scattering together with the assumption that the electrons all start out from the parent-atom in the same direction can be made to account satisfactorily for all the details of the observed space-distribution of the photo-electrons ejected by x-rays. It gives the amount of the spread quantitatively; it gives the form of the distribution curves; it explains the difference between the lateral and longitudinal distributions both as regards the amount of the spread and as regards the falling of the curves to zero; it explains the dependence of the amount of the spread upon the nature of the atoms from which the electrons are ejected and the frequency of the x-rays which do the ejecting; and it accounts for the disagreement among the various observers regarding this dependence.

We conclude therefore that the reality of the space-distribution has not been established and that probably all the photo-electrons ejected by x-rays of a given frequency from the same kind of atom are ejected in one and the same direction with respect to the electric vector.

It should be stated, however, that while nuclear scattering thus seems *adequate* to account for the whole of the space-distribution, it is not necessarily the only effect which is present. If the experimental curves should on

further investigation turn out to be actually not more sharp than a cosine-square curve (and the experiments are probably as yet neither complete nor accurate enough to be sure that this is not the case) the cosine-square distribution *plus nuclear scattering* would also be satisfactory in explaining the facts; for the effect of even a large amount of scattering upon a cosine-square distribution is small except at 90°, but would be large enough to explain both the failure of the curves of the lateral distribution to fall to zero and the dependence of the spread upon the nature of the gas and the frequency of the x-rays. In any case nuclear scattering will be present and must be taken into account.

VI. Acknowledgments

This paper would have been impossible if the writer had not had free access to the important experimental results of Dr. D. H. Loughridge and Mr. C. D. Anderson before they were published and he desires to express his sincere thanks to them both for putting these results completely at his disposal and for freely discussing with him many of the details of the work. The constructive criticism of Dr. I. S. Bowen also played an important part in the paper and the writer gratefully acknowledges his help.

Norman Bridge Laboratory of Physics,
California Institute of Technology,
Pasadena, California.

Note added in proof: Since the manuscript of this paper was sent to the Editors, the arguments against scattering's having any appreciable effect upon the space-distribution have been published by Kirchner [Ann. d. Physik, **84,** 899, (1927)]. As all these arguments have already been discussed only two remarks are called for: (1) The writer still holds that scattering is *adequate* to account for the whole of the space-distribution observed by Bubb, Kirchner, Auger, and Loughridge. This is best shown in the calculations based upon the results of Loughridge in which none of the factors entering into the calculation except t is uncertain and a very conservative value for it is used. Moreover, in the case of Kirchner's own published results, if the relatively large number of tracks which appear to start out at nearly 90° from the direction of the electric vector or if the departures from the cosine-square distribution which he observes in his most recent work [Ann. d. Physik, **83,** 521 (1927)] are to be explained as due to nuclear scattering—and there seems to be no other explanation—then the scattering is adequate to account for the whole of the distribution, for the reason given in the next to last paragraph of this paper. (2) While the distribution curves used by the writer may be statistically less accurate than the corresponding integral curves plotted by Kirchner, they are also far more sensitive than the integral curves. Thus, on the scale which Kirchner uses, a cosine-cube curve can scarcely be distinguished from a cosine-square curve. That the variations shown by the differential curves are real is argued by the fact that they are systematic and by the results of Bothe and Seitz.

This paper is frankly an attempt to push the scattering idea as far as possible. If Williams [Nature, **121,** 134 (1928)] has succeeded in completely eliminating its effect from his results, the arguments here presented are still of value in explaining the variations observed by others and in focusing attention sharply upon the ambiguities in the expansion-chamber results.

THE K ABSORPTION EDGES OF POTASSIUM AND CHLORINE IN VARIOUS COMPOUNDS

By J. M. Nuttall

Abstract

The K absorption edges of potassium and of chlorine were photographed by means of a vacuum spectrometer of the type designed by Siegbahn. Four compounds were used for the absorption of potassium; namely, sylvine, orthoclase, lepidomelane, and phlogopite. In the first two, the absorption occurred in the reflecting crystal itself; in the last two, in thin sheets of the substance placed in the path of the beam which was dispersed by a calcite crystal. The chlorine of the sylvine also gave an excellent Cl K absorption edge. In these photographs as many as five secondary edges were observed. The fine structure of the potassium edge thus extended in wave-lengths from 3429 to 3365 x.u, or over a range of about 67 volts. The fine structure of the chlorine edge extended from $\lambda = 4383$ x.u. to $\lambda = 4341$ x.u., or about 27 volts. That portion of the fine structure which is more remote from the principal edge is not satisfactorily explained by Kossel's original hypothesis, and is perhaps best accounted for by double ionization of the atoms absorbing the x-radiation.

IT IS now well known from the work of Bergengren[1], Lindh[2], Fricke[3] and others that the wave-length of the x-ray absorption edge of an element depends on the chemical compound in which the absorption occurs. The main feature of the results of these observers is that the position of the absorption edge varies with the valence of the atom, the longest wave-length being associated with the lowest valence. The absorption edge for the pure element has the longest wave-length of all.

In addition to this shifting of the principal absorption edge, a certain amount of fine structure is observed on the short wave-length side of that edge, i.e., there are secondary effects represented by white lines and dark lines which may be looked upon as edges of greater frequency than that of the principal edge. This fine structure has been observed by Lindh[2] and Fricke[3] in the edges of the lighter elements, and by Nishina[4] in the L edges of the heavier elements.

The difficulty of experimentally observing the fine structure lies largely in the preparation of absorbing screens of suitable or optimum thickness. The general evidence would appear to show that if the screen is too thick, then the fine structure is not observed. There is one method of avoiding the difficulty of preparing suitable absorbing screens, viz., the use of a reflecting crystal which itself contains the element whose absorption edge is required. This method is necessarily limited in its application to the cases where a crystal can be found with a suitable lattice constant for investigation of the

[1] Bergengren, Zeits. f. Physik **3,** p. 247 (1920).
[2] Lindh, Dissertation, Lund. 1923.
[3] Fricke, Phys. Rev. **16,** 202 (1920).
[4] Nishina, Phil. Mag. **49,** 521 (1925).

desired region. Lindsay and Van Dyke[5] have used this method to investigate the *K* absorption edge of calcium in the crystals calcite, gypsum, and fluorite. In all cases their observations revealed a much more complicated fine structure than that found by previous observers. This has been confirmed by the present investigation of the *K* edges of potassium and chlorine in various compounds. The photographs were taken with an x-ray vacuum spectrograph of the Siegbahn type in which the crystal-plate distance was 182.2 mm. The x-ray tube was evacuated by a mercury diffusion pump preceded by an oil pump. A piece of thin gold beater's skin covered the slit, and separated the x-ray tube from the camera chamber which was evacuated by the oil pump alone. The voltage applied to the tube was supplied by a transformer and was in general regulated so as to prevent the excitation of second order emission lines in the region under investigation.

The average time of exposure was about five hours with a current of approximately 20 m.a. through the tube. The *K* absorption edge of potassium has been examined in the crystals sylvine (KCl) lepidomelane $(K, H)_2 (Mg, Fe)_2 (Al, Fe)_2 (SiO_4)_3$, phlogopite $(K, H)_3Mg_3Al(SiO_4)_3$ and orthoclase $(KSiO_4)$.

In the case of sylvine the dispersion was 14.59 x.u. per mm on the plate, and the position of the principal edge could easily be fixed within 1/10 mm, so that the error in the determination of this edge was about one x.u. The secondary edges in the fine structure are much fainter and could not be determined so accurately as the principal edge, but the probable error was not greater than 2 x.u. As the dispersion in the crystals lepidomelane and phlogopite was about 55 x.u./mm, the fine structure was crowded close to the principal edge and on account of the poor resolution, it was difficult to measure accurately the positions of the secondary edges. Both these crystals, however, are micas and can readily be split into thin uniform sheets a few hundredths of a mm in thickness. Therefore, in the cases of these two crystals the photographs were taken with thin absorbing screens and with *calcite* as the reflecting crystal. The dispersion in the neighborhood of the *K* edge of potassium with a calcite crystal was 13.7 x.u./mm, so that the resolution was about the same as in the case of sylvine and approximately the same order of accuracy was obtained in determining the edges.

In the measurements with orthoclase the absorption was in the reflecting crystal itself and the dispersion (33.7 x.u./mm) did not allow such an accurate determination of the fine structure as in the previous cases.

Throughout the work the $K\beta$ line of potassium was photographed on the plates as a reference line. In all cases the photographs of the *K* edge of potassium show a fine structure which is somewhat similar to that found by Lindsay and Van Dyke in the case of calcium. The main features of the potassium *K* edge as shown by the photographs (See Figs. 1, 2, 3) are as follows. First, a strong principal edge *A*—then an edge *B* so close to the principal edge that its position is only fixed with some difficulty. These are followed by edges *C*, *D*, *E*, which owing to their spacing are not difficult to

[5] Lindsay and Van Dyke, Phys. Rev. **28**, 613 (1926).

fix in lepidomelane and phlogopite, though in the case of sylvine I was unable to locate edge *D*. Succeeding these edges comes a region of more or less uniform blackening on the plate in which it is difficult to see any fine structure then finally a very weak absorption edge *F* which I have attempted to mea-

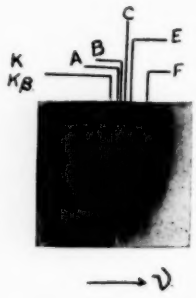

Fig. 1. Fine structure of *K* absorption edge of potassium from sylvine crystal.

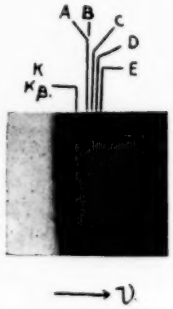

Fig. 2. Fine structure of *K* absorption edge of potassium from lepidomelane.

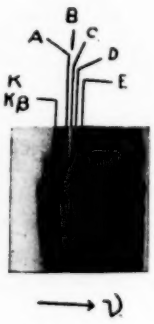

Fig. 3. Fine structure of *K* absorption edge of potassium from phlogopite.

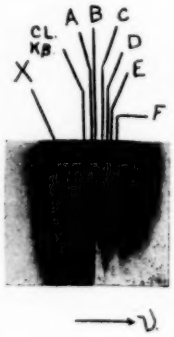

Fig. 4. Fine structure of *K* absorption edge of chlorine from sylvine crystal.

sure on most plates. These main features of the photographs were confirmed by photometer records taken with a Moll microphotometer. Table I gives

TABLE I. *Wave-lengths of absorption edges of potassium in various compounds*

Edge	Sylvine	Lepidomelane	Phlogopite	Orthoclase
A	3429.0 *x. u.*	3426.6 *x. u.*	3426.8 *x. u.*	3427.5 *x. u.*
B	3424.3	3423.6	3424.1	—
C	3414.1	3415.9	3414.6	3414.0
D	—	3408.8	3408.4	—
E	3402.7	3401.7	3401.9	3401.3
F (weak)	3366.0	3363.0	3365.0	3372.0?

the wave-lengths of the absorption edges in the different crystals, and Table II the separation in volts between the principal edge and the various secondary edges.

TABLE II. *Separation (in volts) principal edge—secondary edges*

Edges	Sylvine	Lepidomelane	Phlogopite	Orthoclase
A−*B*	4.9 volts	3.2 volts	2.8 volts	— volts
A−*C*	15.6	11.3	12.8	14.2
A−*D*	—	18.9	19.5	—
A−*E*	27.8	26.4	26.4	27.7
A−*F*	67.4	67.7	65.7	59.2

The figures of Table I show that there is a marked similarity in the fine structure in the different crystals. The edge *D* could be distinctly seen in the

photographs with lepidomelane and phlogopite but not in the case of sylvine. Edge F was weak in all the photographs.

The K absorption edge of chlorine was examined in the sylvine crystal and the fine structure was most marked in all the photographs (See Fig. 4). Rocksalt was the only other crystal containing chlorine which was examined but here unfortunately the photographs were indistinct and were not measured. Lack of time prevented any further examination of the chlorine edge.

The results for chlorine are given in Table III with the corresponding separations of secondary edge from principal edge. The fine structure extended beyond edge F (to approximately 50 volts) but was faint and was not measured.

TABLE III. *Wave-lengths of absorption edges of Cl in sylvine.*

A	B	C	D	E	F
4383.2	4377.0	4366.3	4359.3	4353.5	4341.4 x.u.
	$A \rightarrow B$	$A \rightarrow C$	$A \rightarrow D$	$A \rightarrow E$	$A \rightarrow F$
	4.0	10.9	15.5	19.2	27.3 volts

Lindh[2] has examined the K edge of chlorine in a number of compounds but in no case did he obtain so complicated a structure as that given above. His observations were made with different compounds in which the chlorine had a valence of one, five, or seven.

A remarkable feature of all the photographs of the chlorine edge in the author's experiments with sylvine was the presence of a white line absorption band at approximately 4444 x.u. This is apparently the same phenomenon which has been observed by Berg,[6] and explained by him as being due to the simultaneous reflection of that wave-length from two or more sets of planes in the crystal. The wave-length found for this white line (Fig. 4) was 4444 x.u. For the sylvine crystal the corresponding glancing angle θ is $45° - 0'$. This is an excellent confirmation of Berg's theory, for in the case of a cubic crystal, we should have a strong reflection at $\theta = 45°$ from the set of planes at right angles to the surface being used as the reflector. The angle for this set of planes would then also be 45°; thus the (100) planes and the (010) planes would share about equally in the reflection of this particular wave-length and at the position in the continuous spectrum corresponding to $\lambda = 4444$ x.u. we should have about 1/2 the intensity of adjacent positions. This would result in the white line shown at x (Fig. 4).

It is evident from the results of the foregoing experiments that the structure of these K absorption edges is very complicated. The first possible explanation to account for the fine structure is due to a suggestion originally put forward by Kossel[7] that the ejected electron may possibly stop in the various unoccupied or virtual orbits of the outer part of the atom. On this view the frequency of the principal K absorption edge corresponds to the energy required to remove a K electron to the surface of the atom or to the

[6] Otto Berg, Wiss. Veröff. aus dem Siemans-Konzern, Vol. V, p. 89.
[7] Kossel, Zeits. f. Physik **1**, 119 (1920).

first occupied orbit, and the limiting frequency of the fine structure is the energy corresponding to the work of removal of an electron entirely from the influence of the atom. Between these two frequencies separated by a small quantity $\delta\nu$ we have the whole of the fine structure corresponding to the ejected electron stopping in various virtual orbits. In this event one would expect that the frequency differences between the secondary absorption edges would become less as we moved away from the principal edge. Moreover the extreme difference in energy from principal edge to the limit of the fine structure should correspond (in the case of these experiments) to the work of removal of an electron from the valence orbit of a potassium ion. Assuming that the potassium ion has for the moment had one of its K electrons removed to the valence orbit, then the *additional* energy required to completely remove that electron will be somewhat similar to the energy required to remove an outer electron from a Ca^+ ion. In other words, the energy is comparable with the 2nd ionizing potential of calcium which is known to be 11.8 volts. However, the fine structure certainly extends beyond this point to at least 27 volts and probably to over 60 volts. The suggestion by Kossel may account for the first part of the fine structure, say up to and including edge C (mean value 13 volts) but could hardly account for the full extent observed in these experiments. The second possible explanation is to assume that the fine structure arises from some form of multiple ionization. This means that the same quantum of incident x-radiation ejects not only a K electron but also another electron, say one from the M shell. Clearly a quantum of primary radiation which produced such double ionization would lose additional energy and a secondary absorption edge would be produced. Assuming such a process did occur, then we must conclude that the chance of double ionization by a quantum is much less than that of single ionization of the K shell alone since the secondary edges are not so strong as the principal edge. Coster[8] has considered the possibility of double ionization and made observations on the K absorption of argon with negative results. He obtained a secondary edge very *close* to the principal edge and concluded that double ionization was improbable. On the other hand, Wenzel[9] has assumed the occurrence of double ionization to account for the so-called non diagram or spark lines in x-ray emission spectra. In the case of the present experiments it is extremely difficult to test the theory of double ionization, owing to an absence of data of M energies in the required region. Further, if we had the necessary data, uncertainty arises in the calculation of the energy required simultaneously to remove the two electrons. Assuming that the fine structure is in part due to double ionization of the KM type, then following the scheme proposed by Wenzel, the energy difference between the principal edge and a secondary edge should correspond to the energy required to remove an M electron from an atom of next higher atomic number—in the present case, a calcium atom. As emphasized above, we have no knowledge of M levels of calcium but the

[8] Coster and van der Tuuk, Zeits. f. Physik **37,** 367 (1926).

[9] Wenzel, Ann. d. Physik **66,** 437 (1921); **73,** 647 (1924).

mean difference obtained in the present observations between the main edge of potassium A and the secondary edge E, about 27 volts, is probably of about the right order.

In the case of the K edge of chlorine in sylvine, it seems reasonable to suppose that it would require less energy to remove an electron from a Cl^- ion than that required to ionize a neutral argon atom (15.4 volts). In other words, 15.4 volts represents the limit of the fine structure of the Cl edge on the Kossel assumption of the ejected electron stopping in an outer unoccupied orbit. Again the observations show that the fine structure in this case extends beyond this point and perhaps represents some form of double (KM) ionization.

It has been shown that the structure of the K absorption edges of potassium and chlorine in various crystals is of a complicated nature and it would seem that the theory of the ejected electrons stopping in an outer orbit is inadequate fully to explain the nature of the edges.

In conclusion, I should like to express my thanks to Professor H. M. Randall for providing the facilities for the research which was carried out at the University of Michigan, Ann Arbor, and also to Dr. G. A. Lindsay for much helpful advice during the progress of the work.

MANCHESTER, ENGLAND,
December, 1927.

THE APPLICATION OF THE X-RAY LAWS TO OPTICAL SPECTRA OF HIGHER RANK, AND THE CLASSIFICATION OF GA IV AND GE V

By J. E. Mack, Otto Laporte, and R. J. Lang

Abstract

Spectra of Ga IV and Ge V.—By application of the Moseley law and the two doublet laws of x-ray spectroscopy, the ($3d^9 4s$) and ($3d^9 4p$) levels of Ga IV and Ge V and a tentative ($3d^{10}$) level for Ga IV, have been found. The levels formerly classified as $^3D_1$, $^1P_1(3d^9 4p)$ of Zn III have been interchanged.

Correlation of inverted multiplet levels to series limits.—On the hypothesis that as the nuclear charge increases the levels of an isoelectronic sequence tend to cluster relatively into groups forecasting the next higher ion due to a transition from *ls*- to *jj*-coupling, evidence is adduced to show that of the ^3D, $^1D(d^9 s)$, the $^3D_3$ level approaches the limit $^2D_3(d^9)$, contrary to the theory of Hund. The case is analogous to that of Ne, in whose empirical series $^3P_1(2p^5 3s)$ approaches $^3P_2(2p^5)$.

Distinctions between x-ray and optical spectra, in application of the x-ray laws.—(1) Exact representation of isoelectronic optical spectra on a Moseley diagram generally requires knowledge of series limit correlations of individual levels; the problem is close to that of general term-representation. (2) X-ray energy levels are ionization energies of neutral atoms, whereas in isoelectronic spectra the net charge increases with the atomic number Z; the first order screening number σ_1 increases with Z in x-ray spectra, but decreases to an asymptote in isoelectronic spectra. The difference might be explained by outer screening.

Shape of the σ_1 curve for isoelectronic spectra.—If σ_1 is plotted as a function of Z, the initial slope of the curve depends upon the n- and l-values of the added electron but changes only slowly with the total number of electrons, and substantially not at all with the ion configuration for a given number of electrons; this rule implies that the lines on the Moseley diagram, representing the addition of a given n_l electron to different isoelectronic sequences containing nearly the same number of electrons, are parallel, to a second approximation.

The irregular doublet law applied to isoelectronic sequences in the neighborhood of a closed d-shell (d^{10}), is valid for $(p)^{1/2}-(s)^{1/2}$ but not for $(d)^{1/2}-(p)^{1/2}$ or $(f)^{1/2}-(d)^{1/2}$.

I. Introduction

THE work of Millikan and Bowen[1] extended the application of the following three laws of x-ray spectra into the field of optical spectroscopy:

The Moseley law[2]

$$\nu^{1/2} = \text{a linear function of } Z \tag{1}$$

where ν is the energy value of a level referred to the next higher ion, and Z is the atomic number.

The Sommerfeld law of regular or relativistic doublets[2]

$$\Delta\nu = \frac{\alpha^2 R(Z-\sigma_2)^4}{n^3 l(l+1)} \tag{2}$$

[1] R. A. Millikan and I. S. Bowen, many papers, especially in Phys. Rev., 1924–1927.

[2] The higher degree terms in α^2 that enter into the exact infinite series expressions are extremely small in optical spectra and are omitted in Eqs. (1) to (3).

between two levels of equal n and equal l but different j; where α and R are universal constants and σ_2 is independent of Z.

The irregular or screening doublet law[2] of Hertz

$$\Delta(\nu^{1/2}) \text{ is independent of } Z \tag{3a}$$

or

$$\Delta\nu = \text{a linear function of } Z \tag{3b}$$

between two levels of equal n but different l.

Since the early work of Millikan and Bowen, these laws have been used extensively in the classification of optical spectra, and the doublet laws have been extended in some cases to apply to terms of higher multiplicity. In the first long period, in particular, Gibbs and White[3] and Russell[4] and Lang have applied them to the frequencies of the lines of combination between low terms in systems of several electrons, especially in the first part of the period.* Laporte and Lang[5] have applied them at the other end of the period in the classification of Zn III, by extrapolation from the classifications of the spectra of Ni I[6] and Cu II.[7] In this paper it is shown that these laws may still be used most succesfully in cases where the spectra are of higher rank, i.e., lacking that multiplet structure characteristic of "normal" spectra. They are applied to higher spark spectra at the end of the iron group, isoelectronic with Ni I; namely to Ga IV and Ge V.

While the x-ray laws are used in this investigation in the simple forms expressed in Eqs. (1) to (3), it is shown in Chapter VIII that it is impossible to apply them in general to the optical region, except in the first approximation; and the distinctions between the x-ray region and the optical region from the viewpoint of the applicability of these laws, are examined.

The ten-electron systems are an especially appropriate subject for investigation of higher coupling, since, being at the end of a period, they are a true analogue of neon, the first spectrum where the breakdown of the Russell-Saunders coupling was noticed and other coupling schemes were tested. The similarity between the energy diagrams of the spectra under consideration here, and that of neon, is discussed in Chapter VII.

II. Experimental Procedure

The vacuum-spark between electrodes of pure metallic germanium and aluminum cored with pure metallic gallium was photographed on the two-meter grating as previously described for zinc.[5] The aluminum was of exceptional purity; it was generously supplied by the research department of the Aluminum Company of America.

* See note added to proof, at the end of the paper.

[3] R. C. Gibbs and H. E. White, Natl. Acad. Sci. Proc. **13**, 525 (1927).

[4] H. N. Russell and R. J. Lang, Astroph. Jour. **66**, 13 (1927); H. N. Russell, Astroph. Jour., **66**, 233 (1927); **66**, 347 (1927).

[5] O. Laporte and R. J. Lang, Phys. Rev. **30**, 378 (1927).

[6] K. Bechert and L. A. Sommer, Ann. d. Physik **77**, 351 (1925); K. Bechert, Ann. d. Physik **77**, 537 (1925).

[7] A. G. Shenstone, Phys. Rev. **29**, 380 (1927).

The source of excitation was a large x-ray coil, the primary of which was joined, through suitable resistance, to the 110-volt A.C. 60 cycle mains. To the secondary of the coil two spark-gaps were joined in series, one in vacuum and the other in air. The latter was between brass spheres about one cm in diameter and the gap width varied between one and two cms. Across this circuit, in parallel with the secondary of the coil, sufficient capacity in the form of glass plate condensers was used to give an approximately resonant circuit.

TABLE I. *Classification of lines of Ga IV (see footnote 12).*

$(3d^24p)$ / $(3d^24s)$	$^3D_3$ 0		$^3D_2$ 1455		$^3D_1$ 3575		$^1D_2$ 6512	
	1455		*2120*		*2937*			
$^3P_2$ 74730	74730	(15)	73281	(1)	71146	(0)	68216	(1)
	0		6		−9		−2	
3081								
$^3P_1$ 77811			76356	(9)	74239	(3)	71291	(2)
			0		3		−8	
1820								
$^3P_0$ 79631					76056	(5)		
					0			
−187								
$^3F_4$ 79444	79444	(15)						
	0							
−1271								
$^3F_3$ 78172	78172	(10)	76718	(15)			71658	(4)
	0		1				−2	
2358								
$^3F_2$ 80530	80533	(1)	79076	(10)	76954	(15)	74018	(0)
	3		1		−1		0	
3148								
$^3D_3$ 83678	83678	(10)	82224	(00)			77166	(15)
	0		1				0	
636								
$^3D_2$ 84314	84313	(0)	82857	(10)	80740	(5)	77804	(12)
	−1		−2		1		2	
3080								
$^3D_1$ 87394			85938	(3)	83820	(9)	80881	(3)
			−1		1		−1	
−1968								
$^1F_3$ 85426	85427	(10)	83970	(9)			78920	(18-Ga III)
	1		−1				4	
1375								
$^1P_1$ 86801			85344	(0)	83225	(4)	80289	(12)
			−2		−1		0	
1144								
$^1D_2$ 87945	87947	(1)	86489	(5)	84370	(8)	81434	(10)
	2		−1		0		1	

Very considerable difficulty had been encountered in the past in getting intense spectrograms owing to a fogging effect in the vacuum chamber which caused the Schumann plates to blacken uniformly over the whole film surface very shortly after being placed in the developer. That this was not due to stray light was evident at once because of the absence of shadows. It was therefore attributed to fluorescence of the residual gases in the vacuum chamber, to ions formed from the gases in the vacuum chamber, or to ions formed from the gases in the spark. Following the advice of Dr. I. S.

Bowen, an attempt was made to obtain a higher vacuum. This was done by covering the end castings of the instrument with heavy coats of enamel paint and attaching an all metal "Kaye" diffusion pump to the main body of the spectrograph. These changes resulted in a great improvement in the intensity and contrast of the plates. The absence of a supply of liquid air has been a very great handicap in the successful operation of the instruments.

TABLE II. *Wave-length list of Ga IV (see footnote 12).*

Weinberg		Carroll		This investigation			
λ vac. I. A.	Int.	λ vac. I. A.	Int.	λ vac. I. A.	Int.	ν	desgination $(d^3s)-(d^3p)$
1465.7	4	1466.0	1	1465.93	1	68216	$^1D_2-{}^1P_1$
				1405.55	0	71146	$^3D_1-{}^3P_2$
		1402.88	3	1402.70	2	71291	$^1D_2-{}^3P_1$
		1395.58	3	1395.51	4	71658	$^1D_2-{}^3F_3$
		1364.73	3	1364.60	1	73281	$^3D_2-{}^3P_2$
		1351.2	2	1351.03	2	74018	$^1D_2-{}^3F_2$
		1347.09	3	1346.99	3	74239	$^3D_1-{}^3P_1$
1338.0	8	1338.15	6	1338.15	15	74730	$^3D_3-{}^3P_2$
1314.8	6	1314.86	4	1314.81	5	76056	$^3D_1-{}^3P_0$
1309.7	9	1309.73	5	1309.65	10	76356	$^3D_2-{}^3P_1$
1303.5	11	1303.56	6δ	1303.48	15	76718	$^3D_3-{}^3F_3$
1299.5	9	1299.49	6	1299.48	15	76954	$^3D_1-{}^3F_2$
1295.9	10	1295.91	6	1295.90	15	77166	$^1D_2-{}^3F_3$
1285.2	9	1285.39	5	1285.28	12	77804	$^1D_2-{}^3D_3$
1279.2	9	1279.30	5	1279.23	10	78172	$^3D_2-{}^3F_3$
1267.0	9	1267.19	6	1267.11	18a	78920	$^1D_2-{}^1F_3$
1264.5	8	1264.64	4	1264.60	10	79076	$^3D_2-{}^3F_2$
1258.8	10	1258.81	7	1258.75	15	79444	$^3D_3-{}^3F_4$
1245.4	7	1245.56	4	1245.50	12	80289	$^1D_2-{}^1P_1$
		1241.6	0	1241.73	1	80533	$^3D_3-{}^3F_3$
1238.4	7	1238.58	3	1238.54	5	80740	$^3D_1-{}^3D_2$
		1236.40	3	1236.38	3	80881	$^1D_2-{}^3D_1$
1228.0	9	1228.01	6	1227.98	10	81434	$^1D_2-{}^1D_2$
				1216.19	00	82224	$^3D_2-{}^3D_2$
		1206.9	4δ	1206.89	10	82857	$^3D_2-{}^3D_2$
1201.4	7	1201.55	3	1201.56	4	83225	$^3D_1-{}^1P_1$
1195.0	8	1195.02	4	1195.05	10	83678	$^3D_3-{}^3D_3$
1192.9	8	1192.99	4	1193.02	9	83820	$^3D_1-{}^3D_1$
1190.7	7	1190.81	4	1190.90	9	83970	$^3D_2-{}^1F_3$
				1186.06	0	84313	$^3D_2-{}^3D_2$
		1185.20	4	1185.25	8	84370	$^3D_1-{}^1D_2$
				1171.73	0	85344	$^3D_2-{}^1P_1$
1170.3	13	1170.57	5	1170.59	10	85427	$^3D_3-{}^1F_3$
1163.4	9	1163.58	4	1163.63	3	85938	$^3D_2-{}^3D_1$
1156.0	10	1156.3	4δ	1156.21	5	86489	$^3D_2-{}^1D_2$
1136.9	8	1136.99	2	1137.05	1	87947	$^3D_2-{}^1D_2$

δ Diffuse.
a Also classified in Ga III: $4^3P_1-4^3D_2$.

The degree of ionization attained by the metallic atoms in the source depends on many factors; one of the most important, after the actual potential of the coil, is the width of the spark-gaps, especially the external gap. In spite of the fact that the potential attained is estimated to be between 50,000 and 100,000 volts it was found impossible with the present apparatus to excite the spectrum of Ge V. This failure was perhaps the more unex-

pected owing to the fact that the lines of the less-ionized Ge spectra seem to be rather more easily excited than one might expect. For example, several lines identified as belonging to Ge III appear in the spectrum from a Geissler tube containing $GeCl_4$.[8] On the other hand, the present apparatus brings out but faintly the lines of V V and Cr VI.

III. The Classification of Ga IV and Ge V

The classification of Ga IV is given in Tables I and II, and that of Ge V in Tables III and IV. The data of Table I are all original with this investi-

Table III. *Classification of lines of Ge V.*

$(3d^9 4s)$ / $(3d^9 4p)$		$^3D_3$ 0		$^3D_2$ 1740		$^3D_1$ 4536		$^1D_2$ 7716	
		1740		*2796*		*3180*			
$^3P_2$	89541	89542	(6)	87796	(0)	85012	(0)	81806	(0)
		1		−5		7		−19	
	4083								
$^3P_1$	93624			91886	(8-Ge III)	89095	(1)	85896	(4)
				2		7		−12	
	2487								
$^3P_0$	96111					91575	(5)		
						0			
	−463								
$^3F_4$	95648	95648	(7)						
		0							
	−2113								
$^3F_3$	93535	93537	(5)	91794	(5)			85815	(0)
		2		−1				−4	
	3039								
$^3F_2$	96574			94832	(4)	92039	(5)	88865	(0)
				−2		1		7	
	4382								
$^3D_3$	100956	100959	(5)	99206	(0)			93240	(6)
		3		−10				0	
	362								
$^3D_2$	101318			99582	(6)	96768	(3)	93607	(5)
				4		−14		5	
	4005								
$^3D_1$	105323			103584	(2)	100786	(4)	97618	(0)
				1		−1		11	
	−2362								
$^1F_3$	102961	102955	(6)	101225	(5)			95247	(5)
		−6		4				2	
	1063								
$^1P_1$	104024					99483	(1)	96311	(4)
						−5		3	
	2056								
$^1D_2$	106080	106078	(2)	104341	(3)	101544	(4)	98377	(8δ)
		−2		1		0		13	

δ Diffuse.

gation; in Table II, wave-lengths and intensities are repeated from Miss Weinberg's[9] table, which extends to 157A, and Carroll's.[10] All the experimental data on germanium are from Carroll's[10] table. Both Carroll's tables extend to 600A.

[8] J. Lunt, Roy. Astr. Soc., M. N. **85**, 1 (1924).
[9] M. Weinberg, Roy. Soc. Proc., **A107**, 138 (1925).
[10] J. A. Carroll, Phil. Trans. Roy. Soc., **A225**, 357 (1925).

TABLE IV. *Wave-length list of Ge V.* (Carroll)

λ vac. I. A.	Int.	ν	designation $(d^9s)-(d^9p)$	λ vac. I. A.	Int.	ν	designation $(d^9s)-(d^9p)$
1222.4	0	81806	$^1D_2-{}^3P_2$	1045.5	7	95648	$^3D_3-{}^3F_4$
1176.3	0	85012	$^3D_1-{}^3P_2$	1038.3	4	96311	$^1D_2-{}^1P_1$
1165.3	0	85815	$^1D_2-{}^3F_3$	1033.4	3	96768	$^3D_1-{}^3D_2$
1164.2	4	85896	$^1D_2-{}^3P_1$	1024.4	0	97618	$^1D_2-{}^3D_1$
1139.0	0	87796	$^3D_2-{}^3P_2$	1016.5	8δ	98377	$^1D_2-{}^1D_2$
1125.3	0	88865	$^1D_2-{}^3F_2$	1008.0	0	99206	$^3D_2-{}^3D_3$
1122.4	1	89095	$^3D_1-{}^3P_1$	1005.2	1	99483	$^3D_1-{}^1P_1$
1116.8	6	89542	$^3D_3-{}^3P_2$	1004.2	6	99582	$^3D_2-{}^3D_2$
1092.0	5	91575	$^3D_1-{}^3P_0$	992.2	4	100786	$^3D_1-{}^3D_1$
1089.4	5	91794	$^3D_2-{}^3F_3$	990.5	5	100959	$^3D_3-{}^3D_3$
1088.3	8a	91886	$^3D_2-{}^3P_1$	987.9	5	101225	$^3D_2-{}^3F_3$
1086.5	5	92039	$^3D_1-{}^3F_2$	984.8	4	101544	$^3D_1-{}^1D_2$
1072.5	6	93240	$^1D_2-{}^3D_3$	971.3	6	102955	$^3D_3-{}^1F_3$
1069.1	5	93537	$^3D_3-{}^3F_3$	965.4	2	103584	$^3D_3-{}^3D_1$
1068.3	5	93607	$^1D_2-{}^3D_2$	958.4	3	104341	$^3D_3-{}^1D_2$
1054.5	4	94832	$^3D_2-{}^3F_2$	942.7	2	106078	$^3D_3-{}^1D_2$
1049.9	5	95247	$^1D_2-{}^3F_3$				

δ Diffuse
a Also classified in Ge III: $4^1S_0-4^1P_1$.

In Tables I and III the levels are designated at the heads of the columns and rows, with their values referred to $^3D_3(3d^94s)$; in the body of the tables are the wave numbers of the lines, followed in parentheses by their intensities. Below each wave number is the discrepancy (observed value minus calculated value) between the observed wave number and the wave number calculated from the positions assigned to the levels.

Tables II and IV are lists of the lines of Ga IV and Ge V classified in this investigation.

It will be noticed that all permitted combinations between the configurations (d^9p) and (d^9s) are found in Ga IV and all except three in Ge V, each of which would have been expected to be missing or at any rate very weak. The anomalous absence of $^3D_2(d^9s)-{}^3D_3(d^9p)$, was noted for Cu II and Zn III. This transition is recorded for Ga IV on the evidence of a mere trace found upon close re-examination of the plate, and for Ge V on the basis of a line which shows a deviation considerably greater than the probable error.

The simple average of the deviations in wave-numbers is 1.6 for Ga IV, and 4.6 for Ge V.

It will be seen that for both spectra the intensity relationships for combinations (except the $^3D_2-{}^3D_3$) between terms of the same multiplicity, are qualitatively in agreement with the intensity rules. This regularity persists from Ni I to Ge V. The intercombination intensities, in Ga IV and Ge V, which are anomalous, might have been extrapolated qualitatively from those of the previous spectra.

Table V shows the intensity of each line as a function of the nuclear charge. The levels are designated at the heads of the rows and columns. In the body of the table there appears in each space the intensity of the corresponding line for each of the five isoelectronic spectra. The table gives a survey of the relative change in intensity of the transitions with increas-

ing nuclear charge; of course the intensity standards are different for the different spectra. As the nuclear charge increases, there is a considerable increase in the intensities of intercombinations relative to those of the

TABLE V. *Intensities of lines in the spectra isolectronic with Ni I.*

		$(d^9p)^1P_1$	$^1D_2$	$^1F_3$	$^3P_0$	$^3P_1$	$^3P_2$	$^3D_1$	$^3D_2$	$^3D_3$	$^3F_2$	$^3F_3$	$^3F_4$
(d^9s)	Ni I		5	25R			200R		8	100R	8	70R	150R
	Cu II		2	7			10		1	8	3	4	10
D_3	Zn III		5	8			9		2	8	x	8	15
	Ga IV		1	10			15		0	10	1	10	15
	Ge V		2	6			6		—	5	—	5	7
	Ni I	20R	10	30R		150R	60R	5	100R	70R	20R	150R	
	Cu II	1	2	6		8	5	2	8	—	4	10	
$^3D_2$	Zn III	4	8	6		10	6	5	8	—	10	10	
	Ga IV	0	5	9		9	1	3	10	00	10	15	
	Ge V	—	3	5		8c	0	2	6	0	4	5	
	Ni I	10r	6		80R	50R	15	50R	20r		125R		
	Cu II	1	5		5	5	2	7	3		8		
$^3D_1$	Zn III	6	7		8	7	3	5	7−x		10		
	Ga IV	4	8		5	3	0	9	5		15		
	Ge V	1	4		5	1	0	4	3		5		
	Ni I	80R	100	150R		20	25	12	30r	35r	15	40r	
	Cu II	5	5	6		2	7	4	7	9	0	6	
$^1D_2$	Zn III	9	7	9		7	4	7b	8	10	3	9	
	Ga IV	12	10	18a		2	1	3	12	15	0	4	
	Ge V	4	8δ	5		4	0	0	5	6	0	0	

R, r Reversed.
δ Diffuse.
— Missing.
x, 7−x Intensities of an unresolved pair.
a Includes intensity of a Ga III line.
b Includes intensity of a carbon line.
c Includes intensity of a Ge III line.

singlet-singlet and triplet-triplet combinations; this relative increase is perhaps most marked in the *D-D* intercombinations.

IV. General Survey of the Nickel-Like Spectra

The most stable terms arising from the grouping of twenty-eight electrons can be derived easily from the theory of Hund; they have been discussed in previous papers. [5,7] Based upon the next higher ion ($3d^9$), the important electron configurations in the spark spectra of this sequence, in the order of decreasing stability, and the terms arising from them are:

Configuration	Terms	Spectra
$3d^{10}$	^1S	I II III (IV?)[11]
$3d^94s$	$^3D\,^1D$	I II III IV V
$3d^94p$	$^3F\,^3D\,^3P\,^1F\,^1D\,^1P$	I II III IV V
$3d^94d$	$^3G\,^3F\,^3D\,^3P\,^3S\,^1G\,^1F\,^1D\,^1P\,^1S$	

and so on. The Roman numerals indicate the spectra among those in the isoelectronic sequence Ni I, Cu II, Zn III, for which the terms of a given configuration have been found previously, and Ga IV, Ge V, for which they are reported in this paper. A higher series member ($3d^9,5s$) in Ni I and Cu II, and a number of multiplets in Ni I arising from the addition of an electron to the ion configuration ($3d^84s$), complete the list of known terms for this sequence. Nickel is the only element in this period in whose arc spectrum a term arising from the configuration (d^x) has been identified among the low terms.

[11] See footnote 12.

The failure to establish the ^1S term in the high spark spectra is not surprising in view of the relative faintness which appears to be a general characteristic of spark lines involving (d^s) configurations; Shenstone[7] has mentioned this faintness in the cases of Cu II (d^{10}) and Ni II (d^9). It will be seen below (from Table VI) that the $(d^{10})-(d^9p)$ lines may be expected at about 425A for Ga IV and at about 310A for Ge V[12].

The $(d^9,5s)$ terms would be expected to be absent due to the usual sharp intensity decrease in lines from higher series members, especially where the excitation energy is extremely high as in this case. The $(d^9p)-(d^9,5s)$ lines would lie at about 860A for Ga IV and 610A for Ge V.

TABLE VI. *Approximate[13] ionizing potentials of configurations, referred to the limit configuration* $(3d^9)$.

Spectrum	$(3d^{10})$		$(3d^94s)$			$(3d^94p)$		$(3d^95s)$	
	volts	$(\nu/R)^{1/2}$	volts	$(\nu/R)^{1/2}$	n_{eff}	volts	$(\nu/R)^{1/2}$	volts	$(\nu/R)^{1/2}$
Ni I	6.1	.67	7.7	.75	1.33	4.1	.55	2.5	.44
Cu II	20.4	1.23	17.7	1.14	1.77	12.0	.94	7.2	.73
Zn III	40.4	1.73	30.5	1.50	2.00	22.7	1.30	(13.6)b	1.00
Ga IV	63.9	2.17	45.5	1.83	2.18	35.6	1.62	(21.3)b	1.25
Ge V	(90)	2.58	62.1	2.14	2.28	50.3	1.93	(30.0)b	1.49

b. Extrapolation of the (d^9,s) values by the usual optical method, using a Rydberg table and the n_{eff} values of the (d^9s) configuration, would yield (13.6) volts for Zn III, (21.4) volts for Ga IV, and (31.5) volts for Ge V.

Table VI gives the approximate[13] energy values (recorded in terms of ionizing potentials, 1 volt = 8100 cm^{-1}) of the levels of the Ga IV and Ge V, referred to the most stable configuration (d^9) of the next higher ion. It includes, for completeness, the values of some of the important configurations in the other spectra of this isoelectronic sequence, together with the Moseley ordinates $(\nu/R)^{1/2}$, and the effective quantum numbers n_{eff} of the (d^9s) levels. Predicted values of levels not yet observed, are enclosed in parentheses.

With the aid of Shenstone's[7] determinations of the series limits of Ni I and Cu II, the (d^9s) values were obtained for each successive atomic number by linear extrapolation of the Moseley diagram, Eq. (1), slightly modified by a consideration of the first order screening numbers, fully discussed

[12] *Note added to proof, March, 1928.* The original draft of this article contained, in a footnote, a tentative assignment of the normal level $^1S_0(d^{10})$ of Ga IV. The spectrum of gallium below 1000A has now been rephotographed with the aid of a new grating, and the level established at −149298. The $(3d^{10})-(3d^94p)$ lines are:

λ	Int.	ν	designation	obs.−calc.
440.27	1	227133	$^1S_0-{}^3P_1$	24
423.59	5	236077	$^1S_0-{}^1P_1$	−22
422.49	4	236692	$^1S_0-{}^3D_1$	0

All the tables except I and II have been revised, where necessary, to incorporate the new data.

[13] Russell's consideration (l.c., p. 320) of the errors arising in certain cases in the prediction of series limits from only two members, indicates that the values shown for the ionizing potentials in Table VI may be 1 or 2 percent too high.

in Chapter VIII. The values of the other terms already observed were calculated from those of the (d^9s) configuration by subtraction, and the values in parentheses were extrapolated by the method described in Chapter VIII.

In Table VI, as elsewhere in this discussion where a value depending upon a configuration (that is, upon the n- and l-values of the individual electrons) is used, the value is chosen at the centroid of the configuration, with each level given its quantum statistical weight $2j+1$; not on account of any great significance to be attached to the centroid, but because for the application of the Moseley law in the form of Eq. (1), some representative point for the configuration must be chosen,[14] and the centroid appears to be the most satisfactory.[15]

Chapters V, VI, and VII will be devoted chiefly to a discussion of the (d^9s) and (d^9p) levels, which have all been identified in all the five spectra of the sequence.

V. Application of the Doublet Laws

In addition to the constancy of the frequency differences between the classified lines, and the satisfactory intensity relationships, the validity of the classifications of Ga IV and Ge V presented here rests upon the following three regularities:

1. The total separation of the $^3D(d^9s)$ term is in each case exactly in agreement with that demanded by the regular doublet law, Eq. (2); indeed, the separation was actually predicted in each case within 2 units, by extrapolation of the screening number. The term $^2D(d^9)$ upon which the ten electron system is built, is in one sense[14] identical with the regular x-ray doublet M_{33}, M_{32}. The doublet is inverted; its separation is given by Eq. (2). As Goudsmit and Back[16] have shown in the case of (ps) or (p^5s), if one or two s-electrons are added to the nearly complete shell (d^9), then the total separation of the resulting (d^9s) triplet or (d^9s^2) doublet is independent of the coupling and the same as that of the (d^9) doublet, and the new screening number $\sigma_2(d^9s)$ or $\sigma_2(d^9s^2)$ is equal to the one characteristic of the higher ion (d^9).

Table VII gives the screening numbers calculated from the $^2D(d^9s^2)$ and $^3D(d^9s)$ separations, with the corresponding x-ray screening number for comparison. The numbers are calculated to a higher degree of accuracy than the certainty of α allows $(\alpha^2=5.315\times10^{-5})$; but that fact has no effect

[14] See Chapter VIII.

[15] Table VIII, for instance, shows a much more satisfactory set of second differences than if the strongest line were chosen to represent the transition. Also, in the Gibbs-White graph,[3] where the transition $(d^{z-1}s)-(d^{z-1}p)$ plotted against Z for atoms in a given state of ionization is supposed to have a slope independent of the state of ionization, it is found that between the ten- and the eleven-electron spectra the slope varies from 1508 for Cu I–Ni I to 4660 for Ge IV–Ga IV if the lines $^3D_3-{}^3F_4$ and $^2S_1-{}^2P_2$ are used; while if the centroids are used, the variation is only about half that amount: from 1951 for Cu I–Ni I to 3595 for Ge IV–Ga IV.

[16] S. Goudsmit and E. Back, Zeits. f. Physik **40**, 530 (1926).

TABLE VII. *Relativistic screening number* $\sigma_2(3d^9)$.

Element	spectrum	$^2D(d^9s)$	Screening number $^2D(d^9s^2)$	$^2D(d^9s^2p^6\cdots)$
28 Ni	I	13.693		
29 Cu	I		13.566	
	II	13.516		
30 Zn	II		13.422	
	III	13.370		
31 Ga	IV	13.249		
32 Ge	V	13.161		
41 etc.	x-rays			13.0

Note added to proof. We can now add in a new row and a new column for 27 Co I $^2D(d^9)$, $\sigma_2=13.398$ (M. A. Catalán, Zeits. f. Physik. **47**, 89 (1928)). If all the values in the table are correct, there is a sharp break in the values of $\sigma_2(3d^9)$ for the successive arc spectra Co I, Ni I, Cu I.

on the differences. The second differences of the numbers in the third column are successively 0.031, 0.025, 0.033. This remarkable regularity indicates the accuracy with which the doublet separations can be predicted by the extension of this table, and by similar ones.[17]

2. The irregular doublet law, Eq. (3b), may be applied to the transition $(d^9s)-(d^9p)$. Table VIII shows the distance between the centroids of the two configurations, for the sequence of isoelectronic spectra; together with the differences Δ_1 between the frequencies in successive stages of ionization, and the second differences Δ_2. One would expect the differences

TABLE VIII. *Dependence of* $(d^9s)-(d^9p)$ *upon nuclear charge.*

Spectrum	Frequency	Δ_1	Δ_2
Ni I	28740		
		17965	
Cu II	46705		−1423
		16542	
Zn III	63247		−330
		16212	
Ga IV	79459		−119
		16091	
Ge V	95550		

Δ_1 to approach a constant for high stages of ionization; which in fact they do as the decrease in the absolute value of Δ_2 shows. The approximate linearity of the curves in Fig. 1, discussed in the next paragraph, shows that this linear dependence of the distance between the centroids upon atomic number implies a like linearity for the individual levels.

3. The differences between corresponding levels within each of the two groups due to the configurations $(3d^94s)$ and $(3d^94p)$ respectively, may be

[17] Table VII was calculated from Eq. (2), for convenience in extrapolation. A more accurate equation (A. Sommerfeld, "Atombau und Spektrallinien," 4. Aufl., p. 450, Eq. (14)) taking higher terms into account, yields only slightly higher values for σ_2; the correction in σ_2 ranges from 0.007 for Ni I to 0.014 for Ge V.

represented by smooth, nearly linear curves. These curves[18] are given in Fig. 1; against nuclear charge as abscissa, are plotted the values of the levels composing the (d^9s) and (d^9p) configurations, referred to their re-

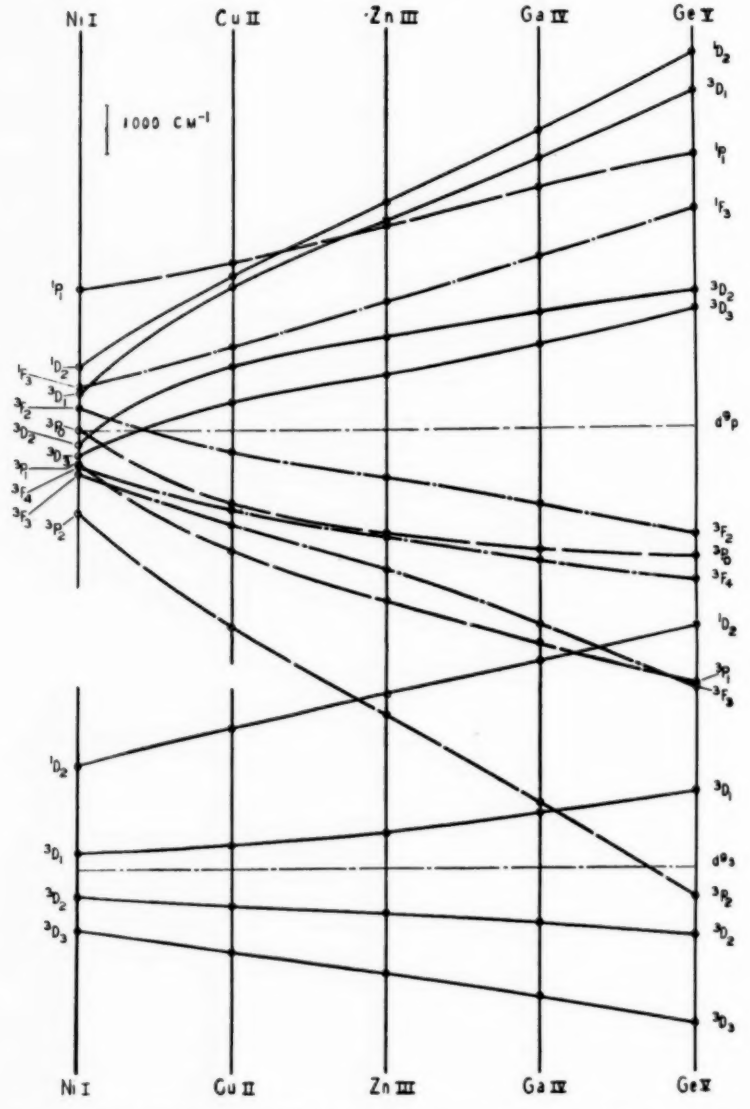

Fig. 1. The ($3d^94s$) and ($3d^94p$) configurations of the nickel-like spectra.

spective centroids. The two horizontal center lines are the centroids; the distance between them in the figure was chosen arbitrarily.

In the (d^9p) group, by far the greatest curvature occurs between the arc and the first spark spectra, as might have been expected. For higher ioniza-

[18] Although continuous smooth curves are drawn and their curvature is discussed, of course no points of any of them have any meaning except the intersections with the vertical lines.

tions, the levels with a given inner quantum number are so far apart and the curvature is so slight that no doubt can be entertained as to the connection of the points; with a single exception in the case of the Zn III levels designated as $^3D_1$, $^1P_1(d^9p)$. In this case the two levels, lying almost at the intersection of the lines, are separated by only 72 cm^{-1}. In an earlier assignment[5] of these levels, made on the basis of an extrapolation from Ni I and Cu II, the lines were not crossed between Cu II and Zn III. The evidence of the higher spark spectra, however, clearly favors the interchange of the two points. Neither assignment is especially favored against the other by the intensities (Table V).

Two of the curves, $^3F_4$ and $^3P_0$, had to be drawn from the evidence of a single transition in each spectrum: but all serious doubt of their reality is removed by the support of the intensities and the smoothness of the curves; together with the fact that in zinc, no line of intensity greater than 3 remains unclassified within 4000 cm^{-1} of either of the ones assigned to these levels. With the curves thus carried through Zn III, there is no choice of points in Ga IV and Ge V.

VI. Assignment of l and s

We come now to a field in which we must proceed most cautiously: namely, the assignment of values to the multiplicities and orbital angular momenta of the several terms.

Goudsmit and Uhlenbeck[19] have shown that the interaction between an outer electron and its ion, depending upon the relative magnitudes of the interaction energies between their several momenta, may be represented by any of several symbolic coupling equations, of which we need consider here only the following: the extreme Russell-Saunders coupling:

$$((l_1l_2)(s_1s_2)) = (ls) = j \tag{4}$$

and the opposite extreme:

$$((l_1s_1)(l_2s_2)) = (j_1j_2) = j \tag{5}$$

where the subscripts 1 and 2 refer to the ion and the electron, respectively, and letters without subscripts indicate momenta of the configuration as a whole. Close coupling or association within a bracket indicates relatively large interaction energy. Eq. (4) shows that the atom as a whole would be characterized by values of l and s only in the ideal case of simple Russell-Saunders coupling.

The interaction energies in the spectra under consideration can be represented by no such pure coupling scheme. According to the usual practice, then, each level is given a symbol intended to indicate the spin and orbital angular momenta that would be expected to result for that level in the case of a continuous change (if that were possible) of the charges and orbital elements of the system until complete Russell-Saunders coupling should occur. The necessity of postulating such an imaginary continuous transi-

[19] S. Goudsmit and G. E. Uhlenbeck, Zeits. f. Physik **35**, 618 (1925).

tion in order to justify our notation, is evidence of the formal nature of the assignment of "multiplicity" and "total orbital angular momentum" to "multiplet" levels where we are not justified in speaking of the quantization of l and s.

Ni I and Cu II having been already classified with the aid of criteria not available for the higher spark spectra, it was found possible on the basis of the Ni I and Cu II assignments to assign l- and s-values unambiguously (with the unimportant exception mentioned above for Zn III $^3D_1$, $^1P_1(d^9p)$) in agreement with the following three plausible rules:

(a) Homologous levels, when plotted with reference to each other or to the centroid of the configuration (Fig. 1) lie on smooth, nearly linear curves.

(b) The intensity rules hold qualitatively (Table V) among the singlet-singlet and triplet-triplet combinations.

(c) Interval ratios are not greatly altered, as the atomic number increases; in particular, there is no crossing of lines with the same l-value, at least for stages of ionization of the order of magnitude of those considered here.

A striking characteristic of the curves drawn according to these rules is that in spite of the departure from the normal, indicated by the non-applicability of the interval rules, the (d^9p) levels are sharply separated by their curvatures in the region of greatest curvature, into three groups, agreeing exactly with their grouping by l-values. The $^{3,1}D$ curves are all sharply concave downward and the $^{3,1}P$ somewhat less sharply concave upward, between Ni I and Cu II; while the $^{3,1}F$ levels show only a slight upward concavity. This similarity of curvature might almost be used as a criterion in similar cases, to associate the singlet levels with their triplets: but more material would be necessary to establish such a criterion.*

Since the assignments, made (except for the levels $^3D_3$, $^3D_1(d^9s)$) chiefly upon the basis of (a), depend for their validity directly upon that of the Ni I and Cu II levels, it is necessary to examine critically the classifications of these two spectra.

Bechert and Sommer were aided in the classification of Ni I by the evidence offered by many combinations with higher lying multiplets. The relative positions of the terms, and the intensity ratios, are quite convincing. Of the two overlapping ^3F terms due to (d^9p) and (d^8sp), the one chosen[5] was selected by rule (c); Russell's[20] recent assignment of this term on the basis of the relative positions of corresponding levels in neighboring arc spectra, confirms this choice.

Shenstone's classification of Cu II was based largely on a Zeeman effect analysis. His g-values from triplet blends are in good agreement with those which would be expected in the case of Russell-Saunders coupling; except in the case of $^1F_3$ and $^3D_3(d^9p)$, which share their g-sum but show a wide departure from normal g-values. The only basis for the present choice (which is in accord with Shenstone's) in the spectra from Cu II to Ge V,

* See note added to proof, at the end of the paper.

[20] H. N. Russell, Astroph. Jour. **66**, 184 (1927).

is the one advanced by Shenstone; the relative positions of the terms, in particular the inversion of the ^3D in agreement with rule (c). On the other hand, the intensity criterion now slightly favors the opposite assignment; and the absence of the intercombination $^3D_2-{}^1F_3$ would be less perplexing than that of $^3D_2-{}^3D_3$, especially in the face of the irregular intensity relationships among the intercombination lines in this isoelectronic sequence, compared with the good agreement among all the other triplet combinations. It must be remembered that although the assignment of l- and s-values on the basis of g-values, appears to have led here to results that are quite satisfactory, such an assignment has not the finality[21] in cases of complex coupling like the present one, that it has in cases of practically pure coupling of one type or another, such as is exemplified in Eqs. (4) and (5).

VII. Coordination of Levels to Series Limits

There are three familiar ways of tracing the dependence of the coupling schemes of similar configurations, upon the nuclear charge and the total quantum numbers of the electrons:

First, by considering an increase in the total quantum number of the added electron, only. Although the lower members of a series may consist of normal terms, the higher members always show the jj-coupling of Eq. (5). Specifically, for higher series members all the other interaction energies are small compared with that of the ion, a fact which may be represented as a special case of Eq. (5) by the scheme

$$((l_1s_1),l_2,s_2)=(j_1,l_2,s_2),=j \qquad (6)$$

where a comma between two momenta indicates that their coupling is negligible.

Second, by comparison of corresponding levels in the arc spectra of elements in the same column of the periodic table; where increasing nuclear charge is accompanied by increasing total quantum numbers. Goudsmit and Back[16] have shown, for instance, that in the case of the configuration (ps) there is a complete change from Russell-Saunders coupling, Eq. (4), for the triplet and singlet $^3P,{}^1P(2p3s)$ of carbon, to the opposite extreme, Eq. (5), for the Pb levels designated $^3P,{}^1P(6p7s)$, which lie in two close pairs.

Third, by comparing regular x-ray doublets with the terms arising from the corresponding optical configurations, as (d^9x) and (p^5x), where the x within the symbol for the configuration stands for any outer electron or electrons. In the transition to the x-ray region, the magnitude of the nuclear charge effective upon the inner orbits (whose total quantum number is the same as in the corresponding optical orbits) is greatly increased; and the total quantum numbers of the outer electrons are greatest for the heaviest atoms. In this case again, the coupling is represented by Eq. (6) (except that

[21] See, for instance, Hund's reassignment ("Linienspektren und Periodisches System der Elemente," p. 200, 1925) of certain of the neon p-lines previously classified by Goudsmit (Zeits. f. Physik **32**, 794, 1925) on the basis of the Zeeman effect.

the pair l_2,s_2 must be replaced by l_2,s_2,l_3,s_3 . . . ; as many pairs as there are outer electrons in the configuration); the case is discussed further in Chapter VIII.

From the similar behavior of the couplings in these three cases, one would expect to find the same trend in a fourth one, in which only the nuclear

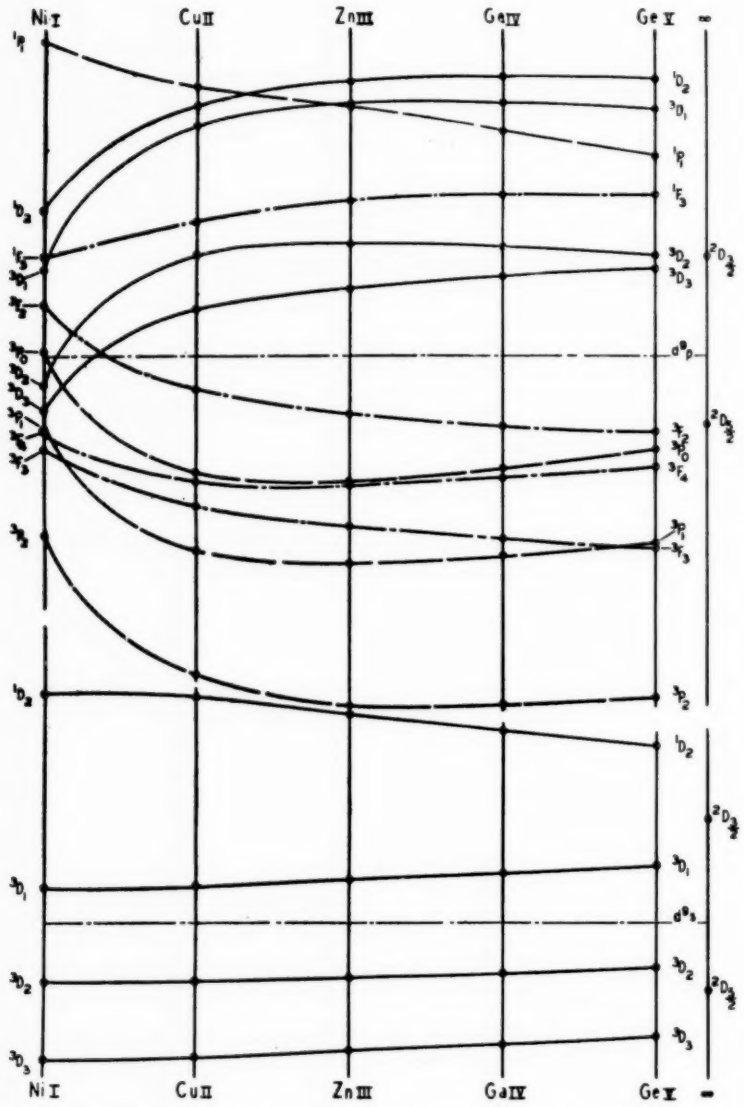

Fig. 2. The $(3d^94s)$ and $(3d^94p)$ configurations of the nickel-like spectra in terms of the regular doublet $(3d^9)$.

charge is altered. This is exactly the case of the isoelectronic sequence under our consideration. We expect, then, that for extremely high ionizations, the (d^9s) and (d^9p) configurations will eventually be split into two subgroups

separated by the difference of the doublet $^2D(d^9)$ of the ion (although this splitting into subgroups may occur much less rapidly with increasing nuclear charge than in the x-ray case, where the total quantum numbers of the outer electrons increase).

Fig. 2 differs from Fig. 1 only in that its ordinates, measured from the centroid for each configuration, are in terms of the relativistic doublet distance $^3D_1-{}^3D_3(d^9s)$ as a unit, instead of in cm^{-1}; and that there is added at the side on a vertical line labelled "∞", the doublet separation about which the levels of the subgroups must cluster with extremly high ionization if the prediction of the paragraph above is correct.

The order of magnitude of the separations for each configuration, is in agreement with the prediction; but the grouping of the levels demands special consideration in the case of each of the two configurations:

1. The method of Hund[22] yields the following correlation between the levels of a (d^9s) or (ds) configuration and the levels of the ion (d^9) or (d):

$$^3D_3, {}^1D_2 \rightarrow {}^2D_{5/2}$$

$$^3D_2, {}^3D_1 \rightarrow {}^2D_{3/2}$$

Upon the postulate that the levels tend to cluster about the relativistic doublet as the nuclear charge increases, the evidence of Fig. 2 indicates that the limits for the levels $^1D_2$ and $^3D_2$ should be interchanged. The ratio:

$$^3D_2-{}^3D_3 : {}^3D_1-{}^3D_2$$

in each of the spectra of the nickel-like sequence, as well as in each of the other known (d^9s) configurations, is given in Table IX. The progressive

TABLE IX. *Ratio of the separations* $^3D_2-{}^3D_3 : {}^3D_1-{}^3D_2$, (d^9s).

$(3d^94s)$	Ni I 0.448	Cu II 0.444	Zn III 0.428	Ga IV 0.407	Ge V 0.384
$(4d^95s)$	Pd I[23] 0.337	Ag II[24] 0.345	Cd III 0.330*	In IV 0.309*	
$(5d^96s)$	Pt. I[25] 0.077a				

a. New assignment of term formerly designated $^1D_2$; the only other possible ratio on the basis of the existing data is .648.

* See note added to proof, at the end of the paper.

decrease of this ratio for the successive isoelectronic spectra from Ni I to Ge V, and the marked decrease in the columns representing the first three stages of ionization, are evidences against Hund's correlation. But the complexity of the progress of the coupling is exemplified by the fact that the ratio is greater for Ag II than for Pd I, in contrast with its decrease in the first row.

[22] F. Hund, Zeits. f. Physik **34**, 296 (1925).
[23] K. Bechert and M. A. Catalan, Zeits. f. Physik **35**, 449 (1925).
[24] A. G. Shenstone, Phys. Rev. **31**, 317 (1928).
[25] W. F. Meggers and O. Laporte, Phys. Rev. **28**, 642 (1926).

Shenstone [7,24] has already pointed out exactly this disagreement with Hund's correlation in the case of the series limits extrapolated from the first two numbers of the (d^9,ms) series in every case where the second member is known: namely, in Ni I, Cu II, Pd I, and Ag II. Shenstone's assignments of multiplicity values to the $^1D_2$ and $^3D_2$ levels of these terms was on the unequivocal evidence of relative positions, separations, intensities, and in the case of Cu II, Zeeman effect.

Indeed, Hund[26] himself would have been confronted with a disagreement in neon strictly analogous with this, had he not rearranged the (p^5,ms) series by interchanging s_2 and s_4 in the higher members of the first subordinate series, arranged by Paschen.[27] The levels of the lowest member $^3P_{210}$ $^1P_1(2p^53s)$ of this series have been determined unambiguously by their relative positions and their Zeeman patterns to be respectively the levels $1s_5$, $1s_4$, $1s_3$, $1s_2$ of Paschen. But Paschen's s_2 and s_3 series approach the upper, and his s_4 and s_5 the lower of the levels of his doublet series limit, the inverted $^2P(p^5)$; giving directly the correlation

$$^3P_2, {}^3P_1 \rightarrow {}^2P_{3/2}$$
$$^3P_0, {}^1P_1 \rightarrow {}^2P_{1/2}$$

in agreement with the findings

$$^3D_3, {}^3D_2 \rightarrow {}^2D_{5/2}$$
$$^3D_1, {}^1D_2 \rightarrow {}^2D_{3/2}$$

of Shenstone and of this investigation, but contrary to the theory.

2. The grouping of the observed (d^9p) levels in Zn III, Ga IV, and Ge V, by j-values can be represented by the following qualitative scheme, where the levels are listed in order of decreasing stability and the larger intervals are represented by commas:

2, 13402, 323112.

The normal grouping pattern from Eq. (4) is

432, 321, 210, 3, 2, 1

and the opposite extreme, from Eq. (5), is

4321, 32, 3210, 21.

The order of the groups here, or of the numbers within a group, is not intended to have any significance. From Eq. (6) we may derive the series limit grouping:

$$43322 1 \rightarrow 5/2$$
$$32211 0 \rightarrow 3/2$$

[26] F. Hund, "Linienspektren und Periodisches System der Elemente," p. 198 (1925).
[27] F. Paschen und R. Götze, "Seriengesetze der Linienspektren," p. 30, 1922.

independent of any complete theory, such as Hund's, for the approach of Russell-Saunders levels to their series limits. The irreconcilability of the observed grouping with the series limit grouping expected asymptotically for high nuclear charge, is best shown by the fact that the levels 0 and 4 are close companions from Cu II to Ge V. The coupling scheme must be, then, of an intermediate sort. As an example of the grouping patterns that may be expected from such intermediate coupling schemes, we may consider the coupling equations

$$(((l_2 s_2) s_1) l_1) = ((j_2 s_1) l_1) = j \tag{7}$$

and

$$(((s_1 s_2) l_2) l_1) = ((s l_2) l_1) = j \tag{8}$$

These yield the same pattern,[28] which in our case becomes

4 3 2 1 0, 3 2 1, 3 2 1, 2

This grouping with its isolated 2 and its grouped 43210, appears to be more nearly in agreement with the observations than any of the other calculated groupings. Of course such a coupling, if it actually occurs, must, like the Russell-Saunders, be considered transient; it is to be expected that for higher ionization it will give way to the $j_1 j_2$ scheme.

Comparison of our $(d^9 p)$ with the analogous neon configuration is not as simple as in the case where the added electron was an s-electron. The observed $(2p^5 3p)$ grouping in neon is

1, 3 2 1 2 1 2 0 1, 0.

The Russell-Saunders scheme, Eq. (4), yields

3 2 1, 2 1 0, 1, 2, 1, 0

the intermediate Eq. (7) or Eq. (8)

3 2 1, 2 1 0, 2 1 0, 1

and the $j_1 j_2$ coupling Eq. (5)

3 2 1 0, 2 1, 2 1, 1 0.

It may be observed that corresponding to $^3P_2$ in the structural scheme $(d^9)+(p) = {}^3F {}^3D {}^3P {}^1F {}^1D {}^1P$, the neon level is $^3S_1$; these, $^3P_2$ and $^3S_1$, are the strikingly isolated low levels of our spectra from Ni I to Ge V, and of Ne, respectively.

[28] Where the added electron is an s-electron, as in 1 above, Eqs. (4), (7), and (8) degenerate into the same form $((s_1 s_2) l_1) = (s l_1) = j$; the atom may be considered both for Ne and for all our isoelectronic spectra, to be already in the intermediate coupling state. The $(d^9 s)$ configuration might be expected, then, to show earlier and more simply than the $(d^9 p)$ configuration, the influence of $j_1 j_2$ coupling. Regarding the plausibility of Eq. (7) and Eq. (8), it must be remarked that the occurrence of l_2 deeper within the brackets than l_1 is less satisfactory in the present case than in the analogous case of neon, where the electrons all have the same l-value, and the subscripts are interchangeable.

VIII. Application of the X-ray Laws to Optical Spectra, in General

Sommerfeld [29] points out in the fourth edition of his book, that in contrast with the situation in x-ray spectroscopy, in the optical region we are far (except in the case of hydrogen) from the achievement of a truly rational term representation.

We shall consider now, more generally than in the previous chapters, the applicability of the x-ray laws, Eqs. (1) to (3), to sequences of isoelectronic optical spectra. Between the x-ray field and the optical field there may be pointed out two[30] distinctions in the application of the laws, which are closely related to the differences in aspect between the fields from the viewpoint of term representation.

First, *in the usual optical Moseley diagram the axis of ordinates represents a manifold of levels, in contrast with the "closed shell" singlet of the x-ray diagram.* In the x-ray diagram the squares of the ordinates represent, in effect, a one-electron configuration (doublet) minus a closed shell (singlet); for the energy differences among the several possible levels of the outer configuration are negligible compared with the energy required to remove an electron from an *inner* closed shell (compare Eq. (6)). The differences within the outer configuration are not negligible compared with the energy required to remove an *outer* electron; so that, strictly, an optical Moseley diagram requires as many graphs (or as many zero points) as there are levels in the higher ion, and, moreover, requires a knowledge of the correlation of the levels to those of the ion. For example, in the case of the nickel-like sequence, the plotting of the (d^9s) levels on the basis of the (d^9) ion requires two zero points, $^2D_{5/2}$ and $^2D_{3/2}$. The ordinates $(^3D_3-{}^2D_{5/2})^{1/2}$ and $(^3D_1-{}^2D_{3/2})^{1/2}$ are (neglecting the minute change in screening number between d^9 and d^9s) exactly the same, and $^3D_2$ lies a little lower (or, according to Hund's correlation, a little higher). This exact representation has in this case the advantage that it attributes the difference $^3D_3-{}^3D_1$ to the ion (d^9) where it belongs and not to the optical electron; this regular doublet difference is easily expressible in the usual doublet term formula built upon the single state (d^{10}). The differences $^3D_3-{}^3D_2$ and $^3D_1-{}^1D_2$ (or from Hund's viewpoint, $^3D_3-{}^1D_2$ and $^3D_2-{}^3D_1$) due to the difference in orientation of the s electron's spin vector, might perhaps be represented with the aid of another screening number as a new function of Z; although obviously not depending in the same way upon Z as the regular doublet, because for high

[29] A. Sommerfeld, "Atombau und Spektrallinien," p. 460, 1924: "Das Problem der Termdarstellung hat also im Röntgengebiet ein ganz anderes Gesicht als im sichtbaren Gebiet. Dort genügen für jedes Element wenige Parameter δ, um mit ihrer Hilfe sämtliche Terme darzustellen durch Formeln, welche sonst nur ganze Zahlen und universelle Konstante, z.B. unser α, enthalten. Hier dagegen ist—ausser im Wasserstoffspektrum —jeder Term letzten Endes empirischen Ursprungs. Eine wirkliche rationelle Termdarstellung liegt für das sichtbare Gebiet noch in unabsehbarer Ferne. Im Röntgengebiet scheinen wir dicht davor zu stehen."

[30] A third distinction, the well-known difference of sign in the Moseley diagrams, need not be discussed here.

values of Z these differences are expected to vanish in comparison with the (d^9) doublet difference, as Chapter VII shows.

The paragraph above concerns exact energy values of levels. In the paragraph below, the complex structure, in the energy diagram, of each configuration, must be neglected. A representative point must be chosen for each configuration, analogous to the ν_{rad} of an x-ray term, which for a given value of Z depends only upon the missing electron (that is, upon the n and l of that electron), and which consists only of the member free from α^2 in the infinite series term formula. Since we do not know the laws of the optical fine structure, the centroid is chosen as the best point available to represent the configuration;[15] the members in α^2 would be expected to represent relatively less energy in optical spectra than in x-ray spectra.

Second, *whereas the optical spectra of a given isoelectronic sequence increase in ionization with increasing Z, all the ordinary x-ray levels represent ionizing potentials of the neutral atom.* Let the first order screening number σ_1, be defined by the relation

$$(\nu/R)^{1/2}=(Z-\sigma_1)/n, \text{ or } \sigma_1=Z-n(\nu/R)^{1/2} \tag{9}$$

where ν is the value representative of a given configuration, referred to any one of its next higher ions (that is, the ion made by removing any one of its electrons) and n is the total quantum number of the removed electron. To every configuration for a given Z there correspond as many values of σ_1, as there are different n_l electrons in the configuration. The x-ray first order screening numbers are derived from Eq. (9) by considering the removal of an inner electron. As a result of the second distinction between x-ray and isoelectronic optical spectra it is found that whereas for x-rays, σ_1 is an increasing function of Z, for isoelectronic spectra it is a decreasing function, approaching an asymptotic value for large Z (see below, Fig. 6).

Fig. 3 is a Moseley diagram for the optical sequence of one-electron copper-like spectra[31] built upon the closed shell $(3d^{10})$; the absolute values are established for the earlier spectra by several series, and for the later ones by the non-penetration of the hydrogen-like $(4f)$ and $(5g)$ orgits. Fig. 4 is a similar diagram for the ten-electron nickel-like sequence, built upon $(3d^9)$; it contains the same material as Table VI. From the data used in Fig. 3 and Fig. 4, it was possible to construct a third Moseley diagram, Fig. 5, for the eleven-electron copper-like spectra built upon the configuration $(3d^9 4s)$; it should be noted that the $3d$-curve of Fig. 5 represents *exactly the same* configuration as the $4s$-curve of Fig. 3.

Now from Eq. (9) and the data of these Moseley diagrams, a screening number curve may be drawn corresponding to each of the Moseley curves. These numbers are shown in Fig. 6, in which the first order screening number is plotted against the atomic number. Since the absolute term values are usually only approximately established, caution must be used in comparing

[31] Cu I: A. G. Shenstone, Phys. Rev. **28,** 449 (1926); Zn II: G. v. Salis, Ann. d. Physik **76,** 145 (1925); Ga III, Ge IV: R. J. Lang, Phys. Rev., **30,** 762 (1927).

the ordinates (this is true to a less extent, of the slopes) of Fig. 6 in cases of configurations built upon different ions. The dotted lines in Fig. 4 and Fig. 6 are the mean values obtained by application of the Moseley law,

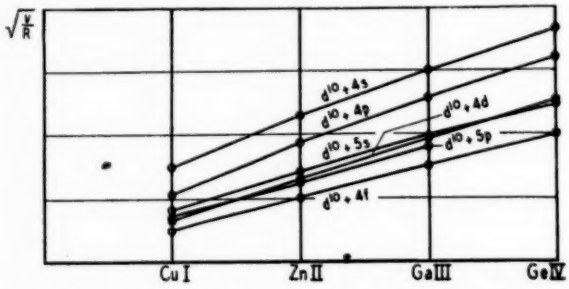

Fig. 3. Moseley diagram, based upon the configuration ($3d^{10}$).

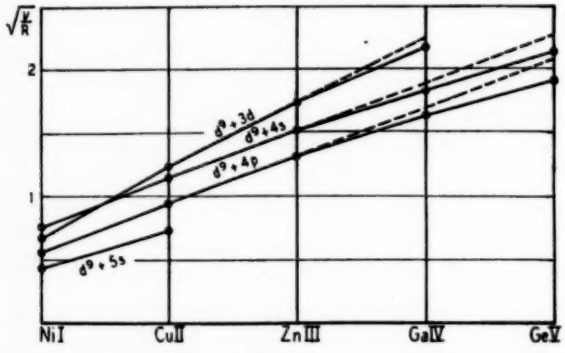

Fig. 4. Moseley diagram, based upon the configuration ($3d^9$).

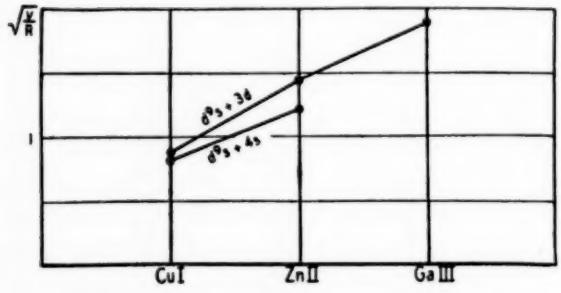

Fig. 5. Moseley diagram, based upon the configuration ($3d^94s$).

Eq. (1), and the irregular doublet law, Eq. (3a), to the configurations (d^9s) and (d^9p). All the other curves tend to approach horizontal asymptotes; with increasing ionization, their slopes decrease approximately in geometric progression like those of exponential curves.

First order screening number curves, plotted for sequences of isoelectronic optical spectra, appear quite generally to possess this property of

decreasing downward slope.[32] (For the hydrogen-like orbits this slope is zero). Moreover, it appears to be a rule that among the curves associated with *the addition of a given electron* to different ion configurations: *The shapes of the curves change quite slowly with changing total number of electrons; and for a given total number of electrons, the shape of the curves is approximately the same for all configurations.*

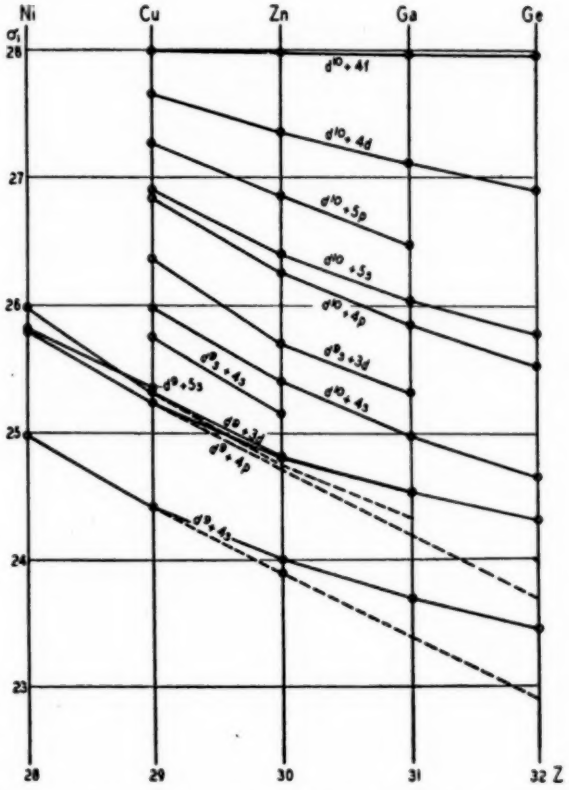

Fig. 6. The first-term screening numbers σ_1 from nickel-like and copper-like spectra.

Table X gives several examples of this rule, chosen from isoelectronic sequences in the neighborhood of closed shells. In each example several ion configurations are listed. The fourth column gives the values of σ_1 for the arc spectrum, calculated from Eq. (9), and the following columns show the negative slopes of the σ_1 curves between the arc and the first spark spectra, the first and second spark spectra, etc. The rule is verified by the slow increase of the values in each column after the fourth for increasing total number of electrons, and the approximate constancy of the values in in the neighborhood of a given total number of electrons. The rule was used

[32] An exponential curve is uniquely determined by the position, slope, and curvature at one point. In the following sentences we shall for convenience speak of the slope and curvature at the initial point (the point representing σ_1 for the arc spectrum) of the exponential curve which most nearly fits the empirical points, as the "shape" of the σ_1 curve.

in determining the values of σ_1 and consequently the absolute energy values in the higher spark spectra of the nickel-like sequence, as follows (so the regularity of the italicized numbers may not be considered a verification of the rule): The italicized numbers in the row representing the addition of a 4*s*-electron to the ion configuration ($3d^9$), were chosen to be equal to the corresponding numbers in the ($3d^{10}$) row; and the numbers in parentheses were derived from those in italics. For Ge V it was necessary to extrapolate the slope. The solid lines departing from the dotted ones in Fig. 4 and Fig. 6, are derived from the numbers in italics and in parentheses in Table X.

TABLE X. *Slopes of first order screening number curves.*

Added electron	Ion configuration	Total number of electrons in ion	I	I–II	II–III	III–IV	IV–V
$3d$	$2p^6$	10[1]	10.00	.02	.03	.04	.03
	$3p^6$	18[1]	17.95	.55	.45	.30	
	$3d^9$	27	25.99	.67	(.50)	(.33)	
	$3d^94s$	28[31]	26.37	.67	.38		
$4s$	$2p^6$	10	9.49	.23	.14	.10	.08
	$3s^2$	12	11.17	.28	.17	.12	
	$3p^6$	18	16.74	.48	.30	.20	
	$3d^9$	27	24.99	.57	*.42*	*.32*	*.24*
	$3d^{10}$	28	25.98	.58	.42	.32	
	$3d^94s$	28	25.75	.60			
$4p$	$2p^6$	10	9.72	.15	.11	.07	.05
	$3s^2$	12	11.50	.22	.14	.10	
	$3p^6$	18	17.21	.41	.28	.19	
	$3d^9$	27	25.79	.55	(.42)	(.30)	(.22)
	$3d^{10}$	28	26.85	.59	.41	.32	
$5s$	$2p^6$	10	9.63	.18	.11	.08	.06
	$3s^2$	12	11.45	.23	.14	.10	
	$3p^6$	18	17.22	.37	.25	.18	
	$3d^9$	27	25.82	.46			
	$3d^{10}$	28	26.91	.50	.37	.32	
	$4d^9$	45[23,24]	42.25	.83			
	$4d^{10}$	46[23]	43.28	.85	.60	.46	.49

The effect on Table VI, of the adoption of the solid lines instead of the dotted ones in Fig. 6, was to lower the ionizing potentials for the (d^9s) and (d^9p) configurations by 1 volt for Zn III, 3 volts for Ga IV, and 8 volts for Ge V; and to decrease the other values accordingly.

If we call M the slope of a curve in the Moseley diagram, then we may see from the definition Eq. (9) that the slope of σ_1 as a function of Z is $1-nM$; and the rule that the screening numbers for a given electron are approximately parallel functions of the state of ionization, implies that in the neighborhood of any atomic number the initial slopes of the lines in the Moseley diagram depend only upon the added electron. Russell[34] has already pointed out several instances of this property of the Moseley diagram. The upward curvature of $\sigma_1(Z)$ as it approaches its asymptotic value,

[23] R. J. Lang, Natl. Acad. Sci. Proc., **13**, 341 (1927).
[34] H. N. Russell, l.c., p. 325, p. 434.

may be seen in the downward curvature of $(\nu/R)^{1/2}$ in the Moseley graph, its slope approaching $1/n$ for high stages of ionization.

The rule concerning the parallelism of the curves representing the addition of a given electron to each of several configurations, is distinct, of course, from the irregular doublet law, which concerns the addition of different electrons to the same ion.

For high values of Z, the x-ray screening number $\sigma_1(M_{32}\,M_{33})$ is a quite accurately known function of Z; but as Z decreases to nearly 28 the first distinction pointed out above, between the x-ray and the optical field, becomes invalid. For instance, the "x-ray $M_{32}\,M_{33}$ doublet" of Ge consists of the totality of the twenty-eight levels arising from the improbable configuration $(3d^9 4s^2 4p^2)$. But in the $^2D(3d^9)$ of Ni II, the x-ray doublet and the optical doublet become identical. The value, at Ni, of the σ_1 curve labeled d^9+3d is in the strictest sense the x-ray $M_{32}\,M_{33}$ screening number of nickel. It would have been just as proper to label the point $3d^{10}-3d$, as $3d^9+3d$, considering the differences in sign in the two fields. The value of σ_1 at this point is 25.99. Since this is very near the value obtained by extrapolating the x-ray screening number down to $Z=28$, and since the x-ray screening number increases and the optical one decreases with increasing atomic number, we see that there is a progressive difference between the optical and the x-ray screening numbers, which might well be accounted for by the outer screening in the x-ray spectra, due to the electrons which are missing in the isoelectronic sequences.

For a given total quantum number, both penetrating and non-penetrating orbits occur; and for non-penetrating orbits, as we have seen, the initial negative slope is zero. But from Eq. (3a) and Eq. (9) we can see that the irregular doublet law, applied as usual to isoelectronic sequences, requires

TABLE XI. *Differences among the first order screening numbers σ_1, as functions of Z.*

Ion configuration	Added electrons	Spectrum	I	II	III	IV	V
$3d^9$	$4p-4s$		0.80	0.82	0.82	0.81	0.84
$3d^{10}$	$4p-4s$		.87	.86	.87	.87	
	$4d-4p$		.81	1.10	1.27	1.38	
	$4f-4d$		.34	.63	.86	1.06	
	$5p-5s$		.37	.45	.44		
	$5d-5p$		.46	.66			
	$5f-5d$		.26	.47			
$4d^{10}$	$5p-5s$		1.06	1.03	1.03	1.04	
	$5d-5p$		.98	1.28	1.44	1.58	
	$5f-5d$		.42	.73	.90	1.08	

that all the σ_1 curves representing the addition of electrons of a given total quantum number to a given configuration, be parallel. Therefore the irregular doublet law cannot be valid for all the added electrons with a given n-value, in general. This invalidity may be seen at once from the divergence of the lines $3d^{10}+4s$, $3d^{10}+4p$, $3d^{10}+4d$, and $3d^{10}+4f$ in Fig. 6, for instance.

In the neighborhood of a closed d-shell the parallelism between the s- and the p-curves appears to hold to a much higher order of accuracy than in the case of higher l-values. Table XI illustrates this fact by recording in rows labeled $p-s$, $d-p$, etc., the values $\sigma_1(p)-\sigma_1(s)$, $\sigma_1(d)-\sigma_1(p)$, etc., as a function of the ionization for each of several ion configurations; the values in the rows $p-s$ remain nearly constant, while the others show large increases. For some of the lighter atoms $\sigma_1(p)-\sigma_1(s)$ appears to show an appreciable increase with increasing ionization, though not as great relatively as $\sigma_1(d)-\sigma_1(p)$. Wentzel[35] has secured, on the basis of the Bohr atom-model, an asymptotic expression for the distance $\Delta(\nu/R)^{1/2}$ between the Moseley ordinates, which he has applied not only to x-ray terms but also to some optical sequences.

In conclusion, the authors wish to express their appreciation to Dr. S. Goudsmit for the valuable advice and criticism they sought and received from him, in the preparation of this paper. Mr. Lang acknowledges gratefully a grant from the Research Council of Canada, to aid him in carrying on this work.

DEPARTMENT OF PHYSICS,
UNIVERSITY OF MICHIGAN (J. E. M., O. L.)

UNIVERSITY OF ALBERTA,
EDMONTON, CANADA (R. J. L.)
February, 1928.

Note added to proof. Gibbs and White (Amer. Phys. Soc. Bull., **3,** 12 (1928) abstract) have identified the levels of the configurations $(4d^{10})$, $(4d^9 5s)$, $(4d^9 5p)$ of the palladium-like spectra Cd III and In IV. Three characteristics of the curves which might be drawn for the palladium-like spectra, corresponding to our Figs. 1 and 2, deserve special notice here:

1. The behavior of the curves is in several respects like that which we would expect for high ionizations in the case of the nickel-like spectra if our Figs. 1 and 2 could be extended to the right. The curvature is much less than in the case of our figures; the sharp curvature near spectrum I, especially, is missing. Several pairs of curves which in Fig. 1 appear to be about to cross, occur in opposite order in the palladium-like sequence; $^3D_2(d^9p)$ is more stable than $^3D_2$ in Pd I, for instance, and its relative stability increases with increasing ionization.

This behavior of the palladium-like sequence as though it were an extension of the nickel-like sequence might be expected from the considerations at the beginning of Chapter VII; it should prove valuable in the classification of the platinum-like spectra.

2. Although the regularities in the l- and s-values, set down in Chapter VI, are for the most part verified in the palladium-like sequence, an exception occurs in the case of the curvature. For each triplet all the levels show similar curvature; but the singlets may no longer be associated with their triplets by the curvature criterion.

3. The ratio of the separations of the $^3D(d^9s)$ term, recorded in Table IX, progresses in the expected direction; in fact, the values in the $(4d^9 5s)$ row run almost exactly parallel to those in the $(3d^9 4s)$ row.

[35] G. Wentzel, Ann. d. Physik **76,** 803 (1925).

THE LOWEST TERMS IN THE SPARK SPECTRUM OF NICKEL AND COPPER (NI II AND CU II)

By R. J. Lang

Abstract

The lowest terms $^2D_{2,3}$ in the spark spectrum of nickel (from the state d^9) are found to lie 6884 and 8391 cm^{-1} below a^4F_5. In the spark spectrum of copper (Cu II) the lowest term is $^1S_0(d^{10})$ and lies 21925 cm^{-1} below a^3D_3.

THE spectra of Ni II and Cu II have been very thoroughly analysed by Shenstone.[1,2] In each of these spectra the lowest term was not found, the lines resulting from combinations between known terms and these lowest terms falling in the region just beyond the absorption of the air.

The author, at the suggestion of Dr. Shenstone, has made a careful search for these lines with the vacuum spectrograph and has succeeded in locating most of them.

Results for Ni II

It was pointed out by Shenstone[1] that the lowest term of the spectrum of Ni II, according to the Hund theory, should be $^2D(d^{10})$ and should have a value of from 5000 to 10,000 cm^{-1} below a^4F_5' which was the lowest term found by him and given zero value. He stated also that its combinations with d^8p might be expected to be very intense.

Several sources were tried including the vacuum-spark, the spark in hydrogen and the inductive vacuum-arc. The latter was found unsatisfactory in the case of nickel. The pure metal was tried and also nickel chloride cored into the pure metal but it was found very difficult to get any radiation from an arc in the region under investigation. All the lines which were obtained appeared also in the spark in hydrogen.

In Table I a summary is given of the results of the investigation in which all the lines are listed which may be expected to appear, whether these were found or not, and the intensities of those found are given for the three types of source used. The term values calculated from the lines found are $^2D_2 = -6884$ $^2D_3 = -8391$. In column two the wave-numbers of the lines calculated from these values for ^2D and Shenstone's values for the terms of d^8p, which may combine with them, are listed and beneath each one the actual wave-number of the line measured is enclosed in brackets. In column three the relative intensity to be expected for each line is given as it was very kindly supplied by Dr. Shenstone to the author.

The intensity of the second, fourth, seventh and twelfth lines is quite anomalous but the wave numbers in all but two cases are remarkably close

[1] Shenstone, Phys. Rev. **30**, 255 (1927).
[2] Shenstone, Phys. Rev. **29**, 380 (1927).

to the calculated values and leave little doubt regarding the validity of the ^2D terms. The term $^2D_3$ should now be given zero value and 8391cm^{-1} added to all the terms of the Ni II spectrum as given by Shenstone.

TABLE I. *Combinations with the low ^2D levels of Ni II. $^2D_2 = -6884$; $^2D_3 = -8391$.*

Designation	ν	Intensity expected	λ(I. A. vac.)	vac. spark	sp. in H_2	arc
$^2D_2-{}^2D_2'$	57195 (96)	strong	1748.37	7	5	1
$^2D_2-{}^2D_3'$	55910 (10)	weak	1788.57	6	4	1
$^2D_3-{}^2D_3'$	57416 (17)	strong	1741.63	7	5	2
$^2D_3-{}^2D_2'$	58702 (03)	weak	1703.49	4	0	
$^2D_2-{}^2F_3$	56983 (83)	strong	1754.90	3	1	0?
$^2D_3-{}^2F_4$	57077 (78)	strong	1751.99	5	5	1
$^2D_3-{}^2F_3$	58490 (89)	weak	1709.72	5	3	1
$^2D_2-{}^4D_2'$	52125	possibly strong				
$^2D_2-{}^4D_3'$	51228 (23)	weak	1952.23	0		
$^2D_2-{}^4D_1'$	52666	weak				
$^2D_3-{}^4D_3'$	52735	possibly strong				
$^2D_3-{}^4D_4'$	51555 (54)	weak	1939.71	4		
$^2D_3-{}^4D_2'$	52632	weak				
$^2D_2-{}^4F_3$	54565 (65)	possibly strong	1832.68	2		
$^2D_2-{}^4F_2$	54914	weak				
$^2D_3-{}^4F_4$	55415 (17)	possibly strong	1804.50	5	1	
$^2D_3-{}^4F_3$	56072	weak				
$^2D_3-{}^4F_2$	56421	very weak				
$^2D_2-{}^4G_3'$	53509	possibly strong				
$^2D_3-{}^4G_4'$	54260	possibly strong				
$^2D_3-{}^4G_3'$	55016 (14)	weak	1817.71	1		
$^2D_3-{}^2G_4'$	56368 (73)	possibly strong	1773.85	6	1	

RESULTS FOR CU II

In the spectrum of Cu II the lowest term[2] should be $^1S_0(d^{10})$ and should lie about 22224 cm^{-1} lower than a^3D_3. The expected combinations are with d^9p and consist of but three lines, one with each of the known terms, $a^3P_1 = 45987.8$, $a^3D_1' = 51173.3$ and $a^1P_1 = 51667.1$. Shenstone states also that the combination with the last of these three terms should give the most intense line.

TABLE II. *Combinations with the lowest term $^1S_0$ of Cu II.*

Designation	λ (I. A. vac.)	ν	arc
$^1S_0-a^3P_1$	1472.48	67913	1
$^1S_0-a^3D_1'$	1368.00	73099	2
$^1S_0-a^1P_1$	1358.84	73592	12

Three lines found in a photograph from an inductive interrupted copper arc in vacuo meet these requirements very well. The strongest of them appears rather intensely in the vacuum spark also but they were not found in the spark in hydrogen because of the absorption of the fluorite window used between the spark chamber and the spectrograph.

The value of the lowest term as calculated from these three lines is $^1S_0 = -21925$. This value should now be added to all the term values of Cu II as listed by Shenstone.

The author's best thanks are due to Dr. Shenstone for supplying him with the information in connection with these spectra and for checking the results. A grant from the Research Council of Canada is also gratefully acknowledged by the author.

UNIVERSITY OF ALBERTA,
EDMONTON, CANADA.
February 23, 1928.

CERTAIN MULTIPLETS IN THE SPECTRA OF CADMIUM III AND INDIUM IV*

By R. C. Gibbs and H. E. White

Abstract

Terms and related wave-lengths and frequencies arising from the configuration d^{10}, d^9s, d^9p of Cd III and In IV.—Guided by the transitions from ^3PDF, ^1PDF, $(4d^95p)$ to ^3D, ^1D $(4d^95s)$ already determined for Pd I and Ag II the corresponding lines have been identified in the spectra of Cd III and In IV. The transitions from $^3D_1$, $^3P_1$ and $^1P_1(4d^95p)$ to $^1S_0(4d^{10})$ the latter being the lowest level in each of these spectra, have also been identified for Ag II, Cd III and In IV. These combinations account for nearly all of the strong lines in each spectrum. The term values for the four iso-electronic systems Pd I, Ag II, Cd III, and In IV, together with those for the corresponding elements in the first long period have been plotted on a Moseley diagram which brings out certain similarities and variations between these two sets of spectra. The validity of the irregular doublet law is again confirmed by the almost constant shift in the corresponding radiated frequencies $(4d^95s-4d^95p)$ on passing in succession from Pd I to Ag II, to Cd III, and to In IV.

THE spectra of cadmium III and indium IV reported in this paper were photographed in this laboratory with a new vacuum spectrograph. A concave glass grating having a radius of curvature of 160 cm ruled and etched at the Johns Hopkins University, with about 15,000 lines to the inch was used. With a Rowland setting a dispersion of 10.5A per mm was obtained at the focal surface. The photographs were made on Schumann glass plates, one by six inches, bent to the focal curve. A thin piece of fluorite, 0.5mm thick, mounted immediately behind the slit, free from sputtering by the spark source, and capable of being rotated into the path of the radiation by means of a tapered rod running to the outside, was used in the region 1300 to 2100A to cut out second order lines from the region below 1300A. By using suitably mounted pairs of electrodes, screened from each other by thin strips of aluminum, and capable of being rotated, raised, and lowered from the outside, several exposures for different elements can be made on the same plate without modifying the vacuum. Usually it is convenient to take three or four exposures on each plate, for example, (1) Cadmium electrodes with fluorite screen, 60 minutes, (2) Cadmium electrodes without screen, 30 minutes, (3) Aluminum electrodes for standards, 15 minutes. If desired a fourth exposure of 5 to 10 minutes can be made for the element being studied, from which more exact measurements of the positions of the stronger lines can be made. An interrupted spark was used so that the actual time of exposure was about 1/10 of that given above.

* This paper was presented at the New York Meeting of the American Physical Society, February 1928.

[1] Data kindly furnished to the authors by A. G. Shenstone in advance of publ cation.

[2] McLennan and Smith, Trans. Roy. Soc. Canada, **20**, 1926.

Recent analysis by Shenstone[1] of Ag II, and the analysis of Pd I as reported by McLennan and Smith[2] and corrected by Shenstone,[1] made the analysis of Cd III and In IV very easy and certain. The normal state of Pd I is given by $(4d^{10})\ {}^1S_0$. Lying just above this are the ${}^3D$ and ${}^1D$ levels of $4d^9 5s$.

TABLE I. *Cadmium III triplets and singlets*

		${}^1S_0$ 000	${}^3D_3$ 80463.2	$(1900.1)\,{}^3D_2$ 82363.3	$(3866.0)\ {}^3D_1$ 86229.3	$(2652.4)\ {}^1D_2$ 88881.7
			15			
			1707.11			
${}^3F_4$	139042		58578.5			
	2817.9		12	15		8
			1793.38	1856.64		2112.31
${}^3F_3$	136224		55760.6	53860.7		47341.4
	6541.3		1?	10	10	9
			1605.08	1655.62	1768.77	1855.84
${}^3F_2$	142765		62302.3	60400.3	56536.5	53883.9
			12	8		9
			1601.50	1651.80		1851.10
${}^3D_3'$	142905		62441.5	60540.0		54021.9
	2464.4		1?	7	12	5
			1667.38	1721.89	1844.67	1939.58
${}^3D_2'$	140441		59974.3	58075.7	54210.2	51557.5
	7196.7	8		7	10	4
		677.33		1532.03	1628.48	1702.02
${}^3D_1'$	147637	147637		65272.9	61406.9	58753.7
			15	3	1?	4
			1874.08	1943.31	2101.17	2225.13
${}^3P_2$	133823		53359.5	51458.6	47592.5	44941.1
	4942.3	8		12	5	6
		720.64		1773.01	1903.52	2004.73
${}^3P_1$	138765	138765		56401.3	52534.5	49882.0
	3358.0				8	
					1789.15	
${}^3P_0$	142123				55892.5	
			5	8		12
			1523.50	1568.92		1747.65
${}^1F_3$	146101		65638.3	63738.1		57219.7
			4	5	7	12
			1470.34	1512.62	1606.59	1678.07
${}^1D_2'$	148475		68011.5	66110.5	62243.6	59592.3
		15		3	5	10
		684.53		1569.33	1670.64	1748.10
${}^1P_1$	146085	146085		63721.5	59857.3	57205.0

Most of the stronger lines of this spectrum result when the transitions take place from ${}^3(PD'F)$ and ${}^1(PD'F)$ levels of $4d^9 5p$ into the levels of these two lower configurations. Lines for the corresponding transitions $4d^9 5p$ into $4d^9 5s$ of Ag II have been identified by Shenstone.[1] The lines

of these triads of singlets and triplets for Pd I lie in the region 3500–3900A, while for Ag II they lie between 2100 and 2600A, being shifted to higher frequencies by approximately 15,000 wave-numbers.

Assuming these multiplets follow relations similar to those for isoelectronic systems in the first long period as previously reported,[3] it was predicted that the corresponding singlets and triplets for Cd III would have wave-numbers about 15,000 larger than those of Ag II. Guided by the relative positions of the lines in Pd I and Ag II, as shown graphically in Fig. 1, the corresponding lines of Cd III, Table I, were easily identified.

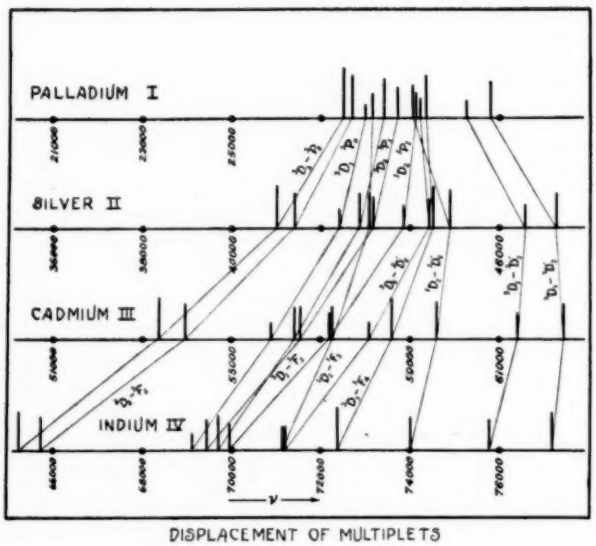

Fig. 1

Inter-combinations between triplets and singlets, as well as relative intensities make certain the assignments and relative positions of the terms arising from the two configurations d^9p and d^9s. With lines of Cd III known, it was an easy matter to indentify the lines of In IV by applying the method of extrapolation shown in Fig. 1, together with relative intensities of lines and common differences between terms.

By a direct analogy with the corresponding elements Ni I,[4] Cu II,[5] and Zn III[6] in the first long period, one would expect to find the most stable electron configuration for Cd III, $(4d^{10})^1S_0$, about 90,000 cm^{-1} lower than $(4d^95s)$. The three combinations with this single level, $^1S_0-{}^1P_1$, $^1S_0-{}^3P_1$ and $^1S_0-{}^3D_1'$ were found at 684.53A, 720.64A, and 677.33A respectively. On the cadmium plates these three lines stand out alone in this region of the spectrum and are very strong. Knowing now the relative positions of $4d^{10}$

[3] Gibbs and White, Proc. Nat. Acad. Sci. **13,** 525 (1927).
[4] Bechert and Sommer, Ann. d. Physik **77,** 367 (1925).
[5] A. G. Shenstone, Phys. Rev. **29,** 383 (1927).
[6] Laporte and Lang, Phys. Rev. **30,** 378 (1927).

and $4d^95p$ for Pd I and Cd III, the $^1S_0(4d^{10})$ level for Ag II and for In IV could be predicted with considerable accuracy from a Moseley diagram as shown in Fig. 2. The three strong lines $^1S_0-{}^1P_1$, $^1S_0-{}^3P_1$, and $^1S_0-{}^3D_1'$ of Ag II were found at 1112.46A, 1195.87A, and 1107.05A respectively, while those for In IV were found at 479.15A, 498.35A, and 472.48A respectively.

TABLE II. *Indium IV triplets and singlets*

		$^1S_0$	$^3D_3$ (2196.8)	$^3D_2$ (4911.7)	$^3D_1$ (2871.3)	$^1D_2$
		000	128785	130981	135893	138764
			15			
			1381.73			
$^3F_4$	201158		72373.0			
	4452.1		5	10		1
			1472.30	1521.52		1725.91
$^3F_3$	196706		67920.9	65723.7		57940.4
	8651.2		1	8	6	4
			1305.99	1344.53	1439.58	1501.66
$^3F_2$	205357		76570.3	74375.4	69464.7	66593.0
			10	7		
			1295.86	1333.82		
$^3D_3'$	205953		77168.8	74972.6		
	3824.0		1	8	7	3
			1363.42	1405.52	1509.74	1578.15
$^3D_2'$	202129		73344.8	71148.0	66236.6	63365.3
	9521.5	10		3	7	3
		472.48		1239.61	1320.00	1372.00
$^3D_1'$	211650	211650.3		80670.5	75757.6	72886.3
			12	?		
			1533.37	1586.82		
$^1P_2$	194004		65215.8	63019.0		
	6658.2	10		7	2	2
		498.35		1435.19	1544.06	1615.67
$^1P_1$	200662	200662.0		69677.2	64764.3	61893.8
	4395.3				7	
					1445.93	
$^1P_0$	205057				69159.6	
			4	5		12
			1233.02	1267.36		1406.05
$^1F_3$	209886		81101.7	78904.2		71121.2
			2	2	5	10
			1190.47	1222.46	1300.54	1351.00
$^1D_2'$	212785		84000.4	81802.3	76891.1	74019.2
		15		3	5	10
		479.15		1286.66	1373.45	1429.83
$^1P_1$	208702	208702.0		77720.6	72809.3	69938.3

The term values given in Tables I and II for Cd III and In IV are taken with respect to $^1S_0$ as zero.

In order to plot a Moseley diagram, however, it was necessary to determine approximately the limits toward which the various levels converge in

series. Having only the first members of any series, extrapolations from the known term values of Ag I were made for Pd I by use of the relations previously reported for the elements in the first long period.[3] The configurations

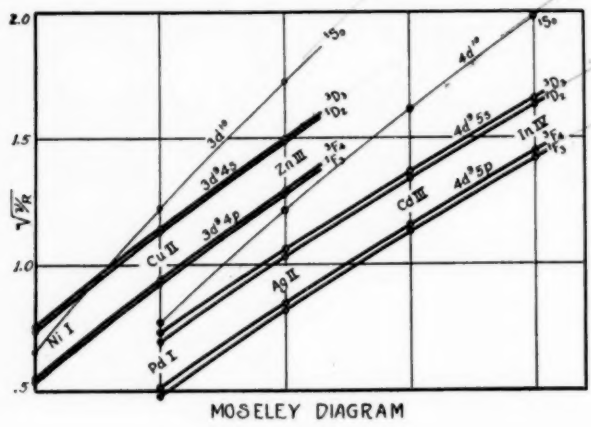

Fig. 2

$4d^{10}$, $4d^95s$, and $4d^95p$ have as a limit $^2D_{2,3}(4d^9)$. The levels $^1S_0(4d^{10})$, $^3D_3$, $^1D_2(4d^95s)$ $^3P_2$, $^3D_3'$, $^3F_4$, $^1P_1$, $^1D_2'$, $^1F_3(4d^95p)$ according to Hund's rule, approach the same level $^2D_3(4d^9)$. The method of extrapolation used to determine the term values given in Table III, is essentially the same as has been explained in a previous report.[7] It will be noted in the alternate columns of this table that the differences in $(\nu/R)^{1/2}$ are remarkably constant between any two elements, except for the $^1S_0$ terms where it should not be the same.

TABLE III. *Values of* $(\nu/R)^{1/2}$

Terms (Limit $4d^9$)		Pd I	Diff.	Ag II	Diff.	Cd III	Diff.	In IV
$4d^{10}$	$^1S_0$	.772	.446	1.218	.397	1.615	.366	1.981
$4d^95s$	$^3D_3$	.732	.330	1.062	.307	1.369	.290	1.659
	$^1D_2$	.699	.333	1.032	.309	1.341	.290	1.631
$4d^95p$	$^3F_4$	.518	.332	.850	.308	1.158	.288	1.446
	$^3D_3'$	.505	.330	.835	.308	1.143	.288	1.431
	$^3P_2$	.534	.334	.868	.310	1.178	.290	1.468
	$^1F_3$	.482	.338	.820	.310	1.130	.289	1.419
	$^1D_2'$	.473	.337	.810	.310	1.120	.289	1.409
	$^1P_1$	.473	.343	.816	.314	1.130	.293	1.423

The regularity with which the term separations increase in going from Pd I to Ag II, to Cd III, and to In IV is given in Table IV. In this sequence of elements the separations are from two to three times the corresponding separations for Ni I, Cu II and Zn III in the first long period. Here also, as in Ni I, Cu II and Zn III, the $^3F_{3,4}$ terms are inverted as may be seen from

[7] Gibbs and White, Phys. Rev., **31**, 520 (1928).

TABLE IV. *Term separations.*

	$^3D_3-{}^3D_2$	$^3D_2-{}^3D_1$	$^3D_1-{}^1D_2$	$^3F_4-{}^3F_3$	$^3F_3-{}^3F_2$	$^3D_3'-{}^3D_2'$	$^3D_2'-{}^3D_1'$	$^3P_2-{}^3P_1$	$^3P_1-{}^3P_0$	$^3D_1'-{}^1D_2'$
Pd I	1191	2339	1628	− 476	3360	− 418	3393	2112	1908	403
Ag II	1577	2998	2306	−1498	4717	−1260	5134	3449	2515	553
Cd III	1900	3866	2652	−2818	6541	−2464	7197	4942	3358	838
In IV	2197	4912	2871	−4452	8651	−3824	9521	6658	4395	1135

Table IV. By the use of extrapolations similar to those discussed above it is planned to extend these investigations to the iso-electronic spectra of Sn V, Sb VI, etc.

Note added to galley proof, March 31, 1928. Since writing this paper a report, dated December 17, 1927, on the spectra of Ag II by Shenstone[8] has been printed, and we have received a reprint of a paper by McLennan and McLay[9] dated January 3, 1928, in which they describe the structure of the spectra of Ag II and make certain corrections to the previous report by McLennan and Smith on the spectra of Pd I. More recently we have received a reprint of a paper by McLennan, McLay and Crawford[10], dated February 8, 1928, in which the transitions $4d^95p$ to $4d^95s$ for Cd III are identified in complete agreement with this report. They did not determine the $^1S_0(4d^{10})$ level.

CORNELL UNIVERSITY,
January 31, 1928.

[8] A. G. Shenstone, Phys. Rev. **31,** 317 (1928).

[9] McLennan and McLay, Trans. Roy. Soc. Canada, **22,** 1 (1928).

[10] McLennan, McLay, and Crawford, Trans. Roy. Soc. Canada, **22,** 45 (1928).

THE ARC SPECTRUM OF GERMANIUM

By C. W. Gartlein

Abstract

Wave-lengths and classification of the lines of the Ge arc spectrum.—The wave-lengths of lines in the germanium arc spectrum have been measured in the region above 1870A with an accuracy of at least 0.03A. From these lines the *relative energy levels* have been determined and transitions corresponding to 73 lines have been identified. In the normal state the germanium atom contains two p valence electrons which give rise to the lower levels $^3P'_{012}$ $^1D_2$ $^1S_0$, with $^3P'_0$ lying deepest as predicted by the theory of Hund. The next higher levels arise from the configurations ps and pd. Data on the persistence of germanium lines were of great value in identification of the levels. At least two members of each of 11 series have been found and approximate limits have been calculated to be 65,300 for $^3P_2$ and 63,600 for $^3P_1$. The first *resonance potential* is 4.65 volts and the *ionization potential* determined by the limit $^3P_1$ is 7.85 volts. The similarities in the arc spectra of Si, Ge, Sn, and Pb are pointed out and the relative term values for these spectra are brought together in a single diagram.

DURING the past few years the arc spectra of silicon, tin, and lead have been analyzed and identified, but little has been done with the arc spectrum of either germanium or carbon. The wave-lengths of the arc lines of germanium have been measured by Rowland and Tatnall and by Exner and Haschek[1] and others to about 2200A. The only analysis attempted was the finding of several constant frequency differences by Paulson.[2]

Since there was available a generous supply of various germanium compounds and of the fused metal, prepared by the Chemistry Department of Cornell University, the author undertook the measurement and analysis of its arc spectrum. From the theory of space quantization the type of spectrum could be predicted; analogy with silicon gave the separations to be expected; and data on the persistence of germanium lines suggested the transitions into the lowest levels.

Theoretical Considerations

According to the Bohr-Stoner scheme of building up the atom the elements of the fourth group each contain two p valence electrons in the normal state and according to the theory of Pauli, Hund, and others it is these p electrons which determine the lowest levels. The levels arising from p electrons given by Hund[3] and by McLennan, Smith, and McLay[4] are $^3P'_{012}$, $^1D_2$, $^1S_0$ with $^3P_0'$ lying deepest.

In the Bohr-Stoner scheme electrons are added in the following order for elements after germanium, p electrons for As, Se, Br, and Kr, s electrons for

[1] Kayser, Handbuch der Spectroscopie, Vol. 5, p. 470.
[2] E. Paulson, Ann. d. Physik, **45**, 419 (1914).
[3] Hund, Zeits. f. Physik **33**, 355 (1925).
[4] McLennan, Smith and McLay, Proc. Roy. Soc. **A112**, 76 (1926).

Rb and Sr and then *d* electrons from Yt to Cd. If one of the *p* valence electrons of the normal atom of germanium is excited, it seems likely that it will go into an orbit which would be occupied by the next tightest bound electron, an *s* orbit, or if excited higher, into a *d* orbit, or a higher *p* orbit. We would expect the next higher levels to be determined by these two valence electrons, one of them still in a *p* orbit but the other displaced successively into *s*, *d*, and *p* orbits. These higher levels would be $^3P_{012}$, $^1P_1$ from a *ps* configuration, $^3F_{234}$, $^3D'_{123}$, $^3P_{012}$, $^1F_3$, $^1D_2'$, $^1P_1$, from a *pd* configuration and $^3D_{123}$, $^3P'_{012}$, $^3S_1$, $^1D_2$, $^1P_1'$, $^1S_0$, from a *p*-*p* configuration. Thus the lowest levels of the normal state are a $^3P'$ and those of the lowest excited state are a ^3P, so a $^3PP'$ multiplet of six lines should contain the strongest lines as well as the most persistent or ultimate lines.

Measurements

Using a six foot concave grating, ruled to give high intensity in the region near 2000A and set up on a Rowland mounting, the arc spectrum produced by germanium metal or germanium dioxide in carbon or aluminum electrodes was photographed below 4700A on Eastman 33 plates and Schumann plates. The glass plates were thin enough to withstand bending to the focal curve during the exposure. The Eastman plates were sensitized with a very thin film of fluorescent oil (Liquid Veneer Furniture Polish) to photograph the region below 2200A. Exposures of 5 minutes gave lines to 1895A, including about 40 new lines below 2200A, while a 15 sec. exposure gave the lines at 2600A. The oiled plates were about one-third as sensitive as the Schumann plates which were later used, but were far superior to unoiled plates.

In measuring the plates iron arc lines were used as standards above 2300A. On the first measures below 2300A silicon lines,[5] which were the only impurity in the germanium spectrum, were used as standards along with the lines from the aluminum spark. The wave-lengths of these lines are not known with sufficient accuracy for use in final measurements. Silver spark lines were used after their wave-lengths were measured on several plates in the second order against iron standards. The wave-lengths of these silver standards will be published in a separate paper. Professor A. G. Shenstone[6] determined wave-lengths of certain copper lines by a different method. Some of these copper lines were present in the germanium spectrum as impurities from the carbons used to hold the electrodes and when measured, using silver standards, the author obtained the wave-lengths given by Professor Shenstone within 0.01 to 0.02A.

The Ge lines were very sharp and characteristic so that they could be separated from the lines due to impurities in the electrodes. The dispersion was about 4.6A per mm so that with a Gaertner comparator reading to 0.001 mm the setting errors amounted to about 0.01A and the absolute

[5] A. Fowler, Phil. Trans. Roy. Soc. **225, 1** (1926).
[6] Shenstone, Phys. Rev. **29**, 380–390 (1927).

wave-lengths are accurate to at least 0.03A as the variation in the frequency differences in Table II indicates.

Table I contains the wave-lengths of all the lines, with the relative intensities in the first column, the wave-lengths in I.A. (in air) in the second, the wave-numbers in vacuo in the third, the persistence in the fourth, and the

TABLE I. *Wave-lengths in the germanium arc.*

Int.	λ (air)	I. A.	ν (vac)	Persistence	Transition
20	4685.86	21334.9	1.f	$4p^2$ $^1S_0-4p5s^3P_1$
50	4226.60	23653.0	.001	$4p^2$ $^1S_0-4p5s^1P_1$
40	3269.51	30576.8	.001f	$4p^2$ $^1D_2-4p5s^3P_1$
20	3124.82	31992.6	.1	$4p^2$ $^1D_2-4p5s^3P_2$
10	3067.04	32595.3	.1	$4p^2$ $^1S_0-4p4d^3D_1'$
60	3039.07	32895.3	.0001	$4p^2$ $^1D_2-4p5s^1P_1$
9	2829.00	35337.8	.01f	$4p^2$ $^1S_0-4p4d^3P_1$
10	2793.93	35781.4	1.	$4p^2$ $^1S_0-4p6s^3P_1$
50	2754.59	36292.3	.001	$4p^2$ $^3P_2'-4p5s^3P_1$
20	2740.43	36479.9	.1	$4p^2$ $^1S_0-4p4d^1P_1$
40	2709.63	36894.5	.001	$4p^2$ $^3P_1'-4p5s^3P_0$
30	2691.35	37145.1	.1	$4p^2$ $^3P_1'-4p5s^3P_1$
20	2651.57	37702.3	.0001f	$4p^2$ $^3P_0'-4p5s^3P_1$
30	2651.19	37707.7	.0001	$4p^2$ $^3P_2'-4p5s^3P_2$
8	2644.20	37807.4	.1	$4p^2$ $^1S_0-4p6s^1P_1$
30	2592.54	38560.8	.001	$4p^2$ $^3P_1'-4p5s^3P_2$
12	2589.19	38610.6	.1f	$4p^2$ $^3P_2'-4p5s^1P_1$
10	2556.32	39107.0	1.	$4p^2$ $^1S_0-4p5d^3D_1$
15	2533.23	39463.4	.1	$4p^2$ $^3P_1'-4p5s^1P_1$
15	2497.97	40020.4	.1	$4p^2$ $^3P_0'-4p5s^1P_1$
5	2436.41	41031.5	1.	$4p^2$ $^1S_0-4p7s^3P_1$
20	2417.37	41354.7	.001f	$4p^2$ $^1D_2-4p4d^3D_3'$
6	2397.90	41690.5	1.	$4p^2$ $^1S_0-4p5d^1P_1$
4	2394.09	41756.8	.1f	$4p^2$ $^1D_2-4p4d^3F_2$
5	2389.48	41837.4		$4p^2$ $^1D_2-4p4d^3D_1$
12	2379.14	42019.2		$4p^2$ $^1D_2-4p4d^3F_3$
4	2359.22	42373.9	.01f	$4p^2$ $^1S_0-4p7s^1P_1$
4	2338.61	42747.3	.1f	$4p^2$ $^1S_0-aP_1$
15	2327.92	42943.6	1.	$4p^2$ $^1D_2-4p4d^3D_3'$
0	2316.44	43156.4		
10	2314.20	43198.2	.1f	$4p^2$ $^1D_2-4p4d^3D_3'$
1	2305.59	43359.5		
00(?)	2262.71	44181.2		
5	2256.00	44312.5		$4p^2$ $^1D_2-4p4d^3P_2$
00(?)	2252.76	44376.2		
1	2252.43	44382.7		
2Cu?	2247.03	44489.4		
2	2242.47	44579.8		$4p^2$ $^1D_2-4p4d^3P_1$
0(?)	2232.27	44783.5		
2	2222.73	44975.7		
4	2220.39	45023.1		$4p^2$ $^1D_2-4p6s^3P_1$
15R	2198.73	45466.6	.1f	$4p^2$ $^1D_2-4p4d^1F_3$
5	2186.46	45721.7		$4p^2$ $^1D_2-4p4d^1P_1$
1	2136.71	46786.1		$4p^2$ $^1D_2-4p6s^3P_2$
5δ	2124.76	47049.2		$4p^2$ $^1D_2-4p6s^1P_1$

Int.	λ(air)	I. A.	ν(vac)	Presistence	Transition
3	2123.83		47069.8		$4p^2$ $^3P_2'-4p4d^1D_2'$
5	2105.83		47472.1		$4p^2$ $^3P_2'-4p4d^3F_3$
3	2102.26		47552.7		$4p^2$ $^3P_2'-4p4d^3D_1'$
10R	2094.27		47734.1		$4p^2$ $^3P_2'-4p4d^3F_4$
5	2086.03		47922.6		$4p^2$ $^3P_1'-4p4dF^1D_2'$
0	2071.98		48247.6		
9R	2068.66		48325.0		$4p^2$ $^3P_1'-4p4d^3F_2$
3	2067.63		48349.1		$4p^2$ $^1D_2-4p5d^3D_1$
6R	2065.22		48405.5		$4p^2$ $^3P_1'-4p4d^3D_1$
2	2058.59		48561.1		
5R	2057.25		48593.0		$4p^2$ $^1D_2-4p5d^3F_4$
5	2054.46		48658.9		$4p^2$ $^3P_2'-4p4d^3D_3'$
7R	2043.79		48912.9		$4p^2$ $^3P_2'-4p4d^3D_3'$
8R	2041.72		48962.2		$4p^2$ $^3P_2'-4p4d^3D_2$
6R	2019.08		49511.5		$4p^2$ $^3P_1'-4p4d^3D_2'$
4R	2011.31		49702.7		$4p^2$ $^1D_2-4p5d^3D_2'$
1	2007.55		49795.8		
0(?)	1999.65		49992.4		
7R	1998.25		50027.5		$4p^2$ $^3P_2'-4p4d^3P_2$
2	1997.18		50054.3		
1	1988.48		50273.2		$4p^2$ $^1D_2-4p7s^3P_1$
4R	1987.64		50294.5		$4p^2$ $^3P_2'-4p4d^3P_1$
2	1987.22		50305.1		$4p^2$ $^1D_2-4p5d^3D_2'$
0(?)	1972.00		50693.2		$4p^2$ $^1D_2-4p5d^3P_2$
4δ	1970.26		50738.0		$4p^2$ $^3P_2'-4p6s^3P_1$
2	1964.76		50880.2		$4p^2$ $^3P_1'-4p4d^3P_2$
1	1962.76		50932.1		$4p^2$ $^1D_2-4p5d^1P_1$
6R	1961.40		50967.4		$4p^2$ $^1D_2-4p5d^1F_3$
4R	1954.49		51147.5		$4p^2$ $^3P_2'-4p4d^3P_1$
0	1953.19		51181.5		$4p^2$ $^3P_2'-4p4d^1F_3$
2R	1944.11		51423.1		$4p^2$ $^3P_1'-4p6s^3P_0$
1	1943.50		51436.6		$4p^2$ $^3P_2'-4p4d^1P_1$
3R	1937.68		51591.1		$4p^2$ $^3P_1'-4p6s^3P_1$
3R	1936.87		51612.6		$4p^2$ $^3P_1'-4p4d^3P_0$
2	1933.42		51704.7		$4p^2$ $^3P_0'-4p4d^3P_1$
4R	1929.23		51817.0		
0δ	1922.87		51988.3		$4p^2$ $^1D_2-aP_1$
3	1916.97		52148.3		$4p^2$ $^3P_0'-4p6s^3P_1$
0	1911.80		52289.3		$4p^2$ $^3P_1'-4p4d^1P_1$
1	1904.09		52500.9		$4p^2$ $^3P_2'-4p6s^3P_2$
0(?)	1899.34		52632.4		
0	1894.61		52763.9		$4p^2$ $^3P_2'-4p6s^1P_1$
0	1889.83		52897.3		
0	1873.62		53354.6		$4p^2$ $^3P_1'-4p6s^3P_2$

transitions in the fifth. The intensities at the short wave-lengths could not be accurately related to those at longer wave-lengths because of the different sensitivities of the two kinds of plates used.

METHOD OF ANALYSIS AND RESULTS

Hicks has shown that for elements in the same group of the periodic table the separations of similar doublets or triplets are nearly proportional to the squares of the atomic weights. In silicon[5] the separations of the lowest $^3P'$ levels are 77 and 146 wave-numbers, so that we should expect separations about 6 times as great in germanium or about 470 and 890 wave-numbers. The PP' multiplet in silicon is located near 2500A so we should expect the multiplet in Ge at a slightly greater wave-length. This alone would indicate the strong lines from 2592A to 2754A as constituting the PP' multiplet. Persistence data verify this guess.

Professor Jacob Papish, Dr. F. M. Brewer, and Mr. Donald Holt of the Chemistry Department of Cornell University have recently worked out the persistence of the germanium lines and kindly allowed the use of their data in advance of publication.[7] Working with solutions they placed small quantities of a germanium compound in the arc and photographed the spectra, noting the quantity of germanium responsible for a given spectrogram. The most persistent spectral lines are those which show when the smallest quantities of the material are present in the zone of excitation. These data are reproduced in the fourth column of Table I. The persistence is there given as the fraction of a milligram of germanium which is just sufficient to make the line appear in a spectrogram. The letter *f* after the figure indicates that the line was visible, but faint with that amount of Ge.

Arranging the most persistent lines around 2650A as a *PP'* multiplet gave separations of nearly 557 and 853 wave-numbers between the lower levels, and very close to the predicted values. This multiplet appears at the top of Table II. The work on the relative levels was begun by assigning the

TABLE II.

	$4p^2\ ^3P_0'$ 0	Δ 557.1	$4p^2\ ^3P_1'$ 557.1	Δ 852.9	$4p^2\ ^3P_2'$ 1410.0	Δ 5715.0	$4p^2\ ^1D_2$ 7125.0	Δ 9242.1	$4p^2\ ^1S_0$ 16366.9
$4p5s\ ^3P_0$ 37451.6			40 2709.63 36894.5						
$4p5s\ ^3P_1$ 37702.1	20 2651.57 37702.3	7.2	30 2691.35 37145.1	2.8	50 2754.59 36292.3	5.5	40 3269.51 30576.8	1.9	20 4685.86 21334.9
$4p5s\ ^3P_2$ 39117.7			30 2592.54 38560.8	3.1	30 2651.19 37707.7	5.1	20 3124.82 31992.6		
$4p5s\ ^1P_1$ 40020.3	15 2497.97 40020.4	7.0	15 2533.23 39463.4	2.8	12 2589.19 38610.6	5.3	60 3039.07 32895.3	2.3	50 4226.60 23653.0
$4p4d\ ^1D_2'$ 48479.7			5 2086.03 47922.6	2.8	3 2123.83 47069.8	5.1	20 2417.37 41354.7		
$4p4d\ ^3F_2$ 48882.0			9δR 2068.66 48325.0	2.9	5δ 2105.83 47472.1	5.3	4 2394.09 41756.8		
$4p4d\ ^3D_1'$ 48962.4	8R 2041.72 48962.2	6.7	6R 2065.22 48405.5	2.8	3 2102.26 47552.7	5.3	5 2389.48 41837.4	2.1	10 3067.04 32595.3
$4p4d\ ^1F_3$ 49144.2					10δR 2094.27 47734.1	4.9	12 2379.14 42019.2		
$4p4d\ ^3D_2'$ 50068.7			6R 2019.08 49511.5	2.6	5 2054.46 48658.9	5.3	15 2327.92 42943.6		

[7] Jacob Papish, F. M. Brewer, and Donald Holt, Jour. Amer. Chem. Soc. **49**, 3028 (1927).

TABLE II. (Continued)

	$4p^2\ ^3P_0'$ 0	Δ 557.1	$4p^2\ ^3P_1'$ 557.1	Δ 852.9	$4p^2\ ^3P_2'$ 1410.0	Δ 5715.0	$4p^2\ ^1D_2$ 7125.0	Δ 9242.1	$4p^2\ ^1S_0$ 16366.9
$4p4d\ ^3D_3'$ 50323.1					7*R* 2043.79 48912.7	4.7	10 2314.20 43198.2		
$4p4d\ ^3P_2$ 51437.4			2 1964.76 50880.2	2.7	7*R* 1998.25 50027.5	5.0	5 2256.00 44312.5		
$4p4d\ ^3P_1$ 51704.7	2 1933.42 51704.7	7.2	4*R* 1954.49 51147.5	3.0	4*R* 1987.64 50294.5	4.7	2 2242.47 44579.8	2.0	9 2829.00 35337.8
$4p6s\ ^3P_0$ 51980.2			2*R* 1944.11 51423.1						
$4p6s\ ^3P_1$ 52148.2	3δ 1916.97 52148.3	7.2	3*R* 1937.68 51591.1	3.1	4δ 1970.26 50738.0	4.9	4 2220.39 45023.1	1.7	10 2793.93 35781.4
$4p4d\ ^3P_0$ 52169.7			3*R* 1936.87 51612.6						
$4p4d\ ^1F_3$ 52591.6					0 1953.19 51181.5	4.9	15*R* 2198.73 45466.6		
$4p4d\ ^1P_1$ 52846.7			0 1911.80 52289.3	2.7	1 1943.50 51436.6	4.9	5 2186.46 45721.7	1.8	20 2740.43 36479.9
$4p6s\ ^3P_2$ 53911.0			0 1873.62 53354.6	3.7	1 1904.09 52500.9	4.8	1 2136.71 46786.1		
$4p6s\ ^1P_1$ 54174.3					0 1894.61 52763.9	4.9	5 2124.76 47049.2	1.8	8 2644.20 37807.4
$4p5d\ ^3D_1'$ 55474.0							3 2067.63 48349.1	2.1	10 2556.32 39107.0
$4p5d\ ^3F_3$ 55718.0							5*R* 2057.25 48593.0		
$4p5d\ ^1D_2'$ 56827.7							4*R* 2011.31 49702.7		
$4p7s\ ^3P_1$ 57398.3							1 1988.48 50273.2	1.7	5 2436.41 41031.5
$4p5d\ ^3D_3'$ 57430.1							2 1987.22 50305.1		
$4p5d\ ^3P_2$ 57818.2							0 1972.00 50693.2		

TABLE II. (Continued)

	$4p^2\ {}^3P_0'$ 0	Δ 557.1	$4p^2\ {}^3P_1'$ 557.1	Δ 852.9	$4p^2\ {}^3P_2'$ 1410.0	Δ 5715.0	$4p^2\ {}^1D_2$ 7125.0	Δ 9242.1	$4p^2\ {}^1S_0$ 16366.9
$4p5d\ {}^1P_1$ 58057.3							1 1962.76 50932.1	1.6	6 2397.90 41690.5
$4p5d\ {}^1F_3$ 58092.4							6R 1961.40 50967.4		
$4p7s\ {}^1P_1$ 58740.8									4 2359.22 42373.9
aP_1 59113.8							0δ 1922.87 51988.3	1.0	4 2338.61 42747.3

value zero to the lowest ${}^3P_0'$ level and the values of ${}^3P_1'$ and ${}^3P_2'$ were determined from two separations in the multiplet. The values of the ${}^3P$ levels were established, the ${}^3P_1$ by three lines and the ${}^3P_2$ by two lines. The great persistence of 2709.63A at once identified it as the transition ${}^3P_1'-{}^3P_0$. It should be noted that this is the only transition possible from ${}^3P_0$. The wave-numbers of all the lines in the spectrum were plotted on a large graph, and a search made for triplets with the two separations 853 and 557 wave-numbers. Five such triplets were found, as well as seven pairs of separation 853. One of the triplets, 2497.97A, 2533.23A, and 2589.19A is just below the multiplet, so it must be a transition from a level just above the ${}^3P$ levels, and seems to be from the predicted ${}^1P_1$ level. The lines of this triplet are of the same persistence but less persistent than the lines of the ${}^3PP'$ multiplet. If this upper level defined by the triplet is the ${}^1P_1$, we should also find transitions from it into the predicted ${}^1S_0$ and ${}^1D_2$ levels. These lines should be above the multiplet, perhaps several hundred Angstroms. The lines at 4226A and 3039A are among the very persistent lines in the spectrum, and might correspond to ${}^1S_0-{}^1P_1$ and ${}^1D_2-{}^1P_1$. These lines would set the values of the ${}^1S_0$ and ${}^1D_2$ as 16367 and 7125 cm^{-1}. Transitions from the ${}^3P_1$ level into these lower levels should give lines at 21334 and 30576 cm^{-1}. The lines at 4685.86 and 3269.51A are in these positions and correspond to ${}^1S_0-{}^3P_1$ and ${}^1D_2-{}^3P_1$, while the line at 3124.82A corresponds to ${}^1D_2-{}^3P_2$. Thus we have established the five levels of the normal state, ${}^3P_0'$ at 0, ${}^3P_1'$ at 557, ${}^3P_2'$ at 1410, ${}^1D_2$ at 7125, and ${}^1S_0$ at 16367 and the four levels ${}^3P_{012}$ and ${}^1P_1$ of the first excited state. The higher levels in Table II were worked out by searching for all the possible wave-number differences between the five lower levels. Since the lower levels have been identified, the upper levels can usually be identified by applying the usual selection rules, that $\Delta k = \pm 1$ or 0, (sometimes violated), and $\Delta j = \pm 1$ or 0, (except that the transition from $j=0$ to $j=0$ is barred); and by applying the intensity rule, that the most intense lines occur when changes in j and k are in the same direction. The persistence

data verify these rules nicely in most cases, and also show that the transitions within the singlet system or within the triplet system are more persistent than similar transitions between the two systems. The line 2691.35, $^3P_1' - {}^3P_1$ is not as persistent as might be expected.

The final identification of terms was made more certain by comparison with the arc spectrum of tin as published by E. Back[8] and Green and Loring.[9] In cases of uncertainty, where intensity rules would permit a choice between two possible identifications, the energy level was identified by comparison with the tin spectrum. The level $4p4d^1D_2'$, 48479.7 was identified by the great persistence of the line 2417.37A which indicated that this line was a transition between singlet terms.

In Table II the values of the lower levels are given at the top of the table, with the differences between the levels in the columns headed Δ, while the term values of the higher levels are given at the left side of the table, with the radiations resulting from transitions into the lower levels opposite these term values. Each radiation is indicated by three numbers; the upper is the relative intensity, the second the wave-length in I.A. in air, and the third the wave-number in vacuum. The difference between the levels at the top of the table is in each case the average of the differences corresponding to transitions from a common level into two adjacent lower levels. The term values of the five lowest levels were found by successive addition of these average differences. The variations in the differences in the Δ columns indicate the accuracy of measurement and are nearly all within 1 wave-number.

It is believed that two members of each of four series of lines are represented by electron configurations $4p5s$, and $4p6s$. Series from these configurations are generally Rydbergian, so approximate limits can be calculated using a Rydberg table. The terms $4p5s^3P_2$, 39117.7 and $4p6s^3P_2$, 53911.0 give the limit 65910 cm^{-1} above $4p^2\,{}^3P_0$. The theory of Hund predicts that these terms as well as all singlet terms will approach the upper series limit. The levels $4p5s^1P_1$, 40020.3, and $4p6s^1P_1$, 54174.3 give the limit 65895 cm^{-1}. The level $4p7s^1P_1$, 58740.8 seems a possible third member of this series. The limit calculated from the second and third members is 65016 cm^{-1}. The levels $4p5s^3P_1$, 37702.1 and $4p6s^3P_1$, 52148.2 give the lower limit 64000 cm^{-1}, while the limit calculated from $4p6s^3P_1$, and the possible third member $4p7s^3P_1$, 57398.3 is 64193 cm^{-1}. Using 64100 cm^{-1} as an approximate lower limit, a prediction was made for the transition from $4p6s^3P_0$ into $4p^2\,{}^3P_1'$ and a reversed line 51423.1 cm^{-1} was found near the predicted position. It was chosen because it was the only strong unidentified line in this region. The terms $4p5s^3P_0$, 37451.6 and $4p6s^3P_0$, 51980.2, give 63867 cm^{-1} as the value of the limit.

In the spectra of silicon, tin, and lead the series limits, from the first two terms, for the levels of the *pd* configurations are several hundred wave-numbers below the limits derived from the *ps* configurations. Thus by

[8] E. Back, Zeits. f. Physik **43**, 309 (1927).

[9] J. B. Green and R. A. Loring, Phys. Rev. **30**, 574 (1927).

choosing a lower limit than that suggested by the *ps* terms the possible series were quite easily identified and a maximum number of the stronger lines could be arranged in series. The value 65300 cm^{-1} was taken for the upper limit and 63600 cm^{-1} for the lower limit. The series thus identified are grouped with those from the *ps* configurations in Table III. The series

TABLE III. *Series approaching the upper limit* $(^2P_2) = 65300$.

	ps $^3P_2$	*ps* $^1P_1$	*pd* $^1D_2'$	*pd* $^1F_3$	*pd* $^1P_1$	*pd* $^3D_3'$	*pd* $^3P_2$
Levels	39118	40020	48480	52592	52846	50323	51437
Term Values	26182	25280	16820	12708	12454	14977	13863
Rydberg Den.	2.047	2.083	2.554	2.938	2.968	2.706	2.813
	53911	54174	56828	58092	58057	57430	57818
	11389	11126	8472	7208	7243	7870	7482
	3.103	3.140	3.598	3.901	3.891	3.733	3.829
		58741					
		6559					
		4.089					
Limit predicted from 1st and 2nd terms	65831	65896	65640	65068	64823	65488	65405
From 2nd and 3rd		65016					

Series approaching the lower limit $(^2P_1) = 63600$.

	ps $^3P_1$	*ps* $^3P_0$	*pd* $^3P_1$	*pd* $^3P_0$	*pd* $^3D_2'$	*pd* $^3D_1'$	*pd* $^3F_3$	*pd* $^3F_2$
Levels	37702	37452	51704	52169	50069	48962	49144	48882
Term Values	25898	26148	11896	11431	13531	14638	14456	14718
Rydberg Den.	2.058	2.048	3.036	3.098	2.847	2.737	2.754	2.730
	52148	51980				55474	55718	
	11452	11620				8126	7882	
	3.095	3.072				3.674	3.730	
	57398							
	6202							
	4.205							
Limit predicted from 1st and 2nd terms	63998	63866				63147	63396	
2nd and 3rd	64193							

approaching the upper limit are given in the upper half of the table. The wave-number of the level is given for the first member of the series, then its term value, obtained by subtracting the value of the level from the limit, and below this the Rydberg denominator, $(\nu/R)^{1/2}$. Below these figures the same data are given for the second and third members of the series. The limit predicted from the 1st and 2nd series members are then given and below it, in a few cases, the limit predicted from the second and third members. The lower half of Table III contains similar data for the series and terms approaching the lower limit.

The average of the limits obtained from the series is about 100 wave-numbers above those chosen, but the values derived from the early members of the series are valuable only as a clue to the real limit obtained from the higher terms. The ionization potential is therefore about 7.85 volts and the resonance potential is 4.65 volts.

The first two members of most of these series are believed to be correctly identified, but the selection for the third members is doubtful. The difference

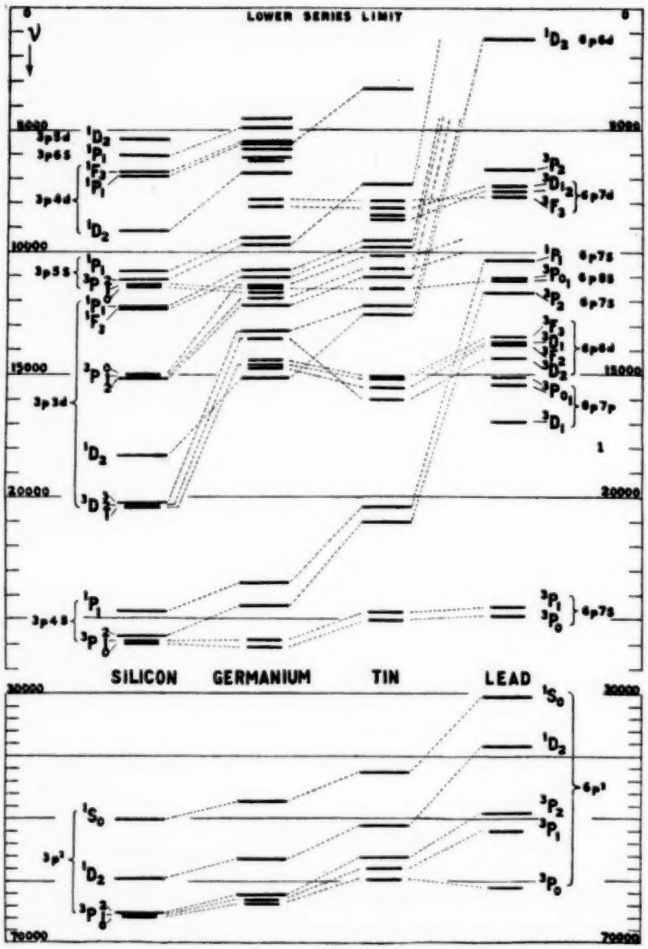

Fig. 1 Energy levels of the elements of the fourth group. The arc spectra.

1700 between the chosen limits is in fair agreement with the separation of the lowest terms in the germanium spark predicted from a comparison of the separations in silicon, tin, and lead. Assuming that these separations are proportional to the square of the atomic weights of the elements, a calculation using the values 287 for silicon and 4253 for tin gave the value 1800 for germanium. No attempt has been made to work out formulae for the series as the identifications did not warrant this.

A diagram of the energy levels of the arc spectra has been drawn (Fig. 1) for the elements of the fourth group. The data on silicon were obtained from Professor H. N. Russell,[10] that on germanium from the author's measurements, that on tin from Back[8] and Green and Loring[9], and the data on lead from Gieseler and Grotrian[11] and E. Back.[12] The four energy level diagrams have been combined in a larger diagram so that their lower series limits coincide at the top and they are set at $\nu=0$. The names of the elements separate the levels of the normal state from those of the excited states. The scale of frequencies above this division is 4 times as large as the scale below and 3000 wave-numbers have been omitted from the graph at the break in the scale. The configurations are indicated both on the left and the right of the diagram. The energy levels which approach the upper limit, according to the theory of Hund, are indicated by a line of slightly greater length than the lines representing the levels which approach the lower limit. The dotted lines connect similar terms in the four spectra.

The regularities of the spectra are brought out in this diagram. 1. The configurations and terms are those predicted by the recent theories and in general both are in the predicted order. 2. As the atomic number increases, the terms approaching the upper limit separate more and more from those

TABLE IV. *Comparison of triplet separations.*

	Separations in Si	Ratio Ge/Si	Separations in Ge	Ratio Sn/Ge	Separations in Sn	Ratio Pb/Sn	Separations in Pb
Atomic number	14	2.29	32	1.56	50	1.64	82
Square of at. no.	196	5.22	1024	2.44	2500	2.69	6724
Term Difference							
$3p^2$ $(^3P_2'-{}^3P_0')$	223	6.317	1410	2.43	3428	3.11	10648
$3p^2$ $(^3P_2'-{}^3P_1')$	146	5.84	853	2.04	1736	1.63	2831
$3p4s$ $(^3P_2-{}^3P_0)$	272	6.13	1666	2.39	3988	3.32	13228
$3p4s$ $(^3P_2-{}^3P_1)$	195	7.26	1416	2.62	3714	3.47	12901
$3p3d$ $(^3P_0-{}^3P_2)$	111	6.59	732	1.11	816		
$3p3d$ $(^3P_1-{}^3P_2)$	67	6.93	465	1.65	303		
$3p5s$ $(^3P_2-{}^3P_0)$	273	7.06	1931				
$3p5s$ $(^3P_2-{}^3P_1)$	218	8.09	1763	2.38	4196		

approaching the lower limit, especially in the excited states. 3. The singlets always lie above the triplets of the same azimuthal quantum number in a given (in each) configuration, (one exception in germanium). 4. Some of the levels of the *pd* configuration invert as the atomic number increases. 5. The separations of the triplets of the p^2 and *ps* configurations are roughly proportional to the squares of the atomic number, especially the $^3P_0$ to $^3P_2$ separation for germanium and tin, as is shown in Table IV. The separations

[10] Professor H. N. Russell kindly furnished the author with his unpublished analysis of the silicon spectrum using data of Fowler[8] corrected.

[11] H. Gieseler and W. Grotrian, Zeits. f. Physik **34**, 374; (1925); **39**, 377 (1926).

[12] E. Back, Zeits. f. Physik **37**, 193 (1926).

are given in a column under the name of the element, and the ratios of the separations for adjoining elements are given in the columns marked ratios. In Table IV the ratios of the separations of the levels of the *pd* configuration for Ge and Sn do not even approximate the ratio of the squares of the atomic number. This may indicate an incorrect assignment of terms in one of these elements. A preliminary analysis of the first spark spectrum of Ge indicates that the separations of the doublet terms of Ge and of the first spark spectrum of Sn are almost exactly in the ratio of the squares of their atomic numbers.

A Schüler tube has been constructed and will be used to study the higher terms of the germanium arc and the entire first spark spectrum and possibly part of the second spark. Gratings will be used to photograph the spectra to 10000A.

Shortly after the results contained in this paper were presented before the meeting of the American Physical Society in December, 1926, a reprint of a paper by McLennan and McLay[13] containing their analysis of the germanium arc spectrum was received. Their analysis covered the lower 12 levels but the identifications are somewhat different from those given in this paper.

More recently a very short paper on the wave-lengths of the germanium arc was published by Richter[14] but only the frequency differences between the lowest 5 levels were given. They are almost identical with those given in this paper.

The author wishes to express his gratitude for the suggestions and assistance given by Professor R. C. Gibbs and Mr. H. E. White, for the assistance in identification of series given by Professor H. N. Russell, for the use in advance of publication of the persistence data by Professor J. Papish, Mr. F. M. Brewer, and Mr. D. Holt, and to the Department of Chemistry of Cornell University for the germanium.

DEPARTMENT OF PHYSICS,
CORNELL UNIVERSITY,
ITHACA, N. Y.
January 26, 1928.

Correction in proof. The $^3P_{012}$ terms of the *pd* configuration approach the upper series limit and should be represented by long lines in Fig. 1. The terms *pd* $^3P_0$ and *pd* $^3P_1$ should be placed in the upper half of Table III. The apparent anomaly in the ratio of the separations of the terms in Sn and Ge is also accounted for and the identifications are probably correct.

[13] J. C. McLennan and A. B. McLay, Trans. of Royal Society of Canada **20**, Sec. 3, p. 355 (1926).

[14] Richter: Naturwissenschaften, p. 266 (March 18, 1927).

THE FLUORESCENCE SPECTRUM OF SODIUM VAPOR IN THE VICINITY OF THE D LINES

By R. W. Wood and E. L. Kinsey

Abstract

Excitation of sodium *D* lines by monochromatic radiation.—When sodium vapor is mixed with hydrogen, air or nitrogen at pressures between 2 and 3 mm it is possible to excite the *D* lines by radiation in the region 5100 to 5250A. Since this radiation is absorbed only by the sodium molecules it is probable that the primary act is the excitation of the molecule. The excited molecule may then cause the *D* line emission by collisions of the second kind with atoms, or by dissociating, either spontaneously or as a result of collisions with the foreign gas, into a normal and an excited atom. To distinguish between these processes further experiments are necessary.

Conditions governing the appearance of a certain fluorescence band-group in the yellow.—A band-group formerly studied by one of us was found to appear in the yellow region of the fluorescence spectrum under white light stimulation when nitrogen or hydrogen was present at a pressure of 6 ± 1 mm and indications are that they are excited by light of their own wave-length. The experiments also verify completely the older work of Wood and Galt on a cathode ray spectrum. Photographs of the absorption spectrum and other considerations indicate that these bands are not the bands ascribed by Barratt and Pringsheim to a sodium-potassium molecule.

I. Introduction

THE spectrum of fluorescing sodium vapor has been thoroughly investigated in a series of previous researches by one of us.[1] Since these researches were undertaken at a time when the present quantum theory of band spectra was unknown, it seemed advisable that some of the results be re-examined and that additional experiments suggested by the present theory be carried out. The fluorescence spectrum, which is attributed to an emitting molecule, exhibits the following general features. Under white-light excitation two major band-groups appear, a band-group in the violet and blue-green region of the spectrum, and a band-group in the red. A region of non-luminosity previously designated by one of us as the "chasm" separates these regions and is bounded on its long wave-length edge by the *D* lines, which appear in the fluorescence spectrum under conditions where they are not reversed. It was found further by one of us that the character of the fluorescence spectrum was greatly affected by the introduction of foreign gases such as hydrogen and nitrogen into the fluorescing vapor.

The present paper describes (1) experiments in which the *D* lines are excited by wave-lengths that are absorbed by the molecule, and (2) experiments upon a yellow band-group in the fluorescence spectrum arising under certain pressure conditions.

[1] Wood and Moore, Astrophys. J. **18,** 94 (1903); Wood, Proc. Am. Acad. **42,** 235 (1906); Wood and Hackett, Astrophys. J. **30,** 339 (1909).

II. D Line Stimulation by Monochromatic Radiation

The first experiments were carried out to determine whether monochromatic radiation of a wave-length other than that of the *D* lines could excite the *D* radiation in the flurorescence spectrum. The arrangement of the apparatus used for the production of fluorescence was as described in previous papers by one of us.[1] A steel tube of "Shelby-seamless-steel" about thirty inches long and two inches in diameter contained at its center a short steel cylinder partly filled with sodium, and provided with holes in its steel end plates which served as windows. The tube was closed by glass plates, hermetically sealed at each end with wax, its middle heated by bunsen burners, and its ends cooled by jackets of wet cotton. Nitrogen prepared by the combustion of phosphorus in a small bulb, could be admitted as desired through a fine capillary and the pressure read by a mercury manometer. Fluorescence was excited by means of a carbon arc, a beam from which was focused at the middle of the retort. The fluorescence light was directed upon the spectroscope slit by a small right angle prism placed at the center of the glass window through which the light entered, or to one side according to the part of the luminous vapor column under observation.

White light excitation produced the well known phenomena previously investigated by one of us.[1] When the pressure of the permanent gases which were present was low, i.e. less than 1 mm of mercury, the red and green bands and the chasm were well defined. If fluorescence occurred in the region surrounding the *D* lines the reversal due to the absorption by the less illuminated vapor through which the light was obliged to pass before reaching the spectroscope destroyed any trace of luminosity.

But now if the pressure of permanent gas present was increased by introducing nitrogen or air, and the spectroscope directed toward the front window of the retort the *D* lines appeared rather strongly. The reversal was prevented by the fact that because of the presence of the nitrogen the rate of diffusion of the sodium vapor out of the retort was diminished, with the consequence that the amount of sodium vapor outside the retort was small. By receiving light into the spectroscope from the region near the front window of the retort reversal due to passage through a long column of vapor was prevented. This was a case in which the right angle prism was placed at the side of the window.

The vapor was then excited by light from the arc filtered through a sheet of very dense cobalt glass and the resulting fluorescence spectrum examined visually. The screen transmitted radiations shorter than about 4200A and cut out completely all radiations in the yellow region. Repeated searches under various conditions of temperature and pressure failed to reveal any trace of the *D* lines in the fluorescence spectrum excited in this way.

A water solution of a neodymium salt was next employed as a screen to filter the exciting light, utilizing for this purpose the very sharp absorption band in these salts covering the region which includes the *D* lines. When the pressure of nitrogen was between 2 and 4 mm and the *D* lines

were fluorescing under white light excitation, introduction of the neodymium cell did not extinguish them. Their intensity was weakened considerably but they unmistakably remained. They were too weak, however, to be photographed. If they were observed as the pressure was changed they were seen to disappear when the pressure rose or fell from its value at 3 mm. The same effect though less clearly cut was obtained later by the use of a cobalt-glass filter of less density than the one previously employed.

Because of the small intensity of the *D* lines when excited by the light filtered through the neodymium cell, objection may be raised to the reality of the phenomenon on the following ground. The exciting light after being filtered may still have possessed sufficient intensity in the yellow to produce the *D* line fluorescence. In fact it was impossible to obtain the phenomenon when the exciting light was filtered through a neodymium cell of such concentration that the light from the arc when viewed directly through the screen, with the spectroscope, did not contain any trace of the *D* lines. Under these circumstances, however, the intensity of the exciting light is reduced considerably throughout the entire green and blue-green regions due to other neodymium absorption bands, and the intensity of the fluorescence is correspondingly reduced since some of the wave-lengths effective in exciting the *D* lines have also been removed.

A solution was made of such concentration that when held between the eye and the spectroscope it cut out completely the *D* lines, as excited by the full radiation of the arc. The cell was then introduced between the arc and the sodium tube and the *D* lines found to be very conspicuous in the fluorescence spectrum. This is a valid criterion of the efficiency of the cell on the assumption that the intensity of the fluorescence radiation is proportional to the intensity of the exciting light. It seemed desirable, however, to check these observations by methods which would be independent of this assumption and the phenomenon was now searched for with fluorescence excited by light obtained from a monochromator.

The slit width was adjusted so as to send into the tube a beam covering a region of about 50A of the spectrum. After repeated failures the phenomenon was finally obtained and we were able to observe the efficiency of various regions of the spectrum in exciting the *D* lines. As before the *D* lines, excited by light in which their wave-lengths were absent, attained their maximum intensity when the pressure was about 3 mm disappearing at higher or lower pressures, i.e. at 2 and 4 mm. By turning the prisms in the monochromator, the wave-length of the exciting radiations could be altered. It was found that as the exciting beam moved into the blue region from the shorter wave-lengths the *D* lines appeared feebly, growing stronger until the wave-length of the exciting light lay between 5100A and 5250A in the green where they reached their maximum intensity. As the wave-length was increased further the *D* lines diminished in intensity and finally disappeared until the yellow region was reached where they were again excited by radiation of their own wave-length.

Similar results were obtained with hydrogen and also with air.

These experiments show conclusively that sodium vapor when mixed with nitrogen, hydrogen or air at a pressure of 3 mm is stimulated to emit the D lines by incident radiations of shorter wave-lengths. Now atomic sodium does not exercise any absorption in the region of the monochromatic radiations used to stimulate the D lines. D_1 and D_2 are the only atomic absorption lines in the visible spectrum, the next absorption doublet of the principal series occurring at 3302A. The tremendous absorption occurring in dense sodium vapor throughout the visible region is due to sodium molecules. The phenomenon described is then one in which radiation is absorbed by the molecule and under certain conditions reemitted as the D lines. Two major alternatives to account for this phenomenon present themselves. The D lines under these circumstances may arise directly from an excited atom or they may arise from an excited molecule, i.e. the energy levels of the molecule may be quite close to those in the atom as is believed to be the case for hydrogen. Considering the first alternative only, the following situations arise:

1. The excited molecule may collide with an unexcited atom and by an impact of the second kind excite the atom, the excess energy appearing as kinetic energy of translation.

2. The excited molecule may collide with a foreign gas molecule and be dissociated into an excited atom and a neutral atom after the manner of H_2^+ when mixed with helium in the positive ray experiments of Smyth and of Hogness and Lunn.[2]

3. The excited molecule may spontaneously break up into a neutral and excited atom after the manner of hydrogen indicated in the experiments of Blackett and Franck.[3]

The controlling factor in the appearance of the D lines under molecular excitation seems to be a proper adjustment of the pressure at 3 mm. The three alternative processes listed above are favored by an increase in pressure. It is not clear why the optimum pressure should occur so far below the pressure at which fluorescence ceases (above 1 cm). Increasing the pressure of a foreign gas prevents a rapid diffusion of the sodium vapor out of the retort and hence increases the density of the sodium atoms and molecules. In this way the number of collisions between unexcited atoms and excited molecules is increased by the addition of a foreign gas and hence the first and third alternatives are favored by an increase in pressure as well as the second. The molecule, excited by λ5100A, possesses 2.4 ± 0.1 volts energy. The energy available for dissociation into one excited and one normal atom is the difference between this and 2.1 volts, the first excitation potential of the atom, i.e., 0.3 volts. Now Pringsheim,[4] using Fredrickson's and Watson's[5] constants for the red and green sodium absorption bands, finds the heat of dissociation of the molecule to be 1.34 volts. If this is

[2] Hogness and Lunn, Phys. Rev. **25,** 452 (1925).
[3] Blackett and Franck, Zeits. f. Physik **34,** 389 (1925).
[4] Carrelli and Pringsheim, Zeits. f. Physik **44,** 651 (1927).
[5] Fredrickson and Watson, Phys. Rev. **30,** 429 (1927).

taken as the correct value for the dissociating potential the energy available is insufficient for processes two and three to occur. But although in the light of this, the first process appears the most probable, it would be foolish to speculate until the results of experiments now in progress by one of us are available.

III. The Fluorescence Spectrum in the Yellow Region

During the experiments outlined above the chance appearance of a group of bands in the yellow region of the fluorescence spectrum discovered by one of us many years ago drew our attention elsewhere, and the second group of experiments about to be described were undertaken for the purpose of studying these bands.

One of us noted in 1910[6] that the character of the fluorescence excited by white light depended greatly upon the pressure of the residual gas. In particular there is mentioned the appearance of a group of bands extending on either side of the *D* lines which arise under white light stimulation when the pressure of the residual gas is around 1 cm. In view of the recent efforts to classify the band spectrum of sodium and the work upon the spectra of mixed alkali vapors, a study of this band group seemed desirable.

Barratt[7] in studying the absorption spectrum of mixtures of sodium and potassium vapors has measured the band heads of a yellow group which arise on either side of the *D* lines. The vapors were mixed with hydrogen at atmospheric pressure. These bands he ascribes to a sodium-potassium molecule. In a later paper, Smith[8] reports a study of the fine structure of one of these absorption bands and gives a band formula which classifies rather well forty six lines. Pringsheim[9] has obtained these bands, or what appear to be these bands in the fluorescence spectrum of a sodium-potassium mixture excited by monochromatic light obtained from a mercury arc. He records the wave-length of the band heads which correspond with those of Barratt's to within 2 or 3A.

In the present experiments technical sodium was employed and its vapor excited by sunlight obtained by the use of a heliostat. A visual examination of the fluorescence spectrum with a small spectroscope showed the usual features when the pump was operating, and the vapor fluorescing in the best vacuum obtainable with a "Cenco High-Vac" pump. Under these conditions the *D* lines were reversed. If nitrogen or hydrogen or air, (it appeared immaterial which gas was employed) was introduced, a series of bands appeared in the region of the *D* lines, when the pressure was higher than 6 mm and less than 1 cm. With all other conditions constant, i.e. temperature constant, intensity of exciting light constant, the bands were consistently absent at the low pressure, appeared at about 5 mm, rose to a maximum between 6 mm and 1 cm and disappeared as the pressure became higher. They were

[6] Wood and Galt, Astrophys. J. **33,** 72 (1911).
[7] Barratt, Proc. Roy. Soc. **A105,** 221 (1924).
[8] Smith, Proc. Roy. Soc. **A106,** 400 (1924).
[9] Pringsheim, Zeits. f. Physik **38,** 161 (1926).

photographed with a two meter grating spectrograph, but neither the dispersion nor the intensity allow of any accurate wave-length measures being made. Four bands appear on the short wave-length side of the *D* lines, each band occupying a region approximately 25A in width. One band appears on some of the plates on the red side of the *D* lines. Whether or not there are more, can not be judged from the present plates, since the familiar red group reached nearly up to the *D* lines and may overlap these bands.

It next seemed desirable to excite them by monochromatic light. Repeated attempts with the mercury arc, which was used successfully by Pringsheim to excite the yellow sodium-potassium bands in vacuum, failed to excite the slightest fluorescence in pure sodium (technical) in gas at 6 mm pressure. Excitation by light from a helium discharge tube and a sodium arc also produced negative results. Since the intensity of the bands under white light excitation is feeble, the failure in these cases may have been due to the weakness of the exciting beam. Sunlight filtered through a monochromator also failed to excite them. Finally, sunlight was filtered through various gelatin color screens and the bands looked for visually. It was found that they were excited by wave-lengths longer than 5700A and were also excited by light filtered through a neodymium cell which cut out wave-lenths between 5700 and 5900A, approximately. These results indicate that the bands are excited by light in the region of their own wave-lengths. But until methods are found whereby their intensity may be increased, it seems useless to attempt to excite them by monochromatic light.

Whether or not these bands are absorbed by the vapor is a question which can only be answered by a study of the fine structure of the absorption spectrum in this region and that of the fluorescence bands themselves. For although the vapor is more transparent to this region than to any other region of the visible spectrum it possesses here a fine lined absorption extending from the red to the green absorption bands, which becomes apparent when the molecular density is sufficiently high. Fine structure studies will be necessary since there is no band structure which is openly apparent.

There appear to be several circumstances which indicate that these bands arise from sodium and not from a compound of sodium with the foreign gases present or with potassium which may exist in the technical sodium as an impurity. First their intensity was unaltered when potassium was mixed with the sodium, and as before failed to appear in vacuum. Second, they were obtained with the greatest intensity when they were viewed from well within the retort, i.e., when a long column of the fluorescing vapor was viewed "end on." Thus they are feebly absorbed by the vapor if at all. Third, a very curious relation exists between these bands and a group which appear under very special conditions in an electrical discharge through the vapor, and which makes it still more difficult to associate them with a compound of sodium.

One of us, in a previous paper,[10] describes a group of bands in the yellow

[10] Wood, Phil. Mag. **15**, 581 (1908).

region of the spectrum which appear in the vapor of sodium, carrying an electrical discharge, under special discharge conditions, and which, as is pointed out, are exactly "out of step" with these bands of the fluorescence spectrum. These bands were more fully investigated by Wood and Galt. Photographs of this spectrum were again obtained and the previous results completely verified. A steel tube 30 inches long and an inch and a half in diameter provided with a glass window at one end served to contain the sodium to be vaporized and also as one electrode. A thin nickel rod extending along the axis of the tube served as the other electrode as described in the previous paper. A large induction coil capable of producing a seven inch spark in air was the source of potential. Ordinarily the discharge appeared as a dull greenish light filling the tube and showing in the spectroscope besides the *D* lines, only the doublets of the first and second subordinate series of the atom. If now the frequency of the vibrator was changed by altering the tension on its spring, and thereby the potential, and if the pressure was the lowest attainable by means of the "Cenco High-vac" pump the discharge suddenly changed its character. A brilliant yellow disc of light appeared in the middle of the tube detached from the axial electrode, which under the best conditions was dazzling in its brilliancy. The appearance of this phenomenon is very sudden and requires a critical adjustment of temperature and potential. It appears when the potential is larger than some critical value which has not yet been measured and when the temperature of the vapor is not too high. The spectrum of this discharge in addition to showing the *D* lines and the doublets of the first and second subordinate series, shows in the photographs obtained in the present work four groups of bands between the *D* lines and λ5688 of the first subordinate series, and two bands on the long wave-length side. The small intensities obtained, however, do not make it seem worthwhile to measure the band heads. If a plate showing these bands is superposed upon one of the fluorescence spectrum, upon which are the yellow fluorescence bands, it is seen that the two band systems are exactly out of step.*

Beutler, Bogdandy and M. Polanyi[11] have obtained bands in the chemical luminescence spectra of reaction mixtures of vapors of sodium, mercury chloride, and chlorine which, as Pringsheim points out, coincide exactly with the bands obtained by Wood in the electrical discharge through sodium. These bands are evidently due to sodium and not to any compound since the same bands appeared for different reacting substances used with sodium.

THE JOHNS HOPKINS UNIVERSITY,
BALTIMORE.
February 1, 1928.

* Recently, Schüler (Zeits. f. Physik **43**, 475 (1927)) has attempted to identify these cathode ray bands with the lithium resonance series of Wood. He, however, erroneously supposes that the fluorescence bands described above have been shown to occur in the absorption spectrum, thus incorrectly interpreting an earlier paper of one of us.

[11] Beutler, Bogdandy and Polanyi, Naturwiss. **9**, 164 (1926).

VOLTAGE-INTENSITY RELATIONS IN THE MERCURY SPECTRUM

By William D. Crozier

Abstract

Voltage-intensity curves have been obtained for twenty lines of the mercury spectrum, when excited by electron impact. The range of accelerating voltage was from excitation to fifty volts, the discharge tube being designed to eliminate most of the disturbance due to positive ion formation. The components of four of the triplet groups were resolved and investigated separately. No significant change appears in the number of atoms in a given energy state as the ionization potential is passed. The components of each of the dD groups of energy levels are excited at practically the same voltage but have quite different excitation functions. *The excitation functions* for d_1, d_3, and s levels and for the $2p_2$ level appear to be similar in form and to have sharp maxima within a few volts of the excitation voltage. The excitation functions for d_2 and D levels also appear similar, increasing uniformly to 30 or 40 volts where they have broad maxima. *The voltage-intensity characteristics* of lines originating in transitions down from the same initial level agree in type but sometimes show certain differences in shape. It appears that the probability of different transitions down from a given energy state may not be independent of the way in which this state is excited. There is evidence that a large number of excitations of $2p_2$ by transitions down from higher levels are not followed by $1S-2p_2$ transitions.

Introduction

THIS work was undertaken with the object of collecting some information as to the nature of the excitation function for certain of the energy levels of mercury. The excitation function is here defined as the fraction of collisions between an electron and an atom which result in the excitation of a given energy level, expressed as a function of the accelerating voltage on the electron. Information as to the nature of the excitation function for a certain energy level may be obtained by studying the variation of intensity with voltage of the spectral lines resulting from transitions down from this level. The exact form of the function may sometimes be somewhat modified by the effect of transitions from higher levels to the one in question and of radiationless transitions out of it.

At the time of starting this problem practically the only information available on voltage intensity relations was for hydrogen[1] and helium.[2,3,4] It had been noticed by Eldridge[5] that the intensities of different lines in the mercury spectrum varied in different ways as the velocity of the exciting electrons was varied over a short range above ionization. During the

[1] Hughes and Lowe, Phys. Rev. **21,** 292 (1923).
[2] Hughes and Lowe, Proc. Royal Soc. **A104,** 480 (1923).
[3] Udden and Jacobsen, Phys. Rev. **23,** 322 (1924).
[4] Bazzoni and Lay, Phys. Rev. **23,** 327 (1924).
[5] Eldridge, Phys. Rev. **23,** 294A (1924).

progress of the work a paper appeared by D. R. White,[6] showing extremely interesting details in the voltage-intensity curves below the ionization potential. This was deemed sufficiently important to warrant a careful exploration of this region with the view of confirming the results and extending them to the lines of the triplet groups which had not been resolved. A paper has also appeared by J. Valasek[7] giving voltage-intensity curves for a few mercury lines in the voltage range 15-300.

Apparatus

The discharge tube is a modification of one described by Eldridge[8] and is shown in cross section in Fig. 1. In front of the flat equipotential cathode were two grids G which were kept at the same potential. The grids were

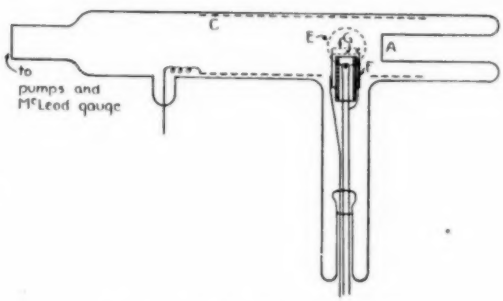

Fig. 1. The Experimental tube.

separated by about 2 mm, the first being about 1 mm in front of the cathode. Blackening of the quartz window A by platinum evaporated from the hot cathode was eliminated by using as the grid support a nickel cylinder F which enclosed the cathode. A side tube indicated at E projected on what was the lower side and contained mercury. The whole tube was enclosed in an oven with an electric heater to maintain the desired mercury vapor density. The pressure of the residual gas was maintained at all times below 10^{-5} mm as indicated by a McLeod gauge.

It was found necessary to limit the current passing through the grids to 0.1 or 0.2 milliamperes to avoid excessive local alteration of potential by space charge. With the currents used the potential over the region between the grids was constant to within 0.1 volt.

A voltage correction of approximately 2 volts was necessary in order to give the true volt-velocity of the electrons. This was determined approximately by the point of appearance of positive ions as described by White. However, if the voltage scale was shifted to make one of the lines appear at its theoretical voltage, then in general the others appeared at their theoretical points. This method is used for a slight final adjustment of the voltage scale for the curves shown. The uncertainty as to the value of the voltage probably does not greatly exceed 0.1 volt.

[6] White, Phys. Rev. **28**, 1125 (1926).
[7] Valasek, Phys. Rev. **29**, 817 (1927).
[8] Eldridge, Phys. Rev. **23**, 685 (1924).

With this arrangement of elements, the tube was reasonably free from disturbances caused by the production of positive ions as the ionization potential was passed. Neither the total emmission from the cathode, nor the current collected by the cylinder *C*, nor the intensity of the light emitted, showed any discontinuity as the ionization potential was passed. The curves between grid voltage and current showed only a slight change in slope. These characteristics of the tube made it possible to carry the observations across the ionization potential with assurance of their correctness.

The final curves were taken with the tube maintained at temperatures from 85°C to 115°C, except in the case of the λ2537 line, which was taken at 28°C. The higher temperatures were used to shorten the time of exposure for the weaker lines. Preliminary observations were made with temperatures ranging from 0°C to 130°C and no appreciable difference was noted in the shape of the curves obtained. It is not certain that the mercury pressure in the tube was exactly that characteristic of the temperature, as some condensation was taking place in the tube leading to the pumps and in the side tube carrying the leads.

The light from between the grids, after passing through the quartz window *A*, was focused on the slit of a quartz spectrograph. Most of the work was done with a spectrograph of aperture F11 having a dispersion of 14.5 A per mm in the region of 3300 and 6.5A per mm in the region of 2600. Exposures ranged from a fraction of a minute to twenty minutes.

Measurement of the density of the lines on the photographic film was made by means of a microphotometer with a photographic recorder. The film was calibrated by taking a series of spectrograms on one film, using different exposure times. The reciprocity law was then assumed to get the density-intensity relation. This method of calibration gave sufficiently good results, voltage-intensity curves taken with different exposures agreeing reasonably well in shape. The precision of the density measurements was for the most part probably within five percent. Practically all the points appearing on the curves are averages of several determinations, partly on different films taken under similar conditions, and partly on the same film.

Results and Discussion

General comments on curves. The curves in Figs. 2 to 11 present the results of some three thousand microphotometer measurements on twenty lines of the mercury spectrum.

Below the ionization potential the results of different measurements on different plates and at different temperatures were very concordant and it is usually possible to draw a smooth curve passing through nearly all the points. Above 10.4 volts the points become somewhat scattered. Most of the irregularities are probably due to some slight instability of current or voltage distribution, associated with the production of positive ions. It was possible to get smoother curves by working at lower temperatures, but then the exposure times became inconveniently long.

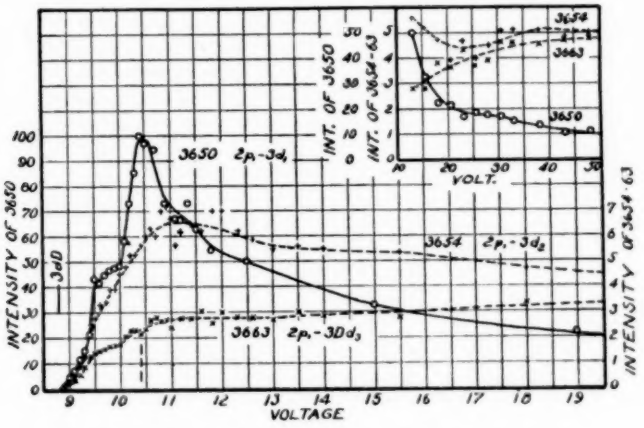

Fig. 2. Voltage-intensity curves of the λ3650 group.

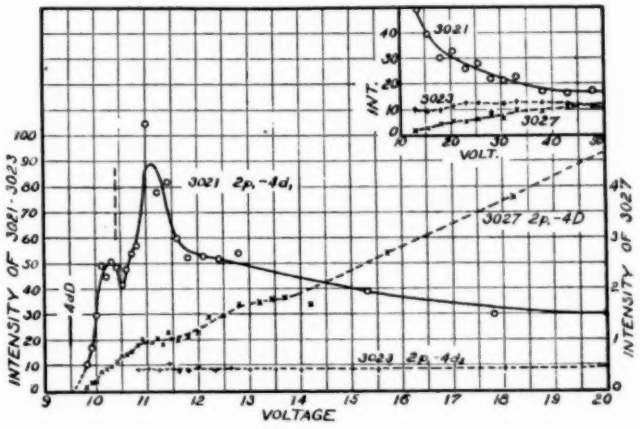

Fig. 3. Voltage-intensity curves of the λ3021 group.

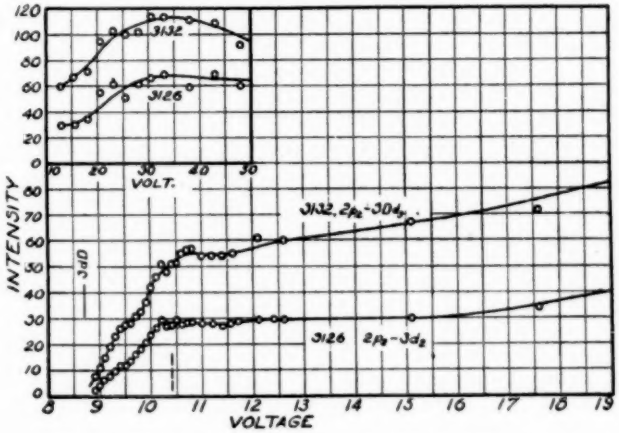

Fig. 4. Voltage-intensity curves of the λ3126 group.

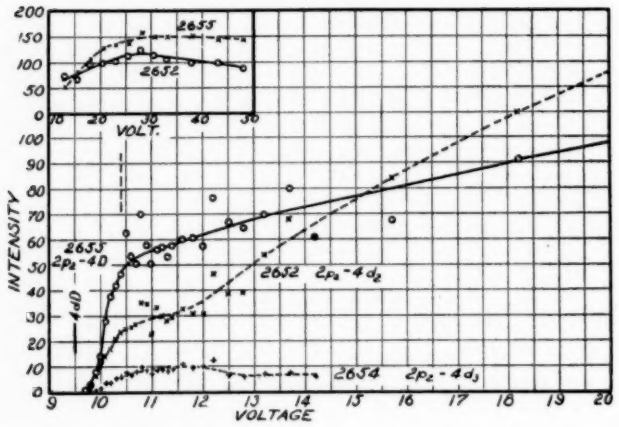

Fig. 5. Voltage-intensity curves of the λ2652 group.

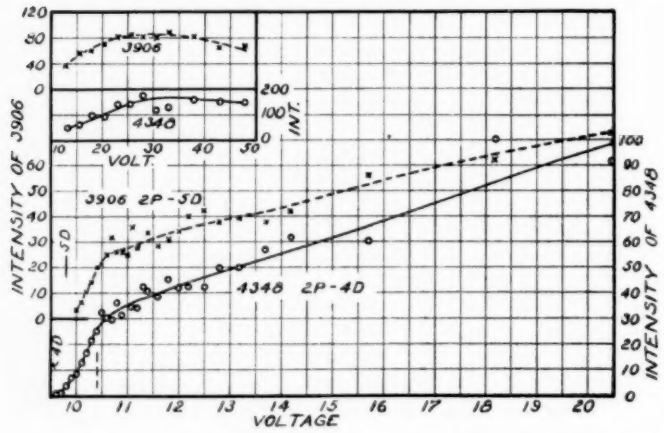

Fig. 6. Voltage-intensity curves of λ4348 and λ3906.

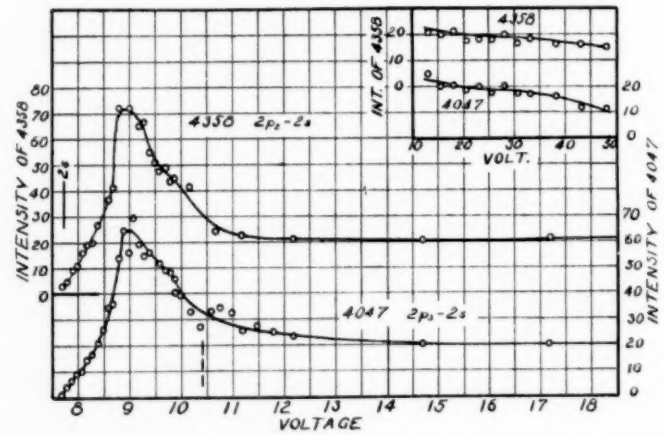

Fig. 7. Voltage-intensity curves of λ4358 and λ4047.

Where the results are comparable with the results of White and of Valasek they are, in general, in excellent agreement with them. In confirmation of the general results of other investigators, it was found that all the lines but one appeared at their respective theoretical voltages, including the components of the triplet groups which have not heretofore been

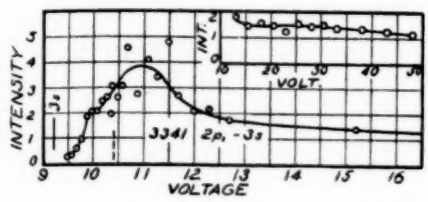

Fig. 8. Voltage-intensity curve of λ3341.

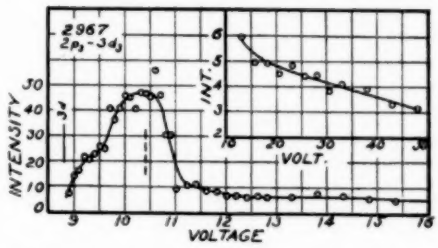

Fig. 9. Voltage-intensity curve of λ2967.

investigated individually, at least photometrically. The exception to this result was in the line 4078, $(2p_2-2S)$.[9] In agreement with the result of White, it was found that this line did not appear in any appreciable strength below about 8.5 volts. The curve in Fig. 10 does not show this as conclusively as

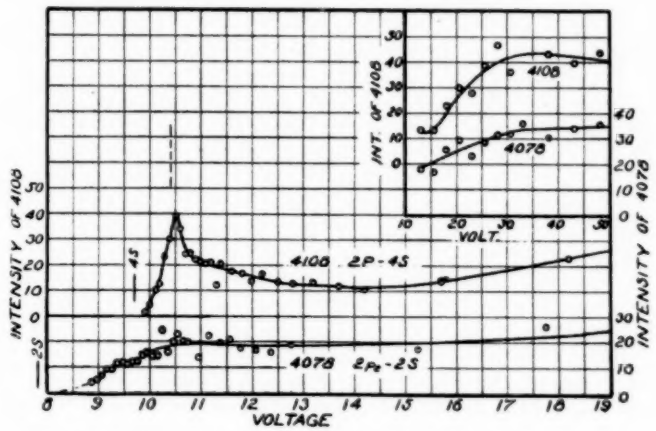

Fig. 10. Voltage-intensity curves of λ4108 and λ4078.

visual observations which were made on plates where the exposure time was sufficient to give a much greater intensity.

Specific results and their interpretation. Non-significance of the ionization potential. In one respect it will be observed that the curves differ from previous curves of the sort, and this is in the fact that in practically no case does a break occur in them at the ionization potential. There is a possible exception in the curves for $2p_1-3d_1$, $2p_3-3d_3$, and $2P-4S$, appearing in Figs. 2, 9, 10, respectively. However, it does not seem likely that the fact that this is the ionization potential has anything to do with this. This result

[9] The Paschen notation is used throughout this article.

is, for example, in sharp contrast with the results of White, which in all cases show a sharp upward break near ionization.

This result is taken to indicate that the role which ionization plays under these conditions in unimportant, at least at lower voltages, as compared with the role of the other inelastic collisions. Were a considerable part of the intensity of the lines due to electrons combining with the atoms after ionization, as was once thought to be the case, then the intensities of all the lines should show an increase at the ionization potential. After Hertz[10] and Eldridge[11] showed that all the arc spectrum could be produced by non-ionizing collisions, it has been thought that the role of ionization is unimportant. The present work definitely confirms this conclusion.

This circumstance is extremely important in discussing the relation of our results to the excitation function. It is fundamentally important to show that the energy states are mainly excited by impacts and not by transitions down from higher levels.

Behavior of the triplet components. The components of four of the triplet groups were resolved, the curves being shown in Figs. 2 to 5. In two instances as indicated it was impossible to separate lines from the d_3 and D levels, but there is every reason to believe that the d_3 line is very weak in comparison with the D line and for the discussion it will be assumed that the composite line is due primarily to D. This assumption is justified by the curves for analogous lines where resolution was possible.

In each case it was found that the lines in each group appeared at practically the same voltage. This fact is important in that it has not been previously verified, at least photometrically, that these lines appear together.

The shape of the curves for different members of a group differs very markedly. This is particularly exemplified by the behavior of the lines from $3d_1$ and $4d_1$ in Figs. 2 and 3 as compared with that of those from the d_2 and D levels. In addition to the obvious difference over all the range of voltage, there is a particularly interesting difference in their behavior for a short range just above their appearance. The curves of Fig. 2 illustrate this best though those in Fig. 3 show a similar effect. After appearing at the same point the lines have an upward curvature of almost the same shape for about 0.4 volt, and then the line from d_1 shows a very rapid increase while the others do not. This is believed to be a true characteristic of the excitation function of the d_1 levels and not to be due to transitions from higher levels. The only other levels which are sufficiently close to the d levels are the $3sS$ and $4sS$ levels. Radiation transitions from these to d_1 are forbidden, and if the transitions were due to collisions of the second kind it would be expected that the relative intensity of the lines from the d_1 levels to lines from the s or S levels should increase with temperature. Some rough measurements were made on the relative intensity of 3341 $(2p_1-3s)$ and 3650

[10] Hertz, Zeits. f. Physik **22,** 18 (1924).

[11] Eldridge, Phys. Rev. **23,** 685 (1924).

($2p_1-3d_1$) at temperatures of 0°C and 130°C, which indicate that this is not the case and that possibly even the opposite is true.

The pronounced drop so characteristic of the d_1 curves at 9.5 and 10.3 volts in Figs. 2 and 3 respectively, may possibly have an explanation in the fact that at approximately these points higher levels are excited in preference to d_1.

Behavior of lines from similar initial levels. Perhaps the most striking characteristics of the curves in general are the sharp maxima which sometimes occur at low voltages. Curves showing this feature in every case, except that of the somewhat anomalous line, $2P-4S$, decrease continuously as the voltage is increased beyond the maximum point.

A second class of lines shows a less interesting behavior; the sharp maximum is missing, and after the initial rise just above the excitation voltage, the curve flattens out. In most cases these curves continue to rise gradually to 30 or 40 volts and then fall off. Adopting this classification it will be seen that, in general, lines from analogous initial levels belong to the same class. For instance, in Figs. 2 and 3 it will be seen that the analogous lines $2p_1-3d_1$, and $2p_1-4d_1$ are very similar and fall into the first class. In the same figures $2p_1-3D$ and $2p_1-4D$ are similar and fall into the second class. The resemblance of $2p_1-3d_2$ and $2p_1-4d_2$ is not so striking. Both show indications of a maximum at lower voltages but their behavior at higher voltages is characteristic of the second class, and they appear to fall naturally into this class. The exact shape of these two curves is not very certain as the lines are in close proximity to much stronger lines, which fact introduces errors due to a peculiarity of the photographic plate. A complete classification of the lines observed is found in Table I, together with the figures in which they are to be found.

TABLE I. *Classification of lines*

Lines of the first class		Lines of the second class	
Type of line	Figure	Type of line	Figure
$X-md_1$	2, 3	$X-md_2$	2, 3, 4, 5
$X-md_3$	5, 9	$X-mD$	2, 3, 4, 5, 6
$X-ms$	7, 8	$2p_2-2S$	10
$2P-4S$	10		
$1S-2p_2$	11		

The only instance of marked dissimilarity between the characteristics of lines resulting from transitions down from levels of the same kind is in the lines from the S levels. Since the line 4078, ($2p_2-2S$), seems to be exceptional in another respect, not appearing at the theoretical voltage for the excitation of $2S$, but about 0.5 volt higher, it seems reasonable to regard the S levels as anomalous.

Behavior of lines from the same initial level. We have several cases before us of lines which originate in transitions from the same initial level to different final levels. Table II shows the type of transitions where this occurs together with the numbers of the figures to which reference may be made.

The shape of curves from the same initial level is practically identical for voltages below ionization, in agreement with the result of White. Above ionization the curves, while showing great similarity in type, are not in general identical and in several cases show marked disagreement. The particularly bad case shown by the lines $2p_1-3d_2$ and $2p_1-4d_2$, in comparison with the lines $2p_2-3d_2$ and $2p_2-4d_2$, is perhaps not to be taken too seriously, as the curves for the first two are not entirely reliable as mentioned above. However, even in other cases where this difficulty is not present there is disagreement between curves for lines with the same initial level.

TABLE II. *Classification of lines*

Type of Line	Figures
$X-3d_2$	2, 4
$X-3d_3D$	2, 4
$X-4d_2$	3, 5
$X-2s$	7
$X-4D$	3, 5, 6

A good example of this is found in comparing the line 3027 ($2p_1-4D$) in Fig. 3 with the line 2655 ($2p_2-4D$) in Fig. 5. 3027 shows an increase in intensity of 12:1 in going from 11 to 50 volts, while 2655 shows an increase of less than 3:1. This fact together with some features to be mentioned in connection with the $1S-2p_2$ line, leads to the suggestion that probabilities of transition from an upper level to lower levels may sometimes depend upon the velocity of the electron which excited the upper level, and that the nature of the dependence may vary with the lower level to which the transition is to lead.

This suggestion while appearing somewhat unintelligible, especially in the light of the older quantum theories, may have an explanation in the fine structure of the levels concerned. By assuming a proper selection principle for the combination of the fine structure terms and proper excitation functions for each of the fine structure levels of the initial term it is easily seen that the probability of the transitons may be made to depend on the voltage of excitation and that the nature of the dependence may be different for different final levels.

It seems that consideration of the ordinary Zeeman sub-levels is not sufficient in this case, as the statistical weight of all the Zeeman sub-levels of the initial state is the same.

The curve of 2537 ($1S-2p_2$). This curve of Fig. 11 is discussed separately because it shows several interesting features, and its interpretation is probably not so simple as in the case of the other lines. The curve shows a great deal of detail below the ionization point. All the features shown were very closely reproducible, and the irregularities are not to be confused with those which appear on some of the other curves at higher voltages. Upward breaks appear at 7.7, 8.8, and 9.1 volts which may be interpreted as due to the excitation of $2p_2$ by transitions from $2s$, $3dD$, and $3s$, respectively, these levels being excited at approximately these voltages. A break

appears at about 8.3 volts, the significance of which is not clear. It was not observed by White. Between 10.0 and 10.5 volts there are two maxima which were not observed by White, and of which the interpretation is also difficult owing to the great number of levels which can be excited at these voltages.

White observed a strong upward break at 5.4 volts which was attributed to transitions to $2p_2$ from $2p_1$ by collisions of the second kind. There is no evidence of such a break in our curve, and this is perhaps to be explained by the fact that our curve is taken at 28° where collisions of the second kind are less frequent than at the pressures presumably used by White.

It is believed that the peak between 6.0 and 7.5 volts is much broader than in the true voltage-intensity function. This is on account of resonance radiation produced in the space between the grids due to the 2537 radiation produced in the space beyond the second grid. Parts of this space

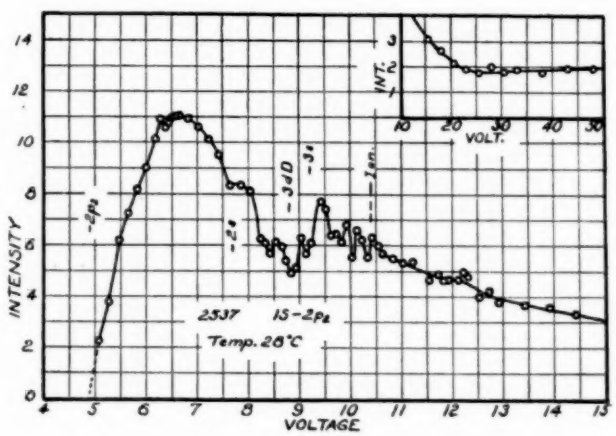

Fig. 11. Voltage-intensity curve of λ2537.

are at quite different potentials from the grids due to space charge, and the result is the same as if there was a rather wide velocity distribution in the electron beam.

Above ionization the intensity decreases as far as 25 volts, and then is constant. This is in qualitative agreement with the result of Valasek though there the intensity decreases to 100 volts.

This curve indicates that the excitation function for $2p_2$ has a strong maximum closely above 4.9 volts and then drops immediately to a very low value. This is in agreement with conclusions reached by Frl. Sponer[12] and by Eldridge[13] by retarding potential methods.

A difficulty arises in the interpretaion of this curve at voltages above the peak. As has been pointed out by Valasek,[7] the total intensity of the $1S-2p_2$ line appears to be much less than the combined intensity of the lines from transitions ending in $2p_2$. Analogous results have been obtained

[12] H. Sponer, Zeits. f. Physik **7**, 185 (1921).
[13] Eldridge, Phys. Rev. **20**, 456 (1922).

in other cases, and, in fact, no one has yet been able to show in any case a quantitative agreement between the number of transitions leading to a given state and the number leading from this state. It seems that the answer must be found in non-radiating transitions (collisions of the second kind). The effect does not appear to depend on pressure. If we assume the $2p_2$ state to consist of several fine structure states, some of which are metastable, we may find an explanation. The ratio of the non-radiating transitions to the radiating transitions will then depend only on the relative population of the fine structure levels and not on pressure.

The present curves render stronger the conclusions of Valasek and bring us more directly in contact with the difficulty. There appears a strong upward break in the intensity of 2537 at 7.7 volts which corresponds to contributions to $2p_2$ from $2s$. The evidence of these strong contributions does not extend to higher voltages. The peak in 2537 at 9.4 volts is much too weak to be associated with the peak which appears in the $2p_2-2s$ curve in Fig. 7. It appears that if $2s$ is excited by electrons having much more than the critical velocity the subsequent fall into the $2p_2$ state often results in an atom which is singularly unable to radiate. This may be explained if we assume as above that a different fine structure $2s$ state is excited by fast electrons from that by slow electrons. More of the first then go to the metastable $2p_2$ states mentioned above and there results a low probability of transition to $1S$ from $2p_2$. This explanation is not altogether improbable. Some recent work by Collins[14] has shown the possibility of influencing the relative population of different fine structure levels by different modes of optical excitation.

Bearing of the results on the excitation function. It is believed that we have here good evidence as to the general form of the excitation functions for the different series of the levels of mercury. The voltage-intensity curves undoubtedly depart to some extent from the true form of the excitation function, one reason being that some of the excitation is indirect, i.e., by transitions down from higher states. This is apparently not sufficient to entirely obscure the form of the curve even in the case of the excitation of $2p_2$, and for most of the other levels considered, it is known that most of the levels which lead into them are rather weakly excited. It is obvious from the curves that ionization contributes little. There may be non-radiating transitions out of some of the levels either by collisions of the second kind, or by the absorption of radiation. Collisions of the second kind do not appear to be of importance in most cases, especially as the preliminary observations showed the shape of the curves to be practically independent of pressure.

It is possible that the shape of the curves is influenced to some extent by absorption in the mercury vapor, some of the light being reemitted at different frequencies.

The discussion becomes somewhat complicated if we accept the method of treatment suggested above, that of considering the excitation of the

[14] Collins, Phys. Rev. **31**, 152A (1927).

fine-structure sub-levels separately. Then we must regard the excitation functions observed as composites of the excitation functions of the sub-levels of the initial level which are involved in the emission of the line observed.

It may be asked if a different curve would not have been obtained if the light had been observed in a different direction relative to the electron beam, since it is known that the light emitted is polarized. Some attempts to measure the polarization of the light in the direction observed indicated that in this tube it was not very strong. In any event the polarization with this type of excitation would not cause a great difference in the shape of the curves obtained looking in different directions and expecially would not account for the great differences in the two classes of curves.

In conclusion I wish to express my appreciation of the friendly interest and helpful attitude of the staff of the Physics Department at the University of Iowa, and of the facilities of the laboratory. I expecially wish to express my thanks to Professor Eldridge who suggested the problem and directed the work.

HALL OF PHYSICS,
UNIVERSITY OF IOWA,
August 12, 1927.*

* Received February 6, 1928.—ED.

THE QUENCHING OF MERCURY RESONANCE RADIATION BY FOREIGN GASES

By Mark W. Zemansky

Abstract

Milne's Theory of the diffusion of imprisoned resonance radiation is applied to Stuart's experiments on the quenching of Hg resonance radiation by foreign gases, and expressions obtained for n_2, the number of excited Hg atoms per cc, and J, the quenching, in terms of k, the number of impacts of the second kind per sec per excited atom. Stuart's experimentally determined values of J are used to give the relation between k and the pressure of the foreign gas, and the result is obtained that the number of impacts of the second kind per sec per excited atom is not a constant fraction of the total number of collisions. The total number of impacts of the second kind per cc is calculated and taken as the reaction velocity, and upon plotting against the pressure it is shown that the reaction velocity varies as the 0.6 power of the pressure for all the foreign gases. It is shown how these results can be explained on the theory that impacts between excited Hg atoms and foreign gas molecules give rise to metastable Hg atoms, which diffuse to the incident wall and meet there adsorbed foreign gas molecules to which they give up their energy. This theory is also capable of explaining the behavior of a large quantity of inert gas on the dissociation of hydrogen and oxygen by excited Hg atoms.

Introduction

IF LIGHT from a Hg resonance lamp at room temperature is incident on a face of another Hg resonance lamp containing a foreign gas, the secondary resonance radiation is quenched by an amount depending on the pressure of the foreign gas.[1,2,3] The relation between the re-emitted resonance radiation, J, and the pressure of the foreign gas, p, called the quenching curve, was obtained and plotted by Stuart for a number of gases among which were O_2, H_2, CO_2, H_2O, N_2, A and He. On the assumption that the resonance radiation is reduced to one half its original value when the probability of an impact between an excited Hg atom and a foreign gas molecule equals the probability that an excited Hg atom will radiate, and upon assuming the radius of an excited Hg atom to be about three times the normal value, Stuart was able to compute the "efficiency" or "yield" of impacts of the second kind. These values varied widely among themselves—being 100% for O_2, 70% for H_2, and about 0.03% for He, the values for the other gases being between these limits. If the radius of an excited Hg atom is taken larger, the efficiencies are reduced, but the general order among the different gases remains the same. The high quenching efficiency of hydrogen is usually explained on the basis that, since it requires only 4.3 volts to dissociate a hydrogen molecule, an excited Hg atom with an energy of 4.9 volts can perform this dissociation upon impact. This is in good agreement with the

[1] Wood, Phys. Zeits. **13**, 353 (1912).
[2] Cario, Zeits. f. Physik **10**, 185 (1922).
[3] Stuart, Zeits. f. Physik **32**, 262 (1925).

experiments of Franck and Cario,[4] but several difficulties still remain. First, one would expect 100% efficiency for hydrogen on this point of view. If the radius of an excited Hg atom is chosen so as to give such an efficiency, however, the efficiency for oxygen comes out greater than 100%. Second, if a 4.9 volt excited Hg atom can dissociate a hydrogen molecule so easily merely because it has sufficient energy, one would expect a 4.9 volt electron, upon impact, to do the same. Hughes,[5] however, found no dissociation by electron impact even at 8.9 volts. Finally the high quenching efficiency of oxygen seems to have no explanation whatever.

Foote[6] recently attempted an explanation of Stuart's quenching curves from a point of view which differentiated sharply between the behavior of hydrogen and that of other gases. According to Foote, *all* impacts between excited Hg atoms and foreign gas molecules are of the second kind, but only in the case of hydrogen is the excitation energy of the excited Hg atom completely used up, partly in dissociating the hydrogen molecule and partly in kinetic energy, giving an efficiency of 100%. Impacts between excited Hg atoms and molecules other than hydrogen produce metastable Hg atoms which, upon further impacts, yield either excited Hg atoms once again, or Hg_2 molecules or, if an impurity is present, normal Hg atoms. Relations between J and p were deduced for the two different cases, and by choosing the unknown constants in these expressions to agree with Stuart's data, information was obtained about the number of metastable atoms, the rate of formation of molecules, and the concentration of impurities.

Foote does not mention, however, the anomalous behavior of oxygen, and although it is conceivable that a slight amount of hydrogen as an impurity might account for the quenching efficiencies of helium, argon and nitrogen, those of O_2, CO_2 and H_2O cannot be accounted for in this way. Moreover, his method of treating the absorptions and re-emissions of quanta of 2537 by Hg atoms was rather approximate, and it was thought worthwhile to apply Milne's theory[7] of imprisoned resonance radiation to this problem, since this theory, extended to include impacts of the second kind has been fairly successful in accounting for the persistance of imprisoned resonance radiation in Hg vapor.[8] In the present paper a relation between J and the number of impacts of the second kind per sec. per cc is obtained for all foreign gases on the basis of Milne's theory. We take into account the geometry of Stuart's apparatus and make only one assumption about the behavior of the foreign gas molecules, to wit: The number of impacts of the second kind per sec. per cc is proportional to the number of excited Hg atoms per cc, the proportionality factor being an unknown function of the pressure of the foreign gas or

$$\left.\begin{array}{l}\text{Number of impacts of second}\\ \text{kind per sec. per cc}\end{array}\right\} = kn_2$$

[4] Franck and Cario, Zeits. f. Physik **11**, 161 (1922); **17**, 209 (1923).
[5] Hughes, Phil. Mag. **41**, 778 (1921).
[6] Foote, Phys. Rev. **30**, 288 (1927).
[7] Milne, Journ. Lond. Math. Soc. Vol. I (1926).
[8] Zemansky, Phys. Rev. **29**, 513 (1927).

where n_2 is the number of excited Hg atoms per cc and $k=f(p)$ is the number of impacts of second kind per sec. per excited atom.

If the number of impacts of the second kind per sec. per excited atom were a constant fraction of the total number of impacts, then k would be equal to a constant times the pressure of the foreign gas. This is the assumption that has always been made. It is not necessary, however, to make any assumptions concerning k at this point, because Stuart's experiments themselves will furnish the functional relation between k and p.

Milne's Theory

If a mass of gas be enclosed between two infinite planes at $x=-a$ and $x=+a$, and if isotropic, monochromatic radiation, for which the gas has the atomic absorption coefficient α, be incident on the face $x=-a$, then, it has been shown by Milne that the number of excited atoms per cc, n_2, is obtained by solving the differential equation

$$(\partial^2/\partial x^2)(n_2+\tau\partial n_2/\partial t)=4\alpha^2N^2\tau\partial n_2/\partial t \tag{1}$$

where τ is the life-time of the excited state, and N is the total number of atoms per cc. Also, the intensity of the radiation advancing in the positive x direction is

$$I_x=\frac{\sigma q_1}{Nq_2}\left[\left(n_2+\tau\frac{\partial n_2}{\partial t}\right)-\frac{1}{2\alpha N}\frac{\partial}{\partial x}\left(n_2+\tau\frac{\partial n_2}{\partial t}\right)\right]$$

and the intensity of the radiation advancing in the negative x direction is

$$I_x'=\frac{\sigma}{N}\frac{q_1}{q_2}\left[\left(n_2+\tau\frac{\partial n_2}{\partial t}\right)+\frac{1}{2\alpha N}\frac{\partial}{\partial x}\left(n_2+\tau\frac{\partial n_2}{\partial t}\right)\right] \tag{3}$$

where σ, q_1 and q_2 are constants with which we do not have to concern ourselves in this problem. In these equations, $\partial n_2/\partial t$ represents the total rate at which excited atoms are forming. To take into account the destruction of excited atoms, it is necessary merely to replace $\partial n_2/\partial t$ everywhere by $\partial n_2/\partial t+kn_2$ according to the assumption made above, and in order to apply the theory to the case of a cylindrical mass of gas, we have merely to transform the differential equation (1) into cylindrical coordinates.

The Problem

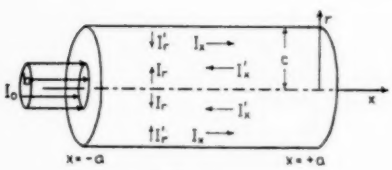

Fig. 1.

The conditions under which the present calculation is carried out are shown in Fig. 1. We have a cylindrical absorption cell of quartz containing N Hg atoms per cc, and a pressure, p, of some foreign gas. A circular portion, of radius b, of the face at $x=-a$ is bathed in radiation from a Hg resonance lamp at room temperature. The radius of the absorption cell is c and the length is $2a$. We wish to find the value of the backward radiation I_x' at

the point $r=0$, $x=-a$ in the steady state ($\partial n_2/\partial t=0$), the boundary conditions being

$$I_x'=0 \text{ when } x=+a,\ 0<r<c \tag{4}$$

$$I_r'=0 \text{ when } r=c,\ -a<x<+a \tag{5}$$

$$I_x=\begin{cases} I_0 \text{ when } x=-a,\ 0<r<b \\ 0 \text{ when } x=-a,\ b<r<c. \end{cases} \tag{6}$$

We have first to obtain the solution of the differential equation

$$\partial^2 n_2/\partial r^2+\partial n_2/r\partial r+\partial^2 n_2/\partial x^2=4\alpha^2N^2\tau k n_2/(1+\tau k) \tag{7}$$

subject to the conditions that

$$n_2+(1/2\alpha N)(\partial n_2/\partial x)=0 \text{ when } x=+a,\ 0<r<c. \tag{8}$$

$$n_2+(1/2\alpha N)(\partial n_2/\partial r)=0 \text{ when } r=c,\ -a<x<+a \tag{9}$$

$$n_2-(1/2\alpha N)(\partial n_2/\partial x)=\begin{cases} Nq_2I_0/\sigma q_1(1+\tau k) \text{ when } x=-a,\ 0<r<b \\ 0 \text{ when } x=-a,\ b<r<c \end{cases} \tag{10}$$

and then to calculate I_x' at $x=-a$, $r=0$.

The solution of (7) is found to be

$$n_2=\frac{2bNq_2I_0}{c^2\sigma q_1(1+\tau k)}\sum J_0(\mu_k r)\times$$

$$\frac{\mu_k J_1(\mu_k b)\left[\cosh p_k(a-x)+(2\alpha N/p_k)\sinh p_k(a-x)\right]}{(4\alpha^2N^2+\mu_k^2)\left[J_0(\mu_k c)\right]^2\left[2\cosh 2ap_k+(2\alpha N/p_k+p_k/2\alpha N)\sinh 2ap_k\right]} \tag{11}$$

where $p_k=(4\alpha^2N^2\tau k/(1+\tau k)+\mu_k^2)^{1/2}$; $\mu_k=y_k/c$; and y_k is the Kth root of $2\alpha NcJ_0(y)=yJ_1(y)$. When there are no impacts of the second kind, $k=0$ and $p_k=\mu_k$ whence, without impacts of the second kind,

$$n_2=\frac{2bNq_2I_0}{c^2\sigma q_1}\sum J_0(\mu_k r)\times$$

$$\frac{\mu_k J_1(\mu_k b)\left[\cosh\mu_k(a-x)+(2\alpha N/\mu_k)\sinh\mu_k(a-x)\right]}{(4\alpha^2N^2+\mu_k^2)\left[J_0(\mu_k c)\right]^2\left[2\cosh 2a\mu_k+(2\alpha N/\mu_k+\mu_k/2\alpha N)\sinh 2a\mu_k\right]} \tag{12}$$

In Stuart's experiments, $2a$ is 10 cm, c is about 2.5 cm, b about 1 cm, and $\alpha N=3$.[9] With these values, it is found that the smallest value of μ_k is about 1, whence $2a\mu_k$ and $2ap_k$ are at least 10, and $\cosh 2a\mu_k$ is very nearly equal to $\sinh 2a\mu_k$.

Eq. (12) enables us to see how the concentration of excited atoms, when there are no impacts of the second kind, varies as we go along the axis of the absorption cell from the incident face toward the origin. Let

[9] Malinowski Ann. d. Physik **44**, 935 (1914); Orthmann Ann. d. Physik **78**, 601 (1925).

$$n_x = 100 \frac{n_2 \text{ at } r=0,\ \tau k=0,\ x=x}{n_2 \text{ at } r=0,\ \tau k=0,\ x=-a}$$

$$= 100 \frac{\sum \dfrac{\mu_k J_1(\mu_k b) e^{-\mu_k(a+x)}}{(4\alpha^2N^2+\mu_k^2)\,[J_0(\mu_k c)]^2(2\alpha N+\mu_k)}}{\sum \dfrac{\mu_k J_1(\mu_k b)}{(4\alpha^2N^2+\mu_k^2)\,[J_0(\mu_k c)]^2(2\alpha N+\mu_k)}}$$

Whence, evaluating the denominator,

$$n_x = 170 \sum \frac{\mu_k J_1(\mu_k b) e^{-\mu_k(a+x)}}{(4\alpha^2N^2+\mu_k^2)\,[J_0(\mu_k c)]^2(2\alpha N+\mu_k)} \tag{13}$$

Eq. (13) is plotted in Fig. 2, and it is seen that 80 percent of the excited atoms lie in a region 1 cm from the incident face.

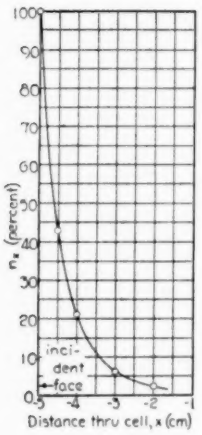

Fig. 2.

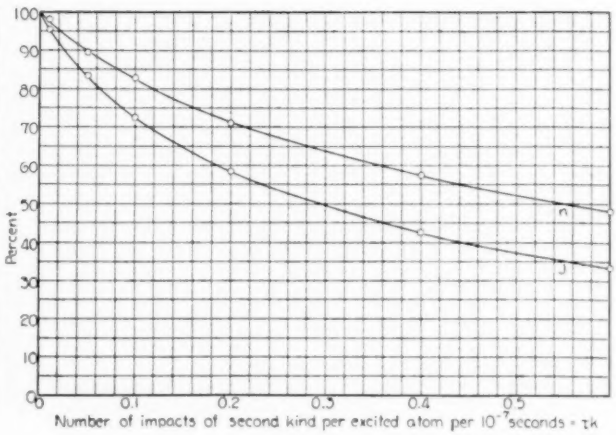

Fig. 3.

How much the number of excited atoms per cc at the incident face is reduced by impacts of the second kind can be calculated from Eqs. (11) and (12).
Let

$$n = 100 \frac{n_2 \text{ at } x=-a,\ r=0, \text{ with impacts of second kind}}{n_2 \text{ at } x=-a, r=0, \text{ without impacts of second kind}}$$

$$= \frac{100}{1+\tau k} \frac{\sum \dfrac{\mu_k J_1(\mu_k b)}{(4\alpha^2N^2+\mu_k^2)\,[J_0(\mu_k c)]^2(p_k+2\alpha N)}}{\sum \dfrac{\mu_k J_1(\mu_k b)}{(4\alpha^2N^2+\mu_k^2)\,[J_0(\mu_k c)]^2(\mu_k+2\alpha N)}}$$

which reduces, upon evaluating the denominator, to

$$n=\frac{170}{1+\tau k}\sum\frac{\mu_k J_1(\mu_k b)}{(4\alpha^2N^2+\mu_k^2)\,[J_0(\mu_k c)\,]^2(p_k+2\alpha N)} \tag{14}$$

Values of n corresponding to values of τk equal to 0.01, 0.05, 0.1, 0.2, 0.4, and 0.6 are given in Table I, and n is plotted against τk in Fig. 3.

TABLE I. *Values of n and J for different values of τk.*

τk	n from Eq. (14)	J from Eq. (15)
0.01	98.4	95.5
0.05	89.7	83.2
0.10	82.7	72.6
0.20	71.4	58.6
0.40	57.3	42.7
0.60	48.2	33.5

From equations (3), (11) and (12), it is found that at $x=-a$, $r=0$, with impacts of the second kind,

$$I_x'=\frac{2bI_0}{c^2}\sum\frac{\mu_k J_1(\mu_k b)(2\alpha N/p_k-p_k/2\alpha N)\sinh 2ap_k}{(4\alpha^2N^2+\mu_k^2)\,[J_0(\mu_k c)\,]^2[2\cosh 2ap_k+(2\alpha N/p_k+p_k/2\alpha N)\sinh 2ap_k]}$$

and at $x=-a$, $r=0$, without impacts of the second kind

$$I_x'=\frac{2bI_0}{c^2}\sum\frac{\mu_k J_1(\mu_k b)(2\alpha N/\mu_k-\mu_k/2\alpha N)\sinh 2a\mu_k}{(4\alpha^2N^2+\mu_k^2)\,[J_0(\mu_k c)\,]^2[2\cosh 2a\mu_k+(2\alpha N/\mu_k+\mu_k/2\alpha N)\sinh 2a\mu_k]}$$

whence J, the quenching, is

$$J=100\,\frac{I_x' \text{ at } x=-a, r=0, \text{ with impacts of second kind}}{I_x' \text{ at } x=-a, r=0, \text{ without impacts of second kind}}$$

$$=100\,\frac{\sum\dfrac{\mu_k J_1(\mu_k b)(2\alpha N-p_k)}{(4\alpha^2N^2+\mu_k^2)\,[J_0(\mu_k c)\,]^2(2\alpha N+p_k)}}{\sum\dfrac{\mu_k J_1(\mu_k b)(2\alpha N-\mu_k)}{(4\alpha^2N^2+\mu_k^2)\,[J_0(\mu_k c)\,]^2(2\alpha N+\mu_k)}}$$

At this point it should be emphasized that both I_x' with impacts and I_x' without impacts represent the *total* energy of radiation emitted backward per second from unit area of the incident face of the absorption cell, whereas Stuart measured the radiation included in the solid angle subtended by a lens some distance away. The final formula for J therefore is correct only if the same fraction of the total radiation passes through the lens when there are impacts, as when there are no impacts. This is undoubtedly so, since the Hg vapor pressure remained constant throughout Stuart's experiments.

Upon evaluating the denominator,

$$J=41\sum\frac{\mu_k J_1(\mu_k b)(2\alpha N-p_k)}{(4\alpha^2N^2+\mu_k^2)\,[J_0(\mu_k c)]^2(2\alpha N+p_k)} \tag{15}$$

values of J for $\tau k=0.01$, 0.05, 0.1, 0.2, 0.4, 0.6, are given in Table I, and J is plotted against τk in Fig. 3.

The curves in Fig. 3 enable us to obtain τk and n for any experimentally determined value of J. Since Stuart measured J at different pressures for many different foreign gases, we therefore have τk and n for all the foreign gases at all the pressures employed by Stuart. The first interesting piece of information is obtained by plotting τk against p. This is done in Fig. 4,

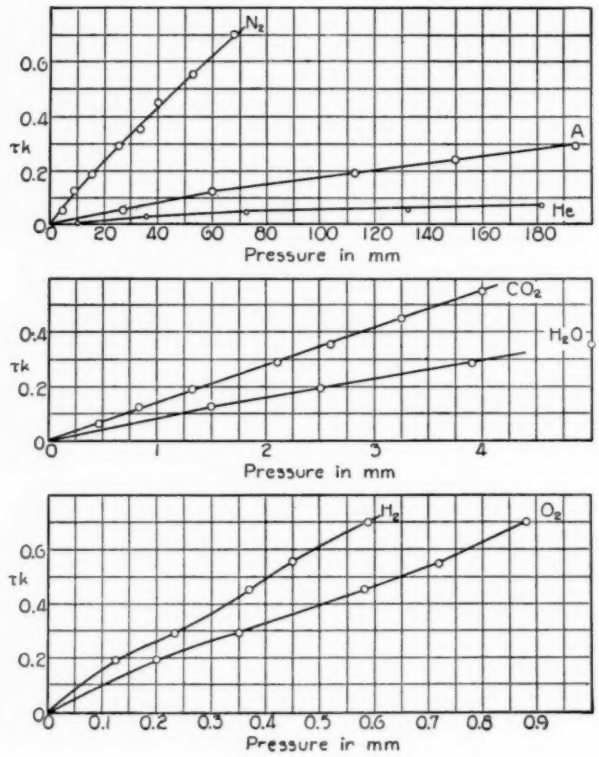

Fig. 4.

and it is seen that the curves are not all straight lines. Some are linear in portions, and others are nowhere linear. The assumption usually made, that the number of impacts of the second kind per sec. per excited atom is a constant fraction of the total number of collisions, is not substantiated by these results. Consequently, we cannot ascribe to a certain gas a constant quenching efficiency.

Instead, let us look at the matter from a different point of view. From the work of Franck and Cario,[4] it is shown that impacts of the second kind

between excited Hg atoms and hydrogen molecules result in the dissociation of the hydrogen molecules. Similar experiments by Taylor and Marshall,[10] Taylor and Bates,[11] Mitchell,[12] Dickinson and Mitchell,[13] and Dickinson and Sherrill,[14] show that excited Hg atoms dissociate many other foreign gases, and perform other chemical reactions as well. Now, since τkn represents the number of times in 10^{-7} secs. that the excited Hg atoms in one cc at the incident face give up their energy to foreign gas molecules, and since most of the excited Hg atoms exist at the incident face, τkn can be taken as a convenient measure of the average reaction velocity. For example, τkn for hydrogen, CO_2, and H_2O represents the rate of dissociation, for O_2 either the rate at which HgO or O_3 is forming or the rate at which O_2 is being dissociated (if this takes place at all), and for N_2, A and He, the rate, possibly of activation, or complex molecule formation, etc. In other words, τkn represents the rate of change of condition of the foreign gas,—therefore the reaction velocity, and curves obtained from plotting τkn

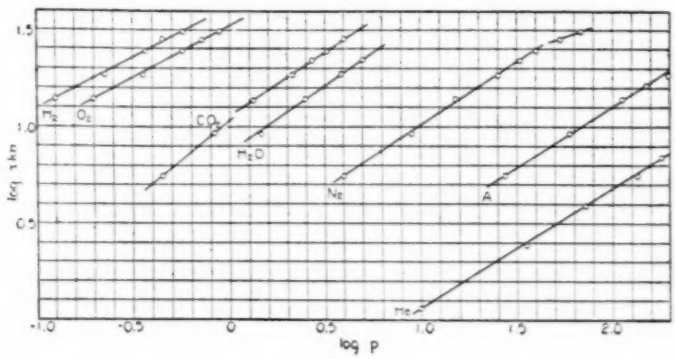

Fig. 5.

against p for all the foreign gases will show how the reaction velocity depends upon the pressure. In Fig. 5, log τkn is plotted against log p and the regularity is apparent. They are all straight lines with slopes varying from 0.54 to 0.66, the average being 0.60. Consequently we have the result that the reaction velocity near the incident face (the only place where any appreciable effect exists) is proportional to the 0.6 power of the pressure, for all the foreign gases.

Discussion

The result just obtained, that the reaction velocity varies as a fractional power of the pressure, suggests that the quenching ability of a foreign gas is evidence of a heterogeneous gas reaction. The only gas reactions of frac-

[10] Taylor and Marshall, Journ. of Phys. Chem. **29**, 1140 (1925).
[11] Taylor and Bates, Proc. Nat. Acad. Sci. **12**, 714 (1926).
[12] Mitchell, Proc. Nat. Acad. Sci. **11**, 458 (1925).
[13] Dickinson and Mitchell, Proc. Nat. Acad. Sci. **12**, 692 (1926).
[14] Dickinson and Sherrill, Proc. Nat. Acad. Sci. **12**, 175 (1926).

tional order that are known are catalytic reactions,[15] and, as a rule, the order is determined by the adsorbing abilityof the catalyst, which, in turn, depends upon the degree to which the catalyst is saturated with adsorbed molecules. The experiments of Wood[16] which show the presence of metastable mercury atoms in a mixture of excited mercury atoms and foreign gas molecules, and the theoretical considerations which require for some of the reactions the presence of a third body, suggest that the catalyst in this case is the incident wall on which are adsorbed metastable mercury atoms. The metastable mercury atoms formed by impacts between excited mercury atoms and foreign gas molecules are known to have a long life, and it was shown by Orthmann and Pringsheim[17] that a metastable mercury atom can travel about ten thousand free paths before it gives up its energy. Therefore, in Stuart's experiments, many of the metastable Hg atoms have time to reach a wall of the absorption cell before they are destroyed, and since the greatest number of excited Hg atoms exists near the incident face, metastable Hg atoms will be arriving at the incident face in large numbers.

If we assume that these metastable Hg atoms meet adsorbed foreign gas molecules at the incident wall, and that the energy of the metastable Hg atoms (4.68 volts) added to the total heat of adsorption is sufficient to activate the foreign gas molecules, then we are in a position to account not only for the energy needed to perform the dissociations and reactions which have been observed, but also for the result that the reaction velocity varies as a fractional power of the pressure.

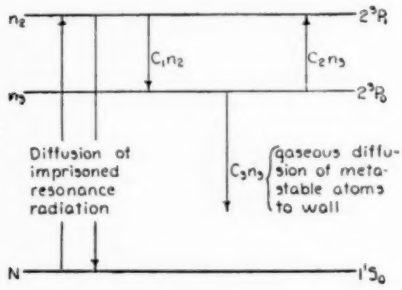

Fig. 6.

In order to derive this relation between reaction velocity and pressure, let us consider a cubic centimeter of mercury vapor near the incident wall, containing N normal Hg atoms, n_2 excited Hg atoms, n_3 metastable atoms, and a pressure p of some foreign gas. Let the rate of formation of metastable atoms be given by C_1n_2, the rate of formation of excited atoms from metastable atoms by C_2n_3, and finally the rate of diffusion of metastable atoms to the wall by C_3n_3. This scheme is shown in Fig. 6.

For equilibrium of the metastable state, we have

$$C_2n_3+C_3n_3=C_1n_2\ ;\ n_3=C_1n_2/(C_2+C_3)$$

whence

$$C_1n_2-C_2n_3=[C_1-C_1C_2/(C_2+C_3)]n_2=kn_2$$

where k has the same meaning that it had in the beginning, that is, the total number of impacts of the second kind per sec. per excited atom. Since

[15] Hinshelwood, "Kinetics of Chemical Change in Gaseous Systems," Oxford University Press, 1926.

[16] R. W. Wood, Phil. Mag. **50**, 774 (1925).

[17] Orthmann and Pringsheim, Zeits. f. Physik **35**, 626 (1926).

$C_1n_2 - C_2n_3 = C_3n_3$, then $kn_2 = C_3n_3$, or, the reaction velocity is equal to the rate of diffusion of metastable atoms to the wall. Now, at equilibrium, the rate of arrival of metastable atoms at the wall equals the rate at which foreign gas molecules are activated at the wall, and this depends upon the degree to which the wall is saturated with metastable atoms, and the amount of foreign gas molecules adsorbed on the wall. With the wall unsaturated, the amount of foreign gas molecules adsorbed depends upon a power of the pressure,[18] and hence, the reaction velocity depends upon a power of the pressure.

If by some other agency, such as the presence of large amounts of nitrogen or argon, so many metastable atoms are produced that the wall is saturated, then the amount of hydrogen or oxygen adsorbed on the wall is independent of the pressure of the hydrogen or oxygen, and we should expect a reaction of the zero order, that is, one whose velocity is independent of the pressure. This is what was found by Meyer[19] and by Mitchell.[12] Meyer illuminated a mixture of Hg vapor, hydrogen at a pressure of 0.12 mm, and N_2 at a pressure of 7 mm, with 2537, and noticed a decrease in hydrogen pressure that was a linear function of the pressure, or $dp/dt = \text{const.}$, showing that the nitrogen provided so many metastable atoms that the amount of H_2 adsorbed by the wall was independent of the hydrogen pressure. Similarly, Mitchell used a mixture of O_2 and A and found a reaction of the zero order.

Since there is no direct evidence of the effect of the walls on gas reactions taking place in the presence of excited Hg atoms, it is not worthwhile to go any further with the ideas suggested in this paper until experiments are performed to test this point. Such experiments are in progress at the present time.

In conslusion, I should like to express my gratitude to Professor H. W. Webb for the opportunity of having many profitable discussions with him on this subject.

PHYSICS LABORATORIES,
COLUMBIA UNIVERSITY.
February, 1928.

[18] Tolman "Statistical Mechanics" p. 256, Chem. Cat. Co. 1927.
[19] Meyer, Zeits. f. Physik **37**, 639 (1926).

THE POSITIVE RAY ANALYSIS OF WATER VAPOR IONIZED BY IMPACT OF SLOW ELECTRONS

By Henry A. Barton and James H. Bartlett, Jr.

Abstract

An electromagnetic method of separating gas ions of different mass, such as that used by Dempster, has been employed in a study of the ions produced by electron impact in water vapor. The principal ions appearing were $(H_2O)^+$ and $(OH)^+$. Of these the $(H_2O)^+$ ions were more abundant. Unmistakable evidence was obtained that a third type of ion, probably $(H_3O)^+$, was produced in very small quantities. H^+ and H_2^+ ions were always very few in number or unobservable. No $(OH)^-$ or any other negative ions were observed.

Ionization potentials for $(H_2O)^+$ and $(OH)^+$.—The ionization potential corresponding to $(H_2O)^+$ was 13 ± 1.5 volts, being probably in agreement with the ordinarily measured ionization potential. The $(OH)^+$ ionization potential was not distinguishably different, but it was difficult to measure this quantity owing to some overlapping of the $(H_2O)^+$ and $(OH)^+$ peaks.

Relative abundance of the ions as a function of pressure.—A study was made of variation in the relative abundance of the ions as a function of pressure. The $(H_2O)^+$ ion appears to be the primary ion, as it predominates at low pressures, but is of the same order of magnitude as the $(OH)^+$ ion at high pressures (0.007 mm).

Introduction

WITHIN the past few years the method of positive ray analysis due to Dempster has been developed and applied to the study of ionization in monatomic and diatomic gases by several experimenters, including Smyth,[1] Hogness and Lunn,[1] Harnwell,[2] Brasefield,[3] and one of the authors.[4,5]. The present research was undertaken as the first step of a similar investigation of several gases composed of molecules of more than two atoms.[6]

Smyth[7] discovered, and one of the authors[4] also later noted, that in a freshly evacuated tube electron impacts of sufficient energy produced water ions. These were doubtless due to water vapor present in the tube, the source of the vapor being layers adsorbed by the glass walls. On account of the polar nature of the water molecule, it would be expected that a large quantity of water could be so retained by a glass surface and then released gradually after evacuation. The experiments to be described confirm this point of view, since sufficient water vapor for detection by ionization was present, even

[1] For references see: H. D. Smyth, Phys. Rev. **25,** 452 (1925), note 1; T. R. Hogness and E. G. Lunn, Phys. Rev. **30,** 26 (1927), note 1.

[2] G. P. Harnwell, Phys. Rev. **29,** 683 and 830 (1927).

[3] C. J. Brasefield, Phys. Rev. **31,** 52 (1928).

[4] H. A. Barton, Phys. Rev. **25,** 469 (1925).

[5] H. A. Barton, Phys. Rev. **30,** 614 (1927).

[6] This field was opened with salt vapors by: V. Kondratjeff and N. Semenoff, Zeits. f Physik **22,** 1 (1924); V. Kondratjeff, idem **32,** 535 (1925) and **39,** 191 (1926), note 2.

[7] H. D. Smyth, Proc. Roy. Soc. **A104,** 127 (1923).

after the system had been standing under a vacuum for two weeks. Conditions were thus favorable to study the nature of the ionization in water vapor as a representative polyatomic gas and to obtain useful information concerning tubes which cannot be baked out and so may contain water vapor as an impurity. In the early part of the present work, when only the nature of the ions was the subject of study, it was not found necessary to augment the water vapor present in the tube. Later, additional water vapor was supplied by evaporation of an adjusted mixture of water and concentrated sulphuric acid.

As in the experiments cited above, [1,2,3,4,5] gas pressures were of the order of 0.001 mm, and the electron impacts were of energies ranging from 0 to 100 volts.

Types of Ion

During preliminary runs, positive ions were noticed in the mass range 24 to 30, approximately, with a maximum near 28 probably due to CO. These

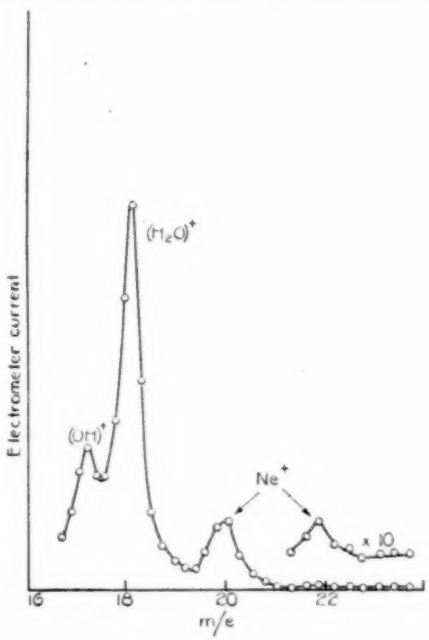

Fig. 1

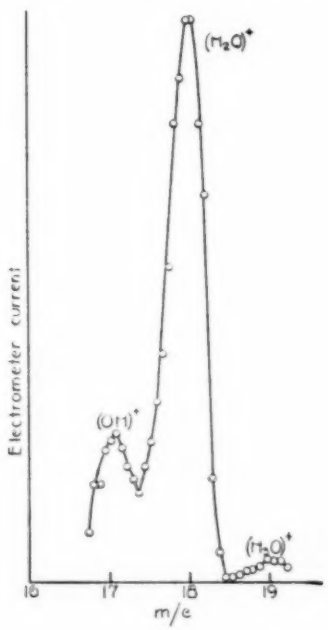

Fig. 2

ions correspond in general to those observed by Aston[8] and attributed by him to the hydrocarbons arising from the waxes and greases present in the tube.

In the study of water vapor, two principal types of ion occurred near $m/e=18$. To fix the mass scale accurately and thus determine the precise composition of these ions, neon, having known isotopes at 20 and 22, was mixed with the water vapor. The mass spectrum which was obtained is

[8] F. W. Aston, Isotopes (1924), p. 66.

shown in Fig. 1. The neon isotopes appear with the expected abundance-ratio, here determined quantitatively and directly for the first time, of approximately 10:1, agreeing with that calculated from the atomic weight of neon on the basis of Aston's[8] work. Since the abscissas of the plot are proportional to m/e, it is obvious, by extrapolating, that the water ion peaks correspond to $m/e=18$ and 17. Accordingly, these must be interpreted as having the compositions $(H_2O)^+$ and $(OH)^+$, respectively.

Later, with neon absent and the resolving power of the apparatus improved, a mass spectrum such as is shown in Fig. 2 was obtained. It is evident that a third type of ion, corresponding to $m/e=19$, occurs, although in small quantities. This third type of ion was present whenever the conditions were such that all the ions were abundant. According to J. J. Thomson,[9] a corresponding line is very frequently found on positive ray photographs. It could be due to fluorine, but as this element could not have been present in more than negligible quantities in the present work, the peak is ascribed to the ion $(H_3O)^+$. It is probable that these ions were formed either by the attachment of protons to neutral water molecules or by some reaction, e.g. $(H_2O)^+ + H_2O \rightarrow (H_3O)^+ + OH$.

Thus, as far as the positive ions are concerned, they agree exactly with the results of Aston,[8] who found the $(H_3O)^+$ ion "always very faint." On the other hand, no negative ions of any sort which might be due to water vapor were found, even though search was made repeatedly. This is in marked distinction from the result of J. J. Thomson[10] who observed $(OH)^-$ ions. Since the apparatus had easily detected Cl^- ions in HCl, there would seem to be no present experimental difficulty involved in the non-detection of such negative ions. In this connection it may be noted that Mohler[11] found that with small electron currents and low pressures, the negative ion current was small in comparison with that of the positive ions. With larger electron currents, the ratio of negative to positive ions increased. This is in good accord with the present results, but it leaves unexplained the large quantities of Cl^- ions observed by one of the writers in HCl.

$(H)^+$ and $(H_2)^+$ ions were always few in number when it was possible to observe them.

Critical Potentials

The lowest potential at which the $(H_2O)^+$ ions appeared was 13 ± 1.5 volts, the weighted mean of ten determinations, as shown in Table I. This agrees well with the lowest ionizing potential of water vapor observed as 13.2 by Mackay and 13.0 by Foote and Mohler.[12] Attempts to determine the critical potential for the appearance of the $(OH)^+$ ion gave roughly the same value. It is impossible to be sure that this properly applies to the $(OH)^+$ ion,

[9] J. J. Thomson, Rays of Positive Electricity (1921) p. 230.

[10] J. J. Thompson, Rays of Positive Electricity (1921) p. 70 and 227.

[11] F. L. Mohler, Phys. Rev. **26**, 614 (1925).

[12] C. A. MacKay, Phys. Rev. **24**, 319 (1924); P. D. Foote and F. L. Mohler, Phys. Rev. **17**, 394 (1921).

since it was difficult to resolve this completely from the $(H_2O)^+$ type. However, if, as appears from the pressure analysis, the $(H_2O)^+$ ion is the primary

TABLE I. *Ionization potential for* $(H_2O)^+$.

Run	I. P.	Wt.	Run	I. P.	Wt.
145	13	21	5–26–1	13	11
146–1	15	8	5–26–2	12	10
146–2	12	11	5–26–3	14	10
146–3	13	12	5–26–4	11	8
147	15	7	5–26–5	14	5
			Weighted mean	13	

ion, and the $(OH)^+$ a secondary type in the sense to be discussed, it would be expected that the critical potentials of the two ions would be the same.

PRESSURE EFFECTS

In most other gases where more than one type of ion was produced, and in hydrogen especially, changes in the gas pressure caused marked changes in the relative intensity of the several types of ion. Such changes are in part interpreted as distinguishing between two classes of ion, called primary and secondary. By primary ions are meant those produced by the electron impact; by secondary ions are meant those produced from the primary ions when they undergo subsequent encounters with other molecules. Obviously, increasing the pressure increases the number of possible encounters and, therefore, the ratio of secondary to primary ions.

It was difficult to test for this phenomenon in water vapor bacause when the water vapor pressure was increased, the filaments were burned out or deactivated. However, it was possible to increase the number of encounters suffered by the primary ions by adding another gas not destructive to filaments, the total pressure being thereby raised. This was done with nitrogen at various total pressures and results obtained, of which those shown in Fig. 3 are an example. It must be acknowledged that the shape of the curves is somewhat doubtful, but it is fairly definite that the $(H_2O)^+$ type of ion predominates at low pressures and so may be regarded as the primary type of ion produced by electron impact in water vapor.

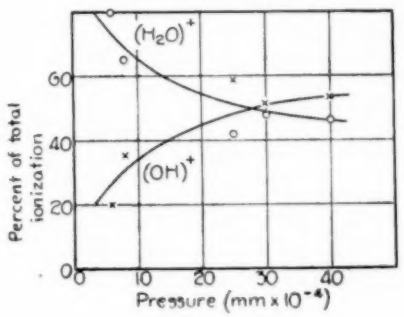

Fig. 3

DISCUSSION

Like most, if not all, non-polar gases and all polar gases which have so far been studied,[13] the water molecule is primarily ionized by the removal of

[13] See summary of results given in reference 5.

an electron without dissociation of the molecule. As in HCl there is no sign of a type of ionization consisting of the separation of the molecule into its polar ions, in this case H^+ and $(OH)^-$ or O^{--}. In both H_2O and HCl a second type of positive ion is observed whose composition is that of the primary ion with one hydrogen atom removed, i.e. Cl^+ and $(OH)^+$ respectively. The possibility in the case of H_2O that still another positive ion could be formed having two hydrogen atoms removed, i.e. O^+, is not realized. In this connection it may be mentioned that the gas logically next in order after H_2O, namely ammonia (H_3N), is now being investigated by one of the writers.

The existence of the positive ion $(OH)^+$ may be regarded as a limiting case of the existence in excited states of the neutral OH molecule, which is generally held to be the emitter of a certain band spectrum associated with water vapor.[14]

The writers wish to acknowledge their indebtedness to Professors T. Lyman, E. C. Kemble and H. D. Smyth for assistance and advice.

BARTOL RESEARCH LABORATORY,
THE FRANKLIN INSTITUTE,
PHILADELPHIA, PENNSYLVANIA.

JEFFERSON PHYSICAL LABORATORY,
HARVARD UNIVERSITY,
CAMBRIDGE, MASSACHUSETTS.
February 14, 1928.

[14] W. Watson, Astrophys. J. **60**, 145 (1924).

IONIZATION IN POSITIVE ION SHEATHS

By Philip M. Morse[1] and W. Uyterhoeven[2]

Abstract

It was found that the positive ion current to a plane auxiliary collector placed in a neon discharge had about twice the value expected from the equations of Langmuir and Mott-Smith. This increase must be due to an ionization within the sheath surrounding the electrode or to an emission of electrons from the surface of the electrode.

Four different possible causes of the increase are analyzed and relations between the voltage drop V, total current to the collector i, and sheath thickness x are obtained. Comparison with data shows that the increase in i is probably caused by the ionization of the metastable atoms within the sheath by radiation from the discharge. The relations; $V=A(Bx^{4/3}+Cx^{8/3})$, and $i=i_0+I_0x^2/2$ hold, and check fairly well with the three experimental curves. Considerations of atomic energy states of the metastable atoms show that this ionization would be most marked in the noble gases, and almost nonexistant in mercury vapor, which was the gas investigated by Langmuir and Mott-Smith.

Introduction

Observations, which will shortly be published in greater detail, have been made by one of us (W.U.) at the Philips Laboratory at Eindhoven, Holland, on the positive ion current to a plane auxiliary collector placed in a neon discharge. These show values for the current of about twice the values expected from the equations of Langmuir and Mott-Smith.[3]

A possible explanation of this increase is that there is a slight amount of ionization within the sheath; an ionization not small enough, however, to be entirely neglected, as Langmuir and Mott-Smith have assumed.

Since the field applied is sufficient to exclude practically all electrons from the sheath, electrons cannot produce this ionization, but it can be brought about in several other ways.

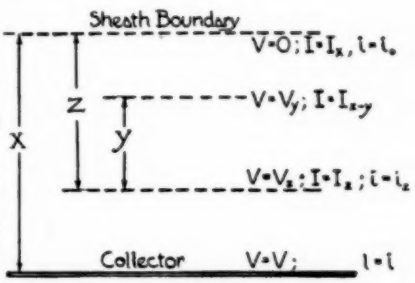

Fig. 1.

In Fig. I, x is the sheath thickness, V the potential drop across it, i the total positive ion current reaching the collector, and i_0 the constant current entering the sheath from the discharge. I_z/e is the number of ions formed per second per cubic centimeter at a point z centimeters from the sheath boundary, and V_z, E_z and i_z are values of potential drop, electric intensity and current density respectively at the same point.

Case 1. The radiation from the arc might ionize the neutral atoms within the sheath. In this case, since the radiation density is constant through-

[1] Fellow in Physics at Princeton University.

[2] Fellow of the C. R. B. Educational Foundation, at California Institute of Technology.

[3] Langmuir and Mott-Smith, G. E. Rev. **27**, 449 (1924).

out the sheath, the number of ions formed per second would be the same throughout the sheath, and, $I_z = I_0$.

Case II. On the other hand, there are neutral atoms in metastable states streaming in from the discharge in a constant flow. Since there are no metastable atoms formed in the sheath, the law of diffusion requires that the concentration of these atoms at any point be proportional to the distance of the point from the collector plate.

These metastable atoms would have a much greater likelihood of being ionized than the neutral atoms, and in this case the ionization per second per cubic centimeter at a point will be proportional to the point's distance from the collector, and; $I_z = I_0(x-z)$

Case III. A less likely case would be that the metastable atoms, in colliding with each other, would release enough energy to ionize one of them. In this case the ionization would be proportional to the square of the distance, and; $I_z = I_0(x-z)^2$.

Case IV. The metastable atoms will also strike the conductor, and give up their energy to an electron, which will ionize the gas in its path across the sheath. Or a photoelectron might be given off by the collector plate. In either case the number of ions formed will probably be small, since the sheath thickness is of the order of a mean free path; and the probability of photoelectric emission from most metals is less than of emission from the metastable atoms in the sheath. In both cases, however, the ionization at any point will be some function of the electric intensity at that point, $I_z = F(E_z)$,

Very likely all four of these effects are present, but Case II will probably be preponderant. At any rate, by solving each of these cases separately and determining which fits the data best, it can be determined which cause of ionization is the important one.

General Considerations

In any of these cases there will be a relationship between n_z, the concentration of ions at point z, V_z and z. The current density i_z will be $n_z eu$, where u is the average drift velocity of the ions at point z. Since the sheath thickness is of the order of one mean free path, we can consider the ion as falling through free space, and;

$$u = [2e(V_z - V_y)/M]^{1/2}$$

where $(V_z - V_y)$ is the potential difference between the point under consideration and the point where the ion was formed. For the constant current density coming from outside the sheath, we have $(V_z - V_y) = V_z$, and;

$$n_z' e = i_0/u_0 = (M/2e)^{1/2} i_0/V_z^{1/2} \tag{1}$$

The number of ions n'' due to ionization within the sheath will be such that the current at z due to them will be proportional to the number formed per second between the sheath boundary and z:

$$i_z'' = n'' e u'' = \int_0^z I_{z-y}\, dy \tag{2}$$

The average drift velocity of these ions, u'', will be the sum of all their velocities divided by their total number;

$$u''=\frac{(2e/M)^{1/2}\int_0^x (V_x-V_y)^{1/2}I_{x-y}\,dy}{\int_0^x I_{x-y}\,dy} \tag{3}$$

Then the total ion concentration at any point will be;

$$n_x e=\frac{i_0}{u_0}+\frac{i_x''}{u''}$$

and from Poisson's Equation;

$$\frac{d^2V}{dz^2}=4\pi\left(\frac{M}{2e}\right)^{1/2}\left[\frac{i_0}{V_z^{1/2}}+\frac{\left(\int_0^x I_{x-y}\,dy\right)^2}{\int_0^x (V_x-V_y)^{1/2}I_{x-y}\,dy}\right] \tag{4}$$

However, we are interested in conditions over the whole sheath. When we let $z=x$, we get two equations; one for the total current flowing in the conductor;

$$i=i_0+\int_0^x I_{x-y}\,dy \tag{5}$$

giving; $$di/dx=I_x \tag{6}$$

and one relating V and x. Letting $4\pi(M/2e)^{1/2}=A^{1/2}$, then;

$$\frac{d^2V}{dx^2}=A^{1/2}\left[\frac{i_0}{V^{1/2}}+\frac{\left(\int_0^x I_{x-y}\,dy\right)^2}{\int_0^x (V-V_y)^{1/2}I_{x-y}dy}\right] \tag{7}$$

This last equation cannot, in general, be solved exactly. However, since we shall find that the second term will be much smaller than the first, it being of the nature of a correction to the first term, an approximate solution will be obtained by setting d^2V/dx^2 equal to each term separately, and then letting the final solution be the sum of the two partial solutions.

The solution of the first term will be the same for all four cases, and will be the Langmuir and Mott-Smith equation;

$$V'=A^{1/3}\left(\frac{9\,i_0}{4}\right)^{2/3}x^{4/3} \tag{8}$$

The solution of the second portion will depend on our choice of I_x.

Case I. Here I_x is constant, and the numerator of the fraction;

$$\left(\int_0^x I_{x-y}dy\right)^2=I_0{}^2x^2.$$

The denominator is undetermined until V is known. However V is probably a function of x to some power between one and two. If we let $V_y=V(x-y)/x$, *i.e.*, a linear function of y, then;

$$I_0\int_0^x (V-V_y)^{1/2}dy=2I_0xV^{1/2}/3$$

and if we let $V_y = V(x-y)^2/x^2$, then;

$$I_0 \int_0^x (V-V_y)^{1/2} dy = \pi I_0 x V^{1/2}/4$$

In other words, if V is proportional to some power of x between one and two, the denominator becomes $I_0 x(V^{1/2}/a)$, where a is a factor between $3/2$ and $4/\pi$. Then the equation becomes;

$$\frac{d^2V''}{dx^2} = A^{1/2}\frac{aI_0}{2}\frac{x}{V''^{1/2}}$$

This has a solution; $V'' = A^{1/3}(aI_0/2)^{2/3}x^2$

and the complete approximate solution will be in this case;

$$V = V' + V'' = A^{1/3}[(9i_0/4)^{2/3}x^{4/3} + (aI_0/2)^{2/3}x^2] \tag{9}$$

and; $$i = i_0 + I_0 x \tag{10}$$

These two relations will completely determine the relationship between i, V and x.

Case II. In this case $I_{x-y} = I_0 y$. By a process similar to that in case I, we obtain;

$$\frac{d^2V''}{dx^2} = A^{1/2}\frac{b}{4}I_0\frac{x^2}{V''^{1/2}}$$

where b is between 15/4 and 3. This equation has a solution which, added to Eq.(8), gives as complete solution;

$$V = A^{1/3}\left[\left(\frac{9i_0}{4}\right)^{2/3}x^{4/3} + \left(\frac{9bI_0}{160}\right)^{2/3}x^{8/3}\right] \tag{11}$$

and the other equation will be;

$$i = i_0 + I_0 x^3/2 \tag{12}$$

Case III. This has as solutions;

$$V = A^{1/3}\left[\left(\frac{9i_0}{4}\right)^{2/3}x^{4/3} + \left(\frac{cI_0}{210}\right)^{2/3}x^{10/3}\right] \tag{13}$$

where c is between 105/16 and $16/\pi$. The other equation is;

$$i = i_0 + I_0 x^3/3$$

Case IV. If we take $F(E) = I_0 E = I_0\, dV/dy$, then;

$$\frac{d^2V''}{dx^2} = 3A^{1/2}I_0 V''^{1/2}$$

giving as complete solution;

$$V = A^{1/3}\left[\left(\frac{9i_0}{4}\right)^{2/3}x^{4/3} + A^{2/3}\left(\frac{I_0}{8}\right)^2 x^4\right] \tag{14}$$

If $F(E)$ were taken as proportional to any higher power of E, V'' would be proportional to an even higher power of x. So, in general, for $I = F(E)$; $V = Bx^{4/3} + Cx^n$ where n is probably higher than 4. Since; $E = B'x^{1/3} + Cx^{n-1}$ then I will vary as the cube or higher power of x.

Experimental Confirmation

Thus four different assumptions as to the cause of ionization in the sheath give four different relations between i, V and x, if one of these relations fits the experimental data with tolerable exactness, then it may be considered as the preponderant cause of the ionization.

The experimental data give the relationship between i and x as shown in Fig. (2). The slope di/dx for different values of x is a straight line going through the origin. From Eq. (6) it is seen that $di/dx = I_x$, so I_x in this case must equal Ax. Then, letting $A = I_0$,

$$I_x = I_0(x - z)$$

which corresponds to Case II.

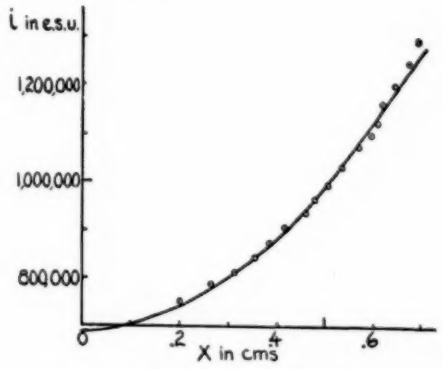

Fig. 2. Variation of positive ion current with sheath thickness. Observations of Uyterhoeven; U5-H, Neon; 450 ma.; pressure 0.02 mm; nickel collector.

Solving the data by least squares to fit Eq. (12), i_0 is found to be 693,000 e.s.u., and I_0 to be 23,160 e.s.u per mm². Putting these values into Eq. (11) a curve is obtained for V in terms of x, which is of the form; $V = C(623x^{4/3} + 57.8x^{8/3})$.

By comparing this with the experimental curve, Fig. (3), the average value of C is found to be .000075. But C is $(8\pi^2 M/e)^{1/3}$, which, for neon, is about .0001, giving a further check.

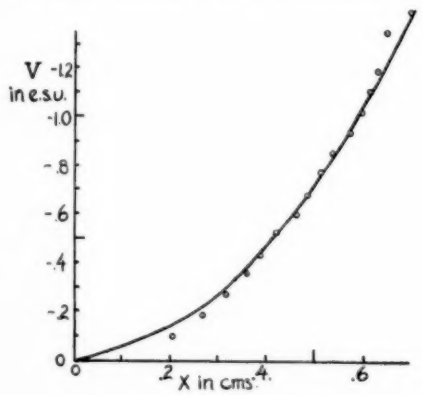

Fig. 3. Variation of potential drop with sheath thickness. Data taken from Uyterhoeven's observations and used in conjunction with Eq. (11).

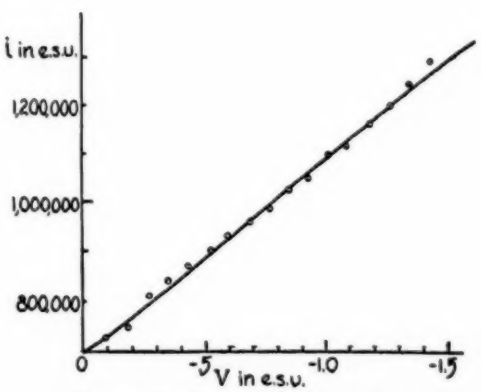

Fig. 4. Variation of positive ion current with potential drop.

Fig. (4) is the experimental curve for i in terms of V. In all these figures the smooth curve represents the curve calculated from Eqs. (11) and (12), and the small circles represent the experimental data.

Conclusion

There are several objections which might be raised against these deductions, but which seem to be satisfactorily answered. The question might

be brought forward as to whether there are enough metastable atoms flowing into the sheath to cause this current. However comparison with an unpublished estimate of the number of metastable atoms diffusing through the sheath, made by W. de Groot, indicates that the number of metastable atoms ionized according to Case II above is about one-tenth of the total number passing into the sheath.

Since the thickness of the sheath is of the order of magnitude of a mean free path of an atom, the validity of the diffusion equation might be questioned. Inasmuch as the mean free path of an excited atom is considerably less than that of the unexcited atom, and as the sheath is but a small portion of the total region across which diffusion is occurring, for lengths of time much larger than a mean free time the diffusion equation will hold with reasonable accuracy.

The approximation made in the integration of Eq. (11), that of solving the two parts of the equation separately, is equivalent to assuming that the total current due to ionization in the sheath is less than i_0. But since i_0 is about 700,000 e.s.u. and I_0 only 23,000 e.s.u./mm^2, it is only for values of x greater than about 6 mm or of V greater than 300 volts that an appreciable deviation from the solution might be expected.

Langmuir and Mott-Smith, in their data on mercury[4] found no such variation from their equation, or, rather, they found a very slight variation (see his Fig. 4; the portion AB of the curve only deviates slightly from the parallelism to the V axis required by his equation). This means that there are less metastable Hg atoms ionized by radiation from a mercury discharge than there are Ne metastable atoms ionized by radiation from a neon discharge. The ionization potential of most of the metastable atoms of both Hg and Ne is about 5 volts. But since there is very little radiation from a mercury discharge of that high a frequency, while a considerable portion of the energy of radiation from a neon discharge has this energy or higher, it is to be expected that the phenomenon will be exhibited in neon to a much more marked degree than in mercury.

This markedly greater ionization of metastable atoms is to be expected in helium and argon also, and may serve to explain why the behavior of the electric discharge through the noble gases has seemed anomalous.

Thus the data available at present seem to show that the ionization within the sheath is due to the ionization of metastable atoms by radiation from the discharge, and that therefore the relations between i, V and x follow Eqs. (11) and (12).

The writers wish to express their appreciation of the considerable aid rendered by Professor K. T. Compton in the preparation of this paper, and of the kindness of Doctor G. Holst, Director of the Philips Laboratory, for his permission to make use of the experimental data.

PALMER PHYSICAL LABORATORY,
PRINCETON UNIVERSITY.

NORMAN BRIDGE LABORATORY,
CALIFORNIA INSTITUTE OF TECHNOLOGY.

February, 1928.

[4] Langmuir and Mott-Smith, G. E. Rev., Vol. 27, 538 (1924).

THE DROP OF POTENTIAL AT THE CATHODE IN FLAMES

By Paul Edward Boucher

Abstract

The theory as given by J. J. Thomson for the drop of potential at plane electrodes has been modified by allowing for recombination in the layer and a similar theory for cylindrical electrodes has been worked out. The equation for plane cathodes is

$$V_2=\left(\frac{32\pi i}{75k_1}\right)^{1/2}x_2^{3/2},$$

and for cylindrical cathodes is

$$V_2=\left(\frac{2i}{3k_1(r_2^2-r_0^2)^2}\right)^{1/2}\left[r_2^3\log\left(\frac{r_2+(r_2^2-r_0^2)^{1/2}}{r_0}\right)-r_2^2(r_2^2-r_0^2)^{1/2}-\frac{(r_2^2-r_0^2)^{3/2}}{3}\right],$$

where V_2 is the potential drop across the sheath, i the current density, x_2 the sheath thickness at the plane cathode, r_0 the radius of the cylindrical cathode, r_2 the radius of the cylindrical sheath about the cathode, and k_1 the velocity of the positive ions for a gradient of one volt per cm. The experimental results for platinum electrodes immersed in pure and NaCl flames agree well with the theoretical equations given. It is found that the drop in potential at the cathode occurs in a sheath of uniform thickness, which completely surrounds the electrode. By plotting the gas potential at various points in the flame against distance from the cathode it is possible to estimate the thickness of the sheath. Over 95% of the potential drop takes place across the sheath at the cathode provided it is of clean platinum. If the cathode is not clean electrons are emitted which partially neutralize the accumulation of positive ions and thus reduce the sheath thickness. By measuring V_2, i, x_2 or r_0 and r_2, and making the proper substitutions in the above equations, the mobility k_1 of the positive ions is found to average 12.4 for a pure flame and 8.1 cms per sec. for one volt per cm for a NaCl flame.

A study of the *characteristic current-voltage curve* for a wire probe in a flame makes it possible to measure the voltage correction to be applied to the measured probe potential in order to obtain the true gas potential adjacent to the test probe. The correction is of the order of +1. volts.

It is found that the current density at the surface of the cylindrical sheath is constant for any given flame conditions, and size of cathode. Thus one can measure the current density existing in the small uniform gradient just outside the sheath. The *current density at the sheath surface* in a pure flame varies from 1. to 2.5 microamperes and for the NaCl flame from 5. to 11. microamperes.

1. Introduction

When more ions of one kind than the other are present in a given space, an electrostatic effect occurs which modifies the potential distribution. The effect is well known in the conduction of electricity through gases at low pressures and in flames. In flames the velocity of the positive ion is much less than that of the negative ions which are mostly electrons, and as a consequence an accumulation of slow moving positive ions gathers about the cathode which produces a large cathode potential drop, expecially in the case of clean platinum electrodes. These regions of large potential gradient

near the electrodes were called by J. J. Thomson layers or sheaths. Thomson[1] has worked out a theory of the current between two parallel plane electrodes with uniformly ionized gas between them. His equation, $V = Ai^2 + Bdi$, where V is the potential difference between the electrodes, A and B are constants, i the current, d the distance between the electrodes, has been successfully applied to the conduction of electricity in flames by H. A. Wilson.[2] The term Ai^2 represents the drop of potential across the layer at the cathode, which is proportional to the square of the current.

A paper on "Positive Ion Currents in the Positive Column of the Mercury Arc" by Langmuir,[3] describing a sheath theory which successfully explains the flow of current in mercury vapor arcs, suggested to the writer that a layer or sheath theory might be applied to the flow of current across the layers near electrodes immersed in a flame.

Thomson's theory assumes in the layers where the electric field is large that recombination is zero and on this assumption the equation representing the state of affairs in the layer near the cathode is $k_1 = \pi i x_2^3 / V_2^2$, where k_1 is the mobility of the positive ion, i the current density, x_2 the thickness of the layer, and V_2 the cathode drop of potential. The assumption that recombination is zero in the layers is reasonable for gases at low pressures where the mean free path is large, but for a bunsen flame where the mean free path is small and collisions numerous recombination is not entirely negligible. At the cathode surface where the current is carried entirely by the positive ions (there being no electron emission from the electrode), the strong electric field drives the electrons away, so that n_2 (electron density) is small and recombination is negligible. But at the sheath surface the electric field is small and the electron density equals the positive ion density; so that as we go from the cathode across the layer recombination will increase from zero at the cathode surface to its normal value at the sheath surface. Thomson's theory[1] for the sheaths about parallel plane electrodes has therefore been modified to agree with this assumption, and a corresponding theory developed for cylindrical electrodes.

Conflicting values of the positive ion mobility k_1 in the bunsen flame, varying from 1. to 400. cm/sec. per volt/cm, have been obtained by various writers. (See Experimental Results). So that it is desirable to obtain k_1 for flames by methods different from those already described. The theory given offers such a possibility. By measuring the sheath thickness, the current density, the potential drop across the sheath at the cathode, and substituting in the proper equations, the mobility, k_1, can be calculated.

Successful experimental tests confirming the modified sheath theory for both plane and cylindrical cathodes in flames have been carried out and values of k_1 for both pure and NaCl flames calculated. The potentiometer method with a galvanometer as the indicating device was used to measure the potential gradient, from which the sheath thickness was deduced. By

[1] Thomson, "Conduction of Electricity Through Gases," p. 64.
[2] Wilson, Phil. Mag. **10**, 476 (1905).
[3] Langmuir, Gen. El. Rev. **26**, 731 (1923).

taking the current voltage relation of a pair of clean platinum electrodes in a flame it is possible to measure the correction to be applied to the probe potential in order to obtain the true gas potential.

2. Theory

It is well known that the potential gradient between two clean platinum electrodes in a flame is far from uniform. A large part of the potential drop occurs at the cathode and this has been called the cathode drop of potential. The writer has measured potential gradients in flames in which more than 95 percent of the potential drop occurs close to the cathode. The explanation offered for this large voltage drop is that the electrons or negative ions travel many times faster than the positive ions.[4] The mobility k_1 for positive ions in a bunsen flame according to the results to be described varies from 7. to 17. cms/sec. volt/cm, while k_2 for the electrons varies from 2000. to 3000. cms/sec. volt/cm. Thus the electrons are immediately driven away from the cathode, while the positive ions because of their slow motion accumulate about the cathode, forming a positive space charge which limits the flow of current just as the space charge effect limits the electron current from a hot filament in a vacuum tube. Experiments described later show that for electrodes immersed in a flame a layer of positive ions of uniform thickness exists on both sides of a plane cathode and completely surrounds a cylindrical cathode. Likewise an electron sheath of comparatively small thickness exists about the anode.

For deriving an equation for the flow of current between infinite parallel plane electrodes in an ionized gas Thomson[1] supposes that the velocities of the ions are proportional to the electric intensity at any point, and also that near the positive and negative plates there are layers in which recombination may be neglected.

First let us consider the case for large parallel plane electrodes. Experiment shows that electron emission may be neglected for clean platinum electrodes. Let n_1 and n_2 be the number of positive ions and electrons per unit volume at any point at a distance x measured from the cathode surface. Let q be the number of positive ions or electrons produced in unit time per unit volume at this point. Let X be the electric intensity, k_1 the velocity of the positive ions due to unit electric field, k_2 the velocity of the electrons due to unit electric field, x_1 the electron sheath thickness at the anode, x_2 the positive ion sheath thickness at the cathode, α the coefficient of recombination, e the charge on an ion, and i the current per square cm of electrode surface. The fundamental equations are[1]

$$dX/dx = 4\pi(n_1 - n_2)e \tag{1}$$

$$n_1 e k_1 X + n_2 e k_2 X = i \tag{2}$$

$$d(n_1 k_1 X)/dx = q - \alpha n_1 n_2 \tag{3}$$

$$d(n_2 k_2 X)/dx = -(q - \alpha n_1 n_2) \tag{4}$$

[4] H. A. Wilson, Phil. Trans. **A192** (1899).

Differentiating Eq. (1) with respect to x and making use of Eqs. (3) and (4) we obtain

$$d^2X^2/dx^2 = 8\pi e(q-\alpha n_1 n_2)(1/k_1+1/k_2) \tag{5}$$

Thomson assumes that recombination is zero in the layer, but perhaps a more satisfactory assumption for flame conditions may be arrived at as follows. At the anode surface where $x=0$, all the current must be carried by electrons, and since the electric field drives all positive ions away from the anode surface, $n_1=0$ and hence $q-\alpha n_1 n_2 = q$. But at the sheath surface where the electric intensity is small compared with that inside, $n_1=n_2$, and hence at $x=x_1$, $dX/dx=0$ and therefore $q-\alpha n_1 n_2=0$. Equation (2) with $n_1=n_2$ shows that the fraction of the current carried by either positive ions or electrons at the sheath surface is proportional to their respective mobilities. All the positive ions which carry current at the sheath surface are produced in the layer and hence the positive ion current increases from zero at $x=0$ to $n_1 e k_1 X$ at $x=x_1$. The same considerations must hold at the cathode, where the current at the cathode surface must be carried entirely by positive ions, and the electron current in the opposite direction increases from zero at the cathode surface to $n_2 e k_2 X$ at the positive ion sheath surface. Furthermore the electrons which carry current at the sheath surface must be produced in this layer. We can therefore assume as an approximation consistent with the above that

$$q-\alpha n_1 n_2 = q(1-x/x_1).$$

This gives $q-\alpha n_1 n_2 = q$ at $x=0$, and $=0$ at $x=x_1$. Thus recombination increases from zero at the electrode surface to its value at the sheath surface instead of being zero throughout the layer. Eq. (5) then becomes

$$d^2X^2/dx^2 = 8\pi eq(1-x/x_1)(1/k_1+1/k_2).$$

We assume that the quantity q is constant for any given flame conditions, and so it can be removed from the above equation as follows. The number of the positive ions produced in the layer which carry the current at the sheath surface will be in accordance with our assumption equal to

$$\int_0^{x_1}(q-\alpha n_1 n_2)dx = \int_0^{x_1} q(1-x/x_1)dx = nk_1X_0,$$

where $n_1=n_2$ and $X_0=$ the electric intensity in the uniform gradient and therefore at the sheath surface. Integrating this we obtain

$$qx_1/2 = nk_1X_0 = ik_1/e(k_1+k_2),$$

which is the number of positive ions which carry the current through unit area at the sheath surface. Then

$$8\pi eq = 16\pi ik_1/x_1(k_1+k_2).$$

Making this substitution we have

$$\frac{d^2X^2}{dx^2}=\frac{16\pi i}{k_2x_1}\left(1-\frac{x}{x_1}\right).$$

Integrating this with respect to x we get

$$\frac{dX^2}{dx}=\frac{16\pi i}{k_2x_1}\left(x-\frac{x^2}{2x_1}\right)+C_1. \tag{6}$$

At $x=x_1$, we have $n_1=n_2$, so that Eq. (1) becomes

$$dX^2/dx=8\pi e(n_1X-n_2X)=0.$$

Hence the constant becomes

$$C_1=-16\pi ix_1/2k_2x_1.$$

Replacing the constant C_1 in (6) with its value and integrating we obtain

$$X^2=\frac{16\pi i}{k_2x_1}\left(\frac{x^2}{2}-\frac{x^3}{6x_1}-\frac{xx_1}{2}\right)+C_2.$$

To determine C_2 we make use of the condition that at $x=x_1$, the electric intensity $X=X_0$, and

$$C_2=X_0^2+\frac{16\pi i}{k_2x_1}\left(\frac{x_1^2}{6}\right).$$

Then substituting the value of C_2 and extracting the square root,

$$X=\left(\frac{16\pi i}{6k_2x_1^2}(x_1-x)^3+X_0^2\right)^{1/2}. \tag{7}$$

The potential drop V_1 across the electron sheath is $\int_0^{x_1}Xdx$; substituting value of X given by Eq. (7), neglecting X_0, since the electric intensity outside the sheath is small compared to that inside, and integrating we have

$$V_1=(32\pi i/75k_2)^{1/2}x_1^{3/2}. \tag{8}$$

Solving for k_2, the mobility of the electrons, we get

$$k_2=32\pi ix_1^3/75V_1^2 \text{ cms per sec. per unit gradient in e.s.u. units.} \tag{9}$$

Dividing this by 300. will give k_2 in cms/sec. for one volt/cm.

Similarly the drop in potential across the positive ion sheath at the cathode is

$$V_2=(32\pi i/75k_1)^{1/2}x_2^{3/2}, \tag{10}$$

and the mobility of the positive ions becomes

$$k_1=32\pi ix_2^3/75V_2^2. \tag{11}$$

Thus by measuring the current density, the thickness of and the potential drop across either sheath, we can calculate the velocities per unit gradient of either the positive ions or electrons. Thomson's original theory gives $k_1=\pi i x_2^3/V_2^2$ for the positive ion mobility, which is 2.3 times the value given by Eq. (11).

The same assumptions used with plane electrodes can be applied to cylindrical electrodes. Let us consider the electron sheath about a long wire of small diameter as anode. With proper change of signs and symbols the the theory will also apply to the positive ion sheath about the cathode. In addition to the symbols already defined, let r be the distance measured normally from center of electrode, r_0 the radius of either anode or cathode, r_1 the radius of electron sheath about the anode, r_2 the radius of positive ion sheath about the cathode, and i the current per cm length of electrode.

The fundamental equations when transformed into cylindrical coordinates become

$$d(Xr)/dr=4\pi er(n_1-n_2) \tag{12}$$

$$2\pi rn_1k_1Xe+2\pi rn_2k_2Xe=i \tag{13}$$

$$d(2\pi rn_1xk_1X)/dr=(q-\alpha n_1n_2)2\pi r \tag{14}$$

$$d(2\pi rn_2k_2X)/dr=-(q-\alpha n_1n_2)2\pi r \tag{15}$$

Multiplying Eq. (12) by X, differentiating it with respect to r, and making use of Eqs. (14) and (15) we find that

$$\frac{d}{dr}\left(\frac{Xd(Xr)}{dr}\right)=4\pi er(q-\alpha n_1n_2)\left(\frac{1}{k_1}+\frac{1}{k_2}\right). \tag{16}$$

As in the case of plane electrodes, the current at the anode surface must be carried entirely by electrons, so that $n_1=0$ at $r=r_0$, and $q-\alpha n_1n_2=q$. At the surface of the electron sheath where the electric intensity is small, $n_1=n_2$, and therefore at $r=r_1$, we have $q-\alpha n_1n_2=0$. A reasonable assumption which fulfills these conditions is to let

$$q-\alpha n_1n_2=q\left(\frac{r_1^2-r^2}{r_1^2-r_0^2}\right).$$

Eq. (16) then becomes

$$\frac{d}{dr}\left(\frac{Xd(Xr)}{dr}\right)=4\pi eq\left(\frac{rr_1^2-r^3}{r_1^2-r_0^2}\right)\left(\frac{1}{k_1}+\frac{1}{k_2}\right). \tag{17}$$

The procedure for carrying out the remainder of the derivation is similar to that for plane electrodes and will be omitted.

The electric intensity in the sheath becomes

$$Y=\left(\frac{2i}{3k_2(r_1^2-r_0^2)^2}\right)^{1/2}\frac{(r_1^2-r^2)^{3/2}}{r}.$$

The potential drop V_1 across the cylindrical electron sheath is $\int_{r_0}^{r_1} X dr$, and substituting the value of X and integrating between the limits r_1 and r_0,

$$V_1 = \left(\frac{2i}{3k_2(r_1^2-r_0^2)^2}\right)^{1/2}\left[r_1^3 \log\left(\frac{r_1+(r_1^2-r_0^2)^{1/2}}{r_0}\right) - r_1^2(r_1^2-r_0^2)^{1/2} - \frac{(r_1^2-r_0^2)^{3/2}}{3}\right]. \tag{18}$$

Solving for k_2, the mobility of the electrons, we have

$$k_2 = \frac{2i\left[r_1^3 \log\left(\frac{r_1+(r_1^2-r_0^2)^{1/2}}{r_0}\right) - r_1^2(r_1^2-r_0^2)^{1/2} - \frac{(r_1^2-r_0^2)^{3/2}}{3}\right]^2}{3V_1^2(r_1^2-r_0^2)^2} \tag{19}$$

In a similar manner the drop in potential across the positive ion sheath about the cathode becomes

$$V_2 = \left(\frac{2i}{3k_1(r_2^2-r_0^2)^2}\right)^{1/2}\left[r_2^3 \log\left(\frac{r_2+(r_2^2-r_0^2)^{1/2}}{r_0}\right) - r_2^2(r_2^2-r_0^2)^{1/2} - \frac{(r_2^2-r_0^2)^{3/2}}{3}\right] \tag{20}$$

and the mobility of the positive ion becomes

$$k_1 = \frac{2i\left[r_2^3 \log\left(\frac{r_2+(r_2^2-r_0^2)^{1/2}}{r_0}\right)^{1/2} - r_2^2(r_2^2-r_0^2)^{1/2} - \frac{(r_2^2-r_0^2)^{3/2}}{3}\right]^2}{3V_2^2(r_2^2-r_0^2)^2} \tag{21}$$

In the uniform gradient outside either sheath practically all the current is carried by the electrons and because of their high mobility only a small fraction of the applied voltage is required to cause the current to flow. The experimental results described below agree well with the theoretical equations for the sheath about the cathode.

3. Experimental Procedure

Those who have worked with flames are familiar with the difficulties in maintaining steady flame conditions for any length of time. Variations in gas pressure and quality of gas are the two prime causes of flame instability. In these experiments the city gas supply was found quit satisfactory so far as constant quality was concerned, in fact much superior to gasoline gas. A fairly constant gas pressure was maintained by connecting a gasometer in the gas line and placing sufficient weights on the movable drum to keep it stationary for any size flame. In this way any small variations in gas pressure were absorbed by the floating drum of the gasometer. The steadiness of the flame was frequently checked by noting the value of the current between two electrodes maintained at some constant potential

difference. Any large variations in current were eliminated by slight adjustment of the control valves in the gas line. It was found that with these precautions the current variations could be limited to less than 5 per cent for periods of two hours or more.

For the electrodes arranged one above the other, the vertical flame of a Meeker burner was found suitable. For the horizontal arrangement of electrodes, a satisfactory burner was made by mounting a number of small quartz tubes, each about 3 mms inside diameter and 2.5 cms long, in holes drilled in a row along the length of a brass tube 2 cms in diameter. This burner will give a flame about 10. cms long, 1.4 cms thick, and any height desirable. The electrodes were supported a short distance above the blue cones in the flame. Compressed air was admitted to produce a well oxidized flame, the cones being about 2 cms high. Solutions of various salts could be sprayed into the flame as desired by means of a Gouy sprayer connected in the air line.

In studying positive ions in a flame electron emission from the cathode must be eliminated so far as possible. At ordinary temperatures in a bunsen flame this is small for clean platinum. It was found that if clean platinum wires or foil were used for the cathode, so that the current was limited by the positive ion sheath about it, that it mattered little what the nature or size of the anode was. In case of the vertical flame the Meeker burner was used as the anode.

Two clean platinum cylinders or plates were used as the electrodes in the horizontal flame. In the sheath theory for cylindrical electrodes the radius of the cylinder occurs in the formula for the flow of current. To test this equation for various cylinder diameters platinum wire of sizes No. 26, 20, and 12 were procured. Cylinders of larger diameter were made of platinum foil. Thus the cylinder diameters tested ranged from 0.0406 cms to 0.60 cms, a maximum ratio of one to fifteen.

The method of taking data for the current-voltage curves was to connect the two electrodes in series with a galvanometer connected to an Ayrton shunt, and a slide wire rheostat of 3200. ohms resistance. A *B* battery of suitable voltage was connected across the high resistance, and thus by making one connection to the movable contact it was possible to vary the applied voltage in as small steps as desired. Suitable means were provided for reversing the direction of the applied voltage, this voltage being read by a Weston voltmeter.

The procedure for obtaining data by which the potential versus distance curves were plotted requires more detailed explanation. A diagram of the circuit used is shown in Fig. 1. This shows the horizontal arrangement of electrodes. The exploring electrode, used for measuring the potential at various points between the two current electrodes, consisted of No. 26 platinum wire. It is desirable to use a probe wire of as small radius as possible, but a smaller size will sag after a short time in a flame. The probe wire, welded to a piece of No. 18 copper wire, was mounted on the movable carriage of a micrometer microscope, the microscope being removed. The

screw of the micrometer scale was oriented so that its axis was parallel to the flow of current between the electrodes. Thus the position of the probe at any point with respect to the electrodes could be ascertained and the distance between the electrodes easily measured. The high resistance slide wire rheostat R in conjunction with the B battery formed a potentiometer device by means of which the probe could be maintained at any potential with respect to the cathode.

With the potential of the probe the same as that of the cathode, $V_2 = O$, positive ions will flow to it. As the probe is moved from the cathode to the anode the potential of the gas about it increases, and the probe current increases. By increasing V_2, the potential of the probe with respect to the cathode, the probe current can be reduced to zero, at which point the probe would be at the same potential as the adjacent gas, if the velocities of the

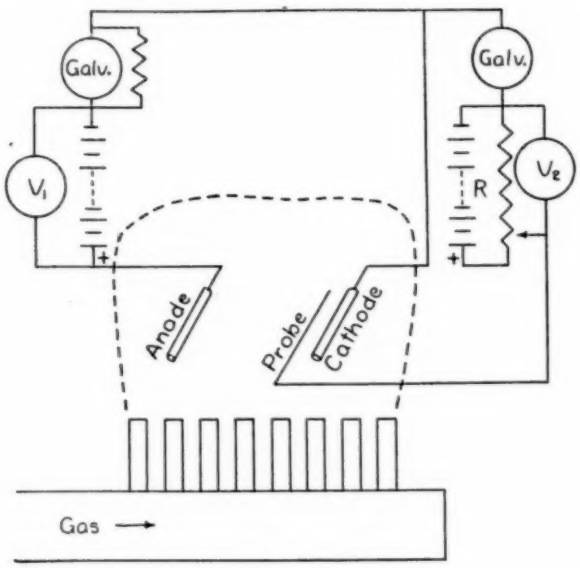

Fig. 1.

positive and negative ions were equal. In reality since the velocities are quite different, the voltage read when the galvanometer indicates zero probe current must have a small correction applied to it to give the true gas potential. This correction is of the order of one volt and must be determined by a preliminary measurement. This is more fully discussed in the Experimental Results. Thus the potential of the gas at various points between and outside the current electrodes can be quickly obtained, and by plotting probe voltage against distance from the anode we have a graph which shows how the gas potential varies as we go from one electrode to the other. If desired it is easy to obtain the potential gradient or electric intensity at any point from the graph.

The above method of obtaining potential gradient data affords a method for measuring the thickness of the positive ion sheath about the cathode.

By means of the probe it is easy to show that the layer or sheath surrounds the cathode, and that it contains an excess of positive ions. In making measurements of potential inside the sheath, one must be careful in noting the exact voltage at which the probe current is reduced to zero, for a further increase in voltage produces a very small increase in current, until the probe voltage becomes equal or greater than the potential at the edge of the sheath. When the probe voltage is greater than this, electrons can enter the sheath and if the probe is not too far inside the sheath surface the current will increase rapidly. If the probe is as much as a 1/2 cm or more inside a thick sheath, its potential will have to be much greater than that of the sheath surface, for at lower potentials the electrons pulled into the sheath are lost by recombination before they reach the probe. This test shows that there are comparatively few free electrons or negative ions in the positive ion sheath expecially near the cathode surface, and proves that the sheath exists not only theoretically but in reality.

As has already been stated the potential drop across the positive ion sheath is much greater than that outside it. So that to obtain data for testing the sheath theory we may choose that point on the potential versus distance graph where it begins to show a sharp change in curvature as the edge of the sheath. The sheath thickness is taken as the distance from the edge of the sheath to the center of the cathode. This distance can be measured to within 10 percent easily, but probably not much greater accuracy should be claimed because of the difficulty in choosing the point at which the density of positive ions increases appreciably over that of the electrons.

4. Experimental Results

The method for obtaining the voltage correction to be applied to the probe potential in order to obtain the true gas potential is described in a paper by McCurdy.[5] The two changes in curvature in the current-voltage graphs where the electrons begin to enter the positive ion sheath, and where the positive ion sheath disappears and the electron sheath begins to grow are easily seen. The results show that in reading the potential of a Bunsen flame by the probe and electrometer method. that a correction of about +0.4 volt for a NaCl flame and about +0.75 volts for a pure flame should be made. This of course will depend on the gas mixture admitted to the burner and the location of the electrodes in the flame.

According to the theory the density n_2 of the electrons increases from zero at the cathode surface to the normal value at the sheath surface. The flow of current to the probe for various potentials applied between it and the cathode throws light on this question. In Fig. 2 are shown curves which give the relation between the probe current and the voltage applied to it for various positions inside a sheath of constant thickness. The potential difference between the current electrodes was maintained constant at 88.6 volts. D is the distance of the probe from the cathode. Curve No. 1 shows the current-voltage relation for the probe placed 0.1 cm from the

[5] McCurdy, Phil. Mag. **48**, 905 (1924).

plane cathode. With the probe potential with respect to the cathode equal to zero, the adjacent gas is at a positive potential and a flow of positive ions to the probe takes place. As the potential of the probe increases the positive ion current decreases until at +18. volts the probe current becomes zero. This is taken as the true potential of the gas at a point distant 0.1 cm from the cathode. It seems reasonable that the correction of +0.75 volts for a pure flame ought not to be applied to obtain the correct gas potential, because there are not sufficient free electrons present in the sheath to change appreciably the probe potential. A further increase of probe potential gives a small increase in electron current which approaches a saturation value at 80. volts. This current remains constant up to 140. volts. The reason for this is that although the probe potential is larger than the potential drop across the sheath, yet the probe can ony gather the few electrons produced in a limited region adjacent to it and any additional electrons that may be pulled into the sheath from the outside will be lost by recombining with the

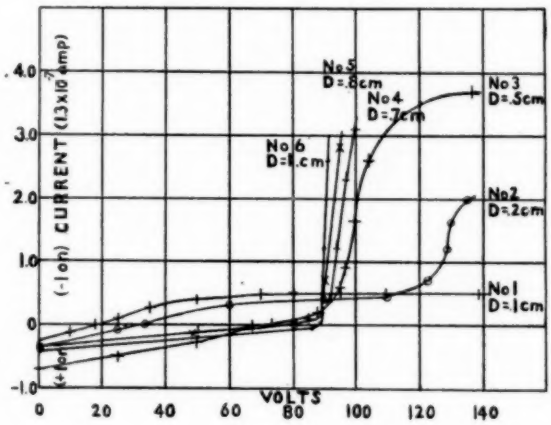

Fig. 2.

positive ions before they reach the probe. This indicates that the strong electric field plays the important part in rapidly removing the electrons from the positive ion sheath, and that the electron density near the cathode surface is small compared with the positive ion density. In curve No 3 the probe current becomes zero at 67.5 volts and this is the potential of the flame at a point 0.5 cm distant from the cathode. A further increase of probe potential gives a small increase in current until the potential attains 90. volts, at which potential electrons from outside the sheath begin to reach the probe and the current increase rapidly. Curve No. 6 shows the condition existing at the edge of the sheath which is 1. cm from the cathode. The probe current becomes zero at 88.5 volts, and a fraction of a volt above this is sufficient to produce a large increase in electron current to the probe. This is what one would expect at the edge of the sheath for the probe is in a region where there are equal densities of positive ions and electrons. Thus we see that the electron density increases from zero at the cathode surface

to $n_2 = n_1$ at the sheath surface. It is proper at the edge of the sheath to apply the correction of $+0.75$ volts to the probe potential to obtain the true gas potential because the probe is now exposed to a large number of electrons having average velocities corresponding to 0.75 volts. The true potential of the gas at this point would therefore be $88.5+0.75=89.25$ volts. In plotting the potential versus distance data this correction has been neglected because it is much less than the sum of the other experimental errors.

In the vertical flame the sheath is thicker above the cathode than below. Some measurements showed that the sheath was as much as 50 percent thicker above than below the electrode, the reason being that the positive ions are carried up by the motion of the flame gases. It was found that better results in testing the sheath theory were obtained by using data obtained with the horizontal arrangement of electrodes.

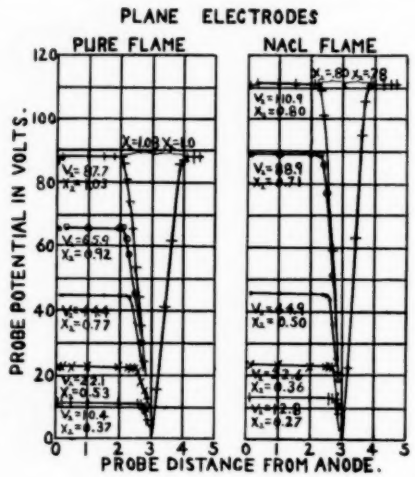

Fig. 3.

Fig. 3 shows the results of plotting two sets of data for plane electrodes, one set for a pure flame and the other for a NaCl flame. The current electrodes were 3. cms apart. The voltage between the current electrodes was kept constant while the data for each curve was obtained. The points plotted are the voltages as read from the voltmeter V_2 when the probe-cathode current was just zero. The cathode is indicated by the heavy vertical line. For the highest voltage applied to the current electrodes the potential has been plotted for points on both sides of the cathode. This proves the existence of the positive ion sheath on both sides of the cathode and furthermore that in a horizontal arrangement of electrodes the sheath has the same thickness on either side. For example in the case of the pure flame the sheath thickness measured from the cathode towards the anode is 1.03 cms and the opposite direction 1.0 cms. For the NaCl flame, x_2 (=sheath thickness) equals 0.80 and 0.78 cms for the same cathode at a higher potential difference. The spraying of NaCl into the flame increases the density of positive and negative ions which causes a 30 to 50 percent decrease in sheath thick-

ness. It will be noted that the change in curvature of the potential versus distance curve at the edge of the sheath is quite abrupt, indicating that the velocities of the positive ions and the electrons are very different. Outside the sheath, the curve is almost horizontal which means that the potential gradient from the edge of the sheath to the anode is small.

The method of measuring was not sensitive enough to measure accurately the potential drop and the electron sheath thickness at the anode. According to the theory, $k_1^2/k_2^2 = V_1/V_2$, and if $k_1 = 10.$ cms per sec. for one volt per cm for positive ions, $k_2 = 3000.$ cms per sec. for one volt per cm for electrons, $V_2 = 88.$ volts = potential drop across the positive ion sheath, then $V_1 = 0.00098$ volts = the potential drop across the electron sheath. It is impossible with the present apparatus to measure such a small potential drop, but assuming the above values of V_1 and k_2, and the corresponding value of $i = 0.693 \times 10^{-7}$ amperes per sq. cm, and substituting these values in c.g.s. units in the equation

$$x_1 = (75 k_2 V_1^2 / 32\pi i)^{1/3}$$

$x_1 = 0.003$ cms is the electron sheath thickness. This is too small a distance to be even approximately measured with the probe used, but certainly the electron sheath thickness for this particular observation was less than the diameter of the probe which was 0.04 cms.

A summary of the data obtained in connection with Fig. 3 is given in Table I. The sheath voltage drop and the sheath thickness were both taken

TABLE I. *Summary of data obtained in connection with Fig. 3.*

V_2 (volts)	I (amp.)	i (amp.)	x_2 (cms)	k_1
		Pure flame		
10.4	1.19×10^{-7}	0.218×10^{-7}	0.37	12.3
22.1	1.75	.32	.53	11.8
44.4	2.64	.485	.77	13.5
65.9	3.10	.567	.92	12.3
87.7	3.79	.693	1.03	11.9
		NaCl flame		
12.8	2.58×10^{-7}	0.471×10^{-7}	0.27	6.92
22.6	3.46	.633	.36	6.96
44.9	5.11	.936	.50	7.0
88.9	7.26	1.33	.71	7.33
110.9	8.25	1.51	.80	7.55

from the graphs. The meaning of the symbols are as follows; V_2 is the potential drop across the positive ion sheath, I the total current in amperes between the electrodes, i the current in amperes per sq. cm of cathode surface, and $k_1 = 32\pi i x_2^3 / 75 V_2^2 300.$ the velocity in cms/sec. for one volt/cm. The effective area of the cathode (both sides) is 5.46 cms.

That the equation given in the theory for the positive ion sheath about the cathode satisfies the experimental results is shown by the good agreement between the values of k_1. The largest deviation from the mean for the pure

flame is 9.7 percent and for the NaCl flame 5.6 percent, and this seems quite satisfactory when it is remembered that the largest experimental error, that occuring in the measurement of the sheath thickness, is probably not much less than 5 percent and may be as much as 10 percent for small values of x_2. The edge correction has also been neglected. The values

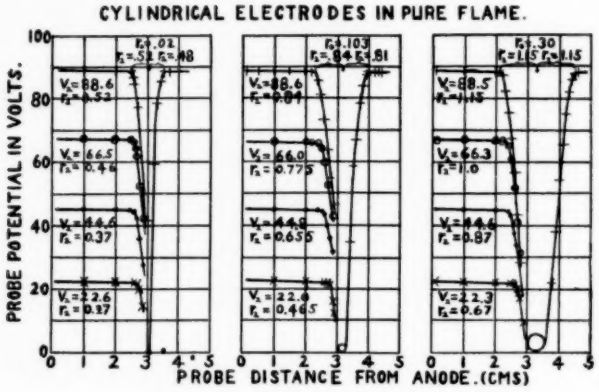

Fig. 4.

of k_1 obtained will be discussed after presenting the results for cylindrical electrodes.

The results for cylindrical electrodes are of perhaps greater interest, for the equations which represent the relations existing between current and volts involved not only the sheath radius but the radius of the electrode. The potential gradient curves for cathodes of radii 0.02, 0.103, and 0.30

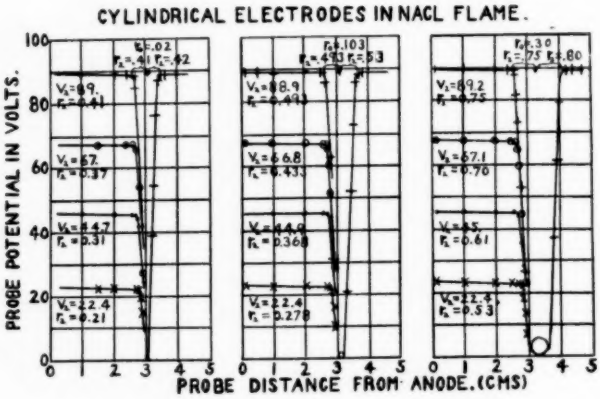

Fig. 5.

cms for various applied voltages in pure and NaCl flames are shown in Figs. 4 and 5. Here again the potentials for points on opposite sides of the cylinders are plotted for the largest value of potential difference used. The middle point of the cylindrical cathode and therefore of the sheath is indicated by the short vertical arrow, and at the bottom the cross-section to scale of

each cylinder is shown. It will be noted that the agreement of the sheath radii as measured on either side of the various electrodes are well within the limits of experimental error claimed. The spraying of NaCl into the flame increases the current and decreases the sheath radius over that in the pure flame for the same applied voltages.

TABLE II. *Results for pure flame.*

V_2 (volts)	I (amp.)	i (amp.)	r_2 (cms)	r_0 (cms)	r_2/r_0	k_1
22.6	0.76×10^{-7}	0.505×10^{-7}	0.27	0.02	13.5	17.1
44.7	1.06	.703	.37	.02	18.5	15.1
66.5	1.35	.90	.46	.02	23.0	16.3
88.6	1.62	1.08	.52	.02	26.0	15.3
				Greatest deviation from the mean =		7.2%
22.0	0.594	0.396	0.465	0.103	4.52	10.2
44.8	.89	.594	.655	.103	6.36	12.1
66.0	1.09	.725	.775	.103	7.52	11.9
88.1	1.42	.943	.84	.103	8.15	11.3
				Greatest deviation from the mean =		10.3%
22.3	1.45	0.97	0.67	0.30	2.23	7.96
44.6	1.98	1.32	.87	.30	2.9	10.1
66.3	2.44	1.63	1.0	.30	3.33	10.7
88.5	2.97	1.98	1.15	.30	3.83	13.1
				Greatest deviation from the mean =		25. %

Tables II and III give the results in tabulated form for the pure and NaCl flames respectively. The meaning of the symbols are as follows; V_2 = voltage drop across the positive ion sheath, I is the total current in amperes, i the current in amperes per cm length of the cathode, r_0 the cathode radius in cms, r_2 the positive ion sheath radius in cms, and k_1 the velocity per volt

TABLE III. *Results for NaCl flame.*

V_2 (volts)	I (amp.)	i (amp.)	r_2 (cms)	r_0 (cms)	r_2/r_0	k_1
22.4	1.19×10^{-7}	0.79×10^{-7}	0.21	0.02	10.5	12.6
44.7	1.48	.99	.31	.02	15.5	12.8
67.0	2.18	1.45	.37	.02	18.5	13.8
89.0	2.74	1.82	.41	.02	20.5	13.2
				Greatest deviation from the mean =		5.3%
22.4	3.47	2.31	0.278	0.103	2.7	5.95
44.9	4.78	3.2	.368	.103	3.57	7.1
66.8	5.77	3.86	.433	.103	4.21	7.5
88.9	6.93	4.62	.493	.103	4.78	8.5
				Greatest deviation from the mean =		18. %
22.4	5.78	3.86	0.52	0.30	1.73	6.3
45.0	8.57	5.71	.61	.30	2.03	6.6
67.1	9.9	6.60	.70	.30	2.33	7.5
89.2	11.9	7.92	.75	.30	2.5	7.3
				Greatest deviation from the mean =		10. %

per cm of the positive ion as given by Eq. (21) in the theory. The effective length of the cylinder was 1.5 cms.

The agreement between the values of k_1 as given for each diameter of cathode is quite satisfactory when one remembers that the accumulated

experimental error can hardly be less than 10 percent. The greatest deviation in k_1 from the mean is given for each size of cathode tested. It will be noted that the ratios of sheath radius to cathode radius vary from 1.73 to 26.

At the surface of the sheath there are equal numbers of plus and minus ions and the current is carried mainly by electrons leaving the sheath. An examination of the graphs shows that the potential gradient just outside the sheath surface is about the same no matter what the size of the sheath or the voltage drop across it. This suggests that the number of positive ions entering and electrons leaving the sheath surface per square cm is constant

TABLE IV. *Data on current density at the sheath surface.*

I (amp.)	r_2 (cms)	r_0 (cms)	Surface area (Sq. cms)	I/Surface area or current density
		Pure flame		
0.76×10^{-7}	0.27	0.02	3.009	2.52×10^{-8}
1.06	.37	.02	4.36	2.42
1.35	.46	.02	5.67	2.39
1.62	.52	.02	6.61	2.44
0.59	0.465	0.103	5.75	1.03
0.89	.655	.103	8.87	1.01
1.09	.775	.103	11.09	0.98
1.42	.84	.103	12.34	1.15
1.45	0.67	0.30	9.18	1.58
1.98	.87	.30	12.98	1.53
2.44	1.0	.30	15.75	1.55
2.97	1.15	.30	19.20	1.55
		NaCl flame		
1.19	0.21	0.02	2.26	5.27×10^{-8}
1.48	.31	.02	3.52	4.21
2.18	.37	.02	4.35	5.01
2.74	.41	.02	4.93	5.56
3.47	0.278	0.103	3.12	11.1
4.78	.368	.103	4.28	11.1
5.77	.433	.103	5.29	10.9
6.93	.493	.103	6.19	11.2
5.78	0.52	0.30	6.6	8.75
8.57	.61	.30	8.09	10.6
9.9	.70	.30	9.68	10.2
11.9	.75	.30	10.62	11.2

for all sizes of sheath and therefore the total current to the cathode for any applied voltage should be equal to the current passing through the sheath surface per square cm multiplied by the total sheath surface area. That is the total surface area of the sheath about a cylindrical cathode varies directly with the total current. Table IV gives data which bears out this supposition. The first, second, and third columns give I the total current flowing to the cathode, r_2 the positive ion sheath radius, and r_0 the cathode radius. The fourth column gives the total sheath surface area including the ends of the cylinders. In the fifth column is given the ratio of I to total sheath surface area, which is the current density. The agreement between

the various values of the ratio of I to sheath area is excellent for cylindrical electrodes, which shows that the total current I to the cathode is equal to the current per square cm of the sheath surface multiplied by the total sheath surface area.

The same calculations were repeated for the plane electrodes. But extreme values of the ratio of I to sheath area vary about 45 percent, so the agreement is not so good. This can be accounted for as follows. It was assumed that the sheath about a plane electrode was of boxlike form and the surface area of the box was computed. It is probable however that the sheath about a plane electrode, where the sheath thickness is comparable in size with the electrode dimensions, assumes an ellipsoidal form and hence it is difficult to calculate even approximately the surface area.

The average of the value of k_1 for the pure flame using cylindrical electrodes is 12.6 and for the NaCl flame 9.1 cms/sec. volt/cm. For the plane electrode $k_1=12.3$ for the pure flame and 7.2 for the NaCl flame. The agreement between the values of k_1 obtained while using either cylindrical or plane electrodes is excellent. No attempt has been made to allow for the edge correction in the case of plane electrodes and the end correction in the case of cylindrical electrodes. Unless the plane electrodes were quite large and the sheaths thin it is probable that from the experimental standpoint cylindrical electrodes would require the smaller correction and would give the most reliable results. Allowing for the edge and end corrections would give smaller values of current density and hence smaller values of k_1.

The simple kinetic theory gives $k_1=e\lambda/mV$, where e/m is the ratio of the elementary charge to the mass of the ion, λ is the mean free path, and V is the mean velocity of agitation. Since λ varies directly with the absolute temperature and V varies directly with the square root of the absolute temperature, k_1 must vary with the square root of the absolute temperature. The accepted[6] experimental value of k_1 for positive ions in air at room temperature (20°C) is 1.4 cm/sec. per volt/cm. Assuming that the bunsen flame is composed largely of air and that the positive carriers are of the same nature at flame temperature, we can apply the temperature correction to the value 1.4. Taking the flame temperature $=2143°K$ and room temperature $=293°K$, $k_1=1.4(2143/293)^{1/2}=3.8$ cm/sec. per volt/cm. The agreement of this value with those obtained is quite satisfactory, when the other factors are taken into consideration. Some of the positive ions consist of charged hydrogen atoms and since their atomic weight is small compared with the average air molecule, their mobility would be larger. Also it is not settled as to whether the positive ion at room temperature consists of a single molecule or a cluster of molecules. High temperature would tend to break up any clusters and thus increase the mobility.

A comparison of the values of k_1 obtained by other investigators using different methods, is of interest. Lusby[7] obtained $k_1=290$ to 350 for tem-

[6] Loeb, Kinetic Theory of Gases, p. 476.
[7] Lusby, Phil. Mag. **22**, 775 (1911).

peratures ranging from 1450° to 1950°K, and Schönborn[8] using radioactive deposits on the anode as the source of positive ions found k_1 to vary from 200 to 400 cm/sec. per volt/cm. These values do not agree with those obtained in this investigation.

The best values obtained by Wilson[9] are $k_1 = 1$ to 2 cms/sec. per volt/cm. Andrade[10] found values of $k_1 = 2.5$ cm/sec. per volt/cm, and Moreau[11] gives values ranging from 10 to 80 cm/sec. per volt/cm. These values are in much better agreement with the values of $k_1 = 7$ to 17 cm/sec. per volt/cm, obtained by applying the modified Thomson sheath theory. Electron emission from the cathode has been neglected in the theory, but any such emission occuring would tend to give larger values of current and hence larger values of k_1. On the whole it seems probable that the formulae derived for the sheath theory and the experimental procedure used give as good values of k_1, the mobility of the positive ion in a flame, as can be obtained by any other method.

In concluding I want to express my appreciation to Professor H. A. Wilson for his interest in these experiments and expecially for his constructive criticism of the theory.

COLORADO COLLEGE,
COLORADO SPRINGS,
November 15, 1927.

[8] Schönborn, Zeits. f. Physik **4,** 118 (1921).
[9] H. A. Wilson, Phil. Trans. **A539** (1915).
[10] Andrade, Dissert. Heidelberg, 1911.
[11] Moreau, Ann. Chim. Phys. (8) **17,** 543 (1912).

LUMINESCENCE EXCITED BY X-RAYS IN COLLOIDAL ALKALINE EARTH SALTS*

By C. H. Boissevain and W. F. Drea

Abstract

The gelatinous precipitates of calcium, strontium and barium fluoride are positive colloids. The precipitates formed in the presence of an excess of calcium, strontium or barium ions luminesce in x-rays. The intensity of luminescence increases after the precipitate has been brought to red heat. The salts that are precipitated in the presence of excess fluoride do not luminesce in x-rays. The positively charged fluorides are changed into negative colloids by washing in dilute alkali; this causes the disappearance of the luminescence. Washing with dilute acid or distilled water is without effect. Colloidal barium sulphate shows a similar behaviour. Calcium tungstate and strontium tungstate are negative colloids; the precipitates formed in the presence of excess tungstate ions fluoresce brightly in x-rays. The precipitates formed in the presence of excess calcium or strontium ions fluoresce very faintly. A table is given showing the extent of the luminescent bands into the ultra-violet. Fluorides that have been heated in a hydrogen atmosphere show a dark discoloration and do not luminesce in x-rays. The presence of impurities diminishes the luminescence of colloidal precipitates. The alkaline earth chlorides and phosphates, calcium and strontium sulphate, and barium tungstate formed only crystalline precipitates that did not luminesce in x-rays. The hypothesis is made that the luminescence of colloidal precipitates is due to a thin layer of metallic oxide which is formed from the double layer of ions that is adsorbed on the surface of the colloidal particles.

IN THE course of a study of ultra-violet flurescence it became necessary for us to prepare calcium fluoride that did not show any luminescence when exposed to x-rays. Urbain and Bruninghaus[1] state that perfectly pure compounds do not phosphoresce. Pringsheim[2] thinks it very probable that chemically pure calcium fluoride does not fluoresce, but does not consider this to have been proved. Gyemant[3] observes that chemically pure calcium tungstate shows luminescence and thinks that the crystalline state is necessary for its appearance. Baly[4] also stresses the importance of the crystalline state and thinks that Urbain's generalisation about the importance of impurities was due to the fact that he worked with oxides of the rare earths, that are amorphous in the pure state. Perrine[5] observed fluorescence during the excitation by x-rays of chemically pure barium sulphate and calcium tungstate amongst others.

* From the laboratory of the Colorado Foundation for research in tuberculosis at Colorado College, Colorado Springs, Colo.

[1] Urbain and Bruninghaus, Ann. Chim. et Phys. **18,** 293 (1909).

[2] Pringsheim, Fluorescenz und Phosphorescenz im Lichte der neueren Atomtheorie, Berlin, 1923.

[3] Gyemant, Chemiker Zeitung, **49,** 493 (1925).

[4] Baly, Spectroscopy, Vol. II, London, 1927.

[5] Perrine, Phys. Rev. **22,** 48 (1923).

We prepared calcium fluoride by precipitating a solution of c.p. calcium chloride with c.p. potassium fluoride. When 5 mols $CaCl_2$ are mixed with one mol KF the calcium fluoride forms a gelatinous precipitate. The dried precipitate which has been centrifuged and washed repeatedly shows a faint greenish fluorescence when exposed to x-rays. This fluorescence is very much brighter when the calcium fluoride has been brought to red heat for one minute before being exposed. The luminescence persists for several hours after sufficient excitation; after its extinction a renewed light emission can be caused by heating. In other words, the precipitate of calcium fluoride behaves in every respect like a phosphor.

When an excess of potassium fluoride (10 mols KF to one mol $CaCl_2$) is used, the precipitate is also gelatinous, but does not show any luminescence in x-rays either before or after heating.

The spectrum of the fluorescence light was photographed on panchromatic plates with a Hilger quartz spectrograph that was shielded from the x-rays. The substance to be studied was contained in a cell of cellophane which is transparent to ultra-violet light and does not fluoresce in x-rays. A Coolidge universal tube was used with a potential of 80 kilovolts and a current of 3 milliamperes. The tube was enclosed in a leaden box and immersed in water-cooled oil as prolonged exposures were needed to obtain the spectrograms. The target distance was 25 cm. A point-plane spark-gap and circuit-breaker were used to protect the tube against reversal of polarity and overload. Under these conditions the x-ray machine could be left running continuously for 24 hours without requiring any attention.

TABLE I. *Wave-lengths of fluorescence bands*

Substance examined	Wave-length of band of fluorescent light	Duration of exposure
Calcium fluoride (excess calcium)	700–270 $m\mu$	72 hours
Calcium fluoride (excess fluorine)	—	72
Calcium fluoride (excess calcium and gadolinium)	700–320	72
Barium fluoride (excess barium)	700–320	72
Barium fluoride (excess fluorine)	—	72
Strontium fluoride (excess strontium)	700–330	72
Strontium fluoride (excess fluorine)	—	72
Barium sulphate (excess barium)	700–330	72
Barium sulphate (excess sulphate)	—	72
Calcium tungstate (excess tungstate)	510–370	24
Calcium tungstate (excess calcium)	500–390	72
Strontium tungstate (excess tungstate)	700–310	72
Strontium tungstate (excess strontium)	—	72

The fluorescence spectra of all the colloidal precipitates that were studied consisted of diffuse bands; their extent and the time of exposure are given in Table I.

The precipitates of strontium fluoride and barium fluoride are colloidal and their luminescence is similar to that of calcium fluoride; only the salts that are prepared in the presence of excess strontium or barium ions show phosphorescence when exposed to x-rays.

Calcium sulphate, strontium sulphate and barium sulphate that were prepared by precipitating solutions of the alkaline earth salts with sulphuric acid are crystalline and do not show any luminescence in x-rays, no matter in what proportion the ingredients are mixed. Von Weimarn[6] described a method by which barium sulphate is precipitated as a jelly; it consists in precipitating a 3–7 mol solution of barium thiocyanate with manganese sulphate. We prepared a colloidal precipitate of barium sulphate in this manner, but used ammonium sulphate instead of manganese sulphate, thus avoiding the presence of all metals except barium. This precipitate that was prepared in the presence of a large excess of barium ions phosphoresced in x-rays.

The chlorides and phosphates were always precipitated in the crystalline state in our experiments and do not show any luminescence in x-rays.

Calcium tungstate forms a colloidal precipitate which phosphoresces in x-rays. Its luminescence offers an important difference from that of calcium fluoride in that it depends upon the presence of an excess of tungstate ions instead of calcium ions. The precipitate that is formed in the presence of an excess of tungstate ions phosphoresces brightly when exposed to x-rays after having been heated. The intensity of its fluorescence is the same as that of the commercial x-ray intensifying screens, from which it only differs by the much slower rate of decay of its phosphorescence. Calcium tungstate prepared with an excess of calcium ions present shows only a very faint luminescence.

Strontium tungstate behaves similarly to calcium tungstate but the intensity of the luminescence of the salt prepared with excess tungstate ions present is much less than that of the corresponding calcium salt. The intensity of the luminescence of the salts prepared with excess strontium or calcium ions is approximately the same and very faint.

The precipitate of barium tungstate was crystalline in all our experiments; it does not show any luminescence in x-rays.

Calcium carbonate prepared by precipitating a solution of calcium hydroxide with CO_2 phosphoresces in x-rays after it has been heated. This phosphorescence is apparently due to the presence of calcium oxide as the salt loses its capacity for luminescence in x-rays after it has been exposed to the air for some time. This made it impossible to obtain a spectrogram because the cellophane cell is not airtight; quartz cells cannot be used in these experiments as all samples of fused quartz that we examined fluoresce in x-rays.

[6] Von Weimarn, Die Allgemeinheit des Kolloidzustandes, Dresden, 1925.

Calcium oxide prepared from freshly precipitated calcium carbonate fluoresces in x-rays; the intensity of its luminescence is less than that of calcium fluoride that is prepared in the presence of excess calcium ions.

It is a surprising fact that only those alkaline earth salts that were precipitated in the colloidal state show phosphorescence in x-rays, and that the appearance of luminescence depends upon the relative concentration of the precipitating ions.

Fajans and Frankenburger[7] have observed a similar relation between optical phenomena and the colloidal state in the case of silver bromide. The bromide precipitated from a solution containing excess Ag ions is a positive colloid and is sensitive to visible light; the limit of its sensitiveness is probably in the infra-red. The bromide precipitated from a solution containing excess bromine ions is a negative colloid and is only sensitive to light of wavelengths smaller than 435 mμ. They could demonstrate analytically that the positive colloid contained an excess of silver over the stochiometric proportions.

Calcium fluoride behaves differently in one respect: both the salt that is precipitated from a solution containing an excess of calcium ions and that which is precipitated from a solution with excess fluorine ions are positive colloids and go to the cathode in an electrophoretic apparatus. All precipitates of calcium tungstate on the other hand are negative colloids.

The colloidal state is due to an electric charge on the colloidal particles which keeps them apart. It is generally believed[8] that this charge is due to the existence of a double layer of ions. In the case of a positive colloid the inner layer consists of positive ions that are adsorbed on the surface of the particle; the outer layer consists of a region where the negative ions of the surrounding fluid are more concentrated to neutralize the charge resulting from the adsorbed ions. The ions that are adsorbed on the particles of the precipitate that was formed by adding one mol KF to five mols $CaCl_2$ may be Ca, K or H. In the precipitate formed by mixing one mol $CaCl_2$ with ten mols KF, only K or H can have been adsorbed. Since only the former shows luminscence, it is possible that this is due to the adsorbed calcium ions.

This supposition is confirmed by the effect of washing the colloidal precipitate in dilute acid or alkali. Calcium fluoride particles that are suspended in water or in dilute acid go to the cathode; the same particles go to the anode when they are suspended in normal NaOH. According to the theory outlined above, suspension in NaOH solution must involve the loss of the layer of adsorbed calcium ions. And indeed, if calcium fluoride that has been freshly precipitated from a solution with excess calcium ions is suspended in normal NaOH and then washed with distilled water, it loses its capacity for luminescence in x-rays. Washing with distilled water alone or with normal hydrochloric acid is without effect on the luminescence.

The second, outer layer that surrounds the particle with the adsorbed calcium ions consists of a zone where the negative ions of the surrounding

[7] Fajans and Frankenburger, Zeits. f. Physik. Chemie, **55**, 255 and 273 (1923).

[8] Bogue, Colloidal Behavior, New York, 1924.

fluid are more concentrated as a result of electrostatic attraction. After the precipitate has been washed repeatedly, these negative ions must be mainly OH ions. The effect of heating the precipitate to red heat will be to transform this double layer of Ca and OH ions into a thin film of calcium oxide. We are inclined to ascribe the luminescence of colloidal salts to this thin oxide film. Nichols and Wilber[9] have observed fluorescence in thin films of calcium, strontium and barium oxide amongst others. The films were prepared by sublimation in the electric arc and fluoresced when bombarded by cathode rays. They also state that this fluorescence does not depend upon the presence of an admixture of foreign material. The phosphorescence of the thin films of oxide surrounding the colloidal particles is entirely similar to the phenomenon described by Nichols and Wilber. The only difference is that our colloidal salts phosphoresce while the thin films of Nichols and Wilber only fluoresce. The electron that is emitted from the CaO molecule under the influence of the cathode rays returns immediately with light emission in the case of the thin films described by Nichols and Wilber. In the case of our colloidal precipitates the emitted electron may apparently be captured by the calcium fluoride particle and return after a longer or shorter interval and so cause the appearance of phosphorescence.

It might be supposed that the effect of heating the calcium fluoride is simply to transform the colloidal precipitate into the crystalline state, and that the excess Ca ions play the role of the impurity postulated by Urbain for the appearance of phosphorescence. However, if we moisten a non-fluorescent sample of calcium fluoride with a few drops of a dilute solution of calcium choloride or calcium hydroxide, dry it and bring it to red heat, it does not acquire the faculty of fluorescing in x-rays. If we treat a phosphorescent sample of calcium fluoride in the same way, we cause a considerable diminution of its light emission or even its entire disappearance. Other impurities than calcium salts have the same effect on the light emission. Urbain[10] showed that the ultra-violet fluorescence of some natural fluorides is due to the presence of gadolinium. If we prepare a fluoride by precipitating a solution containing five mols calcium chloride and one mol gadolinium nitrate with one mol KF, the precipitate shows the same type of fluorescence as that prepared without gadolinium but of much lower intensity.*

When a sample of luminescent calcium fluoride is brought to red heat in a hydrogen atmosphere, it turns dark grey and loses its capacity for luminescence in x-rays. The same change of color and partial loss of the capacity for luminescence in x-rays takes place after prolonged exposition to x-rays. Heating in the air restores in both cases the white color and the original intensity of luminescence. If the discoloration is caused by the formation of metallic calcium as seems likely, this offers another proof that the presence of calcium oxide is the cause of the light emission.

* We wish to express our thanks to Professor B. S. Hopkins of the University of Illinois, who so kindly put the gadolinium that was used in this experiment at our disposal.

[9] Nichols and Wilber, Phys. Rev. **17,** 107 (1921).

[10] Urbain, Ann. d. Chim. et Phys., **18,** 327 (1909).

The calcium ions are very firmly bound to the colloidal calcium fluoride particles, and no amount of washing with distilled water can remove them. Barium sulphate presents an interesting difference from calcium fluoride in this respect. If barium sulphate that has been freshly precipitated in the colloidal state from barium thiocyanate solution is washed and centrifuged three times with large quantities of distilled water, the dried and heated precipitate phosphoresces; if the same precipitate is washed ten times it does not show any luminescence in x-rays. The capacity for luminescence cannot be restored by moistening the precipitate with a few drops of dilute barium thiocyanate solution. The presence of a thin film of barium oxide is again necessary for the appearance of luminescence. The barium ions are not as firmly attached to the barium sulphate as the calcium ions are to the calcium fluoride particles, which explains why special precautions have to be taken to obtain colloidal barium sulphate.

The luminescent qualities of calcium fluoride that has been brought to red heat are not modified by subsequent exposure to air or water although calcium oxide under the same circumstances is changed into non-luminescent calcium hydroxide. The adsorption on the surface of the calcium fluoride particles has apparently not only modified the optical but also the chemical properties of the oxide, unless we want to assume that the adsorbed calcium oxide film has formed a chemical combination with the calcium fluoride particle; the distinction seems however immaterial.

Calcium tungstate is a negative colloid and we must consider the adsorbed tungstate ions as responsible for its luminescence. The precipitate that is formed in the presence of excess calcium ions shows only a faint luminescence of the same spectral character as that of the precipitate with excess tungstate ions. The presence of impurities or moistening the precipitate with dilute solutions of tungsten compounds again diminishes the intensity of the luminescence. None of it is apparently due to calcium ions, but since the precipitate that is formed in the presence of excess calcium ions also phosphoresces, we must assume either that pure calcium tungstate phosphoresces or that the surface of calcium tungstate particles always contains an excess of tungstate ions. The latter supposition is supported by the fact that calcium tungstate is always a negative colloid irrespective of its mode of preparation. On this supposition we ought to expect that calcium fluoride that has been precipitated from a solution with excess fluorine ions ought also to show some luminescence, because it has the same positive charge as the phosphorescent calcium fluoride. This luminescence is perhaps too faint to be observed, as the light emission of all fluorides is much less than that of calcium tungstate. It is impossible to decide between these two possibilities by washing the calcium tungstate with acid, which should remove the excess tungstate ions in the same way as washing with alkali removes the excess calcium ions from calcium fluoride, because calcium tungstate is chemically changed by acids.

Summary

1. Freshly precipitated calcium fluoride, strontium fluoride, barium fluoride, barium sulphate, calcium tungstate and barium tungstate phosphoresce on exposure to x-rays. This phosphorescence is much brighter when the precipitate has been brought previously to red heat for one minute.

2. The precipitated fluorides and sulphates are positive colloids. Their luminescence depends upon the presence of an excess of calcium, strontium or barium ions in the precipitating solution.

3. Calcium tungstate and barium tungstate are negative colloids. Their luminescence depends upon the presence of an excess of tungstate ions in the precipitating solution.

4. No luminescence on exposure to x-rays could be demonstrated in crystalline precipitates of alkaline earth salts.

5. The presence of a thin film of oxide on the surface of the heated colloidal particles is suggested as responsible for their luminescence.

COLORADO COLLEGE,
December 29, 1927.

THE EFFECT OF INITIAL VELOCITY OF ELECTRONS UPON THE ANODE CURRENT OF A VACUUM TUBE

By N. Kato

Abstract

Effective initial velocity of electrons emitted from a tungsten filament at different temperatures.—The initial velocity of electrons causes deviation of anode-current, anode-voltage relation of vacuum tubes as derived from the space charge equation. By eliminating the other causes of deviation, the author measured the degree of deviation of the current-voltage curve from the three-halves power law at various filament temperatures, and found that the effective initial velocity of electrons varies from about 0.5 volt at 2250°K to 4 volts at 3000°K. The effective initial velocity seems to be independent of the dimensions of the electrodes.

Introduction

THE effect of the initial velocity of electrons emitted from a hot cathode upon the current-voltage relation of a diode has been studied by Epstein,[1] Dushman,[2] Fry[3] and Langmuir.[4,5] The writer has investigated the effect of initial velocity of electrons upon the space charge of a tube with coaxial cylindrical electrodes of various dimensions, filament temperature being varied.

Precautions in the Measurement

The deviation of anode current of a diode from the three-halves power law is due to (1) the cooling effect of filament leads, (2) the ionization of residual gas, (3) the voltage drop along filament due to heating current and (4) the initial velocity of electrons emitted from the filament. Discussion of the effect of the last item is the chief object of the present paper.

To eliminate the cooling effect of filament leads, guard rings were used. To get rid of the effect of ionization of residual gas, tubes were as perfectly evacuated as is usual for power tubes, and were immersed in liquid air during the experiment.

For eliminating the effect of voltage drop along the filament due to the heating current, the following method was adopted. The return from the plate battery was connected to the positive end of the filament and one-half the voltage V_n between the neutral point of the filament and the anode was so chosen as to be greater than the filament voltage V_f, where V_n is to be found by the expression $V+V_f/2$. It is shown by the calculation below how the effect of the voltage drop of filament is minimized by this method.

[1] Epstein, Ber. d. Deut. phys. Ges. **21,** 85 (1919).
[2] Dushman, Phys. Rev. **4,** 121 (1914).
[3] Fry, Phys. Rev. **17,** 441 (1921).
[4] Langmuir, Phys. Rev. **21,** 419 (1923).
[5] Langmuir and Blodgett, Phys. Rev. **22,** 347 (1923).

Neglecting the initial velocity, the anode current obtained from the portion of the filament which is at a distance x from the neutral point will be

$$di = C(V_n \pm V_f x/l)^{3/2} dx \tag{1}$$

where $C = 14.65 \times 10^{-6}/\beta^2 r$ and l is the length of filament.

The anode current i_1 coming from the positive half of the filament is therefore

$$\begin{aligned} i_1 &= C \int_0^{l/2} (V_n - V_f x/l)^{3/2} dx \\ &= \frac{2}{5} \frac{l}{V_f} C \left\{ V_n^{5/2} - (V_n - V_f/2)^{5/2} \right\} \end{aligned} \tag{2}$$

Similarly, the current i_2 coming from the negative half of the filament is

$$i_2 = \frac{2}{5} \frac{l}{V_f} C \left\{ (V_n + V_f/2)^{5/2} - V_n^{5/2} \right\} \tag{3}$$

The total anode current i will then be

$$\begin{aligned} i = i_1 + i_2 &= \frac{2}{5} \frac{l}{V_f} C \left\{ \left(V_n + \frac{V_f}{2} \right)^{5/2} - \left(V_n - \frac{V_f}{2} \right)^{5/2} \right\} \\ &= C l V_n^{3/2} \left\{ 1 + \frac{1}{32} \left(\frac{V_f}{V_n} \right)^2 + \cdots \right\} \\ &= 14.65 \times 10^{-6} \frac{l}{\beta^2 r} V_n^{3/2} \left\{ 1 + \frac{1}{32} \left(\frac{V_f}{V_n} \right)^2 + \cdots \right\} \end{aligned} \tag{4}$$

where r is the radius of the anode and $\beta = f(r/r_0)$ where r_0 is the radius of the cathode. The function β is discussed at length by Langmuir and Blodgett.[5]

The second and following terms in the brackets of equation (4) may be neglected when $V_f < V_n/2$, which makes the above anode-current, anode-voltage relation independent of the voltage drop of filament at an error of less than 1 percent.

The above mentioned precautions excluded in the experiments all the causes for the deviation of anode current from the three-halves power law except that due to the initial velocity of electrons. This was experimentally verified by the fact that the anode-current, anode-voltage relation faithfully obeys the three-halves power law under higher anode voltage. The observed deviation under lower anode voltage may therefore be attributed to the initial velocity of electrons as far as the relation $V_f < V_n/2$ holds.

RESULTS

The dimensions of the tubes used in the experiments are as shown in Table I.

TABLE I. *Dimensions of tubes.*

Tube No.	Radius of anode	Radius of filament	Gap between anode and guard ring	Length of anode
1	0.5 cm	0.0035 cm	0.02 cm	0.5 cm
2	0.5	0.0085	0.02	0.5
3	0.5	0.0125	0.02	0.5
4	1.0	0.0085	0.02	0.5
5	1.5	0.0125	0.04	0.7

One set of anode current-anode voltage curves obtained with tube No. 2 is given in Fig. 1, curves being plotted in logarithmic scale and the corresponding temperatures found from Worthing and Forsythe's Table. Full lines in Fig. 1 show the parts where the condition $V_f < V_a/2$ holds. The

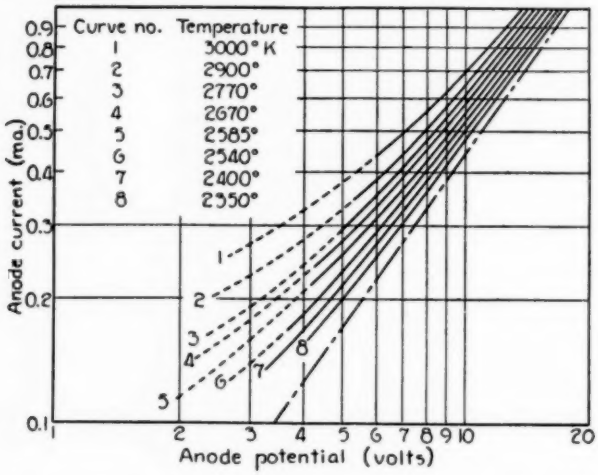

Fig. 1. Anode current, anode voltage relation for tube No. 2.

straight chain line in the figure represents the space charge equation $14.65\times10^{-6}lV^{3/2}/\beta^2 r$ calculated for the tube neglecting the effect of initial velocity. The voltage differences between one of the curves and the straight line represent effective initial velocity at the filament temperature corresponding to the curve. One example obtained from Fig. 1 is shown in Table II

TABLE II. *Values of the effective initial velocity for various anode currents.*

Temp.	V_0' (volts)							
	$i=0.3$ ma	$i=0.4$ ma	$i=0.5$ ma	$i=0.6$ ma	$i=0.7$ ma	$i=0.8$ ma	$i=0.9$ ma	mean
3000°K			3.6	3.6	3.6	3.6	3.7	3.61
2900		2.85	2.75	2.75	2.7	2.75	2.9	2.78
2770		2.15	2.2	2.2	2.25	2.3	2.4	2.25
2670		1.85	1.85	1.85	1.85	1.9	1.9	1.86
2585	1.45	1.35	1.45	1.45	1.5	1.5	1.55	1.46
2540	1.15	1.15	1.2	1.25	1.15	1.15	1.15	1.17
2400	0.8	0.75	0.9	0.8	0.9	0.8	0.9	0.83

from which it may be seen that the effective initial velocity V_0' is almost independent of the anode current.

In Fig. 2 the effective initial velocities measured with the tubes in Table I are plotted against temperatures. It may be seen in the figure that the initial velocity is about 0.5 volt at 2250°K, while it reaches about 4 volts at 3000°K, the value rapidly increasing with temperature. A simple empirical formula may easily be obtained; for example:

$$V_0' = 24.6\, T^{1/2} e^{-17291/T}$$

a curve of which is plotted in Fig. 2.

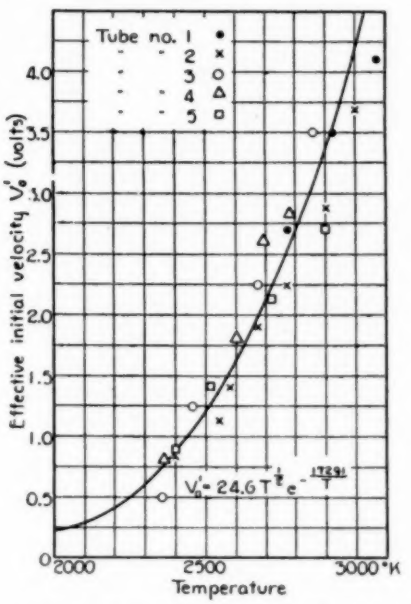

Fig. 2. Relation between effective initial velocity and temperature.

The space charge equation for a diode with cylindrical electrodes in which the effect of initial velocity of electrons is taken into account may also then be represented approximately by the following equation,

$$i = \frac{2\times 2^{1/2}}{9}\left(\frac{e}{m}\right)\frac{l}{\beta^2 r}(V + 24.6\, T^{1/2} e^{-17291/T})^{3/2}$$

The writer noticed the phenomenon in the course of an experiment about the ionization of residual gas in vacuum tubes, and no attempt has been made to make a theoretical investigation nor to enter into further accurate measurement, though it might be, no doubt, very interesting as far as high vacuum technique is concerned.

ELECTRO-TECHNICAL LABORATORY,
MINISTRY OF COMMUNICATIONS,
TOKYO, JAPAN.
October 29, 1927.

THE PHOTO-ELECTRIC EFFECT AND THERMIONIC EMISSION: A CORRECTION AND AN EXTENSION

By P. W. Bridgman

Abstract

In this note the analysis which I recently gave connecting the photo-electric effect with thermionic emission is freed from the assumption that the photo-electric characteristic frequency is independent of temperature. The thermionic work function and the photo-electric work functions are found to differ by a universal constant, which must be zero in the light of the work of Warner and the recent work of DuBridge. Furthermore, it is found that the temperature derivative at 0° Abs of the photo-electric threshold differs by a universal constant, which is also probably zero, from $(S_p-S_m)_0$, the difference of entropy at 0° Abs of surface ions and neutral atoms. The quantity $(S_p-S_m)_0$ enters the constant of the thermionic emission formula, so that there is a connection between this constant and the temperature derivative of the photo-electric threshold. In spite of the known small value of this latter, experiment allows a sufficient range of numerical values to account for the extreme variation of the thermionic emission constant from the "universal" value. The connection found by DuBridge between the thermionic emission constant and the work function is shown to be reasonable from the point of view of this analysis.

IN A recent number of the Physical Review[1] I deduced, among other things, several connections between the photo-electric and thermionic parameters. In this deduction I neglected, as I stated in a note, the variation of the photo-electric threshold frequency with temperature. It is true that experimentally any such temperature variation is so small as not to have been detected in most cases, the experiments of Ives[2] on the alkali metals being perhaps the only ones in which the effect has been definitely established, but nevertheless it appears that a very small temperature variation may involve important variations in other thermodynamically connected quantities, in spite of my over-optimistic statement to the contrary, made on the basis of a hasty preliminary examination. I have now been able to give a more rigorous treatment of the effect of the temperature variation of the photo-electric threshold frequency, and it is the main purpose of this note to give the altered conclusions when this is taken into account.

No change is needed in the analysis of the preceeding paper up to and including the third equation on page 98, from which the conclusion is to be drawn that

$$\frac{(S_p-S_m)_0}{k}+\frac{h\nu-\eta_0}{k\tau}-\frac{1}{k\tau}\int_0^\tau (C_{pp}-C_{pm})d\tau+\frac{1}{k}\int_0^\tau \frac{C_{pp}-C_{pm}}{\tau}\,d\tau \qquad \text{(I)}$$

must be independent of the metal, that is, a universal temperature function.

[1] P. W. Bridgman, Phys. Rev. **31**, 90 (1928).

[2] H. E. Ives, Jour. Opt. Soc. Amer. and Rev. Sci. Instr. **8**, 551 (1924).

$(S_p - S_m)_0$ is here the difference of the entropy at 0° Abs. of a positive metal ion in the surface of the metal and a neutral surface atom, η_0 is the latent heat of evaporation of one electron from the surface at 0° Abs and is the same as the thermionic work function, ν is the photo-electric threshold frequency at temperature τ, and $C_{p\rho}$ and C_{pm} are the specific heats at constant pressure of a surface ion and a surface neutral atom. In expression (I) the factor $1/k$ appears with $(S_p - S_m)_0$; this was inadvertantly omitted in the former paper. Furthermore the notation ν_0 used for the threshold frequency in the former paper is here changed to ν, for a reason which will appear presently.

In the former paper ν was treated as a parameter specifying the metal, and the expression was differentiated with respect to ν as if it were an independent variable. This is evidently allowable only if ν is independent of τ. When ν is a function of τ we may proceed as follows. Differentiate the universal temperature function of (I) with respect to τ and multiply by $k\tau^2$, obtaining

$$-(h\nu - \eta_0) + h\tau d\nu/d\tau + \int_0^\tau (C_{p\rho} - C_{pm})d\tau = \text{a universal temp. function.} \quad \text{(II)}$$

In II allow τ to approach 0° Abs as limit. The right hand side approaches a universal constant. On the left hand side the integral goes to zero, since the specific heats do not become infinite, and also there can be no doubt that the limit of $\tau d\nu/d\tau$ is similarly zero. This gives:

$$\eta_0 = h\nu_0 + \text{a universal constant,} \quad (A)$$

where ν_0 is the threshhold frequency at 0° Abs., and is not to be confused with the ν_o of the former paper, which might be a temperature function. The conclusion expressed in equation A was also reached in the former paper, neglecting the variation of ν with temperature.

Next differentiate II with respect to τ, obtaining:

$$h\left\{\frac{d}{d\tau}\left(\tau\frac{d\nu}{d\tau}\right) - \frac{d\nu}{d\tau}\right\} + C_{p\rho} - C_{pm} = \text{a universal temp. function.} \quad \text{(III)}$$

Divide III by τ, obtaining:

$$h\frac{d}{d\tau}\frac{d\nu}{d\tau} + \frac{C_{p\rho} - C_{pm}}{\tau} = \text{a universal temp. function.} \quad \text{(IV)}$$

Integrate III and IV between 0 and τ, obtaining:

$$h\left\{\tau\frac{d\nu}{d\tau} - (\nu - \nu_0)\right\} + \int_0^\tau (C_{p\rho} - C_{pm})d\tau = \text{a universal temp. function.} \quad \text{(V)}$$

and

$$h\left\{\frac{d\nu}{d\tau} - \left(\frac{d\nu}{d\tau}\right)_0\right\} + \int_0^\tau \frac{C_{p\rho} - C_{pm}}{\tau}d\tau = \text{a universal temp. function.} \quad \text{(IV)}$$

Multiply V by $1/k\tau$, VI by $1/k$, and add to I, obtaining:

$$\frac{(S_\rho - S_m)_0}{k} + \frac{h\nu_0 - \eta_0}{k\tau} + \frac{h}{k}\left(\frac{d\nu}{d\tau}\right)_0 = \text{a universal temp. function.}$$

But since by A, $h\nu_0 - \eta_0$ is a universal constant, this gives

$$\frac{(S_\rho - S_m)_0}{k} + \frac{h}{k}\left(\frac{d\nu}{d\tau}\right)_0 = \text{a universal constant,} \qquad \text{(B)}$$

which is a new relation connecting the difference of entropy of surface charge and neutral metal at 0° Abs with the temperature derivative of the photoelectric threshold at 0°. In the previous paper, in which $d\nu/d\tau$ was neglected, the result was obtained that $(S_\rho - S_m)_0$ is a universal constant, which of course is consistent with the above.

Our problem is now to find what effect the relation B has on the thermionic emission formula. I write here the formula for the electron gas pressure,[3] which is given directly by thermodynamics, rather than the formula for the emission current, which involves further assumptions:

$$p = A\tau^{5/2}\exp\left\{\frac{(S_\rho - S_m)_0}{k} - \frac{\eta_0}{k\tau} - \frac{1}{k\tau}\int_0^\tau (C_{p\rho} - C_{pm})d\tau + \frac{1}{k}\int_0^\tau \frac{C_{p\rho} - C_{pm}}{\tau}d\tau\right\},$$

where A has the universal value $(2\pi m)^{3/2}k^{5/2}/h^3$.

Now if the emission formula is of the type $p = A\tau^{5/2}e^{-b_0/k\tau}$, it is evident at once that $(S_\rho - S_m)_0 = 0$, and $C_{p\rho} - C_{pm} = 0$, conclusions already reached. For all metals of this type, equation B shows that $(d\nu/d\tau)_0$ has the same value.

What now happens if the emission is of the type $p = A'\tau^{5/2}e^{-b_0/k\tau}$, where A' is some constant different from the universal constant above? Differentiation at once shows that the condition $C_{p\rho} - C_{pm} = 0$ continues to hold, but no longer does $(S_\rho - S_m)_0$ vanish. In fact

$$A' = Ae^{(S_\rho - S_m)_0/k}$$

Experimentally it is known that A' may depart by very large amounts form the "universal" value, $A = 60.2$ amp/cm² deg², which it seems to have for W, Ta, and Mo. A' is known to vary over the range from 3×10^{-3} to 5×10^{11}, that is, from $5\times10^{-5}\times A$ to $8\times10^{9}\times A$. Is the formula above able to account for so great a variation? Relation B enables us to answer this question, because although there seems to be no direct method of estimating a probable value of $(S_\rho - S_m)_0$, experminent does put limits on $(d\nu/d\tau)_0$, and so relation B sets numerical limits for $(S_\rho - S_m)_0$.

In the case of tungsten, A' has the universal value, so that for this metal $(S_\rho - S_m)_0 = 0$. We shall also assume that for tungsten $(d\nu/d\tau)_0 = 0$; if this is not strictly the case, the following argument gives the difference between the value of $(d\nu/d\tau)_0$ for other metals and tungsten, instead of the absolute value for the other metals. We shall also neglect, as being entirely outside of

[3] P. W. Bridgman, Phys. Rev. **27**, 173 (1926).

possible experimental detection at present, any variation of $d\nu/d\tau$ with temperature, and in the following omit the subscript. With these assumptions, the universal constant of equation B is 0, so that we have in general, for any metal,

$$\frac{(S_p - S_m)_0}{k} = -\frac{h}{k}\frac{d\nu}{d\tau},$$

or

$$A' = A\, e^{-(h/k)\,(d\nu/d\tau)}$$

The question is, may $-(h/k)\,(d\nu/d\tau)$ reasonably have such values as to give $e^{-(h/k)\,(d\nu/d\tau)}$ values from 5×10^{-5} to 8×10^{9}. The first value, 5×10^{-5}, gives the equation:

$$-\frac{h}{k}\frac{d\nu}{d\tau}\log_{10} e = -4.3$$

or, substituting numerical values, $d\nu/d\tau = 2\times10^{11}$. The second value, 8×10^{9}, gives similarly, $d\nu/d\tau = -4.6\times10^{11}$.

The threshold wave-length is of the order of 2000A for most metals, or ν is of the order of 1.5×10^{15}. Combining this with the values of $d\nu/d\tau$, we see that the required fractional change in ν per degree varies from 1.3×10^{-4} to -3×10^{-4}. The first of these values is for the alkali metals; Ives found between room temperature and liquid air a relative temperature coefficient for K of the order of 2×10^{-4}. The permissible values of $d\nu/d\tau$ seem, therefore, to be consistent with our demands. It appears, then, that *in explaining the the large departures of A' from the universal value we need not have recourse to the hypothesis that the metal has not reached an equilibrium condition, as I did in my previous paper, but rather the variation of A' is to be connected with a temperature derivative of the photo-electric frequency and a non-vanishing of* $(S_p - S_m)_0$.

These conclusions receive valuable support from the results of DuBridge[4] recently published. In the first place, DuBridge finds that within experimental error $h\nu$ of thoroughly outgassed platinum is equal to the thermionic work function. Previously the identity of the photo-electric and thermionic work functions had been established only for tungsten by Warner.[5] It followed by relation (A) that the universal constant in that equation must vanish, so that η_0 and $h\nu$ must be identical for all metals. This conclusion we now find verified for platinum. Actually, of course, it was not the photo-electric work function at 0° Abs that was found equal to η_0, but the value at room temperature; we shall immediately see that the temperature coefficient is so small as to give no significance to this difference. The actual values found by DuBridge were 6.30 volts for the photo-electric work function, with a probable error of not more than 0.5%, and a thermionic work function of

[4] L. A. DuBridge, Phys. Rev. **31**, 236 (1928).
[5] A. H. Warner, Proc. Nat. Acad. Sci. **13**, 56 (1927).

6.35 ± 0.1 volt. DuBridge also found that the constant A' for platinum has the value 14000, or 2.3×10^2 times the value of the "universal" constant. This seems to be the first time that a value definitely different from 60 has been satisfactorily established for a pure metal thoroughly outgassed. This value for A' demands for $d\nu/d\tau$, according to the calculation already given, the value -1.1×10^{11}. But DuBridge found that ν is 1.5×10^{15}, which means that $(1/\nu)(d\nu/d\tau)$ is -0.7×10^{-4}. This, over a 300° range, gives a decrease of ν of 2%. This means that the photo-electric work function, observed at room temperature, should be less than the thermionic function by 2%. Now the photo-electric function as given by DuBridge is actually less than the thermionic function, so that the sign checks, and numerically his extreme values allow more than a 2% difference, for his limits allow a minimum value for the photo-electric function of 6.27 volts, and a maximum thermionic function of 6. 45 volts, differing by 2.9%.

Furthermore, DuBridge, from an examination of all the data has found that there is an approximately linear relation for all substances between the constant A' and η_0, A' increasing as η_0 increases. If $A' \neq A$, then $(S_\rho - S_m)_0 \neq 0$, so that when A' runs through a series of values, $(S_\rho - S_m)_0$ must run through a corresponding set of values. But $(S_\rho - S_m)_0$ is concerned in some way with the physical condition of the surface layers, so that a change in it means a change in the properties of the surface layer. It is most natural to suppose that such a change in the surface layer must also affect the thermionic work function, or the work done by the electron in getting through the surface, and we see that this is actually the case.

The third law of thermodynamics would perhaps predispose us to expect $(S_\rho - S_m)_0$ to vanish, since both S_ρ and S_m refer to the entropy at 0° Abs of condensed phases. The point of view of Lewis and Gibson (6) evidently applies here, namely, that even for a condensed phase the entropy will not vanish at 0° Abs if there is a haphazard element in the structure. At a free surface, where there are surface tension effects tending to disrupt the regular lattice arrangement, it is most natural to expect a haphazard element, and therefore a non-vanishing entropy. More detailed considerations than can be attempted in a thermodynamic treatment are evidently necessary to show why sometimes the haphazard element in the surface ions is greater than in the neutral atoms, and sometimes the reverse. It is perhaps significant that the entropy of the neutral atoms is greater than that of the surface charges in the case of the alkali metals with small A', and we know that the surface tension forces are so great as to entirely disrupt the lattice structure of the heavier alkali metals at ordinary temperatures.

THE JEFFERSON PHYSICAL LABORATORY,
HARVARD UNIVERSITY,
CAMBRIDGE, MASS.
February 12, 1928.

[6] See for example the discussion of the third law of thermodynamics in the Thermodynamics of Lewis and Randall, McGraw-Hill, 1923.

DIFFERENTIAL INTENSITY SENSITIVITY OF THE EAR FOR PURE TONES

By R. R. Riesz

Abstract

The ratio of the minimum perceptible increment in sound intensity to the total intensity, $\Delta E/E$, which is called the differential sensitivity of the ear, was measured as a function of frequency and intensity. Measurements were made over practically the entire range of frequencies and intensities for which the ear is capable of sensation. The method used was that of beating tones, this method giving the simplest transition from one intensity to another. The source of sound was a special moving coil telephone receiver having very little distortion, actuated by alternating currents from vacuum tube oscillators. Observations were made on twelve male observers. Average curves show that at any frequency, $\Delta E/E$ is practically constant for intensities greater than 10^6 times the threshold intensity; near the auditory threshold $\Delta E/E$ increases. Weber's law holds above this intensity, the value of $\Delta E/E$ = constant lying between 0.05 and 0.15 depending on the frequency. As a function of frequency $\Delta E/E$ is a minimum at about 2500 c.p.s., the minimum being more sharply defined at low sound intensities than it is at high. This frequency corresponds to the region of greatest absolute sensitivity of the ear. Analytical expressions are given [Eqs. (2), (3), (4) and (5)] which represent $\Delta E/E$, within the error of observation, as a function of frequency and intensity. Using these equations it is calculated that at about 1300 c.p.s. the ear can distinguish 370 separate tones between the threshold of audition and the threshold of feeling.

1. Introduction

IN THE study of the design and operation of transmission circuits and other apparatus used in the telephone plant, the communications engineer is interested in many phases of the study of speech and hearing. One subject of importance is the investigation of the minimum change in intensity which the ear is able to detect. This information is also of interest to physicists when considering the ear as a physical instrument, to psychologists in formulating relationships between exciting physical stimulus and the resulting sensation and to otologists in the study of normal and abnormal hearing. Since the published data fail to give information over the entire range of frequencies and intensities for which the ear is capable of sensation, the investigation here reported was undertaken with the purpose of covering the range as completely as possible.

The best published information on the sensitivity of the ear to small differences in intensity as well as a good historical survey of the subject is recorded by Knudsen.[1] These data are most conveniently expressed by the ratio, $\Delta E/E$, where ΔE is the minimum preceptible increment in sound intensity and E is the total intensity. This ratio has been variously termed: Weber's constant, Weber-Fechner ratio, intensity sensibility; but in this

[1] The Sensibility of the Ear to Small Differences in Intensity and Frequency, V. O. Knudsen, Phys. Rev. **21**, 84 (1923).

paper it will be called differential sensitivity, a name suggested by N. E Dorsey.

In this investigation the differential sensitivity of twelve observers was measured as a function of intensity and frequency using the method of beating tones. Measurements were made at frequencies of from 35 to 10,000 cycles per second and over an intensity range from the threshold of audition to the threshold of feeling. This practically covers the intensity and frequency range of auditory sensation.[2] As the observers were all of normal hearing, the averaged data may be taken as being representative of the hypothetical average normal ear.

2. Theory of Method Used

The changes in intensity were produced by sending through a special telephone receiver alternating currents whose frequencies were so close together that beats were produced. If two sinusoidal pressure waves, $a_1\cos\omega_1 t$ and $a_2\cos\omega_2 t$, are simultaneously impressed on the ear drum the resultant pressure wave may be expressed as:

$$a = m\cos(\omega_2 t + \Phi)$$

where

$$m^2 = a_1^2 + a_2^2 + 2a_1a_2\cos(\omega_2 - \omega_1)t$$

If $(\omega_2 - \omega_1)$ is small compared with ω_1 and ω_2, there will be a large number of vibrations in each beat cycle and an observer listening to such a sound will not be cognizant of two tones as such but will perceive a single tone whose intensity fluctuates with a frequency $\omega_2 - \omega_1/2\pi$. For beating frequencies such as are used in these experiments, to a close approximation, the amplitude of the resultant wave in the region of maximum intensity is (a_1+a_2) and the amplitude in the region of minimum intensity is (a_1-a_2). The difference between maximum and minimum amplitude is then $2a_2$. In the experiments here described the relative values of a_1 and a_2 for just perceptible beats were determined throughout the intensity and frequency range of the ear.

When listening to slow beats such as are used in these experiments, the ear probably does not make simple direct comparisons between the maximum intensity, proportional to $(a_1+a_2)^2$, and the minimum intensity, proportional to $(a_1-a_2)^2$. The comparison which the ear does make in such a case is dependent on a number of factors, among which are: the magnitude of the difference between maximum and minimum intensity; the rate of change of intensity, which includes rapidity of fluctuations and mode of transition between maximum and minimum intensity. Throughout these experiments the rapidity of fluctuation was kept constant and the changes between maximum and minimum intensity were made so that to a first approximation the amplitude of the resultant wave varied sinusoidally. Thus

[2] The Frequency-Sensitivity Characteristic of Normal Ears. H. Fletcher and R. L. Wegel, Phys. Rev. 19, 553 (1922).

the second of the above mentioned factors was held constant throughout the experiments and for this type of intensity fluctuation, correlating differential sensitivity with the difference between maximum and mimimum intensity, we have:

$$\frac{\Delta E}{E}=\frac{(a_1+a_2)^2-(a_1-a_2)^2}{(a_1-a_2)^2}=\frac{4a_1a_2}{(a_1-a_2)^2} \tag{1}$$

3. Discussion of Method

Although the type of transition from minimum to maximum intensity using the method of beats is not that usually encountered in actual experience, it possesses the advantage that it produces a simple intensity fluctuation which is not complicated by the possible presence of an undetermined amount of transients. If the transitions from minimum to maximum intensity are made abruptly some of the energy will be scattered to frequencies higher and lower than the impressed frequency. Due to the variation of the absolute sensitivity of the ear mechanism with frequency, these introduced transients may be audible, and influence the observer in deciding when he was just able to detect a fluctuation in intensity. The disturbing effect of transients should therefore be greatest at high and low frequencies and least at intermediate frequencies. Knudsen says that at high frequencies his measurements were disturbed by "contact noises," undoubtedly transients. In using the method of beats, the only frequencies present are the two beating frequencies and if these are kept so close together that the ear is unable to distinguish them separately, it is impossible to conceive of the production of any transients. In this investigation no measurements were made of the magnitude of the effect which transients would introduce.

4. Description of Apparatus

A schematic diagram of the circuit used is shown in Fig. 1. Alternating currents of any desired frequency were generated by two special vacuum tube oscillators. The currents, which were read on ammeters A_1 and A_2, were

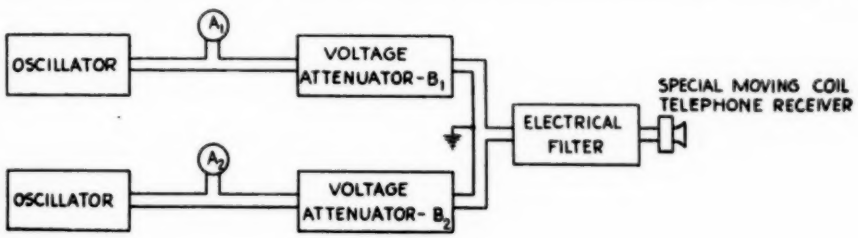

Fig. 1

sent through voltage attenuators B_1 and B_2, whose outputs were in series with the telephone receiver circuit. The attenuators were of the dial type, reading voltage directly on a logarithmic scale and having a range from

1 to 10^{-15}. The filter was necessary to eliminate the effects due to harmonics. Ordinary telephone receivers were found entirely unsuited for this investigation, especially at low frequencies, because of harmonics produced by distortion. A special moving coil receiver was used which was particularly free from distortion. If a pure electrical wave is impressed on the terminals of this receiver the intensity of the harmonics in the acoustic output is less than that of the fundamental in the ratio of $1:10^{-5}$. It was found necessary to make all observations in a sound-proof room.

5. Rapidity of Fluctuations

The differential sensitivity was found to be a function of the rapidity of the intensity fluctuations and a preliminary investigation was conducted to determine the proper rapidity of intensity fluctuation to use. The differential sensitivity for three observers was explored as a function of rapidity of intensity fluctuation at various frequencies and intensities scattered throughout the range of interest. All observers showed practically the same results at all frequencies and intensities. A representative curve of $\Delta E/E$ vs. rapidity of intensity fluctuation is shown in Fig. 2 (the particular frequency used here was 1000 cycles per second). It is characterized by a broad minimum in the neighborhood of 3 cycles of intensity fluctuation per second. The increase in differential sensitivity is probably due, for faster fluctuations, to the fact that the component tones become so far separated in frequency that they are partially resolved by the ear, for slower fluctuations, to a memory effect. Three cycles of intensity fluctuation per second was adopted as the most logical rapidity to use for all measurements.

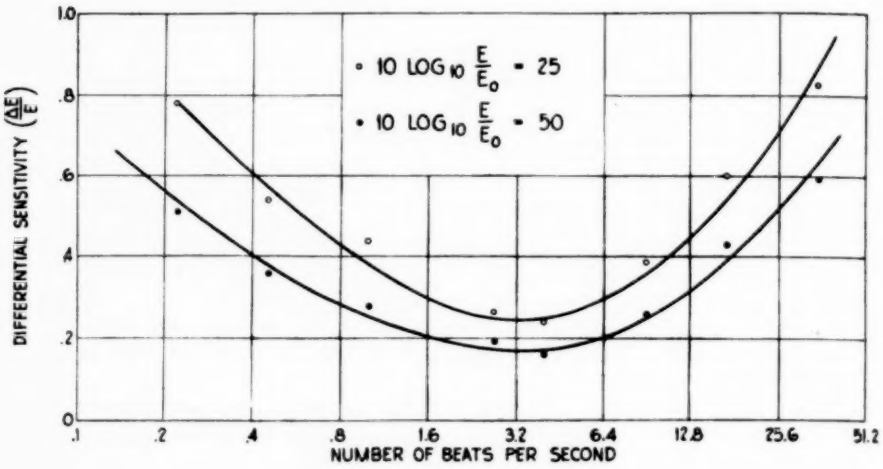

Fig. 2

6. Experimental Procedure

The weight of the special receiver used being 15 lbs., it was necessary to adjust it to the level of the observer's ear by means of a spring suspension. To further insure uniformity of position the receiver was held against

the observer's ear by an elastic strap passing around the head. One oscillator was set at any desired frequency and the other adjusted to give three beats per second. The minimum audible voltage of one attenuator, say B_1, was determined, B_2 being set far below the minimum audible voltage. B_1 was then set at any desired value and B_2 adjusted until the observer signalled that he heard beats. The setting of B_2 was changed each time the observer signalled whether or not the tone seemed to fluctuate. After about 20 such judgments the operator was able to locate with considerable certainty the setting of B_2 for which the observer was just able to detect a fluctuation in intensity. If B_2 was set below this value the fluctuation in intensity was imperceptible. The r.m.s. voltage introduced into the receiver circuit by each oscillator could be calculated from the readings of the ammeters and the settings of the attenuators. At any frequency the r.m.s. alternating pressure on the ear drum is proportional to the voltage introduced into the receiver circuit so that the differential sensitivity can be calculated by Eq. (1). Complete series of measurments were made on twelve male observers at frequencies of 35, 70, 200, 1000, 4000, 7000 and 10,000 cycles per second and at intensities from weak tones near the threshold of audition to very loud tones near the threshold of feeling.

7. Experimental Results

Average curves of differential sensitivity as a function of intensity are shown on Figs. 3 and 4. The crosses are the averages of the twelve observers.

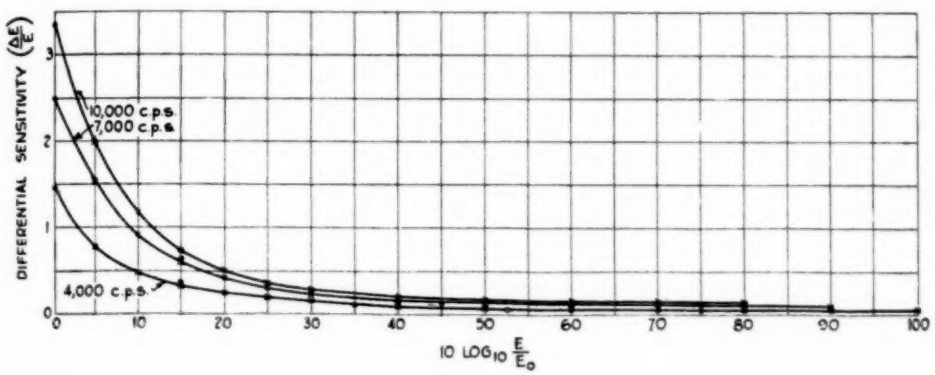

Fig. 3

The intensity is plotted in units of 10 $\log_{10}(E/E_0)$ where E_0 is the threshold intensity. If the data are plotted as a function of absolute intensity, the curves will all be shifted along the abscissa by different amounts. The amount of the shift can be calculated from Fletcher and Wegel's curve of the absolute sensitivity of the average normal ear.[2]

Fig. 5 shows curves of differential sensitivity as a function of frequency for various values of the intensity parameter, 10 $\log_{10}(E/E_0)$. The spread of the observations for the 12 observers was less than $\pm$ 10% of the average value in every case.

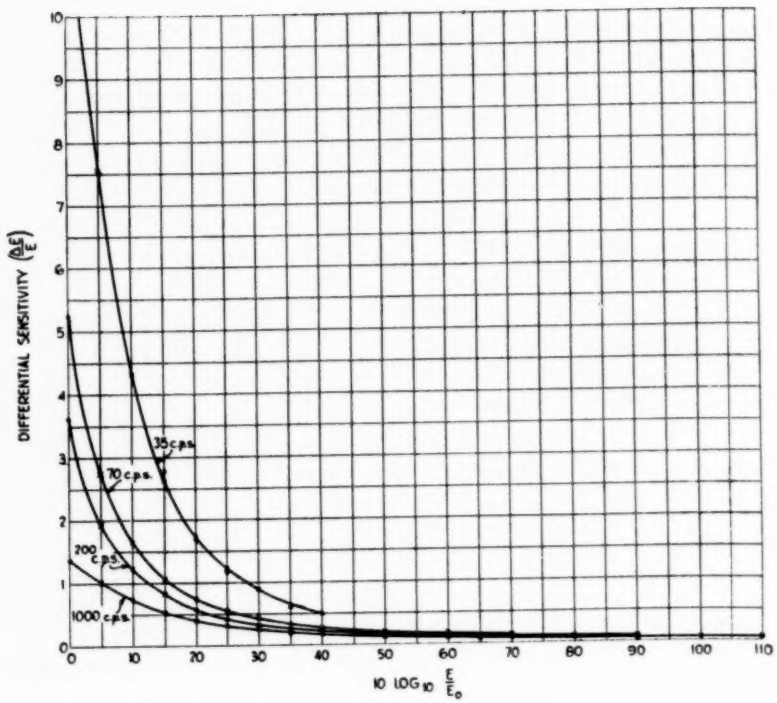
DIFFERENTIAL SENSITIVITY $\left(\frac{\Delta E}{E}\right)$
35 c.p.s.
70 c.p.s.
200 c.p.s.
1000 c.p.s.
10 LOG$_{10}$ $\frac{E}{E_0}$

Fig. 4

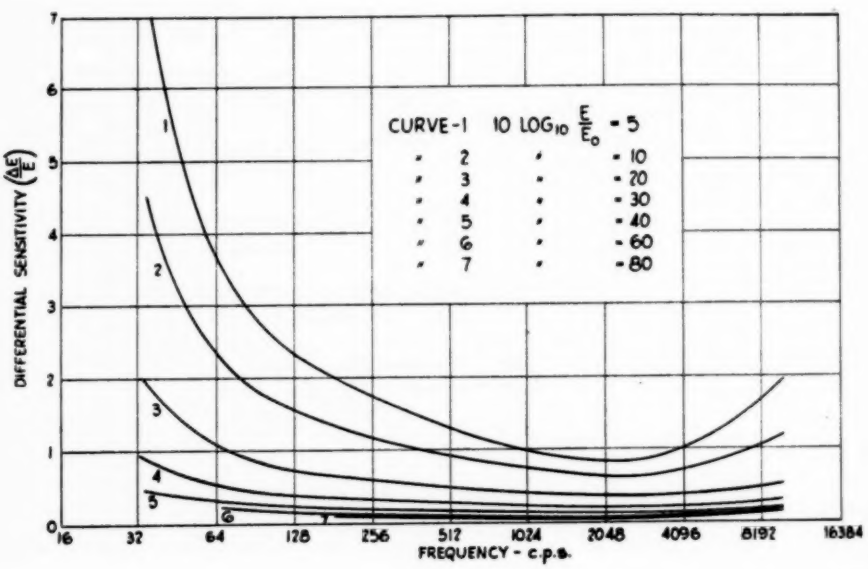
DIFFERENTIAL SENSITIVITY $\left(\frac{\Delta E}{E}\right)$
CURVE-1 10 LOG$_{10}$ $\frac{E}{E_0}$ = 5
" 2 " = 10
" 3 " = 20
" 4 " = 30
" 5 " = 40
" 6 " = 60
" 7 " = 80
FREQUENCY - c.p.s.

Fig. 5

8. Analytical Representation of Data

It is found that an expression of the form:

$$\Delta E/E = S_\infty + (S_0 - S_\infty)(E_0/E)^r \tag{2}$$

can be made to represent $\Delta E/E$ as a function of intensity at any frequency by a suitable choice of the constants S_∞, S_0 and r. S_∞ is the value $\Delta E/E$ approaches at high intensities, S_0 is the value of $\Delta E/E$ at the threshold of audition and r is a number. The above equation is similar to the analogous expression derived by Nutting for the sensation of light.[3] Knudsen attempted to represent his curves by a similar equation but the fit was not very good at the low intensities. The circles shown on Figs. 3 and 4 are points calculated from this expression. Fig. 6 shows S_∞, S_0 and r plotted as functions of frequency. The circles and dots are the values used in calculating

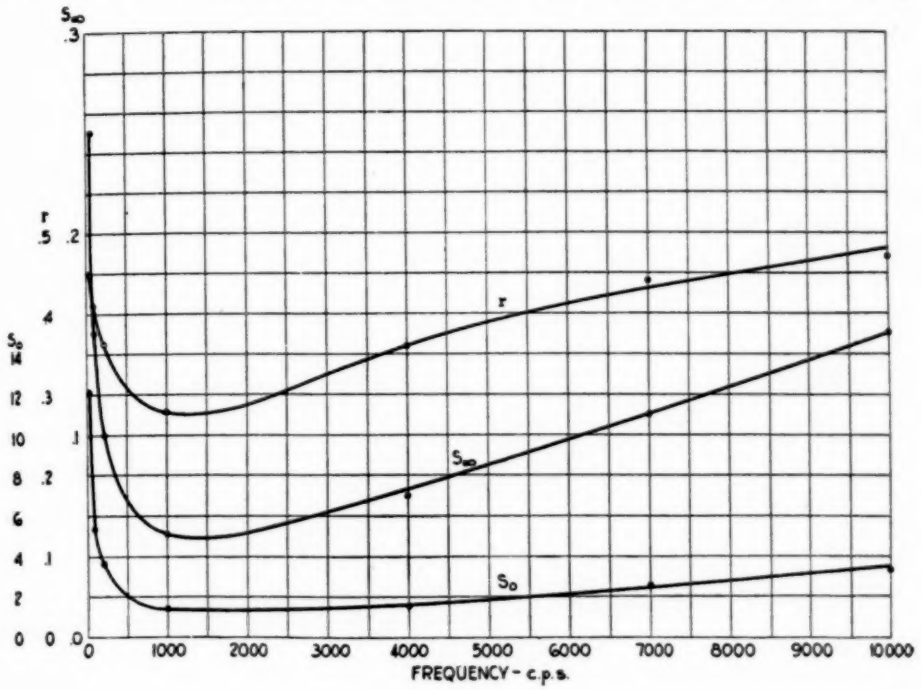

Fig. 6

the points shown on Figs. 3 and 4. The following expressions have been fitted to the points shown on Fig. 6:

$$S_\infty = 0.000015f + \frac{126}{80f^{0.5} + f} \tag{3}$$

$$S_0 = 0.3 + 0.0003f + \frac{193}{f^{0.8}} \tag{4}$$

[3] P. G. Nutting, The Complete Form of Fechner's Law, Bulletin of the Bureau of Standards, Vol. 3, No. 1 (1907).

$$r=\frac{244000}{(358000f^{0.125}+f^2)}+\frac{0.65f}{(3500+f)} \quad . \tag{5}$$

where f is frequency. S_∞, S_0 and r are parameters which, as they vary with frequency in accordance with 3, 4 and 5, determine the family of differential sensitivity versus intensity-curves. The deviation of the values of differential sensitivity given by Eqs. (2), (3), (4) and (5) is of the same order of magnitude as the experimental errors, so that these equations can be considered as completely representing the data.

9. Discussion of Results

Using the method of beats, the differential sensitivity of the average normal ear has been measured over practically the entire range of frequencies and intensities for which the ear is capable of sensation. Figs. 3 and 4 show that at any given frequency the differential sensitivity approaches a constant value for high intensities but increases rapidly as the intensity is reduced toward the auditory threshold. For all frequencies the differential sensitivity is practically constant for values of the intensity parameter greater than $10 \log_{10}(E/E_0)=60$. For intensities greater than this, Weber's law which states that $\Delta E/E=$constant, holds true. This is in qualitative agreement with Knudsen's data.[1] The values of $\Delta E/E$ obtained at low intensities by Knudsen's method of abrupt change from maximum to minimum intensity are lower than the values obtained by the beat method. This is consistent with the fact that at low intensities where ΔE is relatively large, the method of abrupt transition should give the greatest production of transients.

Fig. 5 shows that for any given value of the intensity parameter, $10 \log_{10}(E/E_0)$, the differential sensitivity is a minimum as a function of frequency at about 2500 cycles per second. The minimum is less sharply pronounced at high intensities than it is at low. Thus the region of least differential sensitivity of the ear, which means greatest ability to detect small differences in intensity, corresponds to the frequency range of greatest absolute sensitivity of the ear.[2]

These results show a greater variation of $\Delta E/E$ with frequency than Knudsen's data indicated. They are more in accord with measurements made by A. Deenik, using tuning forks and organ pipes.[4] Deenik found that the most favorable "Unterschiedsschwelle" occurs at a pitch of c^4 which closely corresponds to the frequency of 2500 determined in this investigation.

Eq. (2) permits of the calculation of the number of separate tones which the ear can distinguish at any frequency. This number is expressed by the integral:

[4] A. Deenik. Über das Unterschiedungsvermögen für Tonintensitaten. Konink. Akad. Wetensch. Amsterdam, Versl. 14, pp. 396-400, Nov. 8, 1905.

$$N = \int_{E_0}^{E'} \frac{1}{\Delta E} dE = \frac{1}{rS_\infty} \log \frac{S_\infty (E'/E_0)^r + (S_0 - S_\infty)}{S_0}$$

where E' is the threshold of feeling. Fig. 7 shows the value of N as a function

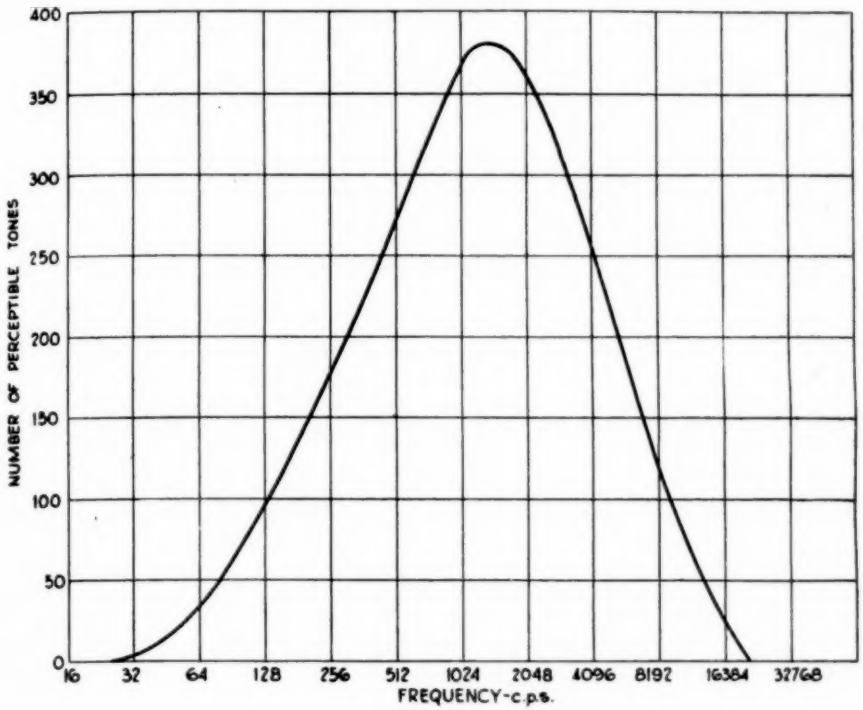

Fig. 7

of frequency. At 1300 cycles per second the ear can distinguish the greatest number of tones as being of different intensity, that number being 370.

BELL TELEPHONE LABORATORIES, INC.,
NEW YORK, N. Y.
December 15, 1927.

ON THE QUANTUM MECHANICS OF A SYSTEM OF PARTICLES

By E. H. Kennard

Abstract

The "*mechanics of a system of particles is developed on the basis of Schrödinger's wave-equation*," without any use of matrices; it is shown that simple cases can be handled as easily by this method as by the matrix method. The passage to classical theory as an approximation stands out very clearly.

The measurement of velocity, momentum, energy and angular momentum as secondary physical qualities is discussed, the usual probability amplitudes being obtained.

The conservation of momentum and of energy is treated in terms of the new theory.

THE foundation of quantum mechanics can fairly be regarded as completed since the publication of Heisenberg's paper of last July,[1] in which an inclusive general principle was at last laid down for the physical interpretation of the theory. In that paper the principle was stated in terms of the generalized matrix theory of Dirac and in this form it was slightly amplified and applied to several simple cases[2] by the present author. To many physicists, however, the matrix theory seems at best pretty abstruse, whereas the wave mechanics of of Schrödinger seems much more tangible. In view of this fact it seemed worth while to show how the entire quantum theory of mechanical systems can be erected with no loss of generality or of simplicity upon the Schrödinger wave-equation for the coordinates as the sole basis.[4] It seems reasonable to hope that the quantum theory of electromagnetism, when finally discovered, will be capable of statement in a similar form.

In the present paper the mechanics of systems of particles is so treated and the simple problems that were solved so easily with the help of the matrix theory are shown to be equally easy to solve without it. In this form of the theory velocity, momentum and energy enter naturally as secondary quantities measurable only indirectly by means of observations of position, just as in classical theory; and the passage to the classical theory as an approximation becomes especially simple. The quantum laws of "Conservation of Momentum and Energy" are easily stated.

[1] W. Heisenberg, Zeits. f. Physik **43**, 172 (1927).

[2] E. H. Kennard, Zeits. f. Physik **44**, 326 (1927).

[4] Cf. also C. G. Darwin, Roy. Soc. Proc. **A117**, 258 (1927). This paper was unaccountably overlooked during the preparation of the present paper. The tenor of both papers is the same, yet there is so little overlapping in detail that it has seemed best not to shorten the present one; it would be beyond the powers of the present author to equal Professor Darwin's fascinating discussion of the general situation, but on the other hand the Heisenberg principle that physical quantities must be physically observable is perhaps carried out here a little more clearly.

1. *The Quantum Mechanics of a System of Particles.* In classical theory one treated a dynamical system of n degrees of freedom by deducing from Newton's Laws of Motion expressions for the values of the coordinates as functions of $2n$ constants of integration and the time. In non-relativistic quantum-mechanics we have, in place of values at a time t, a probability amplitude $\psi(q,t)=\psi(q_1,q_2,\cdots,q_n,t)$ with the property that

$$dP=\psi\psi^*dq_1dq_2\cdots dq_n \tag{1}$$

is the probability that an exact experimental determination of the q's at the time t would yield values lying within $dq_1, dq_2, \cdots, dq_n$. (ψ^* is the complex-conjugate value of ψ). In lieu of Newton's Laws we assume with Schrödinger that

$$\epsilon\partial\psi/\partial t=H(-\epsilon\partial/\partial q,q)\psi \tag{2}$$

where $\epsilon=h/2\pi i$, h being Planck's constant, and $H(p,q)$ or $H(p_1,p_2\cdots p_n; q_1,q_2\cdots q_n)$ is the Hamiltonian function; the p's can be regarded as merely symbolic, an assumption as to the form of H replacing in the new theory the assumption of a particular dynamical structure for the system. The constants of integration representing the initial conditions are then replaced in the new theory by known values of ψ at some given time.

Equation (1) requires that

$$\int dP=\int\psi\psi^*dq=1, \tag{3}$$

where $dq=dq_1dq_2\cdots dq_n$, the integral extending, as do all integrals with unspecified limits in this paper, over the entire physically admissible range of the variables. Either ψ or $P=\psi\psi^*$ may be called with Heisenberg the "probability packet" for the coordinates. The amplitude $\psi'(q',t)$ for another set of n variables q' which are functions of the q's is then

$$\psi'(q',t)=J^{1/2}\psi(q,t)e^{i\zeta(t)} \tag{4}$$

where J is the Jacobian of $q_1\cdots q_n$ with respect to $q_1'\cdots q_n'$ and $\zeta(t)$ is an arbitrary real function.

We shall employ hereafter Cartesian coordinates $x_1, x_2\cdots x_n$ for the $n/3$ particles of the system. Then

$$H=\sum_{r=1}^{n}(\xi_r^2/2m_r)+V(x), \tag{5}$$

ξ_r being the "momentum" for x_r and m_r the mass to which x_r refers, while $V(x)$ or $V(x_1, x_2\cdots x_n)$ is the potential energy.

(2) now becomes

$$\epsilon\partial\psi/\partial t=\tfrac{1}{2}\epsilon^2\sum_{r=1}^{n}\frac{1}{m_r}(\partial^2\psi/\partial x_r^2)+V\psi, \tag{2'}$$

Writing[3]

$$\psi = Re^{2\pi i h^{-1}\theta}, \quad P = R^2, \tag{6}$$

and separating real and imaginary parts in (2′), we find

$$\frac{\partial R}{\partial t} = \sum_\tau \frac{1}{m_\tau}\left[\frac{\partial R}{\partial x_\tau}\frac{\partial \theta}{\partial x_\tau} + \frac{R}{2}\frac{\partial^2 \theta}{\partial x_\tau^2}\right], \tag{7}$$

$$\frac{\partial \theta}{\partial t} = -\frac{h^2}{8\pi^2}\sum_\tau \frac{1}{m_\tau R}\frac{\partial^2 R}{\partial x_\tau^2} + \frac{1}{2}\sum_\tau \frac{1}{m_\tau}\left(\frac{\partial \theta}{\partial x_\tau}\right)^2 + V. \tag{8}$$

From (6) and (7)

$$\frac{\partial P}{\partial t} = \sum_\tau \frac{1}{m_\tau}\frac{\partial}{\partial x_\tau}\left[P\frac{\partial \theta}{\partial x_\tau}\right], \tag{9}$$

which has exactly the same form as the equation of continuity for a fluid of density P flowing with a velocity whose components u_j are given by:

$$m_j u_j = -\frac{\partial \theta}{\partial x_j} = -\frac{h}{4\pi i}\frac{\partial}{\partial x_j}\log\frac{\psi}{\psi^*}. \tag{10}$$

Thus θ/m_j or $(h/4\pi i m_j)\log(\psi/\psi^*)$ is the "velocity potential" for the probability. From (8) and (10):

$$m_j\frac{\partial u_j}{\partial t} = \frac{h^2}{8\pi^2}\frac{\partial}{\partial x_i}\sum\frac{1}{m_\tau R}\frac{\partial^2 R}{\partial x_\tau^2} - \frac{1}{2}\frac{\partial}{\partial x_j}\sum m_\tau u_\tau^2 - \frac{\partial V}{\partial x_j}. \tag{11}$$

The rate of change of velocity for a particular element of the probability is

$$\frac{du_j}{dt} = \frac{\partial u_j}{\partial t} + \sum u_\tau\frac{\partial u_j}{\partial t} = \frac{\partial u_j}{\partial t} + \sum u_\tau\frac{m_\tau}{m_j}\frac{\partial u_\tau}{\partial x_j};$$

hence by (11)

$$m_j\frac{du_j}{dt} = \frac{h^2}{8\pi^2}\frac{\partial}{\partial x_j}\sum_{\tau=1}^{n}\frac{1}{m_\tau R}\frac{\partial^2 R}{\partial x_\tau^2} - \frac{\partial V}{\partial x_j}. \tag{12}$$

Thus each element of the probability moves in the Cartesian space of each particle as that particle would move according to Newton's laws under the classical force plus a "quantum force" given by the h-term in (12).

The motion here considered occurs in a space of n dimensions. We can also, however, replace the n-dimensional packet by n separate packets, one for each particle, all moving in the same ordinary space. The probability that one particle, say the rth, should be found in an element $dx_{3r}\,dx_{3r-1}dx_{3r-2}$ of its space is the integral of Pdx with respect to all other x's except x_{3r},

[3] The equivalent of Eqs. (6) to (12) was given by Madelung, Zeits. f. Physik **40**, 322 (1927).

x_{3r-1} and x_{3r-2}, so that if we call the probability function for this particle alone P_r, we have

$$P_r = \int P dx_{(r)} = \int \psi\psi^* dx_{(r)} \tag{13}$$

where $dx_{(r)} = dx_1 \cdots dx_{3r-3} dx_{3r+1} \cdots dx_n$. (9) gives ($P$ being assumed to vanish fast enough at infinity):

$$\frac{\partial P_r}{\partial t} = \int \frac{\partial P}{\partial t} dx_{(r)} = \frac{1}{m_{3r}} \sum_{3r-2}^{r-3r} \frac{\partial}{\partial x_r} \int \frac{\partial \theta}{\partial x_r} dx_{(r)}. \tag{14}$$

The mean components of velocity of the probability in the space of the rth particle, or the mean components of velocity of P_r, are

$$u_{rj} = (1/P_r) \int P u_j dx_{(r)} \ (j = 3r,\ 3r-1,\ 3r-2)\ ; \tag{15}$$

and, substituting from (10) for θ in (14) and using (15),

$$\frac{\partial P_r}{\partial t} = \sum_{3r-2}^{r-3r} \frac{\partial}{\partial x_r} (P_r u_{rr}). \tag{16}$$

P_r and u_{rj} are functions of t and of x_{3r}, x_{3r-1}, x_{3r-2}, which are the coordinates of m_r and can be regarded simply as coordinates in ordinary space. P_r represents a probability packet for this particle alone; it can be regarded as moving at each point in ordinary space with components of velocity u_{rj} as given by (15). But it is not possible to proceed farther and obtain dynamical equations for P_r in terms of u_{rj} alone: the elements of the probability for one particle alone move, not like a homogeneous fluid, but like the molecules of a gas, the elements located momentarily at a given point having various velocities and being variously related to the other particles of the system.

In terms of these results the relationships between quantum and classical mechanics stand out very clearly. If we put $h = 0$, the probability becomes a distribution of matter moving classically. In general, *if a system is immersed in a uniform force field, its probability packet will simply execute the classical motion in that field in addition to whatever internal motion it may have* by reason of internal classical forces or the quantum force; for by (12) all elements of the probability experience the same classical acceleration in the field in addition to other accelerations of internal origin, and since the accelerations imposed by the field do not alter the relative positions of the particles the internal forces of all sorts are unaffected. The same statement will hold as an approximation if the field is merely approximately uniform over the region occupied by the probability packet.

It follows similarly that the influence of the remainder of the system upon the motion of any one of its particles approximates to the classical influence whenever the classical force upon the particle is approximately the

same in all configurations of the system that stand any appreciable chance of being realized; for then the relative distribution of the probability in the space of that one particle is approximately unaffected by the influence of the remainder of the system. Thus the quantum mechanics predicts no novel interaction between electrons spaced so far apart that their classical interaction is slight.

Finally, let

$$\bar{x}_j = \int x_j dP = \int x_j P dx = \int x_j P_r dx_{3r} dx_{3r-1} dx_{3r-2} \tag{17}$$

denote either the coordinates of the "center of probability" of the n-dimensional packet ($j=1, 2 \cdots n$), or the coordinates of the packet for the rth particle in ordinary space (in which case we limit j to $3r$, $3r-1$ or $3r-2$). Then regarding dP as a moving element:

$$\frac{d\bar{x}_j}{dt} = \int \frac{dx_j}{dt} dP = \int u_j dP, \qquad \frac{d^2\bar{x}_j}{dt^2} = \int \frac{du_j}{dt} dP,$$

$$m_j \int \frac{du_j}{dt} dP = \frac{h^2}{8\pi^2} \int P \frac{\partial}{\partial x_j} \sum_r \frac{1}{m_r R} \frac{\partial^2 R}{dx_r^2} dx - \int P \frac{\partial V}{\partial x_j} dx,$$

by (12). But, putting $P=R^2$ and integrating first by parts with respect to x_j and x_r in turn, and then with respect to x_j:

$$\int P \frac{\partial}{\partial x_j} \sum \frac{1}{m_r R} \frac{\partial^2 R}{\partial x_r^2} dx = \int \sum \frac{1}{m_r} \frac{\partial R}{\partial x_j} \frac{\partial^2 R}{\partial x_r^2} dx$$

$$= \int \sum \frac{1}{m_r} \frac{\partial}{\partial x_j} \left(\frac{\partial R}{\partial x_r} \right)^2 dx = 0.$$

Hence

$$m_j \frac{d^2\bar{x}_j}{dt^2} = m_j \frac{d}{dt} \int u_j P dx = - \int P \frac{\partial V}{\partial x_j} dx. \tag{18}$$

As applied to the separate particles this equation states that *the center of probability for each particle moves in ordinary space as would the particle itself in classical mechanics under the "mean probable" force as given by the right-hand member of (18)*. This result was obtained for a single particle by Ehrenfest[4] and has been given more generally by Ruark[5]; it makes very clear the reason for the approximate validity of classical mechanics.

The quantum force, represented by the term in (12) containing h, thus affects primarily only the relative motion of different parts of the probability packet. This force is responsible for the characteristic quantum indetermination pointed out by Heisenberg; but it is also responsible for other

[4] P. Ehrenfest, Zeits. f. Physik 45, 455 (1927).
[5] Ruark, Phys. Rev., 31, 533 (1928).

departures from classical behavior such as would not result by Newton's laws merely from an indefiniteness in the initial state (e.g. the phenomenon of the quantization of atomic energy). Unfortunately the separation of these two quite different effects presents grave difficulties. The complexity of the quantum force also seems to make it of little use in thinking out directly the solution of simple cases. Nevertheless equation (12) can be made to suggest the solution in all of the simple cases that were so easily handled by the matrix method, and this we shall proceed to show by solving two of those problems.

2. *The Case of Free Motion.* With $V=0$, Equation (2′) is like an equation for the flow of heat[6] with imaginary "conductivity"; we should expect therefore to obtain a solution that represents the part of the field of P or R^2 that is present initially at each point as moving outward with time. Let us seek a simple form of such polar motion. With $V=0$, equation (12) would be very simple if R were uniform in space; then $u_j=$constant for an element of R^2, and a group of elements leaving the point $x_{10}, x_{20} \cdots x_{n0}$ at time $t=0$ would at time $t=t$ have positions $x_j=(x_j-x_{j0})/t$. Inserting this value of u_j in (10) and (8) and integrating (R being assumed uniform):

$$\partial\theta/\partial t=\tfrac{1}{2}\sum m_\tau(x_\tau-x_{\tau 0})^2/t^2,\quad \theta=-\sum_\tau[m_\tau(x_\tau-x_{\tau 0})^2/2t]+f(x)$$

Substituting back in (10) (because we differentiated once in obtaining (12)), we find $f(x)=$constant.
Then by (7)

$$\partial R/\partial t=-nR/2t,\quad R=Ct^{-n/2}.$$

This result justifies our assumption as to R. Choosing a special value of C, we thus have

$$S(x_0,x)=(m_1m_2\cdots m_n)^{1/2}(i/ht)^{n/2}\exp\Big[-(i\pi/ht)\sum_\tau m_\tau(x_\tau-x_{\tau 0})^2\Big] \qquad (20)$$

as a solution of (2′) with $V=0$, S is the "transformation function" from x_0 to x of Dirac and Heisenberg; it cannot itself represent a distribution of "probability", for normalization by (3) would require that $C=0$, but it does represent a mathematically possible distribution of R^2. Now let $\psi_0(x)=\psi_0(x_1, x_2\cdots x_n)$ be the amplitude at $t=0$. Then $\psi(x,t)$ given by

$$\psi(x,t)=\int\psi_0(x_{10},x_{20}\cdots x_{n0})S(x_0,x)dx_0, \qquad (21)$$

where $dx_0=dx_{01}\ dx_{02}\cdots dx_{0n}$, is also a solution of (2′) with $V=0$. We shall show that , with the constant factor chosen as in (20), it reduces to ψ_0 at $t=0$. Put

$$x_{\tau 0}=x_\tau+r_\tau(t)^{1/2}\ ;$$

[6] Cf. Ehrenfest, loc. cit.[4]

then (21) and (20) give:

$$\psi(x,t)=(m_1\cdots m_n)^{1/2}(i/h)^{n/2}\int\psi_0(x+rt^{1/2})\exp\left[-(i\pi/h)\sum m_r r_r^2\right]dr_1dr_2\cdots dr_n.$$

Since

$$\int_{-\infty}^{\infty}e^{-iay^2}dy=\int_{-\infty}^{\infty}(\cos ay^2-i\sin ay^2)dy=(1-i)(\pi/2a)^{1/2}$$

the right member of the preceding equation reduces to $\psi_0(x)$ for $t=0$.

Thus (21) is the general solution of (2′) with $V=0$ corresponding to the initial condition, $\psi=\psi_0$ at $t=0$; and it agrees of course with Heisenberg's result.

The other simple cases referred to above which can be solved by the same method are the case of uniform force field already treated above by general reasoning, the simple harmonic oscillator in n dimensions, and the effect of a uniform magnetic field. As the last named introduces a new feature, we shall treat concisely a simple case of it.

3. *An Electron in a Homogeneous Magnetic Field.* Taking the z axis parallel to the magnetic intensity, M, we have as Hamiltonian,

$$H=\frac{1}{2m}(p_x^2+p_y^2)+\frac{\omega}{2}(yp_x-xp_y)+\frac{m\omega^2}{8}(x^2+y^2), \tag{22}$$

where $\omega=eM/mc$, $e=$charge and $m=$mass of the electron, and as the wave equation:

$$\epsilon\frac{\partial\psi}{\partial t}=\frac{\epsilon^2}{2m}\left(\frac{\partial^2\psi}{\partial x^2}+\frac{\partial^2\psi}{\partial y^2}\right)-\frac{\epsilon\omega}{2}\left(y\frac{\partial\psi}{\partial x}-x\frac{\partial\psi}{\partial y}\right)+\frac{m\omega^2}{8}(x^2+y^2)\psi=0. \tag{23}$$

This equation requires some generalization of preceding results because it contains first-order derivatives. Instead of (7) and (9) we find

$$\frac{\partial R}{\partial t}=\frac{1}{m}\left(\frac{\partial R}{\partial x}\frac{\partial\theta}{\partial x}+\frac{\partial R}{\partial y}\frac{\partial\theta}{\partial y}\right)+\frac{R}{2m}\left(\frac{\partial^2\theta}{\partial x^2}+\frac{\partial^2\theta}{\partial y^2}\right)+\frac{\omega}{2}\left(x\frac{\partial R}{\partial y}-y\frac{\partial R}{\partial x}\right), \tag{24}$$

$$\frac{\partial P}{\partial t}=-\frac{\partial}{\partial x}(Pu_x)-\frac{\partial}{\partial y}(Pu_y), \tag{25}$$

with

$$mu_x=-(\partial\theta/\partial x)+\tfrac{1}{2}m\omega y,\qquad mu_y=-(\partial\theta/\partial y)-\tfrac{1}{2}m\omega x. \tag{26}$$

In (8) two additional terms appear on the right but upon substituting u from (26) we find simply:

$$\frac{\partial\theta}{\partial t}=-\frac{h^2}{8\pi^2mR}\left(\frac{\partial^2R}{\partial x^2}+\frac{\partial^2R}{\partial y^2}\right)+\frac{m}{2}(u_x^2+u_y^2). \tag{27}$$

Now for a particular element of R^2

$$\frac{du_x}{dt}=\frac{\partial u_x}{\partial t}+u_x\frac{\partial u_x}{\partial x}+u_y\frac{\partial u_x}{\partial y};$$

calculating the latter derivatives from (26) and (27), and repeating for u_y, we find:

$$\begin{aligned} m\frac{du_x}{dt}&=\frac{h^2}{8\pi^2 m}\frac{\partial}{\partial x}\left[\frac{1}{R}\frac{\partial^2 R}{\partial x^2}+\frac{1}{R}\frac{\partial^2 R}{\partial y^2}\right]+m\omega u_y,\\ m\frac{du_y}{dt}&=\frac{h^2}{8\pi^2 m}\frac{\partial}{\partial y}\left[\frac{1}{R}\frac{\partial^2 R}{\partial x^2}+\frac{1}{R}\frac{\partial^2 R}{\partial y^2}\right]-m\omega u_x. \end{aligned} \tag{28}$$

With $h=0$ these are the classical equations for the electron (which checks the assumed form for H), and the solution for its position is:

$$\begin{aligned} x&=A\sin\omega t+B\cos\omega t+C,\\ y&=A\cos\omega t-B\sin\omega t+D. \end{aligned} \tag{29}$$

If R is uniform in space, the elements of R^2 will move according to these same equations. Assuming all elements to start out from the point x_0, y_0 at $t=0$, we have $x_0=B+C$, $y_0=A+D$; eliminating the constants by means of these equations and (29) from the values of $u_x=\dot{x}$ and $u_y=\dot{y}$ obtained from (29), we find:

$$\begin{aligned} u_x&=\frac{\omega}{2}\left[\frac{\sin\omega t}{1-\cos\omega t}(x-x_0)+y-y_0\right],\\ u_y&=\frac{\omega}{2}\left[-(x-x_0)+\frac{\sin\omega t}{1-\cos\omega t}(y-y_0)\right]. \end{aligned} \tag{30}$$

We now substitute these expressions for u_x and u_y in (27), omit the term in h and integrate, obtaining:

$$\theta=-\frac{m\omega}{4}\frac{\sin\omega t}{1-\cos\omega t}[(x-x_0)^2+(y-y_0)^2]+f(x,y).$$

Substitution of this value for θ in (26) and comparison with (30) shows that $f(x,y)=\frac{1}{2}\omega(y_0x-x_0y)+\text{const.}$ Then, putting the value of θ into (24) and assuming R independent of x and y, we find after integration

$$R=C(1-\cos\omega t)^{-1/2}.$$

Thus

$$\begin{aligned} S(x_0,y_0;x,y)=\frac{im\omega}{2h}\left(\frac{2}{1-\cos\omega t}\right)^{1/2}\exp\left\{-\frac{i\pi m\omega}{2h}\left[\frac{\sin\omega t}{1-\cos\omega t}((x-x_0)^2\right.\right.\\ \left.\left.+(y-y_0)^2)+2(x_0y-y_0x)\right]\right\} \end{aligned} \tag{31}$$

and

$$\psi(x,y,t)=\int\psi_0(x_0,y_0)S(x_0,y_0\,;x,y)dx_0dy_0 \tag{32}$$

are solutions of (23). Analysis of ψ by the method used above shows that $\psi\rightarrow\psi_0(x,y)$ as $t\rightarrow 0$. Hence ψ as given by (32) and (31) is the general solution of (23) corresponding to the initial amplitude ψ_0. This result agrees with that obtained by the matrix method.[7]

4. *The measurement of Velocity and Momentum.* The ordinary fundamental definition of velocity as space divided by time requires two successive specifications of position. But two *exact* experimental determinations of position made upon the same particle will always yield the velocity of light, because of the indefinitely great Compton-effect or equivalent disturbance produced by the first one; and two inexact determinations leave an indefiniteness in the measured value. There seems to be only one case in which an observation can be made which deserves to be called an exact measurement of velocity, namely, the case of free motion.

Suppose that at time t the amplitude $\psi(x,t)$ differs appreciably from zero only within a distance D from a certain point $(\alpha_1,\ \alpha_2\cdots\alpha_n)$ (i.e. for $\sum(x_r-\alpha_r)^2<D$), and suppose that at a very much later time t' the position of the system is accurately determined, the values thus found for the coordinates being x'. Then we can regard the quantities

$$v_j=(x_j'-\alpha_j)/(t'-t)\qquad(j=1,2\cdots n) \tag{33}$$

as experimental values of the components of velocity of the particles; they become exact as $t'\rightarrow\infty$, since the indefiniteness in the initial positions of the particles is less than $D/(t'-t)$ and vanishes in the limit. We can reasonably regard these values as referring specifically to the time t because the result of such an observation for given $(t'-t)$ would vary statistically in a manner independent of t and it is therefore reasonable to postulate that the lapse of time until t' causes no error.

The amplitude for x' will be, by (20) and (21):

$$(m_1\cdots m_n)^{1/2}\left[i/h(t'-t)\right]^{n/2}\int\psi(x,t)\exp\left\{-\left[i\pi/h(t'-t)\right]\sum m_r(x_r'-x_r)^2\right\}dx \tag{34}$$

and for v by (4) and (33):

$$(m_1\cdots m_n)^{1/2}(i/h)^{n/2}\int\psi(x,t)\exp\left\{2\pi ih^{-1}\sum_r m_r\left[v_rx_r-\right.\right.$$
$$\left.\left.\tfrac{1}{2}(x_r-\alpha_r)^2(t'-t)^{-1}-\alpha_rv_r-\tfrac{1}{2}v_r^2(t'-t)\right]\right\}dx\,. \tag{35}$$

Here the last two terms in the bracket are independent of the variables of integration and so result merely in multiplying ψ by a factor of absolute value unity, which has no effect on the probability: this factor, together,

[7] E. H. Kennard, loc. cit. p. 348.

with i before the integral sign, we shall simply omit. The second term in the bracket vanishes as $t' \to \infty$. Hence in the limit we can take as the amplitude for v at time t

$$M(v) = (m_1 \cdots m_n)^{1/2} h^{-n/2} \int \psi(x,t) \exp[2\pi i h^{-1} \textstyle\sum_\tau m_\tau v_\tau x_\tau] dx \quad (35)$$

and for the momenta $\xi_j = m_j v_j$, by (4):

$$M(\xi) = h^{-n/2} \int \psi(x,t) \exp[2\pi i h^{-1} \textstyle\sum_\tau \xi_\tau x_\tau] dx. \quad (36)$$

The last equation is the familiar result yielded by matrix theory; $M(\xi)$ $M^*(\xi)$ $d\ \xi$ is the probability that an exact measurement of the momenta made as described above would yield values lying within $d\ \xi$. Equation (36) leads at once to the Heisenberg relation between the degrees of indetermination of a coordinate and its momentum.

We shall verify the normalization of $M\ (\xi)$; one of the formulas obtained in doing so will be required later. Putting $I = \int M(\xi)\ M^*(\xi) d\xi$ we have:

$$I = h^{-n} \int d\xi \int\int \psi(x') \psi^*(x'') \exp[2\pi i h^{-1} \textstyle\sum_\tau \xi_\tau (x_\tau' - x_\tau'')] dx' dx'', \quad (37)$$

$$I = h^{-n} \int \psi(x')\ dx' \int d\xi \int \psi^*(x'')\ \exp\ [2\pi i h^{-1} \textstyle\sum_\tau \xi_\tau (x_\tau' - x''_\tau{}')]\ dx''.$$

This change in the order of integration could be made without question if both $\psi(x')$ and $M(\xi)$ vanished outside of certain finite limits (besides satisfying the usual requirements). Now it happens that (as is not hard to show) ψ and M cannot have this particular property simultaneously. Accordingly we shall simply assume that ψ and M vanish at infinity fast enough so that the change of order is possible (caution in regard to this is really necessary; for instance, the integration with respect to ξ cannot be carried out first of all). We now recognize in the double integral following dx' simply the Fourier integral expansion of $\psi^*(x')$, multiplied by h^n. Hence

$$I = \int \psi(x') \psi^*(x') dx', \quad (38)$$

and $I = 1$ by (3).

The physical definition of velocity contained in equations (33) is not immediately applicable to cases other than free motion. According to Heisenberg we are at liberty to imagine the forces abolished at any instant, so that the motion becomes free and exact measurements of velocity and momentum can then be made. If we do not wish to adopt such an assumption then we might still call $M\ (\xi)$ as defined by (36) the "amplitude for the momenta," without asking whether this quantity has an immediate physical meaning or not; this will be done during the remainder of this paper.

5. *The "Conservation of Momentum."* Equ. (36) leads to an important connection between momentum and force. The *total* component of momentum

of all particles in one direction, say that of ξ_α where $\alpha = 1, 2$ or 3, is $\sum_{k=0}^{n-1}\xi_{\alpha+3k}$; the "mean probable" momentum of the whole system is therefore

$$\Gamma_\alpha = \int \sum_{k=0}^{n-1}\xi_{\alpha+3k}M(\xi)M^*(\xi)d\xi \tag{39}$$

$$= h^{-n}\int\sum\xi_{\alpha+3k}d\xi\int\int\psi(x')\psi^*(x'')\exp[2\pi i h^{-1}\sum\xi_r(x_r'-x_r'')]dx'dx''$$

$$= -\frac{1}{2\pi i h^{n-1}}\sum\int d\xi\int\int\frac{\partial\psi(x')}{\partial x'_{\alpha+3k}}\psi^*(x'')\exp[2\pi i h^{-1}\sum\xi_r(x_r'-x_r'')]dx'dx''$$

by (36), after an integration by parts in each term of the sum (ψ being assumed to vanish at the limits). The integrals in the last equation are the same as that in (37) except that a derivative replaces $\psi(x')$; hence, making the corresponding change in (38):

$$\Gamma_\alpha = -\frac{h}{2\pi i}\sum\int\frac{\partial\psi(x)}{\partial x_{\alpha+3k}}\psi^*(x)dx.$$

We can also shift the differentiation onto ψ^* by an integration by parts; hence we can write

$$\Gamma_\alpha = \frac{h}{4\pi i}\sum_{k=0}^{n-1}\int\left(\psi\frac{\partial\psi^*}{\partial x_{\alpha+3k}} - \psi^*\frac{\partial\psi}{\partial x_{\alpha+3k}}\right)dx. \tag{40}$$

Now from (10)

$$\sum_{k=0}^{n-1}m_{j+3k}\int u_{\alpha+3k}P dx = \frac{h}{4\pi i}\sum\int\left(\psi\frac{\partial\psi^*}{\partial x_{\alpha+3k}} - \psi^*\frac{\partial\psi}{\partial x_{\alpha+3k}}\right)dx. \tag{41}$$

Γ_α therefore equals the first member of the last equation and from (18)

$$\frac{d\Gamma_\alpha}{dt} = -\sum_{k=0}^{n-1}\int P\frac{\partial V}{\partial x_{\alpha+3k}}dx. \tag{42}$$

Eqs. (40) and (41) might be interpreted as identifying the total "momentum of the probability" with that of the particles. *Eq. (42) shows that the time rate of change of the total mean probable momentum of the system is equal to the total mean probable classical force upon it, internal forces cancelling out in the usual manner. This is the theorem of the conservation of momentum in the new mechanics.*

The same theorem can be deduced for one particle alone, or for any other separate portion of the whole system, but we shall not elaborate the details.

6. *The Measurement of Energy and other Secondary Magnitudes.* In order to arrive at the Schrödinger theory of atomic energy levels from the present standpoint it is necessary to exhibit each energy value as the result of a mechanical experiment. Now in any measurement the quantity actually observed seems to be always a *position* (on a scale, plate, etc.); from the standpoint of physical observation the coordinates seem to play a funda

mental role, while such things as momentum and energy are arrived at only as subsidiary quantities. The measurement of a magnitude of the latter type can be illustrated as follows:

Let $H\ (p,\ q)=H\ (p_1, \cdots, p_n;\ q_1, \cdots, q_n)$ be the Hamiltonian for a system when the motion of the center of mass is omitted, and let $F\ (p,\ q)$ $=F\ (p_1 \cdots p_n,\ q_1 \cdots q_n)$ be any function of coordinates and momenta which "remains constant in time." In order to "measure" F let us suppose that we are able to immerse the system in a field that exerts a uniform force upon it parallel to the coordinate x of its center of mass and "proportional to F" (an actual example being a non-homogeneous magnetic field exerting a force proportional to magnetic moment, as in the Stern-Gerlach experiment). Then the total Hamiltonian is

$$H_1=H(p,q)+(\xi^2/2M)-\beta F(p,q)x \tag{43}$$

where $\xi=$ momentum corresponding to x, M = mass of system and β is the field constant; and

$$\epsilon\frac{\partial\psi}{\partial t}=H\left(-\epsilon\frac{\partial}{\partial q},\ q\right)\psi+\frac{\epsilon^2}{2M}\frac{\partial^2\psi}{\partial x^2}-\beta xF\left(-\epsilon\frac{\partial}{\partial q},\ q\right)\psi. \tag{44}$$

Putting

$$\psi=\psi_1(q,t)\psi_2(x,t) \tag{45}$$

we find that the variables will separate provided $F(\cdots)\psi=\kappa\psi$ for all t, that is, provided

$$\psi_1(q,t)=\gamma(t,\kappa)u(q,\kappa) \tag{46}$$

and

$$F(-\epsilon\partial/\partial q,q)u(q,\kappa)=\kappa u(q,\kappa), \tag{47}$$

κ being a constant. The usual argument then leads to the equations:

$$H(-\epsilon\partial/\partial q,q)u(q,\kappa)=Wu(q,\kappa), \tag{48}$$

$$\epsilon d\gamma/dt=W\gamma, \qquad \gamma=e^{2\pi i h^{-1}Wt}, \tag{49a,b}$$

$$\epsilon\frac{\partial\psi_2}{\partial t}=\frac{\epsilon^2}{2M}\frac{\partial^2\psi_2}{\partial x^2}-\beta\kappa x\psi_2, \tag{50}$$

where W is a new constant. (We could also add an arbitrary term $\eta(t)\psi_2$ in (50) provided we subtracted $\eta(t)\gamma$ in (49), but this would not alter ψ). We shall suppose that u and ψ_2 are separately normalized to satisfy (3)[9]; to make this possible, κ and W must be "characteristic values" for their respective equations.

If u is to satisfy both of Eq. (47) and (48) it is necessary that the operators F and H should "commute," i.e., if we write $F(\cdots)$, $H(\cdots)$ for

[9] For normalization in the continuous spectrum by the Weyl method cf. E. Fues, Ann. d. Physik 81, 281 (1926)

$F(-\epsilon\partial/\partial q,\ q)$, etc., we must have $F(\cdots)\ H(\cdots)=H(\cdots)\ F(\cdots)$. For, applying $H(\cdots)$ to both sides of (47) and $F(\cdots)$ similarly to (48) and comparing: $H(\cdots)\ F(\cdots)u=\kappa\ H(\cdots)u=\kappa Wu=WF(\cdots)u$ $=F(\cdots)\ H(\cdots)u$. This condition upon F severely restricts the number of mathematical quantities that can be measured physically in this manner; angular momentum is, however, among them.

Assuming that F and H do commute, application of $H(\cdots)$ to both sides of (47) yields the result that

$$F(\cdots)[H(\cdots)u]=\kappa[H(\cdots)u].$$

Thus, if u is a characteristic function of (47), $H(\cdots)u$ is likewise a solution of this equation, and, since we may safely assume that it will satisfy the same boundary condition of finiteness as u, it must also be a characteristic function. If only one such function exists for the value of κ in question, then we have $H(\cdots)u=Au$ where A is a constant, and u satisfies (48) with $W=A$. If κ is a multiple characteristic value, it is easily shown that a corresponding number of linear combinations of the functions belonging to κ can be constructed which are characteristic functions of (48) as well for certain values of W. In short, when F and H commute (47) and (48) have in general a common set of characteristic functions.

Turning now to Eq. (50) this has the same form as the wave-equation for a particle in one dimension subjected to a uniform force $\beta\kappa$(cf. (5) with $n=1$, $v=-\beta\kappa x$). We have seen above (below Eq. (16)) that such a force merely gives to the entire packet the classical displacement $\delta=\frac{1}{2}\beta\kappa t^2/M$. To be sure, the packet also spreads out in the x-direction, just as it would in the absence of the field, but this spreading is easily seen from equation (20) to be ultimately proportional to t, so that the uncertainty in δ due to it can be diminished at will by increasing t. We can then take

$$\kappa=2\delta M/\beta t^2, \tag{51}$$

calculated from observed values of δ and t and the known values of M and β, as a "physically observed" value of F.

Now, in general, we cannot assume that ψ_1 satisfies (45) to (47) initially. Probably we can, however, safely write the initial amplitude for $t=0$ in the form, $\psi_1{}^0(q)\psi_2{}^0(x)$, and we can then expand $\psi_1{}^0(q)$ in terms of the normalized characteristic functions $u(q,\kappa)$ of (47), thus:

$$\psi_1{}^0(q)=\sum\nolimits_n c_n u(q,\kappa_n)+\int c(\kappa)u(q,\kappa)d\kappa,$$

the series extending over the point spectrum and the integral over the continuous spectrum for κ. The complete packet at time t is then

$$\psi=\sum\nolimits_n c_n e^{2\pi i h^{-1}W_n t}u(q,\kappa_n)\psi_2(x,t,\kappa_n)+\int c(\kappa)e^{2\pi i h^{-1}Wt}u(q,\kappa)\psi_2(x,t,\kappa)d\kappa, \tag{52}$$

where $\psi_2(x,\kappa,t)$ is the solution of (50) for the value κ, chosen so as to reduce to $\psi_2{}^0(x)$ at $t=0$, and W_n or W has the value for which $u(q,\kappa)$ is a characteristic function of (48) as well.

The factor $\psi_2(x, \kappa, t)$ will then produce in each term of ψ or partial packet the displacement δ described above. The components of the initial packet corresponding to different values of κ will thus be spread out into a physical spectrum; those corresponding to the discrete values, κ_n, will finally become clearly separated from each other, while those belonging to the continuous spectrum will overlap with components belonging to a continually decreasing range of κ as time goes on. It is easily shown that the probability of finding the system in any particular component packet is equal to $c_n c_n^*$, or to $c(\kappa)c^*(\kappa)d\kappa$; also that the probability for particular values of q is $u(q, \kappa_n)u^*(q, \kappa_n)$ or $u(q, \kappa)u^*(q, \kappa)$, respectively.

A process of this general nature seems to be the justification, from the mechanical point of view, for the common assumption that the coefficients c_n and $c(\kappa)$ represent the probability amplitude for the quantity F.

If we put $F = H$, we have the case of a measurement of the "energy." In this case (47) and (48) both become the ordinary Schrödinger equation without the time factor.

7. *The Conservation of Energy and Angular Momentum.* This topic has been discussed by others but perhaps a few additional remarks from the present standpoint may not be out of place.

Let ψ be expanded in the series (52) with W in place of κ, u denoting characteristic functions of Schrödinger's equation, (48). Then if the system is isolated and conservative the quantities $c_n c_n^*$ or $c(W)c^*(W)$, representing probabilities for the energy, are independent of the time: this is the well-known equivalent of the Conservation of Energy for an isolated system.

But we can sometimes measure the energies of separate parts of a system, as of an electron and atom before and after a collision. To illustrate such a measurement let $H = H_1 + H_2$ where H_1 and H_2 commute with each other and therefore also with H; then we might subject the system simultaneously to a force in the x-direction proportional to H_1, another in the y-direction proportional to H_2 and a third in the z-direction proportional to H and thereby measure by the above method H_1, H_2 and H all at the same time. In that case we should have three equations in place of (47), viz.

$$H_1(-\epsilon\partial/\partial q, q)u = W_1 u, \quad H_2(-\epsilon\partial/\partial q, q)u = W_2 u,$$

and

$$H_1(-\epsilon\partial/\partial q, q)u + H_2(-\epsilon\partial/\partial q, q)u = Wu,$$

which also represents (48). The partial packet that is brought to any given point in xyz space then represents energies W_1 and W_2 for the parts and W for the whole and it is clear from the equations that

$$W_1 + W_2 = W.$$

Thus, as is usually assumed, the conservation of energy holds exactly between a system and its parts.

Finally, if the potential energy V contains the time, we have classically

$$dH/dt = \partial V/\partial t.$$

On the new theory it can be shown that

$$d\overline{W}/dt = \int P(\partial V/\partial t)dq \tag{53}$$

where

$$\overline{W} = \sum_n c_n c_n^* W_n + \int c(W)c^*(W)W dW \tag{54}$$

and represents the "mean probable" value of the energy; the c's are the coefficients in (52) when $F = H$ and $\kappa = W$ and are functions of the time along with V. The proof of this theorem involves only a straightforward use of eqs. (2) and (48) and of the formulas for the coefficients in an expansion in terms of the u's and will not be given here.

Similar results can be obtained for any quantity F which commutes with the Hamiltonian H. The fact that the c's in (52), which are the probability amplitude for F, are independent of the time whenever H is, constitutes the quantum equivalent of the classical theorem that F is conserved during the motion of a conservative system.

An important case is that of angular momentum and magnetic moment, which has been discussed briefly by Oppenheimer[10] and Weyl[11] and more completely by Darwin[4] with special reference to the Stern-Gerlach experiment.

The theory of quantum mechanics has been presented in the present paper from a strictly mechanical point of view. This approach seems to be the most natural one, but it leads unfortunately to very few predictions that are within the reach of experimental verification. The field of atomic energy levels, in which the theory has so far achieved its principal successes, can be explored only with the aid of radiation, employed not as a geometrical clue to position but with reference to the process of its emission and absorption by matter. This process has been treated by Dirac,[12] but in a very abstract manner. The most urgent need at present seems to be a satisfactory theory of the electromagnetic field; when this has been found, we may hope that it will be capable of statement in a readily apprehended form similar to the theory which Schrödinger and Heisenberg have given us for mechanical phenomena.

CORNELL UNIVERSITY,
Feb. 10, 1928.

[10] J. R. Oppenheimer, ZSP 43, 27 (1920).
[11] H. Weyl, ZSP 46, 1 (1927).
[12] P. A. M. Diroc, Roy. Soc. Proc. 114, 243 (1927).

THE PHYSICAL PENDULUM IN QUANTUM MECHANICS

By Edward U. Condon

Abstract

It is pointed out that the Mathieu functions of even order are the characteristic functions of the physical pendulum in the sense of Schrödinger's wave mechanics. The relation of various properties of the functions, as known from purely analytical investigations of them, to the pendulum problem is discussed.

THE problem of the physical pendulum, that is, of the motion of a mass-point constrained to move in a circle and acted on by a uniform force field, has played such a great role in the study of analytic mechanics that a discussion of the same problem from the standpoint of Schrödinger's wave mechanics cannot be without interest. It turns out that the characteristic functions are certain of the Mathieu, or elliptic cylinder, functions and that the arguments from mechanics serve to illustrate in an interesting way many of the properties of these functions.

Let the mass of the particle be μ and let its position in a circle of radius a be designated by the angle θ. It will be supposed that the particle carries an electric charge e, and that there is a uniform electric field acting in such a way that the potential energy function is $-eEa\cos\theta$. That is, the force is in the direction of $\theta=0$. Under these circumstances the wave-mechanical equation becomes

$$\frac{d^2\psi}{d\theta^2}+\frac{8\pi^2\mu a^2}{h^2}[W+eEa\cos\theta]\psi=0,$$

in which W is the energy level parameter. The energy levels are the values of W for which this equation possesses solutions which have the period 2π in θ. Introducing the variable, $x=\frac{1}{2}\theta$, and the abbreviations,

$$\alpha=8\pi^2\mu a^2W/h^2,\quad q=2\pi^2\mu a^2eE/h^2,$$

the equation appears in the usual form for Mathieu's equation,

$$d^2\psi/dx^2+(4\alpha+16q\cos 2x)\psi=0,$$

where, now, one seeks solutions with the period π in x.

The solutions of this equation which have the period 2π in x are known as Mathieu functions.[1] For $q=0$, the case of zero field strength, the problem becomes simply that of a free rotator with fixed axis. The characteristic functions are 1, $\sin 2x$, $\cos 2x$, $\sin 4x$, $\cos 4x\cdots$ with the associated values of α equal to 0, 1, 1, 4, 4 $\cdots$ The problem is degenerate since there

[1] An account of them is given in Whittaker and Watson, *A Course of Modern Analysis*, Chap. 19. (1920). This is, however, quite incomplete now because of the many more recent investigations by British and Scottish mathematicians.

are two distinct characteristic functions associated with each energy level, except the first one. The characteristic function for any degenerate state is an indeterminate linear combination of the two functions associated with that state. In particular, the functions which correspond to progressive rotatory motion in the two opposing senses are e^{2imx} and e^{-2imx}, rather than $\cos 2mx$ and $\sin 2mx$. These latter functions correspond in some way to equal numbers of rotators turning in opposite senses and these connect in a continuous manner with the non-degenerate characteristic functions for $q \neq 0$, as $q \to 0$. The standard notation for the Mathieu functions is $\mathrm{ce}_n(x,q)$ and $\mathrm{se}_n(x,q)$ where as $q \to 0$ these become equal to $\cos nx$ and $\sin nx$ respectively. All of these have period 2π, while those in which n is even have the period π in x and so they are the characteristic functions of the pendulum problem.

It will be observed that the zero from which energy is reckoned in the wave equation is from the position at which $\theta = \pi/2$ or $x = \pi/4$. If instead it is reckoned from $\theta = 0$, the minimum of the potential energy curve, one has to add $4q$ to each value of α.

It is of interest now to consider a number of properties of the functions, which have been obtained by purely analytical means, in the light of the pendulum problem. Firstly, it is clear that the functions will bear an invariant relation to the minimum of the potential energy curve, hence yield such relations[2] as

$$\mathrm{ce}_{2n}(\tfrac{1}{2}\pi - x, \ -q) = (-1)^n \cdot \mathrm{ce}_{2n}(x,q).$$

Jeffreys[3] has shown that there are no allowed values of α such that $\alpha < -4q$. Physically this means that there are no states for which the total energy is less than the minimum potential energy permissible for the system, and therefore appears natural enough. The relation, $\alpha = 4q$, is a critical one for classical mechanics in that for $\alpha > 4q$ the motion is rotatory while for $\alpha < 4q$ it is oscillatory. This value has also shown itself as a critical one in the analytical theory of the functions.

For $\alpha > 4q$, Jeffreys finds (approximately) that α must be such that

$$\int_0^{2\pi} (4\alpha + 16q \cos 2x)^{1/2} \cdot dx = 2\pi m,$$

in which m is an integer. Recalling the meaning of α and q, this requirement becomes

$$\int_0^{2\pi} p_\theta d\theta = \tfrac{1}{2} m h,$$

[2] See e.g. Goldstein, Trans. Cambr. Phil. Soc. **23**, 303, (1927) Par. 1.5. This memoir contains a good many of the newer results not given in Whittaker and Watson.

[3] Jeffreys, Proc. London Math. Soc. **23**, 437, (1924–25). This paper and the one preceding it are especially interesting in that the methods of approximate integration which he uses are closely related to those by means of which the connection between classical mechanics and quantum mechanics is established.

so that the condition reduces to the classical quantum condition for even values of m, the ones which correspond to allowed quantum motions.

The most complete tables of the values of α as a function of q are those of Goldstein (loc. cit.). He has given the values of α for $ce_0(x,q)$, $se_2(x,q)$ and $ce_2(x,q)$ besides several others which are not related to the pendulum problem. He gives an asymptotic expansion good for small m and large q as follows:

$$\alpha \sim -4q+(2m+1)(2q)^{1/2}- \cdots .$$

In this one recognizes that $(\alpha+4q)$ which is the energy counted up from the minimum of potential energy at $\theta=0$ goes linearly with the number m in just the way that the energy levels of the harmonic oscillator go in wave mechanics. Moreover, the interval between levels, $2(2q)^{1/2}$, when expressed as energy is exactly equal to $h\nu$ where ν is the frequency of the small oscillations of a pendulum in the field of strength E, reckoned on classical mechanics, i.e.,

$$\nu=(eE/4\pi^2\mu a)^{1/2}.$$

The rapidity with which the three lowest energy levels approach the values

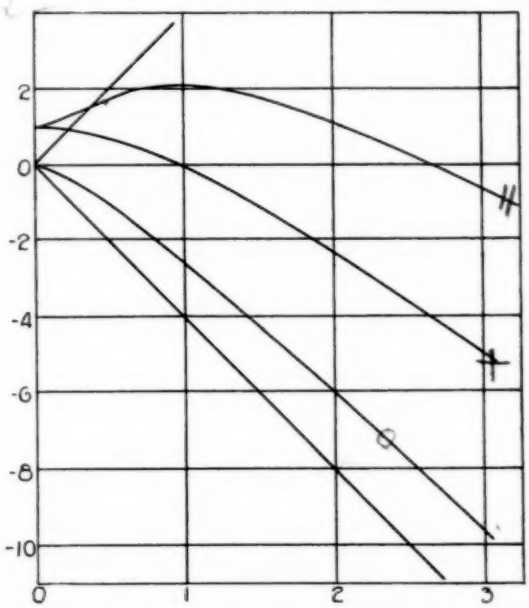

Fig. 1. The three lowest energy levels of the physical pendulum as a function of field strength (abscissas, q. ordinates, α). The straight line of positive slope divides the region of classical rotatory motions from that of classical oscillatory motions. That of negative slope gives the value of the potential energy minimum which forms a more natural origin from which to count the energy of the small oscillation states.

appropriate to the small oscillations theory is indicated in Fig. 1, where α is plotted as a function of q, from Goldstein's tables.

An interesting feature is the way the second and third energy levels cross the line, $\alpha=4q$, without any discontinuity, this being the critical place at which the associated classical motion changes character from rotatory type to oscillatory by passing through a motion of infinite period. The discontinuous behavior of a pendulum moving with constant energy in a field of slowly decreasing strength caused some trouble in the old mechanics, as noted by Ehrenfest and by Bohr. That this discontinuity is not a feature of the wave mechanical treatment was first recognized by Hund.[4] In a sense this discontinuity still appears in wave mechanics but at $q=0$ instead of at $q=\alpha/4$, for the characteristic functions, as $q\to 0$, do not join on continuously with those solutions of the equation for the force-free rotator which represent rotatory motion, as already remarked.*

Similarly one expects for small values of the quantum number and large values of q, that the characteristic functions will go over into the characteristic functions of the harmonic oscillator problem. The Mathieu functions do have just such an asymptotic connection with the Hermitian polynomials or parabolic cylinder functions.[5] This behavior is just what one would expect from the relation to the pendulum problem. Thus it makes clear the theorem of Ince (loc. cit.) concerning the clustering of the zeros of the Mathieu functions within a region of the order of magnitude $-Kq^{-\frac{1}{4}}<x<+Kq^{-1/4}$ as $q\to\infty$, where K is a constant. This is because the wave functions in wave mechanics only show a distinctly oscillatory character inside the region of the associated classical motion, where the de Broglie wavelength, h/p, of the system is real. A simple calculation shows that the amplitude of the classical motion for a given quantum state tends to zero as $q^{-1/4}$ for $q\to\infty$.

It thus appears that the principal properties of the Mathieu functions of even order are simply related to the mechanical problem of which they are the characteristic functions in Schrödinger's wave mechanics.

COLUMBIA UNIVERSITY,
DEPARTMENT OF PHYSICS
February 21, 1928.

[4] Hund, Zeits. f. Phys. **40**, 742, (1927) especially footnote, p. 750.

[5] See e.g., Ince, Jl. London Math. Soc. **2**, 46, (1927).

* *Added in proof:* The ψ function that joins on with $e^{i2\pi x}$ is, of course,

$$\mathrm{ce}_{2n}(x,q)e^{2\pi iE_1t/h}+i\mathrm{se}_{2n}(x,q)e^{2\pi iE_1t/h}$$

where E_1 and E_2 are the energy levels associated with ce_{2n} and se_{2n} respectively. If one compute the quantum mechanical expression for the current associated with this ϕ, it will be seen that it depends on the time through a factor $\cos 2\pi(E_1-E_2)t/h$. For small q, $E_1-E_2\to 0$ so the current reverses itself with a small frequency which becomes zero for $q=0$. This behavior reminds one of the "gallows problem" of Ehrenfest and Tolman (Phys. Rev. **24**, 287 (1924)), although here there are no forces due to twist of thread to cause the long period reversal!

LIGHT QUANTA AND WAVE MECHANICS

By J. C. Slater

Abstract

Light quanta are treated by wave mechanics by analogy with electrons. It is shown that their wave equation is the ordinary optical wave equation. Heisenberg's principle of indeterminateness becomes a description of diffraction. In problems in which localization of quanta is found experimentally, wave packets are to be set up; these are applied to the experiments of Bothe and Geiger, and of Compton. The paths of quanta coincide with the rays of geometrical optics, with a deviation of the error in geometrical optics; by the principle of indeterminateness, more accurate laws for the paths are neither necessary nor possible.

THE wave mechanics has brought out the fundamental resemblance between electrons, with their accompanying Schrödinger waves, and corpuscular light quanta, with their electromagnetic waves. The statistical relations between electrons and Schrödinger waves have been discussed mathematically by Dirac and Jordan,[1] and Heisenberg[2] has supplied a physical description of the situation, in his principle of uncertainty. By analogy, the connections between quanta and light waves can be definitely stated, and no doubt are familiar to many persons. Nevertheless, since no treatment of the subject has apparently been published, and since it furnishes the answer to a problem which has been much discussed, and at the same time a very simple illustration of the principle of uncertainty, it seems worth while to give an explicit treatment. As will be seen from the paper below, for many of the most important problems one can use a simple theory in which the waves exist in a three-dimensional space, and the amplitudes are ordinary c-numbers, rather than q-numbers as Dirac has assumed.[3] The result may be stated as follows: that all experiments can be explained by the hypotheses that the intensity in the radiation field measures the probability of the presence of quanta; and that in those cases where a definite localization of quanta seems to be observed, this localization is to be described, to the accuracy with which it can be observed, by setting up wave packets.

The wave mechanics of a quantum can be formulated by the same principles used with electrons. First one selects coordinates (x, y, z, t) and corresponding momenta $(p_x, p_y, p_z, -E)$. Then, in order to find the function $\psi(x,y,z,t)$ which has the property that $\psi\psi^* dxdydz$ is the probability that a quantum with given energy at time t is in the volume $dxdydz$, one finds a functional relation between $p_x, p_y, p_z, -E$, and, if necessary, x, y, z, t: say $f(p_x,p_y,p_z,-E, x,y,z,t)=0$. In this function, one replaces each

[1] Dirac, Proc. Roy. Soc. **A113**, 621 (1927). Jordan, Zeits. f. Physik **40**, 809 (1927).
[2] Heisenberg, Zeits. f. Physik, **43**, 172 (1927).
[3] Dirac, Proc. Roy. Soc. **A114**, 243 (1927).

momentum by $h/2\pi i$ times the derivative with respect to the corresponding coordinate, so that f becomes an operator; one forms the differential equation

$$f\left(\frac{h}{2\pi i}\frac{\partial}{\partial x}, \frac{h}{2\pi i}\frac{\partial}{\partial y}, \frac{h}{2\pi i}\frac{\partial}{\partial z}, \frac{h}{2\pi i}\frac{\partial}{\partial t}, x, y, z, t\right)\psi(x,y,z,t)=0$$

and the solution is the desired function ψ. To find the relation f, there is no general method given by wave mechanics. But for a quantum, we may take Einstein's equation $E=h\nu$, and de Broglie's[4] relation $(P_x^2+P_y^2+P_z^2)^{1/2}=h/\lambda$, combine with the equation $v/\lambda=\nu$, where v is the velocity, and obtain $v(P_x^2+P_y^2+P_z^2)^{1/2}=E$; in order not to have derivatives under the radical, we may equally well take instead $v^2(P_x^2+P_y^2+P_z^2)=E^2$. Then making our substitution, the equation is

$$v^2(h/2\pi i)^2\nabla^2\psi=(h/2\pi i)^2\partial^2\psi/\partial t^2, \text{ or } \nabla^2\psi-(1/v^2)\partial^2\psi/\partial t^2=0,$$

the familiar wave equation of optics.

To solve the problem of the motion of quanta, then, one solves the optical wave equation, and the intensity of the resulting wave at any point measures the probability of the existence of a quantum at that point. This of course is a connection between waves and quanta frequently proposed before the development of the wave mechanics. Previously, it had to be admitted that this theory was incomplete, in that it did not precisely define the paths of the individual quanta; but now it is seen that this indefiniteness is just what one would expect from Heisenberg's principle of indeterminateness. That principle really involves two statements: first, that it is not mathematically possible in wave mechanics to set up a description of a motion in which the initial conditions (coordinates and momenta) are all precisely defined, but that rather the initial coordinates and momenta must be supposed subject to uncertainties, or probable errors, whose product is at least of the order of magnitude of h; second, that this restriction in the mathematical theory is not of physical importance, for any possible experimental method of fixing the initial conditions would introduce probable errors of at least this magnitude. Applied to optics these statements become, first, that on wave theory one cannot set up a solution in which the initial position and momentum of a quantum are both precisely defined (on account of the diffraction inherent in a wave theory); second, that this is never necessary anyway, since real quanta are deflected to follow the diffraction patterns. From this we can see that definite laws for the motion of quanta are neither possible nor necessary.

The simplest form of solution of the wave equation is a plane wave, $\psi=e^{2\pi i\nu(t-(lx+my+nz)/v)}$. This solution, as we can easily see, corresponds to a quantum whose momentum, with components $lh\nu/v$, $mh\nu/v$, $nh\nu/v$, and energy $h\nu$, are precisely determined, but whose coordinates, x, y, z, t,

[4] This formula may be taken either as a generalization of the equation that momentum of a quantum $=h\nu/c=h/\lambda$, to the case where the velocity is v instead of c; or as an analogy to de Broglie's equation $\lambda=h/(\text{momentum})$, or $(\text{momentum})=h/\lambda$, holding for an electron.

are entirely indefinite (thus obeying Heisenberg's rule). The indefiniteness of the determination of the coordinates is seen by observing that $\psi\psi^* = 1$, independent of position, so that the quantum has equal probability of being at any point of space. On the other hand, the momenta are $\psi(h/2\pi i)(\partial/\partial x)\psi^* = lh\nu/v$, etc., and the energy is $-\psi(h/2\pi i)(\partial/\partial t)\psi^* = h\nu$ quite independent of the coordinates, and definitely determined. This sort of wave is, of course, the one needed in most optical problems; for generally we can determine with great accuracy the direction and frequency of a beam, but we have no idea as to the location of the quanta in it.

One can easily set up an experiment, however, in which there is definite information about the location of quanta, as well is about their momenta. It is only necessary to take a perfectly plane monochromatic wave, allow this to fall on an opaque screen containing a small hole closed by a shutter, and open the shutter, closing it again very soon. Then on the far side of the screen we have light, of which we know that the quanta were at the position of the hole at the time the shutter was open, and were travelling in the direction of the initial beam. It might seem that, by making the hole smaller and smaller without limit, and the shutter faster and faster, we could make as accurate a determination of position and time as we please, without corresponding sacrifice in the accuracy of determination of the momentum. We note, however, in agreement with the first part of Heisenberg's rule, that this would be impossible in the wave theory. For since the wave passes through a small hole, the problem is one of diffraction, and the smaller the hole, the more bending of direction of the wave there is (that is, diversity of the momentum is introduced by the process of passing through the hole); and since the wave train which passes through is limited in time, there is a broadening of the spectrum (resulting in a diversity of energies). The wave theory does not permit of a solution limited to a certain region of space and time, and yet without diffraction and broadening of the spectrum. Next, agreeing with the second part of Heisenberg's rule, one observes that quanta actually travel so as to fill all parts of the diffraction pattern predicted by wave theory; we infer that quanta, originally all of the same momentum and energy, are actually bent and changed in energy by the mere process of passing through a hole and shutter, so that it is useless to try to get exactly precise initial conditions or laws of travel.

The numerical part of Heisenberg's rule is easily verified in our case. Suppose the beam is travelling along the x axis. Let the diameter of the hole be D, the length of time the shutter is open, T. The wave after diffraction can be at once analyzed into plane waves, for this is just what the telescope does in Fraunhofer diffraction. In the theory of that subject, one sees that there will be waves of appreciable intensity in the diffracted beam making angles up to the order of λ/D with the original direction. The spectrum can be found by Fourier analysis, and it appears that frequencies differing by as much as $1/T$ from the original frequency will be present. Thus one infers that in the beam which has passed through, ν will vary from its original value by as much as $1/T$, m and n will differ from

zero by as much as λ/D, and l will equal 1 to the first order of small quantities. The uncertainty of $p_x = lh\nu/v$ will then be of the order of h/vT, of $p_y = mh\nu/v$ of the order of $(h\nu/v)(\lambda/D) = h/D$, of p_z of the order h/D, and of $E = h\nu$ of the order h/T. But the uncertainties in the determination of the coordinates are vT for x (the length of the wave bundle in the direction of its travel), D for y and z, and T for t. Thus in all cases the uncertainty introduced into the momentum, multiplied by the uncertainty in the determination of the coordinate, equals h, as the rule requires.

In the problem we have just discussed, there is a determination of both the initial coordinates and momenta of the quanta; the determination is not perfectly definite, it is true; yet, when one considers the relatively small magnitude of diffraction effects, one is tempted to say that ordinarily the definiteness of the determination is more striking physically than the indefiniteness, as the rectilinear propagation of light is more striking than diffraction. The light transmitted through the hole travels as a fairly compact packet of waves, following the path of the "ray" of geometrical optics, and gradually spreading out. Since the intensity of this wave determines the probability of the presence of quanta, all quanta transmitted will travel somewhere within the packet. Thus we can say that the paths of the quanta are the rays of geometrical optics, with an error of the order of magnitude of the error in geometrical optics. To a greater accuracy than this, we neither have nor require any law of the paths of quanta. In particular, one notes that individual quanta must be deflected, and change their frequency, as they pass through the hole; yet we need not infer from this the existence of forces producing the deflections. For the laws of conservation of energy and momentum, and the concept of force, need not apply precisely to the individual quanta; any more than any other law. They hold, as does the whole of ordinary dynamics, in the approximation to which we may use geometrical optics; beyond that, they need no longer be assumed to apply.

One error, in connection with the wave packet which we have set up by our experiment of the hole and shutter, is particularly to be avoided. This is the supposition that our wave packet is a dynamical "model" of a light quantum, or that it can give any information about the "dimensions" of a quantum. Such questions are entirely foreign to the theory; the dimensions of the wave packet, as we have seen, are derived entirely from the initial conditions of the problem, as regulated by experimental circumstances.

In the actual experiments that have been performed, there are only two in which the localization of light quanta has played a conspicuous part. These are the experiments on the Compton effect, performed by Bothe and Geiger, and by Compton.[5] In them, a plane wave of x-rays fell on atoms which scattered them. Both the recoil electrons, and the photo-electrons ejected by the scattered light, were observed. Bothe and Geiger observed that photo-electrons were ejected simultaneously with recoil electrons; Compton found that, correlating recoil electrons with photo-electrons, the

[5] Bothe and Geiger, Zeits. f. Physik **32**, 639 (1925); A. H. Compton, Proc. Nat. Acad. Sci., **11**, 303 (1925).

scattered quanta must have travelled in such a direction as to have the relation to the direction of the recoil electron demanded by the laws of conservation of energy and momentum. These experiments are somewhat more complicated to discuss than the cases we have taken, for we do not know the exact nature of the interaction processes between light and atoms. Nevertheless, a qualitative explanation can be given, which seems undoubtedly true in its broad outline.

If we knew merely that the plane wave was being scattered by the atoms, we should use a solution of the wave equation in which a plane wave struck the atoms, and spherical scattered waves came off from all of them. From this sort of solution, we can compute the probability of ejection of a recoil electron from an atom; we can also, knowing the intensity of the scattered light, compute the probability of the emission of a photo-electron; and our theory gives us no reason to expect a correlation between the two. But actually in the experiment our information is more precise than this; for in investigating the photo-electrons, it must be assumed that we know from which atom the recoil electron was ejected, and we know when and with what direction and velocity it was sent off. We must set up our wave representing the scattered light, making full use of these observations. The atomic wave function representing the scattering atom is to be so constructed that a wave packet representing the ejected electron is sent off within the limits of time and limits of angle observed in the experiment. Although we do not know in detail how to set up the scattered light wave in such a case, it seems certain that it would be in the form of a wave packet, emitted roughly during the time the recoil electron's packet was being ejected, and in roughly the direction demanded by the corpuscular theory of the Compton effect. The diffuseness of the wave packets, demanded by wave theory, is again to be correlated with the fact that the laws of the quanta are not known in detail, so that they do not precisely obey the law of conservation of momentum and energy in their encounters. We now have a probability of finding scattered quanta only within this wave packet; and the fact that photo-electrons were ejected only in the proper direction and time follows directly from the probability interpretation of the wave. This is a good example of Heisenberg's remark that the mere process of making an observation (in this case, observing the recoil electron), may greatly affect the probability of subsequent observations (in this case, restricting the possible places for the ejection of photo-electrons to a certain small beam); more generally, it illustrates the universal property of statistics, that the probability of an occurrence depends conspicuously on what is assumed known to start with.

JEFFERSON PHYSICAL LABORATORY,
HARVARD UNIVERSITY,
February, 1928.

FIELDS CURRENTS FROM POINTS

By C. F. Eyring, S. S. Mackeown,[1] and R. A. Millikan

Abstract

The laws governing the extraction of electrons from metals in high vacua by fields, first developed through experiments with crossed wires, then with fine wire cathodes discharging to cylindrical anodes, have been now found to hold throughout for field currents between points and planes. The theory needed for the quantitative determination of the potential gradients at points is here given, and critical gradients then determined experimentally. The generality of the linear relation between log i and the reciprocal of field-strength is experimentally established.

1. Introduction

IN OUR paper[2] on "Laws Governing the Pulling of Electrons out of Metals by Intense Electrical Fields" in which were established the laws governing the extraction of electrons from metals under the influence of fields, we did not think it necessary to present all the evidence which we had developed by a long series of experiments to show that the currents which were being measured were indeed field currents, as we named them, the values of which could be reproduced with reasonable accuracy whenever the field was restored to a given value no matter which of the variables governing the field strength was altered. The evidence published in our paper was sufficiently conclusive on this point if it were critically examined, but since the question may come up in connection with the work of many of the other experimenters who have gone into this field since our publication, it is perhaps worth while to present now a more complete statement of the evidence which we had obtained.

This was actually one of the first points for which one of us sought definite evidence in the work published very briefly in 1918[3] and 1920.[4] In this work it will be recalled that crossed tungsten wires were used whose distance apart could be accurately varied by a micrometer screw, and the potential between which could be easily varied three or four fold. The results of such variations were altogether definite and unambiguous. *The currents were reproduced whenever the fields reached certain values quite independently of which of the variables, distance or potential, was altered.*

In these experiments, as well as in those published in 1926,[2] we worked with quite as good vacuum conditions as have ever been used by any one in work of this sort, and proved repeatedly that the quality of the vacuum had no influence upon the currents when electrode distances were small, that is, the changing of the pressure some thousand fold, say from 10^{-5} to

[1] National Research Fellow in Physics.

[2] Millikan and Eyring, Phys. Rev. **27,** 51, January (1926).

[3] Millikan and Shackelford, Phys. Rev. **12,** 167 (1918).

[4] Millikan and Shackelford, Phys. Rev. **15,** 239 (1920).

10^{-8} millimeters had no influence upon the field currents. We did, however, bring to light then[4] and again in 1926,[2] as reported in the latter paper, the very important influences of surface conditions of the wire and of the alteration of surface conditions with time and with heat treatment upon our field currents. Other later observers[5] have checked these results repeatedly, although some[6] of them have interpreted their results as indicating the possible non-existence of field currents at sufficiently high vacuum. The facts are, however, that, as we have established through long experimenting in a great variety of ways, it is wholly the surface condition and not at all the condition of the pressure of the residual gas, provided only that the electronic mean free path is very long in comparison with electrode distances, that determines the strength of the field currents.

As indicated in the first published experiments in this field[3] it is possible to condition the wire so that field strengths of 4,000,000 volts per centimeter produced no currents at all, and in later unpublished experiments we have many times exceeded these values.

In view of this very strong influence of surface conditions, work of the following kind on points of different curvatures is perhaps not as well adapted to the establishment of the unique dependence of the currents from a given surface upon fields as were the experiments above referred to. But it is thought worth while to make record of some of them for guidance of others who may wish to work with points. Accordingly, the method of calculating the field at a point, unpublished data obtained in 1922, and data obtained recently are here presented.

II. Solution of the Field at a Point

The points are shaped, as nearly as possible, in the form of hyperboloids of revolution, and we shall assume them to have such a form in this theoretical consideration. Let the axis of symmetry of the hyperboloid be the X-axis and the plane which contains the Y and Z axes be the metallic plane, then with the point placed at the correct distance from the plane and with a difference of potential between the electrodes we shall have a system of hyperboloids of revolution and an orthogonal system of half ellipses representing the equipotential surfaces and lines of force respectively.

For the free space between the point and the plane we may write the equation of Laplace,

$$\Delta\phi = 0 \tag{1}$$

In generalized orthogonal coordinates this becomes

$$\frac{1}{UVW}\left\{\frac{\partial}{\partial u}\left(\frac{VW}{U}\frac{\partial\phi}{\partial u}\right)+\frac{\partial}{\partial v}\left(\frac{WU}{V}\frac{\partial\phi}{\partial v}\right)+\frac{\partial}{\partial w}\left(\frac{UV}{W}\frac{\partial\phi}{\partial w}\right)\right\}=0 \tag{2}$$

[4] Research Staff of the G. E. C. London, Phil. Mag. (7) **1**, 609, (March 1926). F. Rother, Phys. Zeits. **27**, 471 (1926).

[5] Del Rosario, Frank. Inst. J. **203**, 243 (1927).

where an element of length is given by

$$dl^2 = U^2du^2 + V^2dv^2 + W^2dw^2 \tag{3}$$

In Cartesian coordinates, for figures of revolution about the X-axis, an element of length is given by,

$$dl^2 = dx^2 + dy^2 + y^2d\theta^2 \tag{4}$$

Because of the nature of the equipotential surfaces and the lines of force it is desirable to change to hyperbolic coordinates by these tranformation equations,

$$x = av(u^2+1)^{1/2}\ ;\ y = au(1-v^2)^{1/2}\ ;\ z = y. \tag{5}$$

Making use of equations (5), (4) and (3) and identifying the new coordinate w as the angle Θ we get,

$$U = a\left(\frac{u^2-v^2+1}{u^2+1}\right)^{1/2};\quad V = a\left(\frac{u^2-v^2+1}{1-v^2}\right)^{1/2};\quad W = au(1-v^2)^{1/2} \tag{6}$$

But the hyperboloids of revolution are equipotential surfaces, hence

$$\partial\phi/\partial w = \partial\phi/\partial u = 0.$$

and equation (2) becomes after substituting in the values given in equation (6) and simplifying

$$\frac{\partial}{\partial v}\left[\left(\frac{au(1-v^2)}{(u^2+1)^{1/2}}\right)\frac{\partial\phi}{\partial v}\right] = 0.$$

Solving

$$\phi = \frac{A}{2}\log\frac{1+v}{1-v} + B. \tag{7}$$

On the surface of the metallic point we put $v = v_0$ and $\phi = \phi_0$, and since the metallic plane where $v = 0$, is kept at zero potential we have $\phi = 0$ when $v = 0$. These conditions determine the constants of integration and (7) becomes

$$\phi = \phi_0\frac{\log\left[\frac{1+v}{1-v}\right]}{\log\left[\frac{1+v_0}{1-v_0}\right]}. \tag{8}$$

The potential gradient is given by the equation

$$E = -\frac{\partial\phi}{\partial s_v} = -\frac{1}{V}\frac{\partial\phi}{\partial v} \tag{9}$$

What we wish is the potential gradient at the end of the metallic point, where $v = v_0$ and $u = 0$, hence we have for this particular gradient

$$E_0 = -\frac{2\phi_0}{a \log \frac{1+v_0}{1-v_0}} \cdot \frac{1}{1-v_0^2} \cdot \tag{10}$$

The difference of potential between the point and plane, ϕ_0, can be measured by a voltmeter; a and v are constants characteristic of the point and may be calculated as follows: Eliminating u between the transformation equations (5), and writing $v = v_0$ we get

$$\frac{x^2}{a^2 v_0^2} - \frac{y^2}{a^2(1-v_0^2)} = 1, \tag{11}$$

as the equation of the hyperbola which when revolved about the X-axis gives the surface of the ideal metallic point. Call the distance between the end of the point and the plane x_0, then from equation (11)

$$a = x_0/v_0. \tag{12}$$

Thus a is determined in terms of x_0 and v_0. Now x_0 can be measured by use of a good micrometer microscope, and v_0 can be determined by use of the equation

$$v_0^2 = \frac{x_1^2 - x_0^2}{x_1^2 + y_1^2 - x_0^2} \tag{13}$$

obtained by combining (11) and (12), providing the coordinates (x_1, y_1) of a position on the metallic point can be determined. The coordinates may be obtained from a photomicrograph of the point (Fig. 1) because the edge of this image is a magnification of the hyperbola represented by equation (11) (assuming the point to be a true hyperboloid of revolution, which it is only approximately). But since x_0 is a direct measurement and x_1 and y_1 are measurements made on a photomicrograph (a 127-times enlargement) they must be reduced to the same scale before being substituted in equation (13).

Actually the point is not a true hyperboloid of revolution because of construction difficulties. Hence, within a limited range, there is no one value of x_0 which should be used more than another; that is, no distance between the point and the plane will give *exactly* the electric field described above. However, if for a given value of electrode distance, x_0, a number of calculations are made for v_0 using in each case the coordinates of a different point on the hyperbola (photomicrograph), and if the v_0's thus obtained turn out to have approximately the same value, then a good average value of v_0 is assured and it seems legitimate to use the equations listed above even though the shape of the point and the electrode-distance do not fulfill the ideal conditions set forth in the development of the formulas. This leads to an approximation method to be used in this investigation. The x and y coordinates of a series of points near the vertex of the approximate hyperbola (photomicrograph) are measured, remembering that on this

scale the origin is $127x_0$ from the end of the metallic point. Using each pair of coordinates of the series and a constant value of x_0 a series of v_0's is determined and then an average value of v_0 is calculated—a greater weight being given to the portion of the curve near the vertex. (See Table I). Finally the value of a is arrived at, ϕ_0 is measured on a voltmeter, and E_0 is calculated by use of equation (10). For a rather wide range in electrode distance, x_0, the values of v_0 for a given x_0, show very small dispersion. From this it follows that although theoretically each distance between point and plane should have a slightly different shaped point, yet practically the point serves for a considerable variation of this distance.

TABLE I. *Illustration of the method of calculating the field strength at the end of a point.*

x	y	v_0	
1.64	0.240	0.921	
1.74	.308	.935	Average $v_0=0.935$
1.84	.387	.934	$\phi_0=2950$ volts
2.04	.497	.938	$a=0.0129$
2.24	.594	.940	$x_0=0.0121$ cm
2.44	.689	.940	$E_0=1{,}070{,}000$ volts/cm
2.64	.775	.941	

Especially for large electrode distances, the data of Table I justify the shorter method of taking average values of the coordinates, viz., x_a and y_a, and of determining an average value of v_0 by one substitution in equation (13). Again if the electrode distance is very great as compared with the average dimensions of the point, and the plate is sufficiently large so that it may be considered an infinite plane, that is, if x_0 is very large as compared with $(x-x_0)_a$ and y_a, it is clear from equations (12) and (13) that v_0 is approximately equal to unity and the following relations are true,

$$a \doteq x_0\ ;\ 1+v_0 \doteq 2\ ;\ 1-v_0 \doteq \frac{{y_a}^2}{4x_0(x-x_0)_a} \tag{14}$$

Using these values equation (10) reduces to the simpler form,

$$E_0 = -\frac{4\phi_0(x-x_0)_a}{{y_a}^2\left[\log\frac{8(x-x_0)_a}{{y_a}^2}+\log x_0\right]} \tag{15}$$

which is used in Section IV to calculate the potential gradients.

III. Experimental Work on Tungsten, Platinum, and Nickel Points

Four points, sharp tungsten, blunt tungsten, sharp platinum, and sharp nickel—were made as nearly as possible in the form of hyperboloids of revolution, polished, and cleaned. Then with a projection lantern and a microscope attachment, photomicrographs were made of each point by allowing

its enlarged image to fall upon sensitized photographic paper. These photographs are shown in Fig. 1. The points were then mounted in the glass tube, Fig. 2. The glass structure in which the points are sealed also contains an enclosed soft iron rod. The structure is sealed to a small shaft which is free to turn, and it is easy, by the use of an outside magnet, to bring each point in its turn before a polished stationary tungsten disk, the plane. By means of a sleeve the other end of the shaft is fitted into a threaded

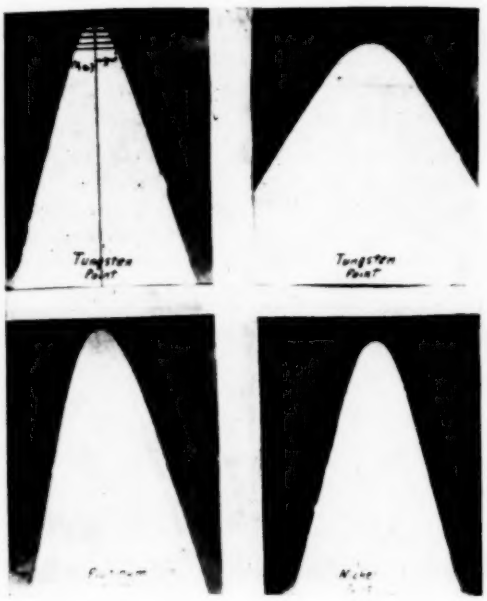

Fig. 1. Photomicrographs of points used.

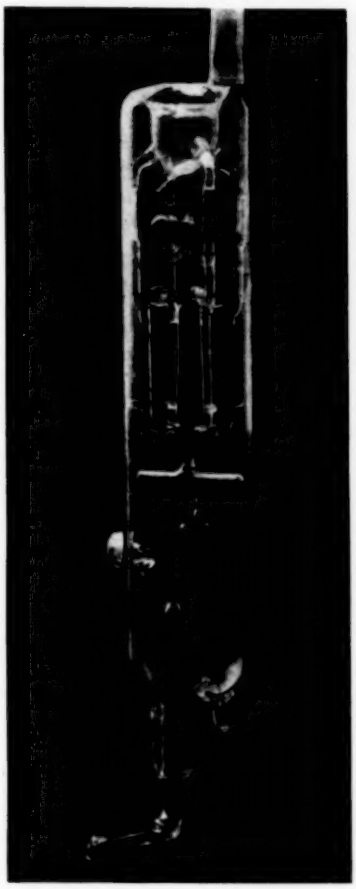

Fig. 2. Photograph of vacuum tube.

journal. A second glass enclosed iron rod is sealed to the screw part of the journal and by the use of an outside magnet a given point may be moved forward and back simply by making the screw turn. Concentric with the tungsten disk is a thoriated tungsten filament which is the source of thermions used in the process of heating the points and plane by electronic bombardment. The tube was baked during exhaust at 350°C for eight hours. The tungsten disk and points were heated to white heat, approxi-

mately 2200°K, a number of times by electronic bombardment. The platinum point was heated to approximately 1900°K and the nickel to approximately its melting point 1725°K. The pressure was always lower than 10^{-6} mm of mercury.

In part of the following experiments the potentials were produced by constant potential, direct current generators in series, capable of yielding up to 15,000 volts. At other times a high frequency (140 kilocycle) alternating current was rectified by a diode vacuum tube used in the manner already described by one of us[7] and capable of producing constant potentials up to 50,000 volts.

Table II gives sample sets of readings on the potential gradients necessary to produce the smallest current capable of accurate measurement with the electrometer used, namely 2.3×10^{-12} amperes. We arbitrarily take the potential gradient necessary to produce this current as the critical gradient. The distance between the point and plane is x_0, ϕ_0 is the potential which is necessary to produce the critical gradient E_0 at the end of the point calculated by use of equation (10) as explained above and as illustrated in Table I. These results were taken after preliminary heating.

TABLE II. *Sample set of readings on the potential gradient necessary to produce a current of 2.3 $\times 10^{-12}$ amp.*

x_0 (cm)	ϕ_0 (volts)	E_0 (volts/cm)	x_0 (cm)	ϕ_0 (volts)	E_0 (volts/cm)
Sharp tungsten point			Dull tungsten point		
0.0057	2100	1.04×10^6	0.0077	4050	0.80×10^6
.0075	2750	1.15	.0057	3000	.76
.0121	2950	1.07	.0102	5000	.83
.0113	2950	1.08	.0198	7100	.83
.0146	3250	1.09	Sharp platinum point		
.0330	4350	1.08	0.0065	6300	2.38×10^6
.0558	5550	1.21	.0048	5600	2.46
.0983	6500	1.10	Very dull nickel point[8]		
			0.0247	7500	0.45×10^6
			.0165	6200	.48

The foregoing data bring out sharply the facts: *first*, that at a given point the current begins to appear at a given field-strength or potential gradient, quite independently of the relations of applied potential and distance; *second*, that the critical field-strenth for tungsten points is of the same order as we obtained and previously published for tungsten wires (from a half million to a million volts per cm), points differing no more from wires than wires or points differ among themselves; and, *third*, that a higher field appears to be necessary to start a current from platinum than from tungsten or nickel. This last result was obtained by Hobbs[9] in the first work ever done on the extraction of electrons by fields.

[7] S. S. Mackeown, Jour. of Opt. Soc. **16**, 727 (1926).

[8] The nickel point had been melted during the heat treatment so it became necessary to estimate its shape by use of the micrometer microscope rather than by use of its photograph.

[9] Hobbs, Phil. Mag. **10**, 17 (1905).

IV. New Field-Current Law Exhibited by Currents From Points

A second sample set of results on field currents from points was obtained with the apparatus shown in Fig. 3, in which steel was used for both anode and cathode. Here the plate was so large that distances as great

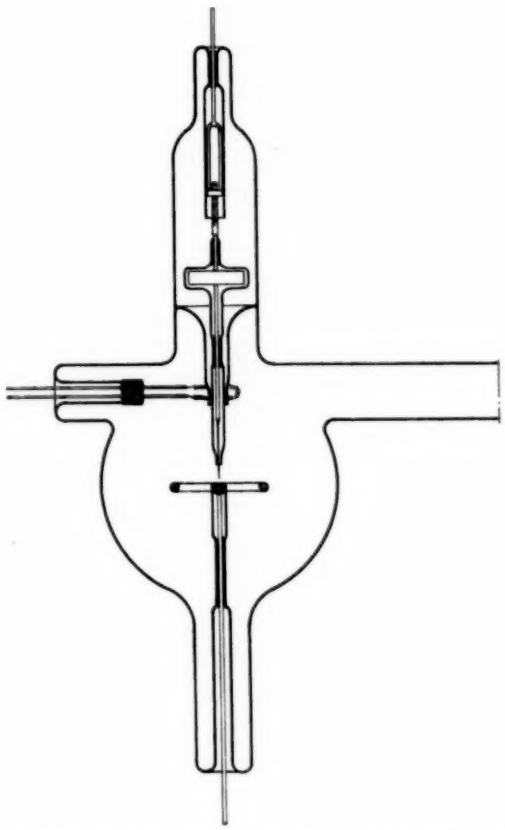

Fig. 3. Diagram of apparatus in which steel was used for both anode and cathode.

as a centimeter between point and plane could be used without introducing an appreciable error by assuming the plane to be infinite. For this case equation (15) was used to calculate the potential gradient. From microphotographs the following average values for $(x-x_0)_a$ and y were obtained,

$$(x-x_0)_a = 21\times10^{-5}\text{ cm},\quad y_a = 26\times10^{-5}\text{ cm}.$$

In exhibiting the results obtained in this run we have first plotted logarithm of the current against the reciprocal of the potential to show that these currents from points follow the field-current law recently brought to light by work on currents from cylinders.[10] (Fig. 4)

[10] Millikan and Lauritsen, Proc. Nat. Acad. Sci. **13**, 45-49 (1928).

It will be seen that these graphs exhibit very beautifully the linear relationship shown by currents from cylinders. The distance between the point and plane was varied by four steps, as shown in the upper right-hand corner of the graph and the four corresponding straight lines were obtained.

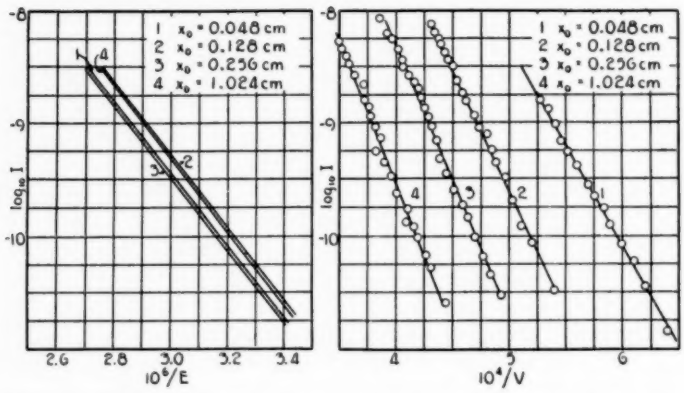

Fig. 4. Variation of logarithm of field current with reciprocal of field strength and with reciprocal of potential.

That field-strength alone determines current is here shown by the method of plotting used in the left half of the figure, all of the four curves reducing to four straight lines which coincide within 2%—closer than the experimental error—when log i is plotted against $1/E$ *instead of* $1/V$.

In this connection it is interesting to note that the research staff of the General Electric Company, London, published a paper in 1926[5] in which

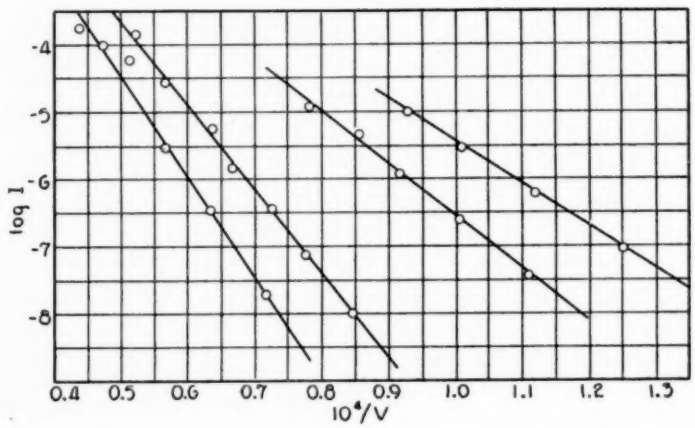

Fig. 5. Variation of logarithm of field current with reciprocal of potentials. Data taken from paper by the research staff of the General Electric Company, London.[5]

they plotted the logarithm of the current against the square-root of the voltage, as we did in our 1926 paper. If, however, we plot the data which they give in their Fig. 7 for "a single point of 0.002 cm wire, rounded by

etching in $NaNO_2$" taking the logarithm of the field-currents as ordinates, and the reciprocal of the potentials as abscissa, we get *straight* lines—an additional evidence of the correctness of the field-current equation. See Fig. 5.

V. No Current From Positive Point with Field Strengths of 35,000,000 Volts Per CM

With a tube similar to that just described, except that the distance between the point and plane was fixed, an attempt was made to draw a current when the point was made the anode. No current was obtained when 100,000 volts was applied from a direct current generator built in this laboratory[11]. This corresponds to a field at the point of 35×10^6 volts per centimeter.

Norman Bridge Laboratory of Physics,
California Institute.
February 9, 1928.

[11] Maxstadt, Jour. A. I. E. E. **43**, 1055 (1924).

BOOK REVIEWS

Pyrometry. WILLIAM P. WOOD and JAMES M. CORK. Pp. 207, 93 figs. and ten tables. McGraw-Hill, New York, 1927.—The authors have performed a valuable task, endeavoring to assemble material which hitherto has been scattered through numerous publications. Although pyrometry is a comparatively young field of work the number of publications has already become quite considerable and the authors have shown good judgment in their selection according to the basis upon which this text book is written, i.e., to meet the needs of the student as well as the more experienced person.

The first two chapters are devoted to the theory and principles of setting up a correct temperature scale and then the obtaining of that scale by the use of the gas thermometer. In this connection Day and Sosman's work, as stated, seems to be the latest and most reliable. It would seem advisable to give in the tables at the end of the book, the value of the melting points obtained by them. Their final reported values were obtained by using a bulb made of platinum alloyed with rhodium instead of iridium as stated by the authors. The number of errors of omission as well as commission are very few.

The text will save a considerable time in lectures, although some additional lectures will be necessary to show the development of formula presented and further discussion of theory. The figures are very good and the index well made. The problems, about thirty-four in number, are the first that have been published in connection with any pyrometry text and will be very acceptable. As for the experiments at the end of each chapter, the instructions are insufficient for laboratory use. Therefore more detailed directions will be required. If the course is to serve the practical or experienced man as well as the student, it would seem advisable to have two or more experiments on comparison of pyrometers, as for example, a resistance thermometer or an optical pyrometer against a standard thermocouple. Table IX is very useful, showing the application of different types of refractory material to pyrometer protection tubes.

The leading feature of the text is its well chosen descriptive material representing the various principles and types of pyrometers.

L. F. MILLER

Wien und Harms Handbuch der Experimental-physik, Vol. 6. Kapillaritat und Oberflächenspannung. G. BAKKER. Pp. 458, 114 figs. Akademische Verlagsgesellschaft., m.b. H., Leipzig, 1928. Price 42 R. M. unbound.—The writer of the treatise is a well known worker in this field since 1899, and the subject has been treated both from the theoretical and experimental points of view. As the first glance over the 450 odd pages shows some of the greatest mathematicians and theoretical physicists have devoted a great deal of effort toward the development of the theoretical aspects of capillary phenomena. It is therefore, gratifying to find also in the volume, a clear description of the experimental technique used in testing the various theories and a large amount of experimental data, so that the reader who is either unable or unwilling to wade through the theory may at least understand what Bridgman would designate as those operations which are "synonymous with the mathematical concepts." ("The Logic of Modern Physics," page 5).

The first four chapters deal with the classical theories of capillarity as formulated by Laplace, Kelvin, Gauss, Neumann and others, also with the form of the capillary surface and the theory of the drop method for measuring surface tension (Lohnstein's investigations.) Chapter V contains a description of the various methods (statical and dynamical) used for the determination of the capillary constants, and in Chapter VI, the effect of temperature (formulae of Eotvos, Ramsay-Shields and Rose-Innes) as well as the relation between surface tension and other properties of liquids are discussed. Tables of capillary constants for pure liquids and solutions are given in Chapter VII, and the next three chapters deal with Gibbs' thermodynamical theory of the surface layer and the surface energy of solids.

The most interesting chapters in the volume are XI and XII, in which are summarized the experimental investigations of Rayleigh, Devaux, Langmuir, Harkins and N. K. Adams on surface layers. The author has laid special emphasis on the significance of Langmuir's views

regarding the orientation of molecules in surface films and has discussed the whole theory in great detail.

The last three chapters deal mainly with the mathematical theories of the capillary layer developed by Fuchs, Rayleigh, van der Waals and the author, but the phenomenon of "oil on troubled waters" also comes in for a few pages of discussion.

SAUL DUSHMAN

Fundamentals of Astronomy. S. A. MITCHELL and C. G. ABBOT. Pp. 307, 56 plates, 42 figs. D. Van Nostrand, New York, 1927. Price $3.00.—A number of textbooks on general astronomy have appeared during the last two years, and of these none is better adapted to the general reader than the work under review. The discussion has been kept non-technical, the authors have presented in clear and attractive form the historical developments of the science as well as the latest results of astronomical research. The work is rather elementary for a serious student, as only the simplest formulae are given, geometrical diagrams are reduced to a minimum, even the Greek letters are spelled out, and no problems or exercises are included. For collateral reference, however, the presentation is likely to increase the interest of the student. The intelligent layman will find this a readable work, especially the chapters on the sun, solar radiation, and eclipses, which are the special fields of the authors; while the technical man of science will find here a fine summary of the present-day status of astronomy.

JOEL STEBBINS

Untersuchungen zur Quantentheorie. LOUIS DE BROGLIE. Pp. 88, figs. 6. Akademische Verlagsgesellschaft, Leipzig, 1927. Price R. M. 5:80.—This is a translation from the French into German of the important thesis of L. de Broglie which originally appeared in *Annales de Physique*, (10) **3**, 22, (1925) The translation is by Dr. Walther Becker. The booklet will therefore interest only those Americans who read German more readily than French.

In a one page preface dated September 8, 1927, de Broglie mentions the rapid developments of the past three years in the direction of a fusion of the methods of dynamics and the theory of waves. The meat of this preface is contained in the paragraph which follows:

"Bien des difficultiés subsistent cepandant. En particulier, on ne parait pas s'être beaucoup rapproché de ce qui peut à justre titre sembler lebut suprème à atteindre: la constitution d'une théorie ondulatoire de la Matiére dans le cadre de la Physique du Champ (Feldphysik). Pour l'instant, on doit se contenter d'une sorte de correspondance statistique entre les corpuscules d'énergie et des ondes à amplitude continue du type de l'Optique classique. A ce sujet, il est intéressant de remarquer que la densité électrique figurant dans les équations de Maxwell-Lorentz parait être seulement une grandeur moyenne; par suite, ces équations ne doivent pas pouvoir être appliquées à une particule isolée comme on le faisait dans la théorie des Electrons et elles ne peuvent pas nous servir à comprendre pourquoi l'électricité a une structure atomique. Le tentative si intéressante de Mie serait donc condamnée."

EDWARD U. CONDON

PROCEEDINGS

OF THE

AMERICAN PHYSICAL SOCIETY

MINUTES OF THE BERKELEY MEETING, MARCH 3, 1928

The 150th meeting of the American Physical Society was held at the Physical Laboratories of the University of California, Berkeley, California, on March 3, 1928. Morning and afternoon sessions were held.

An informal luncheon was held at the Students' Union of the University, attended by thirty-four members of the Society.

The regular scientific session consisted of thirty-two papers, abstracts of which are given on the following pages. Papers 12, 26, 28, and 29 were read by title. An **Author Index** will be found at the end.

LEONARD B. LOEB, Secretary

ABSTRACTS

1. A relation between the variations with temperature and density of the coefficient of recombination of gas ions. A. M. CRAVATH, University of California.—Different writers generally agree as to the nature of the recombination process, but differ greatly in their final theories because of the neglect of different factors in the developments. By the rigorous application of dimensional analysis and the assumption that the masses of the ions do not change with moderate temperature variation, the following relation connecting the temperature and density variations of α, the coefficient of recombination, is derived:

$$\left(\frac{\partial \ln \alpha}{\partial \ln \rho}\right)_\theta \left\{1.5+\left(\frac{\partial \ln k}{\partial \ln \theta}\right)_\rho\right\}+\left(\frac{\partial \ln \alpha}{\partial \ln \theta}\right)_\rho=-1.5$$

k is the average of the positive and negative ion mobilities, ρ is the gas density, and θ is the absolute temperature. This equation may be used as a test of the physical assumptions, or if these are assumed it may be used to calculate the temperature variation from the more easily measured density variation. Present experimental data are too uncertain to permit a significant test. They give from -1.75 to $+0.25$ as compared to the above value -1.5.

2. Radioactive properties of waters and soils in the southern California region. J. L. BOHN, California Institute of Technology.—This work on the radioactivity of soils and waters was started in connection with the work of Dr. Millikan and Dr.Cameron on cosmic radiation to find the activity in the vicinity of their measurements. The radioactivity of the waters of Lake Arrowhead was found to be not more than 1/200th of that of the reservoirs in Pasadena. Also the radioactivity of the soil where cosmic ray readings were taken was twice that of the soil on the Institute campus. The paper also presents measurements of radioactivity as a function of depth.

3. The systematic variation of the constant A in thermionic emission. LEE A. DUBRIDGE, National Research Fellow, California Institute of Technology.—A recent study of the thermionic emission from Pt (Phys. Rev., Feb. 1928) has shown that changes in the work function b during outgassing are always accompanied by changes in A (of the equation $i=AT^2 e^{-b/T}$) in such a way that log A is a linear function of b. Data obtained by other observers show this same relation for other metals. The slope of the straight line depends on the type

of surface studied, being small for coated W (Dushman, Kingdon) and large for liquid surfaces (Goetz, Zeits. f. Physik. **43,** 531(1927)). Dushman's theoretical value of A (60.2 amp/cm^2 deg^2) is observed only when b happens to be about 52,000°K, and nearly all the lines pass near this point. "Abnormal" values of A have usually been attributed (most recently by Bridgman, Phys. Rev. **31,** 90(1928)) to the effect of surface contamination. However for *clean* Pt $b=73{,}500$ and $A=14{,}000$ which is 230 times the theoretical value. Whether these results can best be interpreted by the introduction of a factor involving the surface heat of charging as suggested by Bridgman and Langmuir and Tonks, or by the adoption of the more detailed picture of the process developed by Raschevsky seems as yet uncertain.

4. The cataphoresis of small gas bubbles in various organic liquids. KARL DYK, University of California, (Communicated by Leonard B. Loeb).— The cataphoresis of small gas bubbles in water has been explained as the result of a superficial negative charge caused by an electrical double layer at the gas-liquid boundary (Lenard, Ann. der Physik **47,** 492, 1915). Alty (Proc. Roy. Soc. **A112,** 235, 1926) and McTaggart (Phil. Mag. **44,** 386, 1924) conclude the effect is due to ionic impurities. McLaughlin (Proc. Roy. Dub. Soc. **17,** 13, 1922) investigated organic liquids at low fields and detected no charge on gas bubbles. Experiments were undertaken in this laboratory to test this for high fields since it was suspected that, with lower dielectric constant, the double layers would be less highly charged and would require higher fields for detection. Experiments, by McTaggart's method indicated it to be ill suited to such experiments, because of the high expansion coefficients of the liquids. A new technique has been evolved with the result that the simple behavior observed for water droplets is not observed for organic liquids up to fields of 15,000 volts/cm. Minute bubbles appear to be charged under some circumstances, but change the sign of their charge rapidly in progressing through the field. Polarisation and purification phenomena were also observed in various organic liquids at the high fields used.

5. Mobility of gaseous ions in H_2S–H_2 mixtures. LEONARD B. LOEB AND L. DUSAULT, University of California.—Mobilities of ions in carefully purified H_2S and in H_2S–H_2 mixtures have been measured. The values of mobilities on the ordinary scale of mobilities are 0.588 and 0.572 cm/sec per volt/cm for positive and negative ions respectively; on the new absolute scale they must be multiplied by 1.21. Results obtained at low pressures indicate that the inverse pressure law may not hold accurately for the positive ions, while it does hold for the negative ions. The mobility constant of the former appears slightly *less* than the value at higher pressures. This result for both ions is contrary to the expectations of the ion theory of A. P. Alexeievsky (Phys. Rev. **27,** 811, 1926), which requires an increase of some 10 per cent. In pure samples of H_2S, free electrons were observed in H_2S below 50 mm. This places H_2S between air and O_2 in its power of attaching electrons to form ions. Mobilities of ions in H_2S–H_2 mixtures show that traces of H_2S lower the mobility of both ions well below the values computed from Blanc's law of mixtures. This again indicates clustering.

6. Collector measurements in the positive column of the noble gases. W. UYTERHOEVEN. (Fellow C. R. B. Educational Foundation), California Institute of Technology.—The positive column of the noble gases was studied by using plane collectors of different sizes and materials, and applying Langmuir's theory (Gen. El. Rev. Vol. **27,** 1924). The positive ion currents did not show saturation, nor did the value of the current density computed by means of the measured sheath thickness and the space charge equations agree with the measured current density. The most satisfactory interpretation of these experiments (partly done in the Philips Laboratory, Eindhoven, Holland) seems to be to assume a very large secondary electron emission (50 per cent of the total current, and even more for low accelerating potentials of the collector). As to the cause of this electron emission, the experimental data seem to eliminate the action of the positive ions as a possible explanation. Probably the metastable atoms are responsible for the effect, either by photoelectric ionization in the positive ion sheath, as suggested to me by Prof. K. T. Compton, or by direct action of the excited atoms on the metal surface (conductive photoelectric effect). Further experiments are under way to test these last explanations this secondary emission being an important element in the theory of the cathode fall of the glow discharge.

7. Different types of field currents, their laws and the conditions under which they arise. C. C. LAURITSEN AND R. A. MILLIKAN, California Institute of Technology.—Further evidence is herewith presented for the view earlier advanced (Phys. Rev. **27,** 51, 1925) that field-currents originate only in individual "weak spots" on the emitting surface. These weak spots are of two sorts, first those which are entirely undiscernible by mechanical or optical means; second, those resulting from definite surface explosions or "ruptures" which leave behind them craters with jagged edges. The present paper differentiates the characteristics of the field-currents from both types of weak spots. It however presents further proof that all field-currents whether of one sort or the other follow the law recently reported (Proc. Nat. Acad. Sci. Jan. 1928) by us as a result of experimental studies, and simultaneously given a theoretical explanation by Oppenheimer on the basis of wave-mechanics. This paper also presents experimental proof that field-currents are uninfluenced by temperature changes between ordinary and liquid-air-temperatures, as we previously predicted. (Proc. Nat. Acad. Sci. Jan. 1928).

8. Field currents from points. C. F. EYRING, S. MACKEOWN, AND R. A. MILLIKAN, California Institute of Technology.—The laws governing the extraction of electrons from metals in high vacua by fields, first developed through experiments with crossed wires (Millikan and Shackelford, Phys. Rev. **15,** 239, 1920) then with fine wire cathodes discharging to cylindrical anodes, (Millikan and Eyring, Phys. Rev. **27,** 51, 1926) have been now found to hold throughout for field currents between points and planes. The theory needed for the quantitative determination of the potential gradients at points is here given, and critical gradients then determined experimentally. The generality of the linear relation between log i and the reciprocal offield-strength (Millikan and Lauritsen, Proc. Nat. Acad. Sci., January, 1928) is experimentally established.

9. On the quantum theory of field currents. J. R. OPPENHEIMER (National Research Fellow), California Institute of Technology.—The pulling of electrons out of metals by intense electric fields may be interpreted on the quantum mechanics as the ionization of the metallic atoms by the field. The theory then gives, for the dependence of the field current i (amps) the field strength F (volts) and the work function W (volts)

$$i = 3\times 10^{-8} F^{1/4} W^{5/8} \exp\left\{-10^{8} W^{3/2}/F\right\}$$

per surface atom. The form of the resulting characteristic is that found experimentally by Millikan and Lauritsen: $ln\ i = \text{const.}/F$. The experimental values of the constant, derived by the use of a field strength computed from the geometrical dimensions of the wire, gives for W about 0.4 volt. The introduction of the dimensions of the points surrounding the craters on the wire, which are found experimentally to give the current, raises the value of W to about 5 volts, and shows that only a small number of surface atoms take part in the effect.

10. On the theory of the radiometer. PAUL S. EPSTEIN, California Institute of Technology.—The radiometric effect in extremely rarefied gases has been clear to us since Knudsen's extensive work on this subject. But a treatment of the case of comparatively dense gases (mean free path, l, small compared with the linear dimensions of the vane) has been lacking, though the foundations for it were laid as far back as 1879 by Maxwell. The present computations have the purpose of supplying this want; they are carried through for a thin circular disk. If a is the radius and δ the thickness of the disk, and if I is the energy of radiation falling on unit area of its front surface and absorbed in its surface layer, one obtains a formula for the radiometric force which we give here for two limiting cases:

$$K_1 = -\frac{1.70a}{\kappa_g}\,\frac{pl^2}{T}I, \qquad K_2 = -\frac{2.66\delta}{\kappa_i}\cdot\frac{pl^2}{T}I.$$

K_1 applies to the case for which the thermal conduction of the vane is poor, K_2 when it is good, p,T denote temperature and pressure of the gas, K_g,K_i heat conductivity of the gas and of the material of the vane.

11. The dispersion by hydrogen-like atoms in wave mechanics. BORIS PODOLSKY, California Institute of Technology.—The Schroedinger wave equation for a hydrogen-like atom in the field of a plane electromagnetic wave is solved by a method of expanding the wave function into a series of characteristic functions forming a complete orthogonal set. The result for atomic hydrogen is the following formula: $n^2-1=2.24\times10^{-4}(1+1.228\times10^{-10}/\lambda^2+\cdots)$, where n is the index of refraction and λ the wave-length of the incident light. For the limiting case of electrostatic field, $\lambda=\infty$, this gives the dielectric constant $\epsilon=n^2=1+2.24\times10^{-4}$, in agreement with results previously obtained by Van Vleck, Epstein, and Pauling.

12. The Fermi statistics applied to electrocapillarity. OSCAR KNEFLER RICE (National Research Fellow), California Institute of Technology.—It is assumed that each atom in mercury is ionized into a positive ion and an electron. Due to the crowded state of the positive ions it is supposed that they cannot move in an electric field, while, following Sommerfeld, the electrons are assumed to act like a completely degenerate gas following the Fermi statistics. The distribution of electrons under an electric field due to a charge on the surface of the metal is discussed, and a relation derived which gives the charge on the surface in terms of the potential difference between surface and interior. To a first approximation the charge and potential difference are proportional to each other, as if there were a condenser of constant capacity at the surface. The magnitude of the equivalent capacity is such that, when considered in conjunction with the diffuse layer of ions in the solution, electrocapillary curves can be explained.

13. The gravitational field of a body with rotational symmetry in Einstein's theory of gravitation. P. Y. CHOU, California Institute of Technology.—Einstein's set of field equations in vaccuo, $G_{\mu\nu}=0$, is reduced to such a form that simple problems like the sphere (Schwarzschild's solution), the infinite plane and the infinite cylinder can be solved. The fundamental quadratic differential forms for the latter two cases are respectively,

$$ds^2=-|(1+4\pi\sigma z)^{-1}dz^2+d\rho^2+\rho^2d\phi^2|+(1+4\pi\sigma z)dt^2,$$

$$ds^2=-c_4^2\rho^{-2}[(1+4m\log\rho)^{-1}d\rho^2+\rho^2d\phi^2]-dz^2+(1+4m\log\rho)dt^2,$$

where σ is the surface density of matter on the plane, $z=0$; m the linear density of matter on the cylinder, $\rho=$const.; (ρ, z, ϕ), the cylindrical coordinates, c_4, an undetermined constant and the velocity of light is unity. Setting $g_{44}=$the Newtonian potential+const., we can get the solution of the general gravitational problem for a body whose mass is distributed symmetrically about an axis provided we can solve

$$2\frac{\partial}{\partial\psi}\left((1-2M\psi)\frac{\partial n}{\partial\psi}\right)+\frac{\partial^2}{\partial\theta^2}e^{2n}=0 \qquad (M=\text{mass of the body}).$$

The gravitational field of an oblate spheroidal homoeoid is characterized by

$$ds^2=-\psi^{-4}(1-2M\psi)^{-1}d\psi^2-\psi^{-2}d\xi^2-\psi^{-2}\cos^2\xi d\phi^2+(1-2M\psi)dt^2$$

where $\psi=\kappa^{-1}\cot^{-1}(\sinh\eta)$, $M=$mass of the homoeoid whose equation is $c^2\rho^2+a^2z^2=a^2c^2$, $\kappa^2=a^2-c^2$ and ξ, η are related to the cylindrical coordinates (ρ, z, ϕ) by $\rho+iz=\kappa\cos(\xi+i\eta)$. Analogous expressions for a prolate spheroidal homoeoid are obtainable. The oblateness of the homoeoid causes a slight increase in the advancement of the perihelion of a planet's orbit which was derived from Schwarzschild's solution.

14. Diurnal variation of distribution of the surface charge of the earth around the parallel of 37½° for the year 1927. FERNANDO SANFORD, Stanford University.—That the distribution of the surface charge of the earth is not constant is shown by the existence of earth-currents and the accompanying magnetic variations and by the variations in the electrostatic field of the atmosphere. The fact that all these phenomena show fairly regular diurnal and seasonal changes in both intensity and direction is evidence that they are influenced, if not determined, by the position of the sun relative to the place of observation. The diurnal variation of the surface intensity of the earth's charge at Palo Alto has been almost continuously recorded photographically for the past six years, and recently a new and very sensitive method of recording it has been devised which is free from all possible effects of changes in atmospheric conductivity.

It has been found that there is both a solar and lunar diurnal variation and a seasonal variation which is greatest at the equinoxes and least at the solstices. The average diurnal variation for each month of the year is shown by curves, and the average distribution for the year of the variable part of the charge is shown by a Bidlingmaier diagram.

15. Electron emission at the surface of platinum through which hydrogen is passing. L. T. JONES AND VICTOR DURAN, University of California.—When hydrogen is passing through the walls of a hot platinum tube there is an emission of electrons from the exit surface which far exceeds the Richardson emission for platinum for that temperature. The emission as a function of the voltage removing the electrons exhibits the usual saturation but at very low plate voltages apparently differs from the pure thermionic emission. The phenomenon is complicated by the surface effect examined by H. A. Wilson. Attempts to find electron emission at the exit surface of hydrogen passed electrolytically through platinum and iron have thus far been futile. When hydrogen is admitted to a platinum tube which has been glowing for several hours in vacuum (no emission) electron emission rises to a sharp peak and drops almost as sharply to a constant value. The time of appearance of the peak and its magnitude are both dependent on the previous history of the platinum.

16. The crystal structure of potassium dithionate. M. L. HUGGINS AND GLENN FRANK, Stanford University.—Using x-ray spectra from rotating crystals, the following results have been obtained for $K_2S_2O_6$: The space group is D_3^1 ($3D$-1) of the hexagonal system. The unit of structure has the dimensions $a_0=9.8$ and $c_0=6.45$A and contains $6K$, $6S$ and 18 O atoms. The S atoms are in pairs on the three-fold symmetry axes, each S having three O atoms symmetrically placed around it.

17. Refractive indices of calcite in the wave-length range of two to six Angtrom units. ELMER DERSHEM, University of California.—The indices of refraction of calcite in this region must be known for a precise determination of x-ray wave-lengths by reflection from this crystal and it also desirable to determine what type of anomalous dispersion, if any, occurs near the K absorption limit of calcium. A narrow beam of general radiation rendered nearly monochromatic by reflection from a gypsum crystal was reflected from a polished surface of calcite and the critical angle of total reflection determined. It was found that at 1.98 Angstrom units $1-\mu=17.8\times10^{-6}$ and at 6.00 Angstrom units $1-\mu=137\times10^{-6}$. These values are in excellent agreement with those calculated from the Drude-Lorentz dispersion formula. This is true of other points on the curve except those within two or three tenths Angstrom unit of the calcium absorption limit. In this region the values of $1-\mu$ are depressed on both sides of the absorption edge, being thus in agreement with the quantum theories of x-ray dispersion of Kronig (Jour. Optical Soc. **12**, 547, 1926) and Kallman and Mark (Ann. d. Physik **82**, 585, 1927).

18. An experimental study of the relative intensities of x-ray lines in the L-spectrum of uranium. SAMUEL K. ALLISON, University of California.—The results so far obtained in this investigation, not yet entirely completed, confirm in general the results already published for thorium (Phys. Rev. **30**, 245, 1927). The present work is being done at 55 kilovolts, in order to work in a region in which the exciting voltage is as far above the critical excitation voltages of the L-series as possible. From previous work, notably that of Jönsson (Zs. f. Phys. **41**, 801, 1927) it is known that the relative intensities of the lines $\gamma_3\gamma_2$, $\beta_3\beta_4$ are not 2:1 as demanded by the extension of the Burger-Dorgelo rules to x-ray spectra. In the second order spectrum in uranium it has been possible to investigate the lines β_3, β_4 free from interfering lines and they are found to be of almost equal intensity. This seems also to be true of γ_3, γ_2 although the evidence here is not so conclusive. A further interesting fact is that the lines γ_4, γ_5, which are present in the tungsten L-spectrum are absent in the thorium and uranium L-spectra. The fact that the lines β_3, β_4 are much weaker relative to β_1 in the thorium spectrum than in tungsten has been confirmed in the uranium spectrum.

19. Infra-red absorption by the S-H bond. JOSEPH W. ELLIS, University of California at Los Angeles. The near infra-red absorption spectra have been recorded for ethyl, n-propyl, n-butyl, iso-amyl, phenyl (thiophenol) and benzyl mercaptans and their corresponding sulfides.

This study was undertaken to test an assumption that absorption near 2μ in the spectra of the mercaptans should be modified by the presence of the single S-H linkage. An absorption band was readily found at 2.00μ for thiophenol and benzyl mercaptan, and, although less easily measurable, is detected near that wave-length value in the records of the alkyl mercaptans. The band does not appear with the sulfides. It is regarded as the first harmonic of a band found by Bell (Ber. der Deutsch. Chem. Gesell. **60,** 1749, 1927) at 3.8μ, and is assumed to arise from non-harmonic oscillations in the S-H bond. The sulfur-hydrogen linkage thus seems to behave optically similarly to the carbon-hydrogen and the nitrogen-hydrogen linkages. (See previous abstracts.)

20. Infra-red emission of hydrogen. E. D. McAlister, University of California.—Thermocouple observations of emission from a long hydrogen tube of the Wood type indicate a shift of intensity as a function of pressure. A relative intensity of P_α to H_β of 4 to 1 is observed at a pressure of 1 mm (Hg) of H as compared with 11 to 1 at a pressure of 1/4 mm (Hg) of H. This has an important bearing upon the nature of resonance excitation, since the two lines differ only in final state as to total quantum number. Under this condition of low pressure and with high dispersion the third member of the Brackett series was observed.

21. Vibration spectra of simple hydrocarbons. F. S. Brackett, University of California.—The vibration spectra in the region 0.8 to 2.6μ of liquid hydrocarbons obtained with an effective slit width of 30 A° indicate clear cut differentiation between successive members of the paraffine series. Higher resolving power makes possible the identification of distinct vibration frequencies with the different types of H-C bonds. The spectrum of benzene supports the prevalent hypothesis that little distinction exists between its several H-C bonds. Furthermore the types of H-C bonds present in benzene are distinctly different from those exhibited in the paraffine series.

22. Intensity measurements in the multiplets of TiI. George R. Harrison, Stanford University.—A 10 meter 15,000 line per inch grating has been mounted for photometric measurements in complex spectra so that up to seven plates can be exposed in various parts of the spectrum from 2000 to 7000A at once. Measurements are being made on the intensities of lines in multiplets, and on the relative intensities of the multiplets in the triads and pentads of the elements of the iron group. Results obtained in TiI indicate that the well-known intensity formulas are obeyed almost exactly by most lines of all multiplets measured, but that most multiplets contain some lines which depart from both sum and intensity rules. As examples: In the transition $3d^2.4s^2 - 3d^2.4s.4p$ (Russell, Astrophys. Jour., **66,** 184, 1927) $a^3P' - b^3S'$ and $a^3P' - c^3P$ obey the rules exactly, while $a^3F' - b^3F$ has two lines 100% and 50% too strong, and $a^3F' - b^3D'$ has two 62% and 40% too strong, and one 25% weak. For $3d^3.4s - 3d^3.4p$, $a^5F' - b^5G'$ has its main line 36% strong, $a^5F' - c^5D'$ contains two lines 20% low and two 10% low. For $3d^2.4s^2 - 3d^3.5p$, $a^3F' - b^3G'$ is normal while $a^3F' - b^3F$ has two lines 50% too strong. Frerichs (Ann. der Phys. **81,** 807, 1926) had previously measured two of these multiplets with similar results.

23. Nature of the molecular binding and other properties of the hydrogen halides. R. T. Birge and O. R. Wulf (National Research Fellow), University of California.—In order better to study the properties of certain molecules, comprehensive energy level diagrams have been devised which include the various intermediate products occurring in cyclic processes such as used by Born and others. Using some recent improved data, such diagrams have been plotted to scale for HCl, HBr, HI, and (less completely) HF. Levels are given for the neutral molecule with atomic binding and with (hypothetical) ionic binding, as ionized, and as dissociated into various products. Several additional reasons are deduced for believing, with Franck and Kuhn, that these substances exist with *atomic* binding in the non-vibrational state. In particular this conclusion results from a critical study of their infra-red band absorption, and the heats of dissociation derived by linear extrapolation of the vibrational frequency curve. The actual form of this curve seems however to indicate a dissociation into *ions*, an assumption which the wave mechanics appears to show is not necessarily inconsistent with the preceding. The heat of dissociation of these molecules in the ionized state is roughly zero or negative, and this and other significant relations are discussed in connection with known and predicted experimental facts.

24. New data on H_2 absorption. J. J. HOPFIELD, University of California.—The A-B, and A-C ultra-violet absorption systems of H_2 have been greatly extended. New measurements now include the bands A_0-B_{17}, and A_0-C_{10}. This extension brings both systems near the converging limit, and from these data the heat of dissociation of H_2 with excitation of one of the atoms to the two quantum orbit may be calculated. This limit practically coincides with the beginning of continuous absorption observed by Dieke and Hopfield and interpreted by them as marking this limit. On carrying out the absorption experiments with less hydrogen in the receiver, it was found that this absorption limit is not real and therefore the conclusion of the above authors concerning the heat of dissociation of H_2 is slightly in error. The new experiments show that the absorption limit merely marks the beginning of what appear to be new and stronger absorption band systems of H_2 probably related to still higher electronic excitation. Furthermore the fact of the absence of a real absorption limit in this case is supported by the distribution of intensity among the A-B, and A-C systems. These bands reach their maximum intensity at about the A_0-B_5 and A_0-C_2 bands respectively and become fainter for higher members instead of stronger.

25. Band spectra in the extreme ultra-violet excited by active nitrogen. HAROLD P. KNAUSS, University of California.—A vacuum grating spectrograph was used to observe spectra between λ2500 and λ1000 excited in certain gases in active nitrogen. CO bands were observed originating in a set of vibrational levels (1–6) of electronic level A, with energies from 8.2 to 9.0 volts. NO bands were found to include, beyond the β and γ bands, a progression belonging to another system, with final levels belonging to the normal electronic state of the molecule. The initial level, identified as an electronic state with zero vibration from Leifson's absorption data, is designated as level C, and the bands are called the δ bands of NO. The O-O band is at λ1915.7, and the energy of excitation is 6.44 volts. No trace of the molecular spectrum of hydrogen, requiring 11.1 volts, was found in the afterglow. These results support conclusions reached earlier by R. T. Birge that when atoms of nitrogen combine to form a molecule with 11.4 volts of energy, some of the energy is lost immediately by radiation of the α group bands. The remainder, from 8 to 10 volts, is retained in a semi-metastable configuration, and is the maximum available for the excitation of other bodies in second type collisions.

26. Series spectra of potassium and calcium. I. S. BOWEN, California Institute of Technology.—Several of the strongest extreme ultra-violet lines in the K_{III}, K_{IV}, Ca_{IV}, and Ca_V spectra are given their series designation. In K_{II} several lines are identified in addition to those found by DeBruin. The absolute value of the terms of K_{II} are determined thus fixing the ionization potential at 31.7 volts. 137 lines are classified in Ca_{III} and the term values of the levels involved are calculated. These correspond to an ionization potential of 51.0 volts.

27. Atmospheric or vacuum arc for standard wave-lengths? HAROLD D. BABCOCK, Mount Wilson Observatory.—Unsupported statements in the report of the Optical Society of America (J.O.S.A. *16*, 44, 1928) are controverted by the facts. Typical iron lines from atmospheric and vacuum arcs are shown by photographs to be almost indistinguishable. Equality of errors of setting on these lines is illustrated. Differences from plate to plate, for each of three observers, are found equally great for both arcs. Differences from observer to observer show the same range for both arcs. The present standard arc is as reproducible and as accurately measurable as the vacuum arc. Other features discussed are (1) adaptability to the purpose of producing standards, (2) differences of wave-length between standards and corresponding solar lines, (3) distinction between the study of laboratory spectra from vacuum sources and the practical problem of producing standards of wave-length, (4) pressure displacements for iron lines. New observations, some now in press, will soon make available vacuum iron arc wave-lengths equal in precision to the standards, but not greater. Attempts to discredit the adopted standard arc are without justification. No evidence is found of superiority of the vacuum arc.

28. Astrophysical importance of the rare-earth elements. CHARLES E. ST. JOHN, Mount Wilson Observatory.—Characteristic features: The low values for the rotation of the sun and the high velocities of out flow from spots given by them show that they are at very low level

in the sun's atmosphere. They are present in the ionized state, but their spectra are peculiar for ionized atoms in that their lines are generally stronger in the arc than in the spark, and in flash spectra show marked differences from both the ionized and neutral atoms of other elements. Their lines are greatly enhanced in the spectra of γ Cygni but are weakened in the spectra of sun-spots. Presence in sun and stars: Nine earth-elements are recognized in the sun: namely La^+, Ce^+, Pr^+, Nd^+, Sa^+, Eu^+, Gd^+, Dy^+, and Yb^+. The first seven are found also in γ Cygni. Laboratory data deficient: Accurate measurement of the wave-lengths and study of the relative intensities and appearance of their lines under varied conditions of excitation offer opportunities for laboratory investigations not only of value because of their physical and theoretical importance, but also of interest because of questions of technique and the possibility of solving problems peculiar to this group of elements. Such investigations are within the compass of many laboratories.

29. An improved grating for the extreme infra-red. RICHARD M. BADGER, California Institute of Technology.—A reflection grating has been constructed, consisting of a plate of glass on which is deposited photographically a series of narrow gelatin laminae. These are equally spaced and their width is equal to that of the blank glass spaces between. The even order spectra are absent, and certain wave-lengths, depending on the thickness of the laminae, are absent in the zero order, being concentrated almost entirely in the first order. For these wave-lengths this grating compares favorably with an echlette. The intensity is not quite as great but higher orders are missing, or are weak, and the symmetrical form is very desirable when making absolute wave-length measurements. With such a grating, of 1 mm spacing, the ammonia rotation spectrum has been resolved and six lines measured between 56 and 127μ.

30. The rotational and vibrational energy of molecules. RAYMOND T. BIRGE, University of California.—A literal interpretation of the new wave mechanics indicates that the quantities ω_0, B_0, D_0, etc. of the old mechanics refer, not to a non-vibrating molecule, but to one with a half unit of vibrational energy ($n=1/2$). Hence the theoretical relation $D_0=-4B_0^3/\omega_0^2$ is not necessarily true, using the old mechanics values. From Kemble's theoretical equations, explicit expressions are obtained for the percentage change of each side of this equation, in passing from the new to the old mechanics, and these are applied to a number of molecules for which reliable data are available. In all cases the differential change in the two sides is less than the probable experimental errors, thus accounting for the observed verification of the equation in the old mechanics. With more accurate data it however is a potential means of verifying the above literal interpretation of the new mechanics, originally suggested by the observed electronic isotope effect in BO. Other relations between the constants of band spectra and those of the molecular potential function are discussed and numerically tested on various molecules; in particular, Richardson's indirect method for evaluating the moment of inertia of H_2.

31. Tables of constants for diatomic molecules, derived from band spectra data. RAYMOND T. BIRGE, University of California.—A new table of constants has been prepared, similar to that on pages 230–232 of "Molecular Spectra in Gases," using data available to Nov. 1927. The nature of the electronic transition (such as $^2P-^2S$) is given where known. About twice as many systems are listed as in the older table, and the constants are accompanied by critical remarks as to their source and reliability. *All* numerical values are stated in terms of the *old* quantum mechanics, but transformation equations to the new mechanics are given and discussed. Two additional tables have been prepared. The first gives in order of energy the electronic levels and correlated constants (ω_0, I_0 etc.) of the molecules BO, CO, CO^+, H_2, He_2, N_2 and NO. The other lists heats of dissociation of diatomic molecules, derived from band spectra.

32. The Physical Pendulum in Quantum Mechanics. E. U. CONDON, Columbia University.—The characteristic functions of a physical pendulum in wave mechanics are the Mathieu, or elliptic cylinder, functions of even order. Many of the properties of these functions are illuminated by considering their interpretation in the pendulum problem, especially their asymptotic connection with the parabolic cylinder function, which is the quantum mechanical analogue of the harmonic-oscillator-like behavior of the physical pendulum for oscillations of small amplitude.

AUTHOR INDEX

Allison, Samuel K.—No. 18

Babcock, Harold D.—No. 27
Badger, Richard M.—No. 29
Birge, Raymond T.—Nos. 30, 31
———— and O. R. Wulf—No. 23
Bohn, J. L.—No. 2
Bowen, I. S.—No. 26
Brackett, F. S.—No. 21

Chow, P. Y.—No. 13
Condon, E. U.—No. 32
Cravath, A. M.—No. 1

Dershem, Elmer—No. 17
Du Bridge, Lee A.—No. 3
Duran, Victor—see Jones
Du Sault, L.—see Loeb
Dyk, Karl—No. 4

Ellis, Joseph W.—No. 19
Epstein, Paul S.—No. 10
Eyring, C. F., S. Mackeown and **R. A. Millikan**—No. 8

Frank, Glenn—see Huggins

Harrison, George R.—No. 22
Hopfield, J. J.—No. 24
Huggins, M. L. and **Glenn Frank**—No. 16

Jones, L. T., and Victor Duran—No. 15

Knauss, Harold P.—No. 25

Lauritsen, C. C., and **R. A. Millikan**—No. 7
Loeb, Leonard B. and L. Du Sault—No. 5

Mackeown, S.—see Eyring
McAllister, E. D.—No. 20
Millikan, R. A.—see Eyring
———— see Lauritsen

Oppenheimer, J. R.—No. 9

Podolsky, Boris—No. 11

Rice, O. K.—No. 12

Sanford, Fernando—No. 14
St. John, Charles E.—No. 28

Uyterhoeven, W.—No. 6

Wulf, O. R.—see Birge